Chemoselective Reduction of Nitroarenes using Hydrogen Sulphide under Phase Transfer Catalysis

Dissertation submitted to the

National Institute of Technology Rourkela

In partial fulfillment of the requirements of the degree of

PhD

in

Chemical Engineering

by

Ujjal Mondal

(Roll Number: 512CH1008)

under the supervision of

Prof. Sujit Sen

Department of Chemical Engineering
National Institute of Technology Rourkela

Department of Chemical Engineering
National Institute of Technology Rourkela

January 26, 2017

Certificate of Examination

Roll Number: 512CH1008

Name: Ujjal Mondal

Title of Dissertation: Chemoselective reduction of Nitroarenes using Hydrogen Sulphide and Phase Transfer Catalysis

We, the below signed, after checking the dissertation mentioned above and the official record book (s) of the student, hereby state our approval of the dissertation submitted in partial fulfillment of the requirements for the degree of Doctor of Philosophy in Chemical Engineering at National Institute of Technology Rourkela. We are satisfied with the volume, quality, correctness, and originality of the work.

Sujit Sen
Supervisor

Raghubansh Kumar Singh
Chairman (DSC)

Basudeb Munshi
Member (DSC)

Abanti Sahoo
Member (DSC)

Sourav Chatterjee
Member (DSC)

Vaibhav V. Goud
Examiner

Department of Chemical Engineering
National Institute of Technology Rourkela

Dr. Sujit Sen
Assistant Professor

January 26, 2017

Supervisor's Certificate

This is to certify that the work presented in this dissertation entitled "**Chemoselective reduction of Nitroarenes using Hydrogen Sulphide under Phase Transfer Catalysis**" by "Ujjal Mondal ", Roll Number 512CH1008, is a record of original research carried out by him under my supervision and guidance in partial fulfillment of the requirements for the degree of *Doctor of Philosophy in Chemical Engineering*. Neither this dissertation nor any part of it has been submitted for any degree or diploma to any institute or university in India or abroad.

Sujit Sen

Dedicated to My Family

Declaration of Originality

I, Ujjal Mondal, Roll Number 512CH1008 hereby declare that this dissertation entitled "Chemoselective reduction of Nitroarenes using Hydrogen Sulphide under Phase Transfer Catalysis " represents my original work carried out as a doctoral student of NIT Rourkela and, to the best of my knowledge, it contains no material previously published or written by another person, nor any material presented for the award of any other degree or diploma of NIT Rourkela or any other institution. Any contribution made to this research by others, with whom I have worked at NIT Rourkela or elsewhere, is explicitly acknowledged in the dissertation. Works of other authors cited in this dissertation have been duly acknowledged under the section "Bibliography". I have also submitted my original research records to the scrutiny committee for evaluation of my dissertation.

I am fully aware that in the case of any non-compliance detected in future, the Senate of NIT Rourkela may withdraw the degree awarded to me on the basis of the present dissertation.

January 26, 2017 Ujjal Mondal

NIT Rourkela

Acknowledgement

I wish to thank and express my heartfelt gratitude to my supervisors ***Dr. Sujit Sen,*** *Assistant Professor, Department of Chemical Engineering, National Institute of Technology Rourkela guiding me to this interesting research work. I thank him for being for constantly motivating me through his valuable counsel as well as his excellent tips to build my research and writing skills.*

I would also like to thank my Doctoral Scrutiny Committee members Prof. Saurav Chatterjee (Associate Professor, Department of Chemistry) Prof. Raghubansh Kumar Singh (Professor, Department of Chemical engineering), Prof. Basudeb Munshi (Associate Professor, Department of Chemical Engineering) and Prof. Abanti Sahoo (Associate Professor, Department of Chemical Engineering) for their helpful suggestions and discussions in developing my thesis.

I wish to convey my sincere gratitude to the Director, NIT- Rourkela for providing me the opportunity to pursue my research in this Institute.

I am also thankful to all lab mates, Preeti Jha, Gaurav Singh, Sivamani, Devipriya Gogoi, Saroj Kumari, Pratik Mishra, Gajendra Kumar and Tatinaidu Kella for their time-to-time help, encouragement and creating an excellence atmosphere both inside and outside the department.

I am obliged to all my friends NVS Praneeth, Suresh Kumar, Selva Kumar Irshad Mattan, Dani Varghese, Asheley Thomas, Balmiki Kumar, Harjeet Nath, Sourav Mukharjee, Bhaskar Das, Gajendra Kumar, Aslam Puthankot, Priya Nakade and Kasturi Ganguly for their friendships and encouragements. I cannot be what I am, without the blessings of my father Uttam Mondal and support of my mother Mrs. Sumita Mondal, my sister Mrs Laboni Mondal to whom I shall give all the credit for my existence and the position I'm in now.

Lastly, I wish to thank my loving grandfather Late Upendra Nath Mondal, whose blessings always give me strength to overcome all obstacles and difficulties in my life.

Ujjal Mondal

Abstract

Hydrogen Sulphide gas (H_2S) is the major source of sulphur as an impurity in gasification process of fossil fuels, biogas plant, syngas production plant, petrochemical and various industrial gases. H_2S gas is highly corrosive, toxic and odorous in nature. It is very necessary to remove H_2S from gas streams as it can damage mechanical and electrical components of any control system, corrode energy generation and heat recovery units. In the present work, our main aim is utilise this toxic unwanted H_2S and synthesise value added fine chemicals such as aromatic amines. In order to achieve our aims two industrially used alkanolamines such as mono ethanolamine (MEA) and n-methyldiethanolamine (MDEA) have been used to absorb H_2S and this H_2S-laden aqueous alkanolamine solution is used as a reducing agent. Mono nitro, dinitro, polynitro, heterocyclic nitro compound have been reduced selectively to their corresponding aromatic amines in the liquid-liquid or liquid-liquid-solid phase transfer catalysis mode of reaction in the presence of phase transfer catalysis. In this current work insoluble PT catalyst have been used such as Amberlite IR400 (Cl) and a number of soluble PT catalyst have been used such as Tetrabutylammonium bromide (TBAB), Tetrabutylphosphonium bromide (TBPB), Tetramethylammonium bromide (TMAB), Tetrabutylammonium iodide (TBAI) and Ethyltriphenylphosphonium bromide (ETPPB), Tetrapropylammonium bromide (TPAB). The main objectives of this work are to maximise conversion of the organic substrate, maximise selectivity of the desired product and to deveolop a suitable mechanism to explain the whole reduction process. Six different system have been studied and in those five system chloronitrobenzene (CNB) reduction have been studied in L-L and L-L-S PTC mode of reaction and 1-nitronapthalene (1-NN), nitroacetophenone (NAP), dinitrotoluenes (DNT) have been studied in the biphasic mode of reaction. In last system total sixteen nitroaromatic compounds have been reduced under an identical set of parameters. For all the system parametric study, mechanistic investigation was performed and kinetic and statistical model have been established. The studied parameters are stirring speed, catalyst concentration, temperature, reactant concentration, sulphide concentration, MDEA loading, elemental sulphur loading. The developed model have been validated with the experimental data and the model predicts the conversion well.

Keywords: Hydrogen sulphide, Zinin reduction, Phase transfer catalysis, selectivity, alkanolamines, mathematical modelling.

Contents

List of Figures

List of Tables

Nomenclature

$[QX]_o$	Concentration of QX in the organic phase (kmol/m^3)
$[QX]_a$	Concentration of QX in the aqueous phase (kmol/m^3)
$[QHS]_a$	Concentration of QHS (also $[Q^+HS^-]_a$) in the aqueous phase (kmol/m^3)
$[QHS]_o$	Concentration of QHS in the aqueous phase (kmol/m^3)
$[QSQ]_o$	Concentration of QSQ in the organic phase (kmol/m^3)
$[QSQ]_a$	Concentration of QSQ in the aqueous phase (kmol/m^3)
$[QS_2Q]_o$	Concentration of QS_2Q in the organic phase (kmol/m^3)
$[QS_2Q]_a$	Concentration of QS_2Q in the aqueous phase (kmol/m^3)
$[QSHO_3]_a$	Concentration of $QSHO_3$ (also $Q^+SHO_3^-$) in the aqueous phase (kmol/m^3)
$[QSHO_3]_o$	Concentration of $QSHO_3$ in the aqueous phase (kmol/m^3)
$[S_2O_2^{2-}]_a$	Concentration of $S_2O_2^{2-}{}_3$ in the aqueous phase (kmol/m^3)
$[S^{2-}]_a^2$	Concentration of $[S^{2-}]^2$ in the aqueous phase (kmol/m^3)
$[ArNO_2]_o$	Concentration of $ArNO_2$ in the organic phase (kmol/m^3)
$[QX]^*$	Concentration of catalyst QX initially fed to the aqueous phase (kmol/m^3)
$[Q^T]$	Concentration of total catalyst Q in the organic phase (kmol/m^3)
$[ArNO_2^*]$	Concentration of total reagent ($ArNO_2$) added in the organic phase (kmol/m^3)
K_{app}	Apparent first order reaction rate constant [m^3/(mol of catalyst .min)]
k_1	Forward reaction rate constant [m^3/(mol of catalyst .min)] aqueous phase
k_1'	Backward reaction rate constant [m^3/(mol of catalyst .min)] aqueous phase
k_2	Reaction rate constant [m^3/(mol of catalyst .min)] organic phase
k_3	Reaction rate constant [m^3/(mol of catalyst .min)] organic phase
k_3	Reaction rate constant [m^3/(mol of catalyst .min)] organic phase

V^o	Volume of organic phase (m^3)
V^a	volume of aqueous phase (m^3)
X	fractional conversion
t	time (min.)

Abbreviation

ATU	Amine treating unit
CNB	Chloronitrobenzenes
m-CNB	m-Chloronitrobenzenes
p-CNB	p-Chloronitrobenzenes
o-CNB	o-Chloronitrobenzenes
m-CA	m-Chloroaniline
MDEA	N-Methyldiethanolamine
MEA	Monoethanolamine
TEA	Triethanolamine
DEA	Diethanolamine
DIPA	Diisopropanolamine
1-NN	1-Nitronapthalene
1-NA	1-Napthylamine
2,4-DNT	2,4-dinitrotoluene
4A2NT	4-amino-4-nitrotoluene
2A4NT	2-amino-4-nitrotoluene
p-NAP	p-Nitroacetophenone
p-AAP	p-Aminoacetophenone
3CA	3-chloroaniline
4CA	4-chloroaniline
2CA	2-chloroaniline
TBAB	Tetrabutylammonium bromide
TBAC	Tetrabutylammonium chloride
TBPB	Tetrabutylphosphonium bromide
TMAB	Tetramethylammonium bromide
CTMAB	Cetyltrimethylammonium bromide
ETPPB	Ethyltriphenylphosphonium bromide

Thesis Overview

This chapter provides an outline of the research work presented in the thesis. This chapter describes the motivation behind the proposed work. Also, it provides an overview of the research approach taken, industrial application and as well as of the results obtained. Finally, it introduces the structure of the thesis.

1.1 Motivation

Hydrogen sulphide (H_2S) is a poisonous, odiferous and corrosive gas. H_2S normally come into the atmosphere as the major impurity via fossil fuel processing plant, biogas plant, syngas production plant and pharmaceutical industries along with some natural sources like a volcanic eruption, sulphur spring, bacterial activity.

It is essential to process H_2S gas before releasing it to the environment with other gaseous waste. The presence of H_2S gas can equally harm mechanical and electrical unit of any plant. There are copious technologies available for the removal of H_2S gas. Chemical scrubbing and absorption in different media are most practiced methods in industry and research labs. In petroleum refineries, H_2S gas is removed from by-product gas stream in Amine treating unit and then regenerated H_2S is treated in Claus unit.

Some approaches have already been undertaken for utilizing H_2S gas in a more productive manner. Production of hydrogen and sulphur by treating H_2S gas in thermal [1], photochemical [2], electrochemical [3–5] or thermochemical processes [6]. When a significant amount of H_2S gas is mixed with CO_2, it is called acid gas. Acid gas can be pyrolyzed to produce Syngas (H_2, CO) which is used in fuel gas engines. All of the investigated processes mentioned above are having some limitations which include, (i) difficult and expensive mode of operation (ii) strict environmental regulations (iii) limited scope of utilization of sulphur, produced as an end product. The main focus of our work is, therefore, to search for an alternative process to utilize H_2S for producing valuable fine chemicals.

In our current work, H_2S has been used for the selective reduction of nitroaromatic compounds to aromatic amines, a type of value-added chemicals. Selective reduction of a nitro group attached to an aromatic ring is tough to achieve. H_2S laden alkanolamine solution has been used as a reducing agent. Various kinds of absorbents have been used for research and commercial purpose, among which some are NaCl, copper sulphate, hollow fibre membrane contractors, activated carbon, iron-based sorbents, FeOOH,

Fe_2O_3, aqueous ammonia and alkanolamine solution. For our current study, we have used alkanolamines like monoethanolamine (MEA) and methyldiethanolamine (MDEA) and the main reasons for choosing alkanolamines over other absorbing agents are a wide range of operating conditions, easily recyclable, not harming the main reaction, solvent loss due vaporization is minimum.

Aromatic amines are useful intermediate for the preparation of photographic chemicals, pesticides, rubber and extensively used in dye, food and pharmaceutical industries. Selective reduction is challenging work, and it was done with many approaches which include Bechamp reduction [7], catalytic hydrogenation [8] and Zinin reduction [9]. The reduction reaction of nitroaromatic compounds by negative divalent sulphur in the form of sulphide, hydrosulphide and polysulphide is called Zinin reduction. The presence of sulphide and hydrosulphide ions made aqueous H_2S-laden aqueous alkanolamine solution a potential reducing agent. The reaction between reducing agent present in the aqueous phase and nitroarenes which remain in the organic phase is very slow. One of the most efficient ways of enhancing reaction rate and product selectivity in a multiphase reaction is to employ Phase Transfer Catalyst (PTC) that intensifies the reaction rate by transporting inorganic nucleophiles (anions) to the organic phase from the aqueous phase and vice versa [10]. PTC is a very well-practiced technique, and the main advantages include reaction milder and safer environment through high reactivity, higher yield as selectivity is more, utilization of reusable raw materials and catalyst makes the whole process cheaper, product separation is easy. Phase transfer catalysis systems can be classified into different types, based on the number and properties of the phases. In the present work liquid- liquid (L-L), and liquid-liquid-solid (L-L-S) PTCs have been employed to achieve the goal.

Very little research is available in the area of Zinin reduction with the utilization of PTC in the literature. Kinetic modeling based on the proposed mechanism and parametric study have also rarely been developed. Parameters which are the most influencing for the reduction reaction has to be optimized for achieving highest output while keeping the whole process economical.

1.2 Work Methodology and Objectives

Among the processes of removing H_2S gas from the different industrial gaseous by-product, Claus process is the mostly practiced approach. Elemental sulphur is the only end product produced during this process. Due to increased number of concern has against this process, such as strict environmental emission rule for H_2S emission,

environmental hazards possessed by the huge amount of unutilised elemental sulphur deposition. The current process has been engineered to employ H_2S gas to yield fine value-added chemicals such as anilines and substituted anilines in a cost-effective and environment-friendly way. The methodology is outlined in Fig. 1.1.

The aim of this research is to establish a process for better utilization of H_2S gas.

To this end, the main objectives of this research are:

1. To develop a process for selective reduction of various aromatic nitro compounds with the use of H_2S gas absorbed in alkanolamines as a reducing agent under L-L and L-L-S mode of reaction.

2. Different types of PTC have to utilize in the current reaction to identify the best catalyst for our system, and recyclability of solid catalyst have to be analyzed.

3. Study the effect of different process parameters (stirring speed, catalyst concentration, reactant concentration, temperature, sulphide concentration, alkanolamine (MEA/MDEA) concentration, elemental sulphur loading) on the conversion of reactant and selectivity of desired product.

4. Establishment of a suitable reaction mechanism of PTC catalyzed reduction reaction for L-L and L-L-S mode of PTC reaction.

5. To identify most influencing operating parameters and to optimize operating parameters after statistical modeling to achieve the highest conversion and selectivity of desired product.

6. To develop a mathematical model of L-L and L-L-S PTC based on the mechanism proposed which can predict the conversion of the reactant.

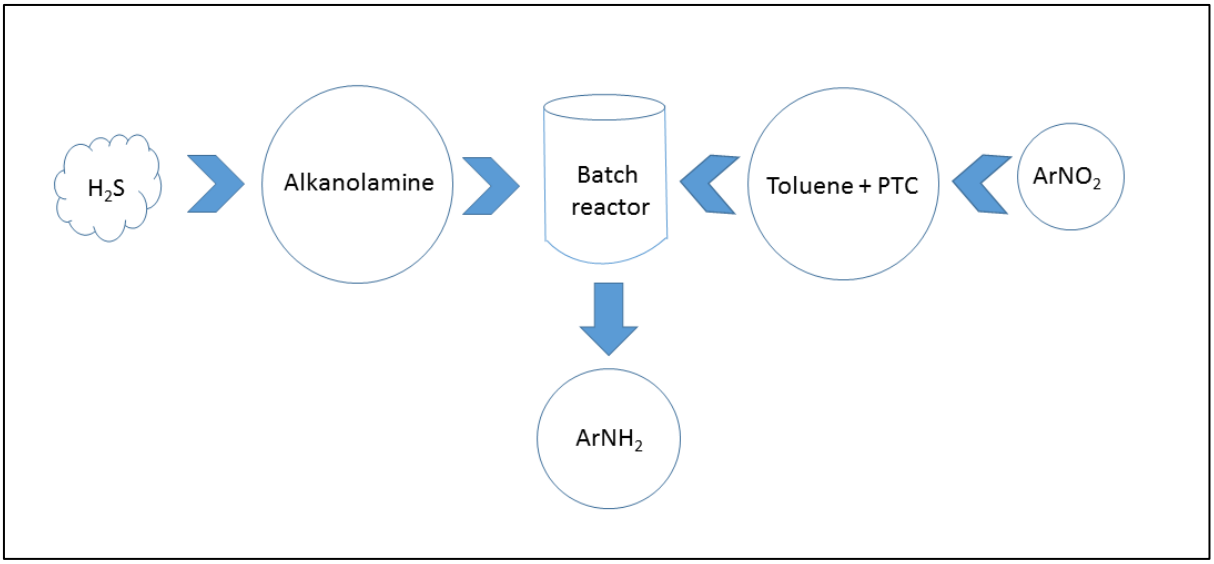

Figure 1.1: Schematic diagram of proposed work

1.3 Main contributions

This research work offers a comprehensive solution to voluminous H_2S production from different industries. It can use as an alternative technique for H_2S treatment other than most popular Claus process. The current approach is an improvement over the presently available reduction techniques of nitroaromatic compounds. Zinin reduction is normally a slow reaction involving disulphide, sulphide and polysulphide ions as a reducing agent. In this research, we have used PTC to accelerate the rate of reaction.

1.4 Industrial application

Selective reduction of nitroaromatic compounds is an industrially important reaction as the amino group can be further derivatized to give commercially important products [11]. The production of Aniline and its derivative is a cornerstone of the modern chemical industry. In 2013 value of global aniline market was £6.25 billion and expected to reach £ 10.17 billion by 2020 [12]. Aniline and its derivatives are found to be very useful in plenty of industries such as pharmaceutical, polymer, and materials (e. g. rubber, polyurethane), herbicides, pesticide, bulk chemicals, photographic chemicals, and sometimes as an inhibitor of the polymerization reaction, as antioxidants and as stabilizing agent for many chemicals [13–17]. Azo and azoxy compounds are prepared through oxidation of aromatic amines which is having ubiquitous usage in dye industry as a raw material for the production of dyes, optical brighteners, and pigments (e.g. indigo) [14,18,19].

Anilines can be used as a corrosion inhibitor in mild steel in the picking process. p-nitrotoluene is the largest produced aniline as 6200 t was produced in the United States in 1983 and it is used for the production of dyes, pharmaceuticals, and antioxidants. But the main share (67%) of Aniline production is utilized to manufacture isocyanates, mainly for 4,4′-methylenebis (phenylisocyanate), to prepare polyurethanes. 20-27% of total aniline production is utilized in rubber industry for the preparation of antioxidants, vulcanization accelerators (2-mercaptobenzothiazoles). Many herbicides, insecticides, fungicides and animal repellent are made from aniline or its derivative. Some important pharmaceuticals which are produced from aromatic amines are sulphonamides and analgesics.

4-aminoacetophenone (4-AAP) is used for the preparation of novel phenyl azochalcone derivatives that are having antitubercular, anti-inflammatory and antioxidant activity.[20] 4-AAP is one of the reactants used for the synthesis of 1,3,4-oxadiazole-based chalcone derivatives as novel bio-active antimicrobial agents against multidrug-resistant bacteria and fungi.[21] It is employed in the synthesis of HIV-1 growth inhibitors and for the synthesis of aryl semicarbazone of 4-AAP for their anti-HIV activity.(Vibha Mishraa, S.N. Pandeyab, E. DeClercqc, Christophe Pannecouquec 1998) Reduction of 2, 4-dinitrotoluene lead to the formation of 2-amino-4-nitrotoluene, 2-nitro-4-aminotoluene and 2, 4-diaminotoluene. These products are industrially used as an intermediate for the production of dyes, artificial pigments [23,24]. Some other examples of usage of aromatic amines are as follows o-anisidine is an important intermediate in pigment and azo dye industry, chloroanilines is mainly used for manufacturing agricultural products, 1-aminoactophenone is used as a precursor for the Victoria blue dyes, 8-Aminoquinoline is used to produce the drug tenoxicam.

1.5 Thesis organization

The structure of the thesis is illustrated in the Figure1.2. In more detail **Chapter 2** provides an introduction in the area of different H_2S capture and utilization methods, a comprehensive study on the different phase transfer catalyst and mechanism of all existed PTC systems and detailed research background on different nitroaromatic compound reduction techniques has been discussed along with a brief discussion about Zinin reduction, which is main operating method been followed in the in this study and a comprehensive discussion of past approached of Zinin reduction have been included. At the end of **Chapter 2,** a brief description about optimization of a chemical reaction by changing one variable at a time (OVAT) method and statistical methods such as response surface methodology have been included. Optimization of a chemical process is all needed to be done before its industrial implementation and practice, which includes

understanding and finding variables responsible for a good outcome (yield, conversion). Furthermore, **Chapter 3** elaborates on the available techniques of absorption of H_2S in different media and utilization of H_2S gas in the industry or at the laboratory scale. A detailed discussion on the different reducing agent used for the reduction of nitroaromatic compounds and the use of different phase transfer catalyst for the reduction of nitroarenes have been included.

To this end **Chapter 4** provides an insight about the chemicals has been utilised during the reactions, preparation process of the stock solution of H_2S laden Alkanolamines (MEA, MDEA) and a detailed experimental process for L-L-S PTC and L-L PTC systems have been shown followed by analysis procedure of collected samples from organic phase in GC and GC-MS, and aqueous phase samples by iodometric titration method are included.

Chapter 5 encompasses the use of solid catalyst Amberlite IR400 (Cl-) for the reduction of Chloronitrobenzene under Liquid-Solid-Liquid (L-S-L) mode of reaction by H_2S-laden N-methyldiethanolamine (MDEA). A detailed parametric study has been done and based on the proposed mechanism a mathematical modeling has been established. Catalyst recyclability has been optimized, and model has been validated against the experimental data.

Chapter 6 deals with the reduction of chloronitrobenzene under Liquid-Liquid (L-L) mode of reaction by H_2S-laden Monoethanolamine by using tetra-n-butyl phosphonium bromide (TBAB) as phase transfer catalyst. A detailed parametric study has been done in order to optimize operating conditions, a verity of PTC and organic solvents have been examined for getting the highest conversion and selectivity. A reaction mechanism has been proposed and based on the reaction mechanism a mathematical modeling has been proposed, and the model has been validated against the experimental data.

Chapter 7 presents a reduction of 1-nitronaptalene by H_2S-laden MDEA under the Liquid-Liquid (L-L) mode of reaction in the presence of TBAB as phase transfer catalyst. A detailed parametric study has been done in order to optimize operating conditions, and a reaction mechanism has been proposed and based on the reaction mechanism a mathematical modeling has been proposed. The model has been validated against the experimental data.

Chapter 8 deals with the improved Zinin reduction of 4-Nitroacetophenone (4-NAP) was studied with refinery generated toxic H_2S dissolved in aqueous N-methyldiethanolamine (MDEA) solution under Liquid-Liquid (L-L) phase transfer catalysis. Response Surface

Methodology (RSM) was employed to model the system and optimize the controlling parameters for maximum 4-NAP conversion.

Chapter 9 incorporates the selective reduction of one of the nitro group present in dinitro toluene compounds by a novel Zinin reagent, H_2S-laden N-methyldiethanolamine (MDEA) solution, has been explored in the presence of Tetra-n-butyl phosphonium bromide (TBPB) as phase transfer catalyst (PTC) under the liquid-liquid (L-L) mode of reaction. A detailed parametric study has been done in order to optimize the reaction condition to achieve the highest conversion and selectivity, and a variety of PT catalysts and solvents have been tried out to find out most suitable catalyst and solvent for the system. A mathematical model has been developed for the complex system, and it was validated against the experimental data.

Chapter 10 consists of selective reduction of a number of aromatic nitro compounds by H_2S-laden N-methyldiethanolamine (MDEA) solution under the liquid-liquid (L-L) mode of reaction in the presence of TBAB as phase transfer catalysis and a reaction mechanism has also been proposed.

Chapter 11 enlisted the conclusions of the present work and the future recommended work which can be carried out for more useful utilizations of H_2S gas.

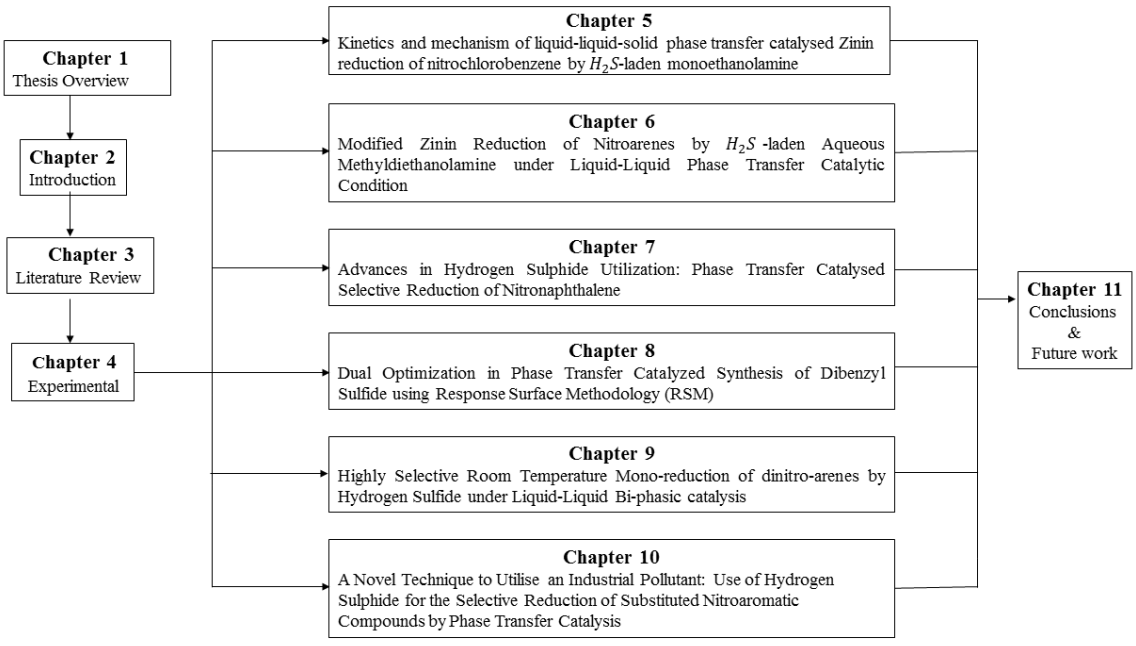

Figure 1.2: Schematic diagram of the Organisation of the thesis

References

1 F. Faraji, *Int. J. Hydrogen Energy*, 1998, **23**, 451–456.

2 S. Cervera-March, L. Borrell, J. Giménez, R. Simarro, *Int. J. Hydrogen Energy*, 1992, **17**, 683–688.

3 H. Huang, Y. Yu and K. H. Chung, *Energy & Fuels*, 2009, **23**, 4420–4425.

4 K. Petrov and S. Srinivasan, *Int. J. Hydrogen Energy*, 1996, **21**, 163–169.

5 S. Srinivasan. and A. J. A. Z. Mao, A. Anani, R. E. White, *J. Electrochem. Soc.*, 1991, **138**, 1299–1303.

6 J. O. N. E. Noringt and E. A. Fletchers, *Energy*, 1982, **7**, 651–666.

7 Y. Zheng, K. Ma, H. Wang, X. Sun, J. Jiang, C. Wang, R. Li and J. Ma, *Catal. Letters*, 2008, **124**, 268–276.

8 P. G. Jessop, T. Ikariya and R. Noyori, *Nature*, 1994, **368**, 231–233.

9 H. K. Porter, *Org. React.*, 2011, **20**, 455–481.

10 C. M. Starks, *Am. Chem. Soc*, 1987, 1–7.

11 M. Kumarraja and K. Pitchumani, *Appl. Catal. A Gen.*, 2004, **265**, 135–139.

12 K. Zhu, M. P. Shaver and S. P. Thomas, *Chem. Sci.*, 2016, **7**, 3031–3035.

13 M. H. Lin, B. Zhao and Y. W. Chen, *Ind. Eng. Chem. Res.*, 2009, **48**, 7037–7043.

14 F. E. Catino SC, *Concise Encyclopaedia of Chemical Technology*, John Wiley & Sons, New York, 1985.

15 S. Sakaue, T. Tsubakino, Y. Nishiyama and Y. Ishii, *J. Org. Chem.*, 1993, **58**, 3633–3638.

16 A. P. A. Shabbir, H. Gheewala, *Water Sci. Technol.*, 1997, **36**, 53–63.

17 N. Boon, L. De Gelder, H. Lievens, S. D. Siciliano, E. M. Top and W. Verstraete, *Environ. Sci. Technol.*, 2002, **36**, 4698–4704.

18 R. S. Downing, P. J. Kunkeler and H. vanBekkum, *Catal. Today*, 1997, **37**, 121–136.

19 H. G. Abdessamad Grirrane, Avelino Corma, *Science*, 2008, **322**, 1661–1664.

20 R. M. Rohini, K. Devi and S. Devi, *Der pharma Chem.*, 2015, **7**, 77–83.

21 D. Joshi and K. S. Parikh, *Med. Chem. Res.*, 2014, **23**, 1855–1864.

22 M. W. Vibha Mishraa, S.N. Pandeyab, , E. DeClercqc, Christophe Pannecouquec, *Pharm. Acta Helv.*, 1998, **73**, 215–218.

23 X.-L. Chen, Jin-Fang; Jia, Tao; Huang, *Yingyong Huaxue*, 2000, **17**, 672–674.

24 A. Z. Manieh, A. A.; Sayed, *Al-Azhar Bull. Sci.*, 1995, **6**, 35–48.

Abstract

This chapter covers a brief introduction to the sources of hydrogen sulphide (H_2S), physical and toxicological properties of H_2S, H_2S emission controlling methods operated in industries, different nitroarenes reduction techniques, different types of phase transfer catalysis techniques and optimization techniques.

2.1 Sources of Hydrogen sulphide

Hydrogen sulphide gas is evolved from a variety of natural sources and one of the major component of natural gas, volcanic gas, crude petroleum oil and sulphur spring [1]. Animal and vegetable proteinaceous mass decomposed by bacteria are one of the natural sources of H_2S gas. Natural source contributes 90-100 million of H_2S into the atmosphere, among that 60-80 million tons is coming from land-based sources and rest 30-40 million is evolved from aquatic sources. Besides natural sources, H_2S emission is three million/ year from different polluting sources [2]. The anthropogenic source of H_2S includes petrochemical refineries, natural gas plants, coke oven plants, kraft paper mills, viscose rayon manufacturer, sulphur production, iron smelters, food processing plant, and tanneries. Processing of high sulphur content crude oil produces H_2S gas during purification and production of commercial grade fuels and other intermediate stocks. Petroleum refineries are mostly recovering these sulphur and sulphur containing compounds. Processing of 20,000 barrels high sulphur content generates 50 tons of H_2S.

H_2S is being produced as a by-product from many chemical operations where sulphur compounds come into contact with organic compounds. Some of the responsible reactions for H_2S production are the production of CS_2 from methane and sulphur, production rayon and cellophane, etc. Other H_2S polluting sources includes pesticide, fatty-acid, grease production plant, animal processing plant, tanneries, dairy and wool scrubbing plant.

H_2S originated from natural, and anthropogenic sources form the major component of "Global sulphur cycle" [3,4]. In the presence of hydroxyl radical and O_2, H_2S is oxidized to SO_2 in the atmosphere. The sulphur cycle is consisting of four action phases.

1. Atmospheric phase: the natural and anthropogenic sources of H_2S includes volcanos and burning sulphur.
2. Bacterial phase: a wide variety of bacteria species are taking part in oxidation or reduction of H_2S, animal, and plant proteinaceous biomass, sulphur, and sulphate.
3. Plant phase: sulphur is incorporated into plant protein via reduction of sulphate and further reduction of plant protein by bacteria to produce H_2S.

4. Animal phase: animal protein is produced from plant protein and then reduced by bacteria to generated H_2S.

2.2 Physical and toxicological property/ Characteristic of H_2S

Hydrogen sulphide gas is a colourless gas with a strong foul odor like "rotten eggs". H_2S is heavier than air, flammable, poisonous, explosive (when mixed with air) and corrosive. H_2S is highly toxic, and high exposure can lead to fatal consequences. The direct contact of H_2S with mucous membrane results in irritation and inflammation of eyes and respiratory tract. The nervous system can also get affected by H_2S, and the respiratory centre became paralyzed and usually, leads to death. If it is present more than 3ppm, H_2S can cause corrosion in pipes and instruments in industries [5–7]. If the presence of H_2S gas exceeds more than 1ppm, then it is enough to poison catalyst used in fuel processing unit (FPUs) and electrolytes of fuel cells (FCs) [8,9].

Table 2.1 Effect of different levels H_2S exposure on human physiology

H_2S concentration in ppm	Physiological effects
0.003-0.02	Odour threshold
3-10	Sensible unpleasant odor
20-30	Strong "rotten eggs" like odor
30	Strong odor but not intolerable
50	Conjunctival and respiratory tract irritation
50-100	respiratory tract irritation and
100-200	Loss of smell (olfactory fatigue)
150-200	Olfactory nerve paralysis
250-500	Long-time exposure leads to pulmonary edema, threat to life
700	Rapid faint which may lead to death if not rescued
700-1000	Rapid unconsciousness death in minutes caused by respiratory paralysis, immediate collapse, neural paralysis, cardiac arrhythmias, death

H_2S is capable of damaging electrical and mechanical components used in energy generation, control system, heat recovery unit of the petroleum industry, power plants. Some chemical and physical properties of H_2S is listed in listed in **Table 2.2**.

Table 2.2. Chemical and physical properties of H_2S

Formula	H_2S
Molecular mass	34.0809 g/mol
Boiling	-60˚C
Density	1.36 kg/m^3
Melting point	-82 °C
Vapour pressure	15,600 mm Hg at 25°C
Water solubility	3980 mg/L at 20°C

2.3 H_2S emission controlling methods

A variety of methods has been in existence for the controlling and removal of H_2S gas. H_2S gas removal process is mainly divided into three main processes like physical, chemical and biological processes. Some methods are practical in the industry in a combination of a different process. The main factor for choosing a process of H_2S removal is based on the gas composition, physical and chemical properties, the end use of the gas and the total amount of the gas requires to be removed.

2.3.1 Amine absorption unit

An aqueous solution of various amines is used in industry to absorb acid gases. As alkanolamines contains at least one hydroxyl group and one amine group, the aqueous alkanolamine solution can selectively absorb the dissolved acidic H_2S gas. Then the stream can be heated to regenerated concentrated H_2S stream which is valorised in a Claus unit or the other process for better utilization. Amines are oxidized in the presence of oxygen, so this process can be used for the anaerobic gas stream, which is the main limiting factor behind the use of amine absorption unit. Some of the commonly used alkanolamines are diethanolamine (DEA), monoethanolamine (MEA) and methyldiethanolamine (MDEA). Natural-gas purification plant and petrochemical plants are major industries to use alkanolamine solution. A copious amount of literature is available on the solubility study of acid gas mixture (CO_2 and H_2S) [10,11], pure H_2S [10–12] in diethanolamine (DEA) and monoethanolamine (MEA) solution. H_2S is selectively removed from the gasses produced in refinery and coal gasification unit by an aqueous solution of methyldiethanolamine (MDEA) [13–16].

Different types of alkanolamines are most popular for acid gas absorption as alkanolamines have less vapour pressure and it can, therefore, be used in a broad range of operating conditions (regarding temperature, pressure, concentration), recyclable and cause minimum loss via vaporization [17]. Problems associated with this process are a loss of some portion of amine solution during the process, complicated flow schemes, foam formation, disposal issue of foul regenerated air.

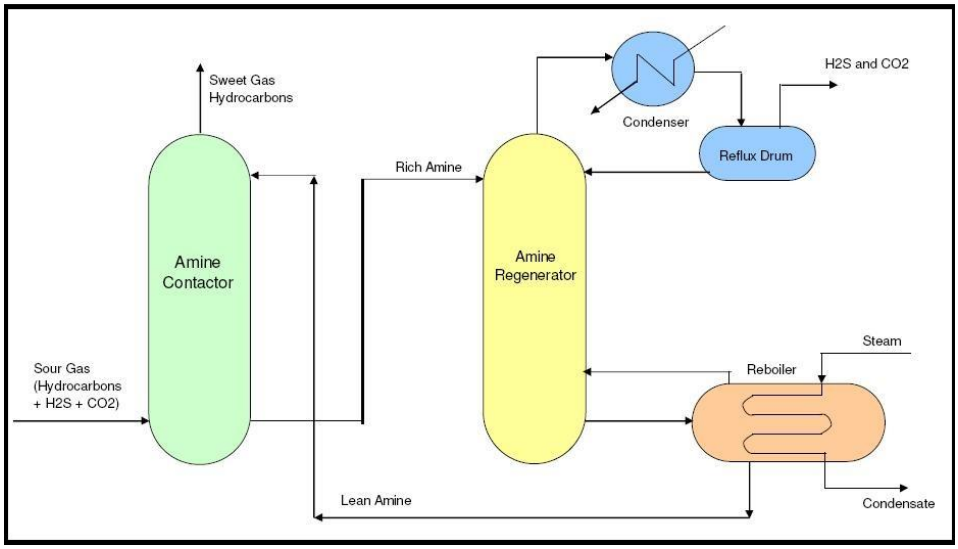

Figure 2.1: Amine Treating Unit

2.3.2 Claus process

Claus process is very popular in petrochemical and natural gas industry and during the process, H_2S is oxidized to produce elemental sulphur as an end product [18]. Reactions shown below is occurring in a different unit of Claus process, and efficiency of this process depends on the number of catalytic reactors used. 95% efficiency found when two catalytic reactors used, and four reactor gives 98% efficiency.

$$H_2S + {}^{3}/_{2}\, O_2 \rightarrow SO_2 + H_2O$$

(2.1)

$$2H_2S + SO_2 \rightarrow 3S^0 + H_2O$$

(2.2)

$$H_2S + {}^{1}/_{2}\, O_2 \rightarrow S^0 + H_2O$$

(2.3)

The O_2 to H_2S ratio is to be strictly maintained otherwise chances of excess SO_2 emission and poor H_2S removal efficiency, become higher. The Claus process is advantageous for large, consistent and higher concentration (15%) of H_2S gas. The shortcoming of Claus process is many: (i) insufficient utilization of valuable hydrogen source; (ii) requirement of highly precise air rate control; (iii) presence of trace sulphur compounds in the spent air. Hydrogen sulphide removal efficiency of Claus process is 95-97%, so emission from this process are now becoming a source of H_2S pollution. Claus process releases tail gas at 100-315˚C, and it contains H_2S as high as 0.8-1.5% with other impurities such as COS, CO_2, CS_2 at various concentrations. Due to all these reasons, Claus process is required to reduce H_2S emission from the tail gas [19].

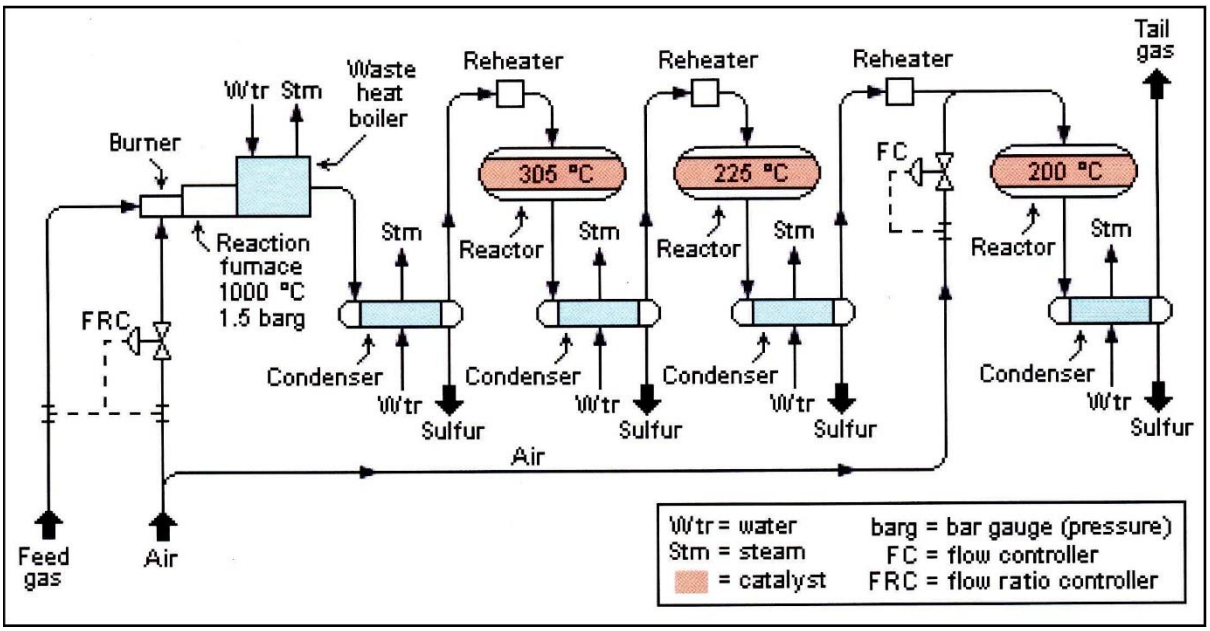

Figure 2.2. Sulphur recovery utilizing Claus Unit

2.3.3 Chemical oxidation

Waste water treatment plants often use chemical oxidants to remove odorous and toxic H_2S gas. With this process, other odorous compound which is generated in the anaerobic process can also be eliminated. The combination of sodium hydroxide (NaOH) and sodium hypochlorite (NaOCl) are popular chemical oxidants as they are cheap, easily available and higher oxidation capability. The oxidation steps are as follows:

$$H_2S + 2NaOH \leftrightarrow Na_2S + 2H_2S$$
(2.4)

$$Na_2S + 4NaOCl \rightarrow Na_2SO_4 + 4NaCl \quad (2.5$$

In this process, the requirement of oxidants is proportional to the amount of H_2S to be treated, and so continuous supply of oxidants is necessary. In this process, the only low concentration of H_2S gas stream can be treated in an economical manner. The gas phase is required to be converted into liquid phase as a reaction are occurring in the aqueous phase in the scrubber. Counter current packed columns are preferred type of scrubbing process, but other types of scrubbing processes are also used such as mist scrubber, spray scrubber, and ventures. For avoiding salt precipitations, the scrubbing solution is periodically or frequently removed and fresh solution is being added.

Caustic scrubbers

Removal of H_2S using sodium hydroxide (NaOH) solution is an established technique and it is known as caustic scrubbing process. This process is like other chemical oxidation process, but the main difference is that it is an equilibrium limited process. So with the addition of caustic, H_2S is removed, but when pH of the solution become acidic, then H_2S is re-produced. NaOH reacts with H_2S dissolved in the aqueous solution to form sodium bisulphide (NaHS) and sodium sulphide (Na_2S).

$$H_2S_{aq} + NaOH_{aq} \rightarrow NaHS_{aq} + H_2O \quad (2.6)$$

$$NaHS_{aq} + NaOH_{aq} \rightarrow NaS_{aq} + H_2O \quad (2.7)$$

Since spent caustic is very difficult to regenerate, the caustic scrubbing process is often applied to situations where a small amount of H_2S is required to be removed. The presence of CO_2 in the effluent stream complicates the use of this process because CO_2 readily scrubbed into the caustic and produce Na_2CO_3.

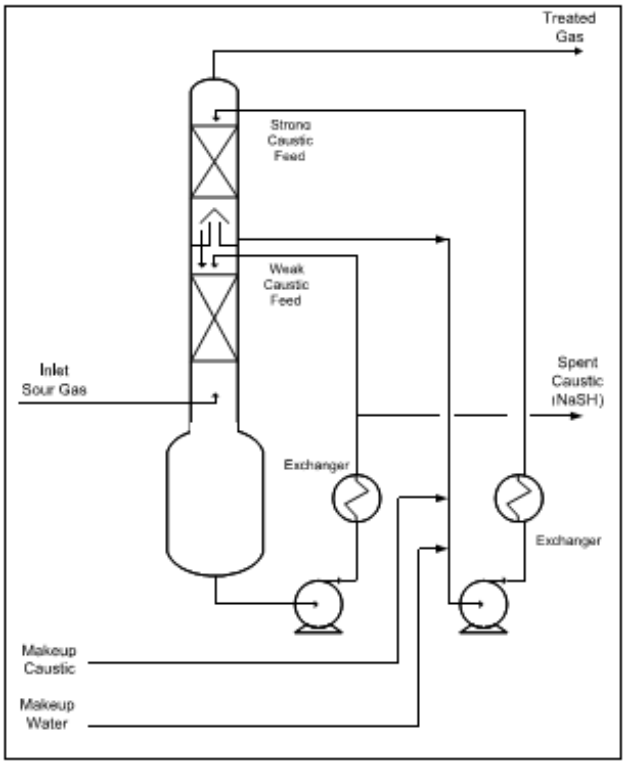

Figure 2.3: Caustic Scrubber Unit

2.3.4 Adsorption

The role of adsorbent material is to attract polluting molecules from the effluent gas stream on its surface, and by this way, gaseous effluent can be treated. The adsorption process is functional until the adsorbent surface is fully occupied by the adsorbed molecules and then adsorbent is needed to either replaced or regenerated (undergo desorption) if possible. The regeneration process is very expensive and also time-consuming. Carbon Materials are often used to remove H_2S gas by physical adsorption, and activated carbons are mostly employed for this purpose. It is found in several studies that the factors other than surface area and pore volume can contribute to the H_2S adsorption process. Activated carbon can be impregnated with sodium hydroxide (NaOH) and potassium hydroxide (KOH), which catalyzed the process of H_2S removal. Surface treatment of activated carbon with nitric acid and ammonia significantly enhances H_2S removal efficiency [19–21].

2.3.5 Hydrogen sulphide Scavengers

Sulphide scavengers refer to such chemicals (usually additives) that can react with single or multiple sulphide species and convert them to a nonreactive inert form. This scavenging process is more effective when the reaction is irreversible and complete reaction takes place between sulphides and scavengers. Most scavengers remove the sulphide species either through surface adsorption manner or by ionic precipitation. If the surface adsorption technique is adopted, then the mud must be in constant flow for the required interaction (collision) between the additive and the sulphides for the complete reaction. For this purpose, turbulent flow regarded as best flow scheme as the molecules are randomly colliding with each other which leads to higher reaction rate. Detailed properties of scavengers have to be understood which follows ionic precipitation process to assure that the properties like pH, salinity are favourable to the usage of the scrubbers [22].

Few examples of scavengers are caustic and sodium nitrate solution, amines, iron-based adsorbents, zinc-containing chemicals. Depending on the chemicals used the end product will be different. These systems are supplied under trademarks by different companies. LO-CAT® (US Filter/Merichem) process is an example commercially available of H_2S scavenging system which utilizing chelated iron. This process removes 200 kg of S/day, and this process is ideal for land filling gas [23].

2.3.6 Liquid phase oxidation systems

Liquid phase oxidation systems convert hydrogen sulphide into elemental sulphur through redox reaction by electron transfer from sources such as vanadium or iron. The first liquid-phase oxidation system is known as the Stretford process. During this process, H_2S is initially absorbed into an aqueous alkali solution and then it is reacted with vanadium. During this process, vanadium is reduced, and H_2S is oxidized to produce elemental sulphur. But this process is very slow, and it requires packed columns or venturies. As the vanadium is toxic, this unit must be designed in such a way that both the solution and 'sulphur cake' can be cleaned easily. Due to these disadvantages now iron-based reagents are utilized instead of Stradford process. By air oxidation, ferrous iron (Fe^{2+}) can be regenerated and the reaction is faster than Stretford process. LO-CAT by US Filter/Merichem, is a H_2S removal system that utilises chelated iron solution. The basic reaction are shown below in equation 2.8 and 2.9 below.

$$2Fe^{3+} + H_2S \rightarrow 2Fe^{2+} + S + 2H^+ \quad (2.8)$$

$$2Fe^{2+} + {}^1/_2\, O_2 + H_2O \rightarrow 2Fe^{3+} + 2OH^- \quad (2.9)$$

2.3.7 Physical solvents

Physical solvents are also used in practice to remove acid gases, such as H_2S. During the process, H_2S is dissolved in a liquid and later H_2S is recovered by reducing the pressure of the system. For higher H_2S removal efficiency, selection of liquid is important. Water is widely available and free. Water is used in physical solvent- utilizing the process for H_2S removal. As water can also absorb CO_2, this process is not economical for selective removal H_2S.

There are a number of other solvents are available like propylene carbonate, methanol, and ethers of polyethylene glycol. The main criteria for selecting solvents are high absorption capacity, very low reactivity with process instruments and gas constituents and low viscosity. Loss of product is usually happening during this process. Losses as high as 10% is observed during this process.

2.3.8 Membrane process

This process is popular in biogas industry which utilizes a membrane to purify gas from impurities. Permeation through the membrane is controlled by the partial pressure on either side of the membrane. This membrane system is not mainly for selective removal of H_2S, but it is used to upgrade biogas to natural gas standards. Membrane process is mainly two types (i) high pressure with gas phase on both sides of the membrane, (ii) low pressure with a liquid adsorbent on one side. Biogas produced in anaerobic digesters is upgraded by passing through cellulose acetate membrane.

2.3.9 Biological methods

Biogas can be treated with microorganisms to remove H_2S. Microorganisms can use CO_2 present in biogas as a carbon source (extra nutrient input can be neglected) and can degrade H_2S to produce elemental sulphur. Elemental sulphur build up in this process can be removed easily without affecting the biomass and biomass clogging problem can be avoided and thus this process can be operated under a wide range of process parameters (O_2/H_2S ratio, temperature, moisture). Among many species of bacteria especially Chemothrophic bacteria, particularly from the Thiobacillus genus shows the highest efficiency in removing H_2S. Chemotrophic thiobacteria can be operated in both aerobic and anaerobic conditions. This bacteria can utilize CO_2 a carbon source and acquired chemical energy from the reduction reaction of H_2S present in the medium. In both reaction, H_2S first dissociates shown in Eq. 2.10.

$$H_2S \leftrightarrow H^+ + HS^- \quad (2.10)$$

Elemental sulphur is produced under limited oxygen condition as shown in Eq. 2.11

$$HS^- + 0.5O_2 \rightarrow S^0 + OH^- \quad (2.11)$$

Under excess O_2 conditions, sulphate is produced, which leads to acidification as shown in Eq. 2.12

$$HS^- + 2O_2 \rightarrow SO_4^{2-} + H^+ \quad (2.13)$$

Thiobacillus ferroxidans is a bacteria which can remove H_2S by oxidizing Fe_2SO_4 to $Fe_2(SO_4^{2-})_3$. The resulting solution can be utilised to dissolve H_2S and H_2S can be further oxidised to produce elemental sulphur. Biofilter and bioscrubber can be utilised to remove H_2S by biological removal processes. Thiopaq® is a commercially available H_2S removal system which utilises chemotrophic bacteria in alkaline environment to oxidise sulphide to elemental sulphur. H2SPLUS SYSTEM® is another commercially available system which operates on chemical and biological methods to remove H_2S. In this system a filter consisting an iron sponge inoculated with bacteria is used and this system is having capacity of treating 225 kg H_2S/day.

2.4 Phase transfer catalyst

Chemists always find difficulty to bring together two reagents which are mutually insoluble in sufficient amount to attain required reaction rate. The useful solution for this problem is to use a solvent which can dissolve both reagents. Use of a solvent is not always an ultimate solution, and industrially it is not always viable to use solvents. The technique of phase transfer catalysis is an alternative process that can be used efficiently instead of solvents [24–26].

In 1965 Mieczyslaw Makosza published a series of papers on the two-phase reaction which he called “extractive alkylation” [27]. At the same time, Charles M. Starks filled patents on “Catalysis of heterogeneous reactions”. Arne Brandstrom has worked with reactions of quaternary ammonium salts in nonpolar media, and he mentioned non-catalytic part as “ion pair extraction” [28]. Although Starks was the first person termed this process as “phase transfer catalysis” and thereafter this is widely accepted [24,25,28].

Currently, phase transfer catalyst has been utilized in total 600 industrial processes in a variety of field such as dyestuff, perfumes, pharmaceuticals, flavors, polymers, etc. and the total cost of phase transfer industry is as high as US $12 [29,30]. Phase transfer catalyst are very popular due to these advantages, (i) reaction medium and condition is milder and safer, (ii) it can easily enhance

reaction rate of slow reaction, (iii) selectivity and yield for products are higher, (iv) use of phase transfer catalysis can reduce or eliminate requirement of solvent, (v) total cost of operation is comparatively low, (vi) product separation is easier. Most of the phase transfer catalysis reactions are conducted in the bi-phasic (Liquid-Liquid) mode of reaction. During the reaction phase, transfer catalysts remain dissolved in both of the phases depending on the lipophilicity or hydrophilicity of the catalyst, and it transfers inorganic reagents from the aqueous phase by forming ion pair to the organic phase, which is the main reaction phase. Researchers have examined different types of phase transfer catalysts such as ammonium and phosphonium salts, cryptands, crown ethers, polyethylene glycol, etc. Among these catalysts, the popularity of ammonium and phosphonium slats are very high as they are cheap, moderately stable at basic conditions and can withstand temperature up to 100˚ C but the recovery of these salts are difficult. Crown ethers cryptands are expensive, but the stability at basic conditions and temperature is as high as 150-200˚ C. Both possess high toxic effects and environments hazards. Polyethylene glycol is very cheap, very stable, can be used in more quantities without poisoning the reaction and it is very easy to recover.

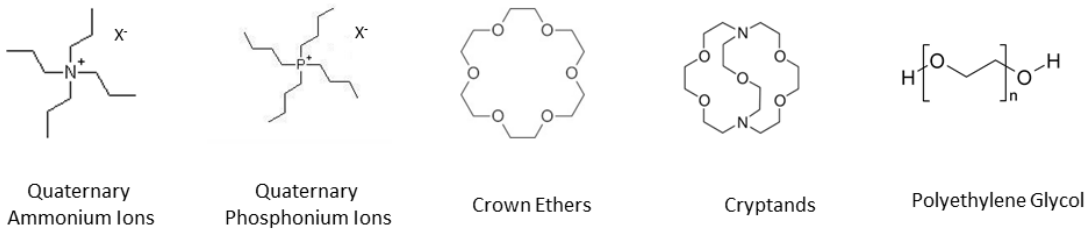

Figure 2.4: Different types of PT catalyst used

2.4.1 Classification of PTC reactions

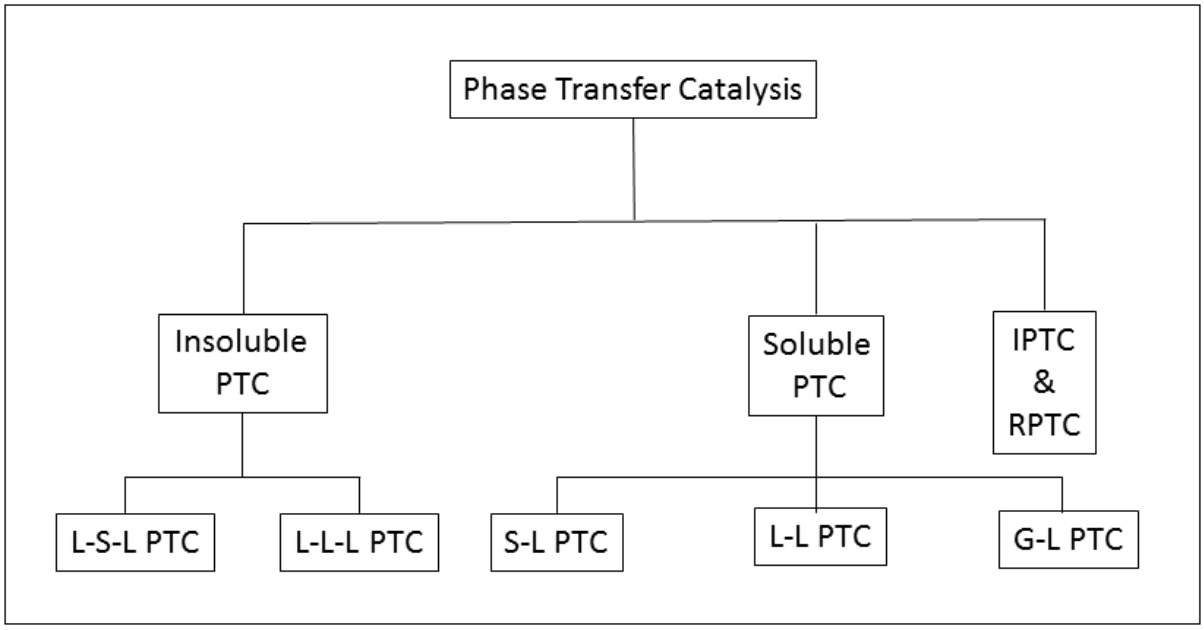

Figure 2.5: Classifications of PTC

2.4.2 Mechanism of Liquid-Liquid PTC (L-L PTC)

The most used PTC used in L-L PTC are quaternary salt, crown ether, cryptands, and polyethylene glycol. For last few years, the L-L PTC mechanism is explained by two mechanisms, Stark's extraction mechanism, and Makosza interfacial mechanism.

2.4.2.1 Starks extraction mechanism

This is a widely accepted mechanism which describes catalyst transfer between the reaction phases. This catalytic process involved following steps (i) intermediate catalyst-reactant formed when reactants react with catalyst in its normal phase, (ii) then the intermediate transfers to the main reaction phase, (iii) after that intermediate catalyst-reactant reacts with unreacted reagent present in reaction phase and forms product and catalyst, (iv) then catalyst transfers to its normal phase. Starks reaction mechanism can be categorized into three types based on catalysis path and it discussed below.

Normal Liquid-Liquid PTC (N L-L PTC)

This is the most applied PTC process reported in the literature, and this process involved in many reactions such as alkylation, etherification, esterification and this process involves simple displacement reaction where the nucleophilic reactant is transferred to the organic phase with pairing soluble catalyst. This reaction mechanism (2.6) is first presented by Starks for the reaction of 1-chloro-octane and aqueous sodium cyanide [25].

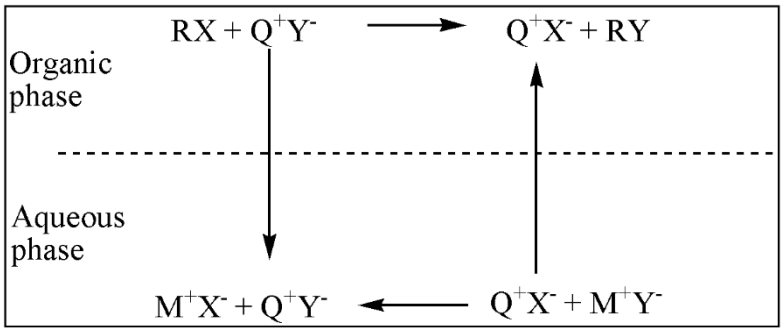

Figure 2.6: Normal Liquid-Liquid PTC mechanism by Stark's

Inverse liquid phase PTC (I-L-L PTC)

During this process, organic reagent reacts with the catalyst in the organic phase and forms an ionic intermediate, which is partially soluble in the organic phase. Then the intermediate is transferred into the aqueous phase and reacts with an inorganic reagent to form product and this process is called inverse PTC.

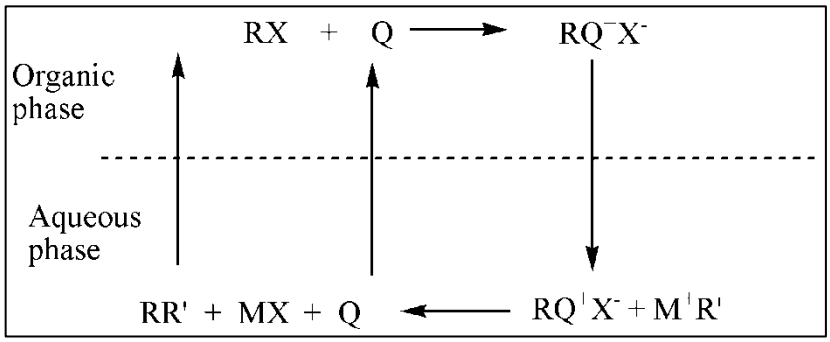

Figure 2.7: Inverse liquid phase PTC mechanism

Reverse Liquid-Liquid PTC (R-L-L PTC): the mechanism of the third type of reaction is shown below in Figure 2.8.

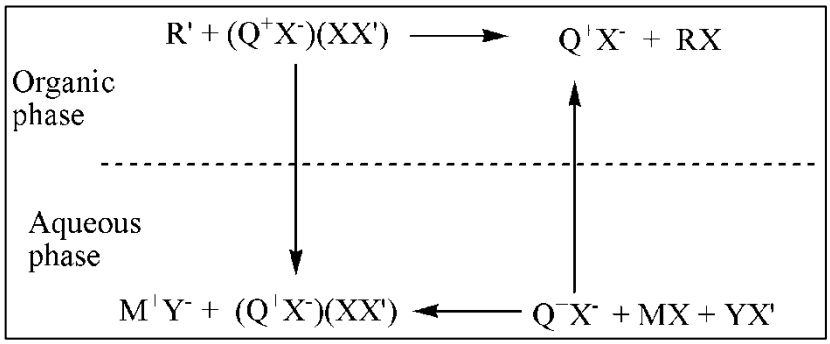

Figure 2.8: Reverse Liquid-Liquid PTC mechanism

2.5.2.2 Makosza interfacial mechanism

This is the mechanism of transporting of catalyst between two phases and is proposed by Makosza and Bialecka [31,32]. The reaction steps involved are (i) catalyst form the reaction phase and ionic reactants from its normal phase transfer to the interfacial region, (ii) then at the interfacial region ionic reactant reacts with the catalyst to form intermediate catalyst-reactant. (iii) after that, the intermediate complex is transferred to the reaction phase and reacts with unreacted reagent to form product and catalyst. This reaction mechanism is shown Figure 2.9.

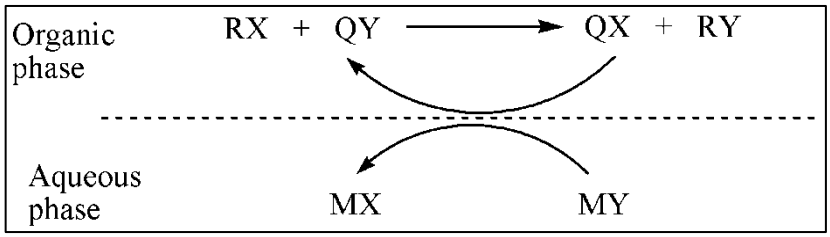

Figure 2.9: Makosza interfacial mechanism

2.4.3. Solid-Liquid PTC (S-L PTC)

Solid-liquid PTC is used to conduct the reaction between organic reactant dissolved in the organic phase and solid inorganic salt in the absence of water. A variety of catalyst is used for this reaction like tertiary amine, quaternary salts, cryptands, crown ethers. For

the normal bi-phasic system, the nucleophile present in the aqueous phase is insoluble or slightly soluble in the organic phase. In the absence of water, the inorganic salt should produce anion nucleophile, such that unwanted side reaction can be avoided. Other than this SL PTC can promote the weak nucleophiles and it enhances the reactivity by minimizing hydrolysis effect.

The advantages of this process include (i) easy separation of products from reactants, (ii) easy selection of organic solvents, (iii) easy recovery of catalyst, (iv) elimination of a side reaction, (v) high potential for commercial application.

2.4.4 Gas-Liquid PTC (G-L PTC)

In this process, the organic reagent present in gaseous form passes over the solid inorganic reactant which is coated with PTC in a semi-liquid form. It is advantageous over L-L PTC as a continuous flow of organic gaseous reactant over the solid surface of inorganic reactant, which gives higher reaction rate. Recovery of the catalyst is easy as it is directly loaded on inorganic phase and easy to avoid unwanted side reaction due to the absence of hydrolysis. For GL PTC operation, PTC should be thermally stable as high energy is required to carry out the process in gaseous form.

2.4.5 Liquid-Solid-Liquid PTC (L-S-L PTC)

L-L PTC mode of reaction allows reaction between two immiscible phases. However, this bi-phasic system always encounters the problem of purifying the product from the mixture and recycling of catalyst. Regen was the first person to use solid catalyst, which was a polymer-supported catalyst, in which a tertiary amine was immobilized on the polymer support. For the industrial use, this catalyst is most suitable to use as it can be separated very easily by filtration or centrifugation. Plug flow reactor and continuous stirred tank reactor can be used effectively to carry out this L-S-L PTC system. Thus this process is having a high potential for industrial application.

The steps involve the reaction of triphase catalysis are as follows (i) reactants from both the phases will transfer to the surface of the catalyst pellet, (ii) diffusion of reactants through the pores of the catalyst to reach out the active site of catalyst (the sites where quaternary salts are impregnated on polymer support), (iii) intrinsic reaction between the reagent present at the active site of the catalyst with the unreacted reagent present in the bulk phase. Diffusion of both the phases within the solid support is important, and a number of the mechanism is proposed for a variety of reactions. The reaction mechanism is shown in the Figure 2.10.

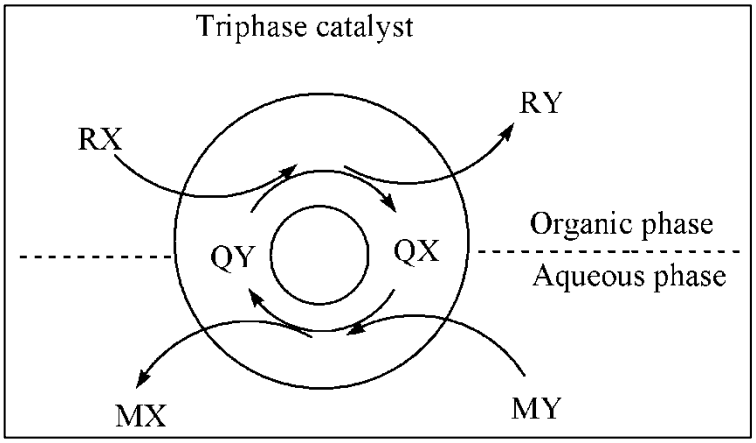

Figure 2.10: Liquid-solid-Liquid PTC mechanism

2.4.6 Liquid-Liquid-Liquid PTC (L-L-L PTC)

In 1987, Wang and Weng studied the L-L PTC reaction system utilizing Tetra-n-butylammonium bromide as PTC, and they found that reaction rate increases with the addition of PTC beyond the critical concentration of the catalyst. During the reaction, a viscous liquid phase was formed which constitute mostly by PTC and a little amount of organic and inorganic reagent. This viscous third layer is insoluble in both the phases and this third phase is enhancing the reaction rate in several folds in comparison with the L-L-PTC mode of reaction. From the industrial point of view, the formation of the third phase is not only good for enhancement of reaction rate; it is increasing the recycling possibility of catalyst and separation of product from the reaction mixture is easy. The operating condition which is influencing the formation third liquid phase are (i) type, and quantity of aqueous reactant, (ii) quantity and type of PTC, (iii) organic reagent concentration in the organic phase, (iv) addition of another inorganic salt, (v) polarity of organic is lower, (vi) temperature of reaction medium. The reaction mechanism is shown below.

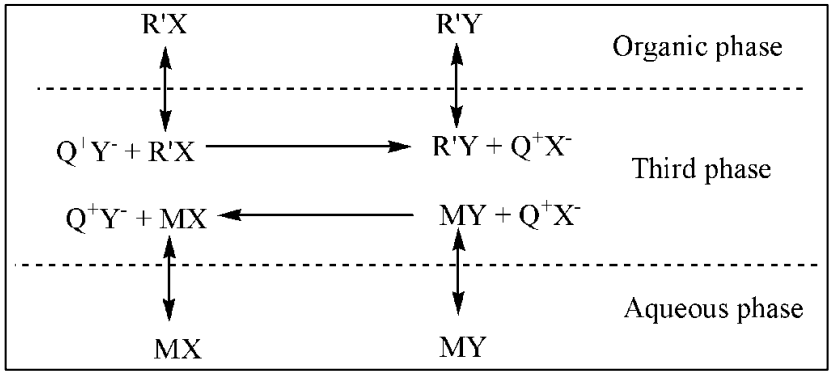

Figure 2.11: Liquid-Liquid-Liquid PTC mechanism

2.5 Optimization methods:

Optimization term refers to enhance the performance of a process, a reaction or a product in order to achieve highest output and performance from it. In chemical engineering, optimization of a reaction system involves discovering conditions at which the process produces the best possible response. Optimization of a chemical process is all needed to be done before its industrial implementation and practice, which includes understanding and finding variables responsible for a good outcome (yield, conversion). Traditionally optimization of a chemical process is done by either changing one variable at a time (OVAT) approach or by multivariate optimization technique.

2.5.1. One variable at a time approach (OVAT)

The most common approach to optimizing a chemical reaction is by changing one variable at a time (OVAT) [33]. This optimization technique involves changing one parameter with fixing others at a constant level. The interaction between the operational variables of the process can be understood from this univariate approach. The major disadvantage associate with this approach is that it does not take account the interactive effect among the variables studied and consequences this study does not take account the complete effects of the variables on the response. Furthermore, OVAT approach is laborious, non-feasible and costly [34].

2.5.2 Design of experiment (DoE)

In order to overcome the problem associated with OVAT approach, a multivariate statistical approach has been considered. During recent times, the inefficient OVAT approach is replaced by effective chemometric methods, such as response surface

methodology (RSM), based on statistical approach as the design of experiments (DoE) [35]. RSM is used for modeling engineering problems, and its main approach of solving is a combination of statistical and mathematical methods [36]. This statistical method can be applied to study the relationship between independent variables and response for multivariable systems [37,38]. Moreover, maximum response is achieved through determination of the optimal factorial combination of variables. RSM is a combination of mathematical and statistical techniques based on the fit of a polynomial equation to the experimental data, which must trace the behavior of the experimental data set in order to make statistical previsions.

An experimental design should be adopted which will specify the number of experiments to be carried out in the experimental region, before applying RSM methodology. Some experimental matrixes are available for this purpose. When the experimental data does not represent curvature, experimental designs for first order design can be adopted. In order to approximate a response function based upon experimental data set is unable to describe by linear functions, for those quadratic response surface should be used, such as Box-Behnken, three-level factorial, Doehlert and central composite design.

References

1 D. F. Adams, S. O. Farwell, M. R. Pack and W. L. Bamesberger, *J. Air Pollut. Control Assoc.*, 1979, **29**, 380–383.

2 P. Urone, *Air Pollution, Vol 1*, Academic Press, New York, 3rd edn., 1976, p. 23.

3 J. P. Friend, in *Chemistry of the Lower Atmosphere*, ed. S. I. Rasool, Springer US, Boston, MA, 1973, pp. 177–201.

4 P. J. Maroulis, A. R. Bandy, *Science.*, 1977, **196**, 647–648.

5 S. K. Maity, N. C. Pradhan and A. V. Patwardhan, *Appl. Catal. B Environ.*, 2008, **77**, 418–426.

6 K. Polychronopoulou, J. L. G. Fierro and A. M. Efstathiou, *Appl. Catal. B Environ.*, 2005, **57**, 125–137.

7 S. Rezaei, A. Tavana, J. A. Sawada, L. Wu, A. S. M. Junaid and S. M. Kuznicki, *Ind. Eng. Chem. Res.*, 2012, **51**, 12430–12434.

8 P. Dhage, A. Samokhvalov, D. Repala, E. C. Duin and B. J. Tatarchuk, *Phys. Chem. Chem. Phys.*, 2011, **13**, 2179–2187.

9 L. Li and D. L. King, *Catal. Today*, 2006, **116**, 537–541.

10 J. D. Lawson and A. W. Garst, *J. Chem. Eng. Data*, 1976, **21**, 20–30.

11 E. E. Isaacs, D. Otto and E. Alan, *Engineering*, 1980, 118–120.

12 J. I. I. Lee, F. D. Otto and A. E. Mather, *J. Chem. Eng. Data*, 1976, **21**, 207–208.

13 A. B. G. Astarita, D. W. Savage, *Gas Treating with Chemical Solvents*, John Wiley & Sons, 1983.

14 S. K. Maity, N. C. Pradhan and A. V. Patwardhan, *Appl. Catal. A Gen.*, 2006, 301, 251–258.

15 B. P. Mandal, A. K. Biswas and S. S. Bandyopadhyay, *Sep. Purif. Technol.*, 2004, **35**, 191–202.

16 H. Xu, C. Zhang and Z. Zheng, *Simulation*, 2002, 2953–2956.

17 A. Kohl and R. Nielsen, *Gas purification*, Gulf Publishing Company, Houston,TX, 1997.

18 M. Plummer, *US Pat.*,US5334363 A, 1994.

19 W. Feng, S. Kwon, E. Borguet and R. Vidic, *Environ. Sci. Technol.*, 2005, **39**, 9744–9749.

20 T. J. Bandosz, *Catal. Today*, 1999, **37**, 483–491.

21 T. J. Bandosz, *J. Colloid Interface Sci.*, 2002, **246**, 1–20.

22 G. Nagl, *Chem. Eng.*, 1997, **104**, 125–131.

23 N. Abatzoglou and S. Boivin, *Biofuels, Bioprod. Biorefining*, 2009, **3**, 42–71.

24 C. M. Starks and R. M. Owens, *J. Am. Chem. Soc.*, 1973, **95**, 3613–3617.

25 C. M. Starks, *J. Am. Chem. Soc.*, 1971, **93**, 195.

26 S. S. Dehmlow, E. V.; Dehmlow, *Phase Transfer Catalysis*, Verlag Chemie Weinheim, 2nd edn., 1983.

27 M. Makosza, *Tetrahedron Lett.*, 1966, **38**, 4621–4624.

28 W. Weber and G. W. Gokel, *Phase transfer catalysis in organic synthesis*, Springer Science & Business Media, 2012, vol. 4.

29 G. D. Yadav, *Top. Catal.*, 2004, **29**, 145–161.

30 M. E. H. Charles M. Starks, Charles L. Liotta, *Phase-Transfer Catalysts*, Chapman and Hall Publications, New York, 1994.

31 E. Makosza, M.; Bialecka, *Tetrahedron Lett.*, 1977, **2**, 183–186.

32 M. Makosza, *Pure Appl. Chem.*, 1975, **43**, 439–462.

33 M. A. Schwindt, T. Lejon and L. S. Hegedus, *Organometallics*, 1990, **9**, 2814–2819.

34 O. W. Gooding, *Curr. Opin. Chem. Biol.*, 2004, **8**, 297–304.

35 M. S. Tanyildizi, D. Özer and M. Elibol, *Process Biochem.*, 2005, **40**, 2291–2296.

36 P. Elavarasan, K. Kondamudi and S. Upadhyayula, *Chem. Eng. J.*, 2009, **155**, 355–360.

37 D.C. Montgomery, *Design and Analysis of Experiments*, John Wiley and Sons, New York, fifth., 2001.

38 A.I. Khuri, J.A. Cornell, *Response Surfaces: Design and Analyses*, Dekker, New York, 1987.

Abstract

This chapter contains all the literature that have been utilised in order to carry out this investigation.

3.1 H_2S removal form gaseous stream

H_2S is an acidic gas and its separation from natural gas, and gaseous by-product stream is one of the major challenges faced by the industry. H_2S is a hazardous gas when is oxidised to SO_2; it can cause acid rain. The removal process of H_2S gas is very critical as H_2S is very malodorous and toxic. Among the available techniques H_2S removal process falls into the following categories, (i) absorption in a solution which is either aqueous and caustic solution, (ii) absorption on solid materials such as activated carbon or impregnated activated carbon, (iii) sulphur oxidizing microorganism can convert sulphur compounds to elemental sulphur[1]. During the investigation of different techniques of removal of H_2S, different types of solid adsorbents have been found like metal oxides, activated carbon and zeolites. Activated carbon is used to absorb H_2S from a gas stream as a virgin or impregnated activated carbon. Impregnated activated carbon with alkaline or oxide solids yield enhanced the efficiency of removing H_2S in comparison with virgin activated carbon [2,3]. The most common disadvantages of activated carbon are its mechanical stability which causes tortuosity and presence of a large number of micropores lead to the formation of fines [4]. A variety of metal oxides (Cu, Zn, Co, Ce, Fe, Mo, Sn, Mn, W and Ni) have been used to remove H_2S. Among these metals, desulfurization abilities of tungsten and molybdenum are highest but their application in limited in a narrow temperature range due to carbide formation [5]. Zn-based sorbents have also found widespread use in H_2S removal, and it can be used at the higher reaction temperature [6–8].

At the temperature range of 400-500 °C, zinc oxide can be used to capture pure H_2S gas but at a reduced temperature of 200-300 °C, ZnO losses the efficiency of sulfidation. Doping ZnO with Cu helps to accelerate the sulfidation reaction [9]. During adsorption of H_2S by Copper oxide, it reduces to metallic copper by the H_2 and CO present in the gas, and it reduces the efficiency. Similar studies also show that metal oxides are not proper adsorbent to remove H_2S gas due to their thermodynamic equilibrium. Zeolites are very effective in removal of H_2S, and it is certainly known as molecular sieves [10]. Natural zeolites have been investigated for the adsorption of H_2S at different temperatures between 100 °C to 600 °C [11]. Graphene is achieving popularity as an adsorbent for H_2S, and it can selectively adsorb H_2S gas. Thus it can be used as H_2S sensor [12]. H_2S adsorbing capacity of graphene can be enhanced by doping it with metal/ non-metal or relevant functional groups [13,14]. A novel process has been developed for removing H_2S gas using cupric chloride solution. It removes H_2S by reaction with it and produces CuS deposition, and it is followed by the oxidation in the presence of an excessive cupric ion in another reactor [15]. Triamine-grafted pore-expanded mesoporous silica (TRI-PE-MCM-41) can adsorb H_2S and CO_2 selectively. However the adsorption of both gases is diffusion limited but the optimum temperature of CO_2 adsorption was 348 K, and for H_2S it is 298K [16]. Hollow fibre membrane contractors equipped with expanded polytetrafluoroethylene (ePTFE) hollow fibres was used to remove H_2S gas at high pressure. In this module, a mixture of distilled water, sodium hydroxide and amine solutions has been used as a chemical solvent [17,18].

Room temperature ionic liquids (ILs) are metal salts that remain in liquid form over a wide array of temperature. In the past few years, a number of research have been done on the solubility of H_2S in ILs and solubility data of the absorption of H_2S in different ionic liquids such as 1-butyl-3-methylimidazolium-based ILs with different anions, bis(trifluoromethyl) sulfonylimide based ILs with different cations [13], [bmin] [PF_6], [bmim] [BF_4], [bmim] [Tf_2N] have been documented. Caprolactam tetrabutyl ammonium bromide has also been tried out [19–22]. H_2S is selectively removed from the gaseous mixture by methanol when the various contactor is employed such as a tray, spray or packed tower in which the gas mixture is released upwardly in counter current to the liquid flow [23]. Stretford process uses an aqueous solution of sodium carbonate, sodium bicarbonate and anthraquinone disulfonic acid to dissolve oxygen in the aqueous solution in the order to oxidise the H_2S to sulphur. But the reaction is slow and for enhancing the reaction rate, alkali vanadates are added. Vanadats are toxic, and the main disadvantages of this process are a high amount of sulphur cake formation and release of discharge solution [24]. Alkaline hypochlorite, hydrogen peroxide, sodium hydroxide has been traditionally used as an economical absorbent. Sodium hydroxide solution is very

effective, but it is non-generable absorbent for H_2S. Thus the use of caustic soda is limited for absorption these impurities [25].

Ammonium hydroxide has been popularly used to remove and recover H_2S gas from different gas streams. A continuous process of H_2S removal has been proposed where gas streams are contacted with a solution of ammonium hydroxide to produce ammonium sulphide. Then the ammonium sulphide is fed to the heating zone and with the supply of oxygen, it got oxidised to elemental sulphur [26]. Ammonium sulphide recovered from the contacting zone can also convert to ammonium polysulphide in an electrolytic cell at ambient pressure and temperature. Then it is oxidised in the heating zone to produce elemental sulphur [27]. Rumpf et al. (1999) have studied the solubility of ammonia and H_2S in a simultaneous manner at a temperature range of 313 K to 393 K at a total pressure of 0.7 MPa.

Among the green sulphur bacteria, the phototropic bacteria are one of the species such as *Cholorobium limicola* which is capable of oxidising H_2S to elemental sulphur under anaerobic condition. The bacteria requires CO_2 and inorganic nutrients for growth [27,28]. The most common bioreactor which has been used for H_2S removal involving phototropic bacteria are gas-fed batch reactor, continuous flow reactor, photo tube reactor. Chemotrops are species of bacteria such as *Thiobacillus, Thermothrix, Beggiato* has been studied for the oxidation of sulphide compounds (hydrogen sulphide, thiosulphate)[28]. The gas-fed batch reactor, scrubbers, biofilters, biotrickling filters are the reactors that use chemotropic bacteria [29].

Alkanolamine based solvents are one of the most commonly used solvents for the removal of acid gases. H_2S gas will react with an alkanolamine solution via a reversible, exothermic reaction in a gas/liquid contactor. The absorption step is followed by the regeneration of acid gas. The most commonly used industrially important alkanolamines are monoethanolamine (MEA), diethanolamine (DEA), di-isopropanol amine (DIPA), N-methydiethnolamine (MDEA) [30]. Alkanolamine based separation process are more popular as it is having more advantageous over ammonia-based processes due to its unique property like less vapour pressure that allows flexible process operation (regarding concentration, temperature, pressure), minimum vapourisation loss, easily recyclable [31]. Study on equilibrium solubility and mathematical model of pure H_2S [32–34], a mixture of H_2S and CO_2 in diethanolamine (DEA) and monoethanolamine (MEA) solution have been established based on the experimental solubility data. An aqueous solution of methyldiethanolamine (MDEA) can absorb H_2S gas selectively from natural gas, refinery exhaust gases and produce from the coal gasification unit [35–38]. MDEA is advantageous over other alkanolamines as it possesses some qualities like minimum corrosion effect,

reduced solvent loss due to less vapour pressure, chemically stable and economically beneficial. H_2S selectivity can further be enhanced with the use of a non-aqueous solvent such as ethylene glycol, N-methyl pyrrolidone, etc.[38,39] As our main aim is to utilise harmful H_2S gas from the gas stream containing both CO_2 and H_2S gases, so selective absorption of H_2S is one of the main criteria for choosing MDEA among other alkanolamines.

3.2 Nitroarenes reduction

Nitroaromatic compounds with nitrogen oxidation number ≥-2 can be reduced to aromatic amines. Reduction of nitroaromatic compounds is an industrially important reaction because aromatic amines can be used as a starting material for a number of products.

3.2.1 Catalytic reduction

In this process of reduction of aromatic nitro compounds, hydrogen is being taken up from the solvent, sometimes from water or the acid present. The most important reductants are iron, tin and Zinc, although phosphorus, sulphur dioxide, sulphide and sulphites also used as reducing agent. Bechamp reduction is a process of reducing nitro compounds with a stoichiometric amount of Fe metal (but also Zn, Al, Sn) or a metal sulphide such as Na_2S in the presence of acid. During this process, reducing agent may result in the formation of useless by-products, which are very difficult to dispose of in the environmentally safe way [40].

3.2.1.1 Reduction with iron

Iron is the most important reducing agent which can easily reduce almost every nitroaromatic compounds with water and acid [41]. Side products are often produced when molecules are attached with other easily reducible substitutes (nitroso, sulfoxide, hydrazine and other nitro group) or can be saponified. Mobay (United States) and Bayer (Germany) both have used this process and produced iron oxide with the generation of anilines as a by-product [42].

3.2.1.2 Reduction with other metal

A number of other metals (Zinc, Tin and Aluminium) and their salts are used to reduce aromatic nitro compounds in neutral, acidic or alkaline medium [43]. This process operates in a mild operating conditions and during the reaction, other functional groups (-OH, -

COOH, -OR, halogen or -CN) attached to the aromatic ring is not getting affected by this process. This process is practised mostly in laboratory scale [44].

3.2.1.3 Reduction with sulphide, hydrogen sulphide and sodium dioxide

A stoichiometric amount of sulphide can selectively reduce multi-nitro aromatic compounds to nitro aromatic amines. The reduction reaction of aromatic nitro compounds by negative divalent sulphur in the form of hydrosulphide, sulphide, disulphide and polysulphide is called Zinin reduction [45]. There are several kinds of literature available for the reduction of aromatic nitro compounds with sodium sulphide and ammonium sulphide. Ammonium hydrogen sulphide is also used as reducing agent, and it can be used in an excess amount in the presence of ammonia [42,46]. The reduction of aromatic nitro, nitroso, or azo compounds with sulfite or hydrogensulfite to the corresponding aromatic amines is known as the Piria reaction (PIRIA, 1851). Nitro and nitroso group can be reduced quantitatively by sodium dithionite.

3.2.1.4 Electrochemical reduction

This is a special technique in chemical reduction. During this process, an inorganic compound is used to reduce an oxidised chemical compound at the cathode and can react again. The cathode can be made up of Cu, Pb, Sn, Ni and 15-20% of the hydrochloric acid is used as the electrolyte at cathode side separated by a membrane from the anode. On the anode side, 30% of the sulphuric acid is used. This process has existed for several decades but commercially it is not established. Nowadays some products are produced electrochemically like p-aminobenzoic acid, p-aminophenol [47,48].

3.2.2 Catalytic hydrogenation

3.2.2.1 Hydrazine as a reducing agent

Hydrazine is also used as a source of hydrogen for the reduction of aromatic nitro compounds in the presence of a catalyst. The decomposition mechanism of hydrazine on the metal catalyst is different at various pH level - at the higher pH level, the amount of hydrogen liberated is also higher. Without the presence of catalyst also hydrogenation can be done, but the hydrogenation is done in the presence of a catalyst such as Pd/carbon, $Pd/CaCO_3$, and Raney nickel [49,50]. Hydrazine hydrate can be used as a source of hydrogen in the presence of heterogeneous catalyst Faujasite Zeolites [51], activated Zn-Cu, Zn-C, iron oxide and hydroxide [52], Metallic nanoparticles Rh_3Ni_1 [53], Ni/ Co [54].

3.2.2.2 Hydrogen as a reducing agent

Poly nitro aromatic compound is reduced to their corresponding primary aromatic mono or polyamines by the catalytic hydrogenation reaction, either in the liquid or vapour phase, in the presence or absence of a solvent. This is an exothermic reaction. If this excess heat is not dissipated properly, then explosion can happen. In order to reduce these hazards the partial pressure of hydrogen, concentration of the nitro compound, the activity of the catalyst and temperature are controlled [40].

3.2.2.3 Vapour phase hydrogenation

Utilisation of this process is limited to the boiling point and the thermal stability of the nitro compound [55,56]. Copper-silica catalyst is used for the production of aniline in the United States [40].

3.2.2.5 Liquid phase hydrogenation

Most of the reduction reaction nitro aromatic compounds have been done in the liquid phase. During this process temperature and pressure can be changed independently. The nature of this reaction is exothermic, and thus a number safety precautions have to be taken, especially for hydrogenation reaction of the aromatic poly-nitro compound in the liquid phase without solvent [57–59].

3.3 Preparation of aromatic amines with Zinin reducing agent

3.3.1 Sodium sulphide/disulphide as reducing agent:

Hojo is the first person to study the reduction of a nitro aromatic compound such as nitrobenzene by aqueous sodium monosulphide and disulphide under a different mode of reaction (Solid-Liquid, Liquid-Liquid)[60]. He found that the reaction rate is proportional to the square root of the sodium disulphide concentration. Bhave and Sharma studied the reduction of p-nitroaniline, m-choronitrobenzene, m-dinitrobenzene by sodium mono sulphide and sodium disulphide under biphasic reaction condition. The reaction was found to be first order with respect to the nitro compounds and sulphide [61]. In 1992 Pradhan and Sharma carried out the reduction of chloronitrobenzene with sodium sulphide in the presence or absence of PTC. Without catalyst usage in the S-L mode of reaction with solid sodium sulphide as reducing agent, the o-chloroaniline and p-chloroanile were the only product formed from their respective nitro compound and the other experiment with utilising catalyst results 100% nitro aromatic compound conversion to dinitrodiphenyl sulphide. Meta isomer of chloronitrobenzene is the only compound which gave 100% chloroaniline in the presence or absence of PT catalyst[62]. But in the L-L

mode of reaction, all isomers have produced chloroanilines in the presence and absence of a catalyst. Reduction of p-nitrochlorobenzene has been carried out in the presence of sodium sulphide in S-L, L-L, L-L-S mode of reaction with utilising PT catalyst [63].

Nitrotoluenes in the form of *o,p,m* isomers have been reduced to the corresponding toluidines with sodium sulphide as reducing agent in the S-L and L-L mode of reaction and tetrabutyl phosphonium bromide (TBAB) as phase transfer catalyst. When L-L mode of the reaction was applied, then all isomers have shown kinetically controlled reaction but in the S-L mode ortho and para isomers have shown kinetically controlled reaction and the meta isomer was found to be mass transfer controlled [64].

A detailed kinetic study of the reduction reaction of p-nitroanisole to the corresponding amine by sodium sulphide under the L-L mode of reaction in investigated by Yadav. The rate of the reaction was found to be proportional to the catalyst, organic reactant and sodium sulphide concentration [63].

In 2007, Yadav and Lande used sodium sulphide as a reducing agent for the reduction of 4-nitro-oxylene in the Liquid-Liquid-Liquid mode of reaction. The reduction reaction results in 100% selectivity of the product 3,4-dimethyl aniline.

3.3.2 Ammonium sulphide as a reducing agent:

Besides sodium sulphide, ammonium sulphide can also be used as a reducing agent. Different types of ammonium sulphide have been used to reduce nitro aromatic compounds such as (i) aqueous ammonium sulphide [65], (ii) alcoholic ammonium sulphide [66], (iii) ammonium sulphide prepared by mixing ammonium chloride and sodium sulphide dissolved in ammonium hydroxide or alcohol[67].

Nitrochlorobenzene has been reduced with the ammonium sulphide in the Liquid-Liquid mode of reaction in the presence of PTC, and 100% selectivity was observed for the only product chloroaniline, and the rate of the reaction was found to be proportional to the cube of sulphide concentration [68].

The reduction of nitro toluene (o-, m- and p-) using ammonium sulphide has been conducted under the biphasic or triphasic mode of reaction with utilising TBAB/ anion exchange resin (AER) as phase transfer catalyst. Both modes of the reaction have shown toluidine as the only product, and the rate of the reaction was proportional to the square of the sulphide concentration [36,69].

3.3.3 H_2S rich Alkanolamines as reducing agent

Aqueous alkanolamines are used as an absorbent of H_2S gas in amine treating units (ATU). Thus the H_2S rich alkanolamines can be acquired from the ATU units and subsequently used a reducing agent for Zinin reduction. In 2006 Maity et al. have investigated the use of H_2S-rich ethanolamine as a reducing agent for the reduction of nitrotoluenes under the Liquid-Liquid mode of reaction in the presence of phase transfer catalyst (TBAB). It was found that the rate of the reaction was proportional to the square of the concentration of sulphide and cube of the concentration of nitrotoluenes [70].

The role of H_2S-rich diethanolamine as a reducing agent has also been examined by Maity for the reduction of o-anisidine (ONA) in an organic solvent under the biphasic mode of reaction. The rate of the reaction of ONA was found to be proportional to the 1.63 power of the sulphide concentration, to the cube concentration of ONA [71].

3.4 Phase transfer catalysis

Phase transfer catalysis process involves a number of sequential steps and good knowledge of the parameters which influence every step, is very much desirable for full application of the technique. There is two important feature that a PTC must possess such as it should have the ability to transfer one reagent from its normal phase to the other phase where the second reactant is present and as soon as the first reagent reached to the second phase, it must be in highly active form.

For a successful anion transfer reaction the main criterions are:

(i) A cationic catalyst must have large organic structure so it can be subsequently partitioned in the organic phase.

(ii) The cation-anon complex bonding must be “loose” enough to allow high anon reactivity.

In 1971, mechanism of phase transfer catalysis was first developed by Starks and later on the name was given as “phase transfer catalysis”. Afterwards, Napis and Starks patented their research on heterogeneous catalysis using quaternary salt [72]. The commonly used PT catalyst are onium salts (ammonium and phosphonium salts), aza-macrobicyclic ethers (cryptands), macrocyclic polyethers (crown ethers) and open chain polyethers (polyethylene glycols and their dimethyl ethers) [73].

The group, VA elements (nitrogen, phosphorus, arsenic etc.) of the periodic table of elements, are very stable and forms strong bases which are highly ionised in the aqueous phase, forms a stable cation containing pentavalent element covalently bonded to hydrocarbon substituents. These quaternary salts are more effective than sodium and

potassium salts. Ammonium and phosphonium quaternary salts are most popular in the industry. Different ammonium quaternary salts have been utilised extensively such as tetrahexylammonium bromide (THAB), tetrabutylammonium bromide (TBAB), tetraethylammonium bromide (TEAB), benzyltetrabutylammonium bromide (BTEAB) for the reaction between n-bromobutane and sodium sulphide in a biphasic reaction condition. The result shows THAB gave highest reaction rate and the reason may be the higher carbon number in the alkyl group of the ammonium slats [74]. Phase transfer catalysed the reaction of dibromo-o-xylene and 1-butanol have been investigated in the presence of a number of quaternary cations such as tetrabutylammonium iodide (TBAI), tetrabutylammonium bromide (TBAB), tetrabutylammonium hydrogensulfate (TBAHS). After comparing, the obtained results the reactivity order of the anions attached to the quaternary cation is $I^- > Br^- > HSO^-$ [75]. Similar results were obtained by Yadav et al. when he compared same group of catalyst while synthesizing p-chlorophenyl acetonitrile under liquid-liquid phase transfer catalysis reaction [76]. Reactivity of ammonium salts such as TBAB, TBAHS and phosphonium salts such as ethyl triphenylphosphonuium bromide (ETPB), tetrabutylphosphonium bromide (TBPB) has been compared in the synthesis of 3-methyl-4′-nitro-diphenyl ether by reacting sodium salt of m-cresol and p-chloronitrobenzene under biphasic mode of reaction. The order of activity was as follows TBAB> TBPB> TBAHS> ETPB [77]. Liquid-Liquid phase transfer catalysed synthesis of 2,4-dichlorophenoxyacetic acid by using 2,4-dichlorophenol and chloroacetic acid has been investigated in the presence of different quaternary cations which are as follows tetrabutylammonium bromide (TBAB), tetramethylammonium chloride (TMACl) and tetraethylammonium bromide (TEAB). Results obtained reveals that TBAB is the least performing catalyst and TEAB gave best results [78].

Ming-Ling Wang has been investigated L-L PT catalysed the reaction of dibromo-*o*-xylene and 1-butanol [79], n-bromobutane and sodium sulphide [80] by using TBAB as PT catalyst. He carried out reaction between bisphenol A and allyl bromide in the presence of a variety of conventional phase transfer catalyst such as benzyltriethylammonium chloride (BTEAC), diallyldimethylammonium chloride (DADMAC), poly(ethylene glycol) 400, tetrabutylammonium iodide (TBAI), tetrabutylammonium hydroxide (TBAOH) and tetraheptylammonum chloride (THAC)[81].

O-alkylation reaction of *p-tert*-butylphenol with benzyl chloride have been carried out under microwave irradiated liquid-liquid phase catalysis (MILL-PTC) with using TBAB as phase transfer catalyst. The reaction was greatly accelerated by the use of microwave irradiation [82]. TBAB have been utilised as an efficient PTC for a variety of reactions which includes oxidation [83,84], alkylation [85], aromatic ether preparation[86], *O*-alkylation [87],

selective etherification [88]. Yadav et al have investigated phase transfer catalysed the reduction of nitroarenes by sodium sulphide under liquid-liquid (L-L) PTC mode of reaction such as *p*-nitrochlorobenzene [89], p-nitroanisole [63] and reaction under liquid-liquid-liquid PTC system by utilising TBAB as phase transfer catalysis [90,91]. Tetrabutylammonium hydrogen sulfate (TBAHS) is used as an effective PTC for the reduction of nitroaromatic compounds by sodium dithionite in solid phase synthesis [92].

NC Pradhan has done a reduction of nitrochlorobenzene and nitrotoluene by sodium sulphide in the presence of TBAB as phase transfer catalysis in biphasic reaction conditions [64,93]. L-L mode of reaction system has been investigated for the reduction of nitrochlorobenzene [68], nitrotoluene [36,70], nitroanisole [71] by TBAB as phase transfer catalysis by Maity et al.

Soluble PTCs are very difficult to recover and not reusable. Thus the biphasic liquid-liquid PTC process is cost expensive and also minimizes the purity of the product and possess environmental hazards when it gets disposed of into water bodies [94]. Liquid-Solid-liquid phase transfer catalysis is having lots of advantages over liquid-liquid phase transfer catalysis [95]. Catalyst recovery and then reuse made tri-liquid phase transfer catalysis more advantageous with little spare in conversion. Impregnating catalysts on solid micro porous or macro porous supports solve this recovery problem, and it is called Triphase catalyst [96]. Triphase catalysts are not commercially popular because they are less catalytically active than soluble catalyst and production cost of Triphase catalyst is also high [97]. The comparison of different polymer supported PTC for industrial synthesis of bisphenol –A from phenol and acetone has been documented [98]. The mechanism and kinetics of the selective synthesis of benzaldehyde from benzyl chloride using polymer supported chromium salt as a PTC have been studied [99]. Researchers have studied catalytic activity of different Ion-Exchange resigns as a phase transfer catalyst, such as esterification [100], aldol condensation [101] and reduction of p-nitrotoluene [69].

References

1 S. Pipatmanomai, S. Kaewluan and T. Vitidsant, *Appl. Energy*, 2009, **86**, 669–674.

2 T. J. B. Andrey Bagreev, *Carbon N. Y.*, 2001, 2303–2311.

3 L. Wang and R. T. Yang, *Front. Chem. Sci. Eng.*, 2014, **8**, 8–19.

4 J. M. Nhut, R. Vieira, L. Pesant, J. P. Tessonnier, N. Keller, G. Ehret, C. Pham-Huu and M. J. Ledoux, *Catal. Today*, 2002, **76**, 11–32.

5 W. F. Elseviers and H. Verelst, *Fuel*, 1999, **78**, 601–612.

6 S. H. Kang, J. W. Bae, H. T. Kim, K. W. Jin, S. Y. Jeong, K. V. R. Chary, Y. S. Yoon and M. J. Kim, *Energy and Fuels*, 2007, **21**, 3537–3540.

7 D. Jiang, L. Su, L. Ma, N. Yao, X. Xu, H. Tang and X. Li, *Appl. Surf. Sci.*, 2010, **256**, 3216–3223.

8 J. W. Bae, S. H. Kang, G. Murali Dhar and K. W. Jun, *Int. J. Hydrogen Energy*, 2009, **34**, 8733–8740.

9 S. Cheah, D. L. Carpenter and K. A. Magrini-Bair, *Energy and Fuels*, 2009, **23**, 5291–5307.

10 M. Ozekmekci, G. Salkic and M. F. Fellah, *Fuel Process. Technol.*, 2015, **139**, 49–60.

11 S. Yaşyerli, I. Ar, G. Doğu and T. Doğu, *Chem. Eng. Process.*, 2002, **41**, 785–792.

12 O. Faye, A. Raj, V. Mittal and A. C. Beye, *Comput. Mater. Sci.*, 2016, **117**, 110–119.

13 Y. Chen, X. Yang, Y. Liu, J. Zhao, Q. Cai and X. Wang, *J. Mol. Graph. Model.*, 2013, **39**, 126–132.

14 E. Ashori, F. Nazari and F. Illas, *Int. J. Hydrogen Energy*, 2014, **39**, 6610–6619.

15 J. Zhang and Z. TONG, *Chinese J. Chem. Eng.*, 2006, **14**, 810–813.

16 Y. Belmabkhout, G. De Weireld and A. Sayari, *Langmuir*, 2009, **25**, 13275–13278.

17 S. A. M. Marzouk, M. H. Al-Marzouqi, N. Abdullatif and Z. M. Ismail, *J. Memb. Sci.*, 2010, **360**, 436–441.

18 R. Faiz, K. Li and M. Al-Marzouqi, *Chem. Eng. Process. Process Intensif.*, 2014, **83**, 33–42.

19 A. H. Jalili, M. Rahmati-Rostami, C. Ghotbi, M. Hosseini-Jenab and A. N. Ahmadi, *J. Chem. \& Eng. Data*, 2009, **54**, 1844–1849.

20 F. P. Bernardo and P. M. Saraiva, *Am. Inst. Chem. Eng. J.*, 2014, **61**, 1–15.

21 B. Guo, E. Duan, Y. Zhong, L. Gao, X. Zhang and D. Zhao, *Energy & Fuels*, 2011, **25**, 159–161.

22 E. M. Broderick, A. Bhattacharyya and B. J. Mezza, *US Pat.*, US20150093313 A1 2015.

23 J. W. Tierney, *US Pat.*, US2813126 A, 1957.

24 F. Kohl, A. Riesenfeld, in *Gas Purification*, Gulf publishing, Houston, Houston, TX, 4th edn., 1985.

25 E. Üresin, H. İ. Saraç, A. Sarıoğlan, Ş. Ay and F. Akgün, *Process Saf. Environ. Prot.*, 2015, **94**, 196–202.

26 D. Chang and M. C. McGaugh, *US Pat.*, US 4765873 A, 1988.

27 D. Chang and M. C. Mcgaugh, *US Pat.*, US4765969 A, 1987.

28 H. Larsen, *J. Bacteriol.*, 1952, **64**, 187–196.

29 M. Syed, G. Soreanu, P. Falletta and M. Beland, *Can. Biosyst. Eng.*, 2006, **48**, 2.1-2.14.

30 A. H. Zare and S. Mirzaei, *World Acad. Sci. Eng. Technol.*, 2009, **37**, 194–203.

31 A. Kohl and R. Nielsen, *Gas purification*, Gulf Publishing Company, Houston,TX, 1997.

32 J. D. Lawson and A. W. Garst, *J. Chem. Eng. Data*, 1976, **21**, 20–30.

33 E. E. Isaacs, D. Otto and E. Alan, *Engineering*, 1980, 118–120.

34 J. I. I. Lee, F. D. Otto and A. E. Mather, *J. Chem. Eng. Data*, 1976, **21**, 207–208.

35 A. B. G. Astarita, D. W. Savage, *Gas Treating with Chemical Solvents*, John Wiley & Sons, 1983.

36 S. K. Maity, N. C. Pradhan and A. V. Patwardhan, *Appl. Catal. A Gen.*, 2006, 301, 251–258.

37 B. P. Mandal, A. K. Biswas and S. S. Bandyopadhyay, *Sep. Purif. Technol.*, 2004, **35**, 191–202.

38 H. Xu, C. Zhang and Z. Zheng, *Simulation*, 2002, 2953–2956.

39 H. Xu, C. Zhang and Z. Zheng, *Society*, 2002, 6175–6180.

40 P. F. Vogt and J. J. Gerulis, in *Ullmann's Encyclopedia of Industrial Chemistry*, Wiley-VCH Verlag GmbH & Co. KGaA, 2000.

41 A. Agrawal and P. G. Tratnyek, *Environ. Sci. Technol.*, 1996, **30**, 153–160.

42 M. J. Potter, *U.S. Geol. Surv. Miner. Yearb.*, 2002, **1983**.

43 D. Gowda, B. Mahesh and S. Gowda, *Indian J. Chem.*, 2001, **408**, 75–77.

44 F. A. Khan, J. Dash, C. Sudheer and R. K. Gupta, *Tetrahedron Lett.*, 2003, **44**, 7783–7787.

45 W. G. Dauben, *Organic reactions*, John Wiley & Sons, Inc., New York, 1973.

46 A. McKenzie and G. W. Clough , *J. Chem. Soc. Trans.*, 1910, **97**, 1016–1023.

47 J. L. Sadler and A. J. Bard, *J. Am. Chem. Soc.*, 1968, **90**, 1979–1989.

48 D. Meenakshisundaram, M. Mehta, S. Pehkonen and S. W. Maloney, *Electrochemical Reduction of Nitro-Aromatic Compounds Product Studies and Mathematical Modeling*, 1999.

49 S. Gowda and D. C. Gowda, *Tetrahedron*, 2002, **58**, 2211–2213.

50 D. Balcom and A. Furst, *J. Am. Chem. Soc.*, 1953, **75**, 4334.

51 M. Kumarraja and K. Pitchumani, *Appl. Catal. A Gen.*, 2004, **265**, 135–139.

52 M. Benz and R. Prins, *Appl. Catal. A Gen.*, 1999, **183**, 325–333.

53 S. Cai, H. Duan, H. Rong, D. Wang, L. Li, W. He and Y. Li, *ACS Catal.*, 2013, **3**, 608–612.

54 R. K. Rai, A. Mahata, S. Mukhopadhyay, S. Gupta, P. Z. Li, K. T. Nguyen, Y. Zhao, B. Pathak and S. K. Singh, *Inorg. Chem.*, 2014, **53**, 2904–2909.

55 R. Langer, H-J. Buysch, U. Pentling, P. Wagner, *US Pat.*, 5,877,350A, 2000.

56 S. K. Mohapatra, S. U. Sonavane, R. V Jayaram and P. Selvam, *Org. Lett.*, 2002, **4**, 4297–4300.

57 Y. Huang and W. M. H. Sachtler, *Appl. Catal. A Gen.*, 1999, **182**, 365–378.

58 A. S. Kulkarni and R. V. Jayaram, *Appl. Catal. A Gen.*, 2003, **252**, 225–230.

59 D. F. S and H. Greenfield, *US Pat.*, US3350450 A, 1967.

60 Y. O. M. Hojo, Y. Takagi, *J. Am. Chem. Soc.*, 1960, **82**, 2459–2462.

61 R. R. Bhave and M. M. Sharma, *J. Chem. Technol. Biotechnol.*, 1981, **31**, 93–102.

62 N. C. Pradhan and M. M. Sharma, *Ind. Eng. Chem. Res.*, 1992, **31**, 1606–1609.

63 G. D. Yadav, Y. B. Jadhav and S. Sengupta, *Chem. Eng. Sci.*, 2003, **58**, 2681–2689.

64 N. C. Pradhan, *Indian J. Chem. Technol.*, 2000, **7**, 276–279.

65 H. Gilman, Wiley, New York, 1941, p. 52.

66 N. F. Lucas, H J, Scudder, *J. Am. Chem. Soc.*, 1928, **50**, 244–249.

67 D. E. W. M. J. Murray, *J. Am. Chem. Soc.*, 1938, **60**, 2818–2819.

68 S. K. Maity, N. C. Pradhan and A. V. Patwardhan, *Appl. Catal. B Environ.*, 2008, **77**, 418–426.

69 S. K. Maity, N. C. Pradhan and A. V. Patwardhan, *Chem. Eng. J.*, 2008, **141**, 187–193.

70 S. K. Maity, N. C. Pradhan and A. V Patwardhan, *Ind. Eng. Chem. Res.*, 2006, **46**,

7767–7774.

71 S. K. Maity, N. C. Pradhan and A. V. Patwardhan, *Chem. Eng. Sci.*, 2007, **62**, 805–813.

72 D. R. Napier and C. M. Starks, US Pat., 3992432, 1976.

73 S. D. Naik and L. K. Doraiswamy, *AIChE J.*, 1998, **44**, 612–646.

74 M.-L. Wang and Y.-H. Tseng, *J. Mol. Catal. A Chem.*, 2003, **203**, 79–93.

75 M.-L. Wang and Y.-H. Tseng, *J. Mol. Catal. A Chem.*, 2002, **179**, 17–26.

76 G. D. Yadav and Y. B. Jadhav, *J. Mol. Catal. A Chem.*, 2003, **192**, 41–52.

77 G. D. Yadav and S. A. Purandare, *J. Mol. Catal. A Chem.*, 2005, **237**, 60–66.

78 G. D. Yadav and Y. B. Jadhav, *J. Mol. Catal. A Chem.*, 2002, **184**, 151–160.

79 M. Wang and Y. Tseng, 2002, *J. Mol. Catal. A Chem.*, **179**, 17–26.

80 M. L. Wang and Y. H. Tseng, *J. Mol. Catal. A Chem.*, 2003, **203**, 79–93.

81 M. L. Wang and Z. F. Lee, *Ind. Eng. Chem. Res.*, 2006, **45**, 4918–4926.

82 G. D. Yadav and P. M. Bisht, *J. Mol. Catal. A Chem.*, 2005, **236**, 54–64.

83 G. D. Yadav and B. V Haldavanekar, *J. Phys. Chem.,* 1997, **5639**, 36–48.

84 G. D. Yadav and J. L. Ceasar, Org. Process Res. Dev., 2008, **12**, 740–747.

85 G. D. Yadav and N. M. Desai, *Org. Process Res. Dev.*, 2005, **9**, 749–756.

86 G. D. Yadav and P. M. Bisht, *J. Mol. Catal. A Chem.*, 2004, **223**, 93–100.

87 G. D. Yadav and O. V. Badure, *J. Mol. Catal. A Chem.*, 2008, **288**, 33–41.

88 G. D. Yadav and S. V. Lande, *J. Mol. Catal. A Chem.*, 2006, **244**, 271–277.

89 G. D. Yadav, Y. B. Jadhav and S. Sengupta, *J. Mol. Catal. A Chem.*, 2003, **200**, 117–129.

90 G. D. Yadav and S. V. Lande, *Ind. Eng. Chem. Res.*, 2007, **46**, 2951–2961.

91 G. D. Yadav and S. V. Lande, *Adv. Synth. Catal.*, 2005, **347**, 1235–1241.

92 R. Kaplánek and V. Krchňák, *Tetrahedron Lett.*, 2013, **54**, 2600–2603.

93 N. C. Pradhan and M. M. Sharma, *Evaluation*, 1990, 1103–1108.

94 G. D. Yadav, *Top. Catal.*, 2004, **29**, 145–161.

95 S. Desikan and L. K. Doraiswamy, *Ind. Eng. Chem. Res.*, 1995, **34**, 3524–3537.

96 J. A. B. Satrio, H. J. Glatzer and L. K. Doraiswamy, *Chem. Eng. Sci.*, 2000, **55**, 5013–5033.

97 S. L. Regen, *J. Am. Chem. Soc.*, 1975, **20**, 5956–5957.

98 G. D. Yadav and N. Kirthivasan, *Appl. Catal. A Gen.*, 1997, **154**, 29–53.

99 G. D. Yadav and B. V Haldavanekar, *React. Funct. Polym.*, 1997, **32**, 187–194.

100 Y. S. OU Zhize, XU Mancai, *Lizi Jiaohuan Yu Xifu*, 2000, 162–166.

101 D. W. P. S. W. Park, H.B. Cho, *J. Ind. Eng. Chem. Seoul, Repub. Korea*, 2003, 464–472.

4. Material and Methods

4.1 Materials

Toluene (>99%), Monoethanolamine (MEA) (≥99%), Ferrous sulphide sticks (FeS) and N-Methyldiethanolamine (MDEA) (≥99%) of analytical grade obtained from Merck (India) Pvt., Ltd., Mumbai, India. *o,m,p*-chloronitrobenzene (m-CNB) (>99%), 1-nitronapthalene (1-NN), 4-chloro-3nitrotoluene, 4chloro-2nitro toluene, *p*-iodonitrobenzene, 3-nitroacetophenone, 4-nitroacetophenone, o,p-nitroanisole, 8-aminoquinolene, 2,6-dinitrotoluene, 2,4-dinitrotoluene, 4-amino-4-nitrotoluene, 2-amino-4-nitrotoluene, 1-(2-nitrophenoxy)benzene, 1-(4-nitrophenoxy)benzene all of the analytical reagent grade, were procured from Sigma-Aldrich, Mumbai, India. Catalysts taken for the comparison studies are Tetrabutylammonium bromide (TBAB), Tetrabutylphosphonium bromide (TBPB), Tetramethylammonium bromide (TMAB), Tetrabutylammonium iodide (TBAI) and Ethyltriphenylphosphonium bromide (ETPPB), Tetrapropylammonium bromide (TPAB). The catalyst tributylmethylphosphonium chloride polymer-bound was purchased from Sigma-Aldrich, Mumbai, India. The FeS sticks used for H_2S production has been bought from Rankem, India. Amberlite IR-400 has been procured from Ranken. Potassium iodide (KI), Sodium hydroxide (NaOH), potassium iodate (KIO_3), starch powder, sodium thiosulfate ($Na_2S_2O_3$) and 98% pure

sulfuric acid (H_2SO_4) have been bought from Renken for absorption of H_2S and determination of sulfide concentration.

4.2 Preparation of Aqueous of H_2S-rich N-methyldiethanolamine

FeS sticks and sulfuric acid was used to generate H_2S gas. Here, the source of Sulphur is FeS act and after reacting with sulfuric acid it produces H_2S gas. Kipp's apparatus was used for serving the purpose of reacting FeS and H_2SO_4 (1M) and it was invented by a Dutch pharmacist Peter Jacobus Kipp (Fig. 4.1). The reaction involved in H_2S production in Kipps apparatus is shown below.

$$FeS + H_2SO_4 \rightarrow H_2S + FeSO_4 \qquad (4.1)$$

For aqueous phase preparation H_2S gas was bubbled through 35 wt% aqueous MEA/MDEA solution kept in an ice bath. The gas bubbling process was carried out till desired sulphide concentration attained, which was analysed by iodometric titration method [1].

Figure 4.1 H_2S generation and absorption assembly

4.3. Measurement of sulfide concentration (Idometric titration)

Preparation of Stock Solution

1. 0.0254 kmol/m^3 is the concentration of KIO_3 was prepared first.

2. 0.1 M sodium thiosulfate was prepared for which 25 gm of $Na_2S_2O_3$. H_2O was mixed with 1 liter of distilled water with 0.1 gm of sodium carbonate and three drops of chloroform were added to storing the solution.
3. 10 M NaOH, 5% of KI and 4 M H_2SO_4 and solutions were also prepared.
4. Starch-iodide solution (which is an indicator of the titration) of 0.2% concentration was prepared. For preparing so first 100 ml of distilled water was boiled, and then of 0.2 gm of starch is added to it followed by addition of 2.5 gm of KI.

Estimation of Sulfide Concentration

1. 1 ml of the solution was taken out from the stock solution of H_2S laden MEA/MDEA in a 100 ml of volumetric flask and then the flask was make up with distilled water for 100 times dilution of the sample. Then 10 ml of the solution is taken is a conical flask, and 15 ml of KIO_3 solution was added followed by addition of 10 ml of NaOH solution.
2. After that the mixture was boiled for 10 min on a heating plate and then transferred to the refrigerator for cooling the solution.
3. Thereafter 5 ml of KI solution was added to the mixture followed by addition of 20 ml of H_2SO_4 solution and the color of the mixture turned brown.
4. Titration 1: titration of the solution was carried out against the thiosulfate solution till the color of solution changes to pale yellow.
5. Therefore the solution was again diluted up to 200 ml by adding distilled water followed by addition of few drops of starch solution and the color of the solution changes to violet.
6. Titration 2: Solution was again titrated against the thiosulfate solution dropwise till the solution becomes colorless.

The reaction involved in the process of sulphide concentration estimation is as follows, Eq. (4.2) – (4.3):

$$KIO_3 + H_2SO_4 + 5KI \leftrightarrow 3K_2SO_4 + 3I_2 + 3H_2O \quad (4.2)$$

$$2Na_2S_2O_3 + I_2 \leftrightarrow Na_2S_4O_6 + 2NaI \quad (4.3)$$

$$4IO_3^- + 6OH^- + S^{2-} \rightarrow 4SO_4^{2-} + 4I^- + 6H_2O \quad (4.4)$$

Thus, the 1 mole of KIO_3 = 3×2 moles $Na_2S_2O_3$,

$$\therefore \text{Strength of Thiosulfate Solution } (S_{th}) = \frac{6 \times \text{Strenth } (KIO_3) \times \text{Volume } (KIO_3)}{\text{Volume (Consumed Thiosulfate)}}$$

Here**,** the volume of thiosulfate consumed in the titration is for the first titration.

And, 4 moles of liberated iodine $\left(IO_3^-\right) = 3$ moles of sulfide (S^{2-}) (for the second titration)

$$\text{so, the Concentration of } H_2S = \left[15 \times S_{KIO_3} - \frac{V_{th} X S_{th}}{6}\right] \times \frac{3}{4} \times \frac{N_{dl}}{10}$$

Where,

V_{th} = Thiosulfate volume

N_{dl} = Number of times of dilution

S_{KIO_3} = KIO_3 Strength

S_{th} = Thiosulfate Strength

4.4 Experimental set-up

The main reaction was carried out in an isothermal baffled three neck batch reactor of 150 ml capacity and the stirrer blade diameter was 2 cm with six blades. The reactor was provided with digital speed regulation system. The whole reaction system is kept in an isothermal water bath with a PID temperature controller (±1°C). The whole reaction setup is shown in the Figure 4.2.

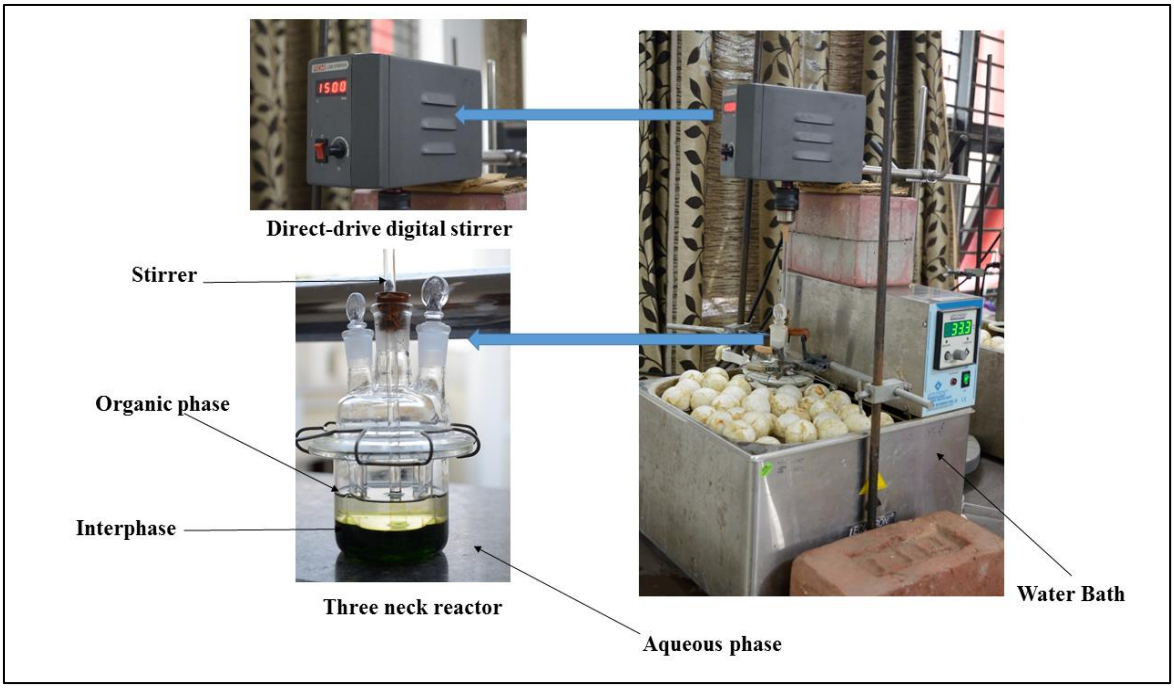

Figure 4.2 The Experimental Assembly

4.5 Experimental Procedure

The reaction system consisted of an equal volume of aqueous phase (H_2S-laden aqueous MEA/MDEA) and an organic phase (toluene used an organic solvent to dissolve nitroarenes) and a catalytic amount of phase transfer catalyst (soluble or insoluble). The aqueous phase was first introduced into the reactor followed by stirring the solution till it reached the desired temperature. Then after stopping the stirrer, organic reactant dissolved in toluene is introduced in the reactor. At last measured quantity of catalyst is added in the three neck batch reactor. The reaction commenced as soon as the stirrer was switched on again. 0.1 ml of sample was collected from the upper organic phase layer after switching off the stirrer to allow the phase separation.

4.6 Analysis of the Phases

Post experiment the quantitative analysis of the organic sample was done using GC-FID (Agilent GC 7890B) equipped with a capillary column (DB-5MS, 2 m × 3mm) using a flame ionization detector (FID). The qualitative analysis to identify the product produced in our system was done using GC-MS (Agilent 5977A).

4.6.1 Qualitative Analysis using GC-MS

1µl of organic sample was injected into the injector port of GC using a micro syringe and helium was used as a carrier gas. The compounds present in our organic sample were identified by GC-MS. Separation process of the molecules (present in the sample) is done in a capillary column is used in the GC-MS. After separation in the column the molecules goes to the mass spectrometer, then it ionizes, accelerates, deflects and the molecules are finally detected separately. During deflection the ions are separated accordingly to their charge/weight ratio. The different molecular weight of the different compound is given in the spectra. A detailed program followed for the identification in GCMS is given below:

MS Program

Inlet conditions. (Split mode)

Purge Flow = 3 ml/min, Heater = 300^0C, Pressure = 11.724 psi

Column specifications. Agilent DB-5ms, Flow = 1 ml/min, Pressure = 8.2317 psi, Holdup Time = 1.365 min

Oven condition. Initial Temperature = 60 ^{0}C, Maximum temperature = 300 ^{0}C.

Table 4.1 Temperature Programme for MS

	Rate (^{0}C/min)	**Value (^{0}C)**	**Holdup Time (min)**	**Retention Time (min)**
Initial		60	0	0
Ramp 1	45	190	2	4.6
Ramp 2	20	280	5	7.4

4.6.2 Quantitative analysis using GC-FID

Gas-chromatography accompanied with flame ionization detector (GC-FID) is being widely used natural gas, petroleum, and pharmaceutical markets. For the analysis, we inject a known volume of the sample using microsyringe into the capillary column. In the present analysis, nitrogen acts as a carrier gas which carries the molecules of the sample through the column and the molecules get adsorbed in the fillings present in the column which is the stationary phase of the column. Every molecule differs in their progression rate and leaves the column at a different time which is called the retention time of that molecule. The molecules which are leaving the column is detected by a flame ionization detector. The sample passes through a Hydrogen/Air flame to oxidize organic molecules and produces electrically charged ions. These ions get collected and generate an electrical signal which is then measured. The concentration of the organic compound is

proportional to the number of ions formed, and this theory was used quantification of the organic phase. The detailed program followed for the quantification using GC-FID is mentioned below:

FID Program

Inlet Condition. Heater = 200 ^{0}C, Purge Flow = 3ml/min, Pressure = 15.345 psi

Column Condition. Agilent DB-5ms, Flow = 1.5 ml/min, Holdup Time = 1.427 min, Pressure = 15.345 psi.

Oven Condition. Initial temperature = 60 ^{0}C, Maximum temperature = 300 ^{0}C.

Detector. Heater = 300 ^{0}C, Column Flow (N_2) = 15 ml/min, Make up Flow (N_2) = 25 ml/min, H_2 Flow = 30 ml/min, Air Flow = 400 ml/min.

Table 4.2 Temperature Programme for FID

	Rate (^{0}C/min)	**Value (^{0}C)**	**Holdup Time (min)**	**Retention Time (min)**
Initial		60	0.0	0.0
Ramp 1	45	190	0.0	2.8
Ramp 2	20	300	0.0	8.4

References

1 Scott WW, *Standard Methods of Chemical Analysis*, Van Nostrand, New York, 6th Editio., 1966.

Abstract

Parametric studies were performed to find out the kinetics of the Zinin reduction and to optimize the influence of process parameters like stirring speed, concentration of m-CNB, concentration of aqueous sulphide, catalyst concentration etc. on reaction rate and conversion of m-CNB. The reusability of catalyst was investigated and catalytic activity of used catalyst was found to change a little even after three recycle run in comparison to fresh catalyst. Also waste

minimization was achieved by the use of reusable catalyst which can also act as a green alternative.

5.1 Introduction

Kinetics of Zinin reduction between m-chloronitrobenzene (m-CNB) and H_2S-laden monoethanolamine (MEA) in liquid-liquid-solid (L-L-S) system catalysed by anion exchange resin Amberlite IR-400 (Chloride form) was investigated. Selectivity of the product m-Chloroaniline (m-CA) was 100%. The reaction was found to be kinetically controlled with an apparent activation energy of 56.16 kJ/mol. Parametric studies were performed to find out the kinetics of the Zinin reduction and to optimize the influence of process parameters like stirring speed, concentration of m-CNB, concentration of aqueous sulphide, catalyst concentration etc. on reaction rate and conversion of m-CNB. The reusability of catalyst was investigated and catalytic activity of used catalyst was found to change a little even after three recycle run in comparison to fresh catalyst. The kinetic model and mechanism of complex L-L-S phase transfer catalytic process have been developed and kinetic model has been validated against experimental data. The present reaction is an example of intensification of multiphase reaction with 100% selectivity to the desired product and can replace amine treating unit (ATU) of petroleum refinery as a key process for utilizing hazardous H_2S gas. Also waste minimization was achieved by the use of reusable catalyst which can also act as green alternative.

5.2 Results and discussion

5.2.1 Proposed mechanism of reduction of nitro-aromatic compound under L-L-S PTC

The overall stoichiometry of the Zinin's original reduction of nitrobenzene by aqueous ammonium sulphide as proposed by Zinin in 1842 is given by Equation 5.1 [1]. Reduction of nitroarenes by sodium sulphide follows same stoichiometry. [2–6]

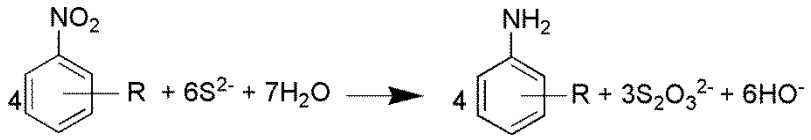

(5.1)

Some other reports have shown that elemental sulphur can be produced as a by-product instead of thiosulphate when aqueous ammonium sulphide is used as a reducing agent in the reaction. p-aminophenylacetic acid can be prepared from p-nitrophenylacetic acid using aqueous ammonium sulphide and it has been reported that the sulphide ions are

oxidised to elemental sulphur instead of thiosulphate following the stoichiometry of Equation 5.2. [7]

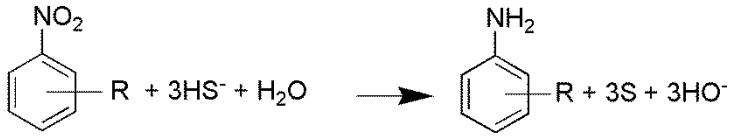

(5.2)

Above reactions (Equation 5.1 & 5.2) show that two different anions ($S^{2-}$and HS^{-}) have participated in the reduction reaction and elemental sulphur and thiosulphate are produced as a by-product respectively. In the presence of a base, ammonia, the dissociation equilibrium favours toward more ionization [7,8]and the concentration of sulphide ions (S^{2-}) relative to hydrosulfide (HS^{-}) ions increases in the aqueous phase with the increase in the ammonia concentration. [9]

The overall stoichiometry of the reduction reaction using sodium disulphide as the reducing agent is shown below. [2]

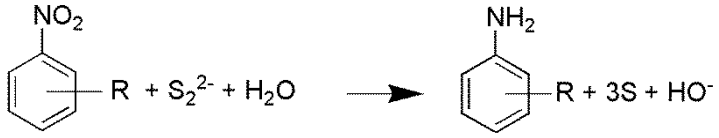

(5.3)

During the reduction of ntroarenes, it is found that all three reactions mentioned in Equation 5.1, 5.2 and 5.3 are co-existed.[7,8] Sulphur can exist in multiple valency state ranging from (-2) to (+6) and therefore can form different anions (HS^{-},HSO^{-}, HSO_2^{-}, HSO_3^{-}) which are capable of pairing with quaternary cations of anion exchange resin. The nitro group present in the nitroarens are reduced by the transfer of electrons from sulphide ions during the reduction by H_2S-laden MEA solution.

Ionic equilibrium of sulphide ions (S^{2-}) and hydrosulphide ions (HS^{-}) in H_2S-laden alkanolamine solution resembles aqueous ammonium sulphide solution, as represented by Equation 5.4 to Equation. 5.7 in the Scheme 5.1. [9] These two ions are responsible for the formation of elemental sulphur or thiosulphate in the process of reduction of nitroarenes by H_2S-laden aqueous MEA solution. The presence of both ions (sulphide, hydrosulphide) makes H_2S-laden aqueous alkanolamine and aqueous ammonium sulphide solutions different from other reducing agent like sodium sulphide, sodium disulphide etc. [10]

Liquid-Liquid-Solid (L-L-S) triphase reaction system consists of an organic phase containing organic substrate (forming dispersed phase), an aqueous phase containing inorganic reagent (normally continuous phase) and catalyst impregnated on a solid

support. Unlike Stark's extraction mechanism, catalyst movement is restricted between the phases and organic and aqueous reagents must come contact to the catalyst cations in a sequence. Only those sites, which are present on the interphase between the phases are involved in the reaction. [11]

In the aqueous phase H_2S gas reacts with MEA to form sulphide (S^{2-}) and hydrosulphide (HS^-) anions (Scheme 5.1). Quaternary cations present at the interphase readily form Q^+HS^- ion pair as soon as it comes into contact with the aqueous phase. Then, a series of reactions take place at the interphase as shown in Scheme 5.1. Reactions occur near the interphase in the vicinity of the solid catalyst.The contribution of several elementary reactions in the interphase to the overall rate of the reaction is elaborated by the following mechanism. In a series of complex elementary reactions, m-CNB is converted to m-CA through the formation of intermediates m-chloronitrosobenzene and m-chlorophenylhydroxylamine, both of which have not been detected in GC-MS analysis. The existence of these two intermediates during Zinin reduction has long been established. [5,12] While the catalyst cations are pairing with the HS^- anions, some water molecules transfer to the interphase and are taking part in the reaction as shown in Equation. 5.12. After a series of elementary reactions the ion pair $Q^+HSO_3^-$ is formed which reacts with remaining S^{2-} ion to regenerate Q^+HS^- to complete the catalyst cycle (Equation 5.13). The product amine that is hydrophobic in nature transfers to the organic phase as soon as it forms. The quaternary cations present on the surface of the resin are pairing with different anions during reactions but majority of the catalyst cations remains in Q^+HS^-form and the catalysis cycle goes on. Three reactions as shown in Equation 5.4 – 5.7 take place in the aqueous phase and all other reactions (Equation 5.8-13) take place consecutively in the interphase region between the phases where the active sites of the catalyst are alternatively available for the reaction because of the dynamic nature of the interphase.

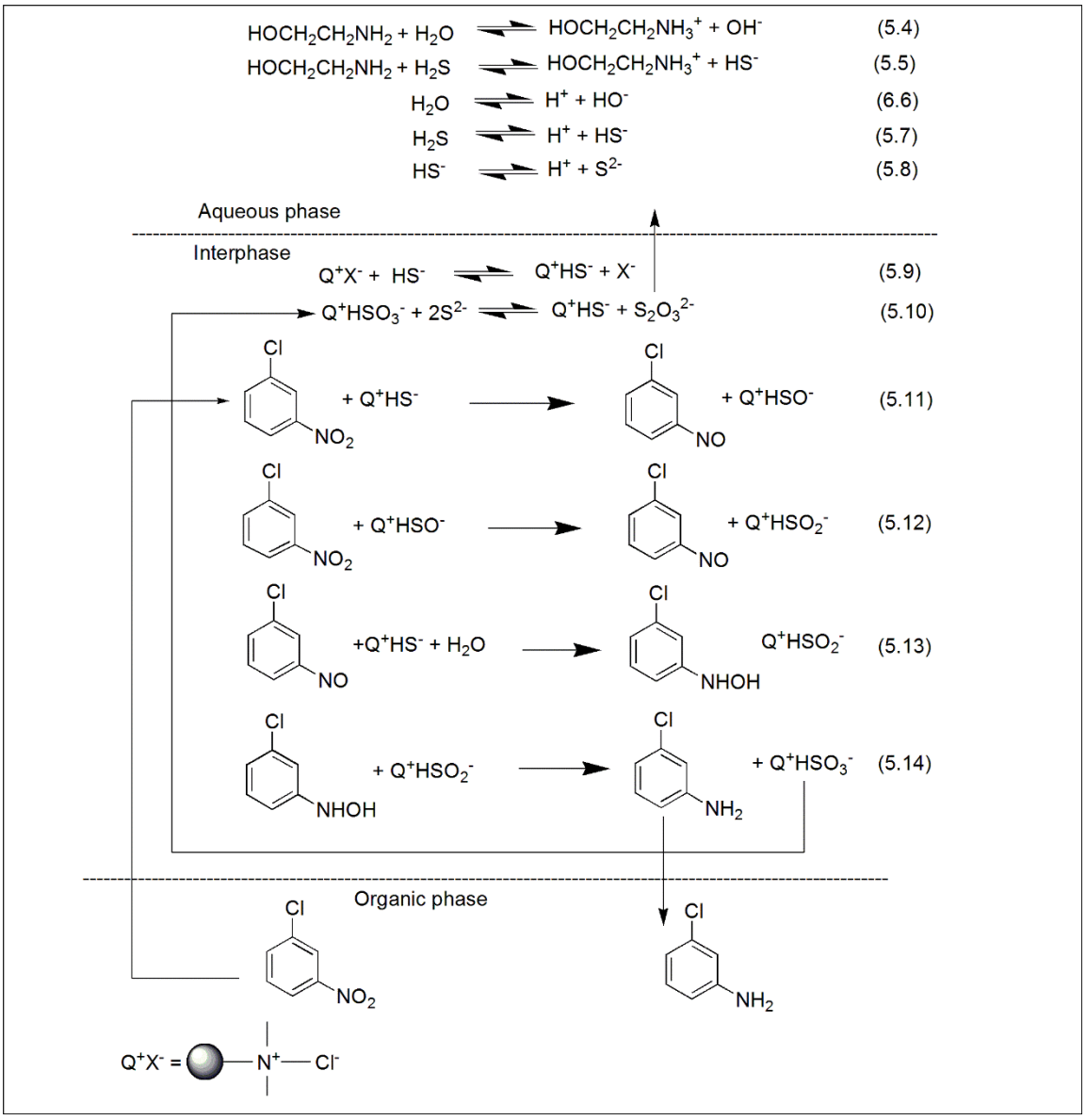

Scheme 5.1. Proposed mechanism of reduction of m-CNB by H_2S-laden MEA under L-L-S PTC.

5.2.2 Kinetic modelling

Modelling of triphase catalytic (TPC) system incorporates mass transfer of reagents into the bulk aqueous and organic phases followed by diffusion of reactant molecules within the catalyst particle, then intrinsic ion-exchange reaction along with organic reaction at the active site of the catalyst, which was first proposed by Wang and Yang.[13] One of the assumption made in developing the model was the steady state nature of mass balance equations which was further modified to dynamic model by the same authors in 1992. [14] An additional modification was done by Desikan and Doraiswamy [11,15] as they have included reversibility of ion exchange reaction and non-isothermality in their model.

Almost all the kinetic models of TPC system assume that the reactions consist of a number of elementary reactions that are independent in their respective phases. This model elaborated how reduction reaction involves TPC where intrinsic reaction at the active site of the catalyst is the rate limiting step.

Let us assume a triphase catalytic reaction system where m-CNB dissolved in toluene is reduced by H_2S-laden MEA aqueous solution to yield m-CA as the sole product and $S_2O_3^{2-}$ as a by-product in their respective phases as shown in Scheme 5.1. The overall reaction can be expressed in a single reaction as Equation 5.1.

Mechanism of triphase catalysis is different from traditional heterogeneous catalysis, where adsorption and reaction steps take part at an active site. For triphase catalysis quaternary cations, Q^+ present on the surface is referred as a site. When a site adsorbes inorganic nucliophile, (HS^-in this case) the site is called active site and when a site gets attached to catalyst's orginal anion or the by-product anion (in this study Cl^- and $Q^+HSO_3^-$), it is called as in-active site.

The reaction medium was agitated with a stirrer at 1500 rpm to make the reaction as reaction rate controlled as mass transfer effects were minimized. The reaction initiated at the interphase with ion exchange between HS^- and chloride ion of the ion exchange resin (Q^+X^-) to form an active site Q^+HS^-. During the progress of the reaction, different transition anions were formed at the active sites and finally they became in-active site as HSO_3^- ions got attached to quaternary cations. Then in-active site underwent redox reaction with S^{2-} ions and active sites Q^+HS^- were regenerated.

The whole reaction mechanism can be compaired to an Eley- Redieal reaction mechanism [16], where an adsorbed reactant reacts with an un-adsorbed reactant from the bulk phase. Here reactant dissolved in organic phase reacted with adsorbed reactant present on the active site of the catalyst at the interphase to form the final product (m-CA), followed by inactivation of active site ($Q^+HSO_3^-$). The regeneration step can be treated as adsorption step where sulphide ions (S^{2-}) got adsorbed on inactive site and after redox reaction site became active again (Q^+HS^-) as shown in Figure 5.1. Among many elementary reactions shown in Scheme 5.1 (Equation 5.10-5.13), the reaction shown in Equation 5.10, where the first intermediate product m-chloronitrosobenzene formed, has been considered as the slowest and rate determining step.

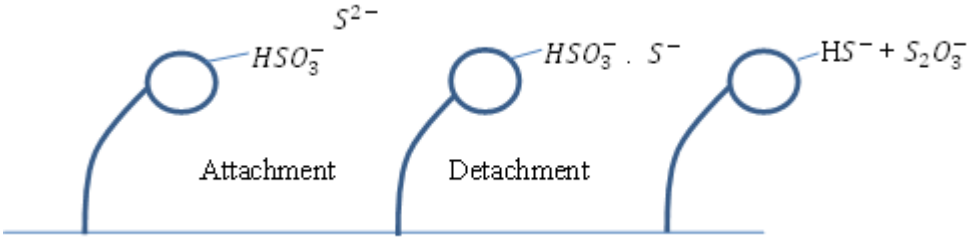

Figure 5.1. Schematic diagram for catalyst regeneration.

The reversible regeneration reaction may be compared to the Langmuir-Hinshelwood adsorption/desorption mechanism as shown in Figure 5.1.

$$Q^+X^- + HS^- \leftrightarrow Q^+HS^- + X^- \tag{5.14}$$

A transitional site ($S^{2-}Q^+HSO_3^-$) was assumed to be formed between forward and backwards reaction steps during regeneration reaction of active site, i.e.

$$Q^+HSO_3^- + 2S^{2-} \leftrightarrow S^- Q^+ HSO_3^- \leftrightarrow Q^+HS^- + S_2O_3^{2-} \tag{5.15}$$

This reaction can be thought to be consisting of two distinct attachment/detachment steps. In the forward reaction step, sulphide ions (S^{2-}) gets attached to the inactive site $Q^+HSO_3^-$, which can be assumed as "attachment/detachment" step of sulphide ions (S^{2-}), i.e.,

$$Q^+ HSO_3^- + 2S^{2-} \leftrightarrow S^- Q^+ HSO_3^- \tag{5.16}$$

The backward reaction can be assumed as "attachment/detachment" of thiosulphate ion ($S_2O_3^{2-}$) at the active site, i.e.

$$Q^+HS^- + S_2O_3^{2-} \leftrightarrow S^{2-} Q^+ HSO_3^- \tag{5.17}$$

Considering each of the attachment and the detachment steps are in equilibrium, Equation 5.18 and Equation 5.19 can be obtained from reaction Equation 5.16 and Equation. 5.17 respectively, as

$$Q_{S^{2-}HSO_3^-} = K_S\ [S^{2-}]_{aq}^2 \left(1 - Q_{HSO_3^-} - Q_{S^{2-}HSO_3^-}\right)$$
(5.18)

$$Q_{S^{2-}HSO_3^-} = K_{S_2O_3}\ [S_2O_3^{2-}]_{aq}\left(1 - Q_{HS^-} - Q_{S^{2-}HSO_3^-}\right) \tag{5.19}$$

Here K_S and $K_{S_2O_3}$ are the equilibrium attachment/detachment constants for S^{2-} and $S_2O_3^{2-}$ nucleophiles, respectively; $[S^{2-}]$ and $[S_2O_3^{2-}]$ are the concentrations of S^{2-} and $S_2O_3^{2-}$ anions in the aqueous phase, respectively; and $Q_{HSO_3^-}$, Q_{HS^-}, $Q_{S^{2-}HSO_3^-}$ are fractions of the total number of triphase cations occupied by HSO_3^-, HS^-, $S^{2-}HSO_3^-$ anions, respectively.

It can be postulated that the transition site $S^{2-}HSO_3^-$ formed at the catalyst cations instantaneously converted to an active site Q^+HS^- or in-active site $Q^+\ HSO_3^-$, so Equation 5.18 and Equation 5.19 can be rewritten as shown below.

$$Q_{HS^-} = K_S\ [S^{2-}]_{aq}^2\left(1 - Q_{HS^-} - Q_{HSO_3^-}\right) \tag{5.20}$$

$$Q_{HSO_3^-} = K_{S_2O_3}\ [S_2O_3^{2-}]_{aq}\left(1 - Q_{HSO_3^-} - Q_{HS^-}\right) \tag{5.21}$$

Now combining Equation 5.20 and Equation 5.21 would yield a hyperbolic functions for the fraction of active sites as,

$$Q_{HS^-} = \frac{K_S\ [S^{2-}]_{aq}^2}{(1 + K_S\ [S^{2-}]_{aq}^2 + K_{S_2O_3}\ [S_2O_3^{2-}]_{aq})} \tag{5.22}$$

And in the terms of catalyst concentration:

$$[Q^+.HS^-] = [Q]_{tot}\ \frac{K_S\ [S^{2-}]_{aq}^2}{(1 + K_S\ [S^{2-}]_{aq}^2 + K_{S_2O_3}\ [S_2O_3^{2-}]_{aq})} \tag{5.23}$$

Since $K_{S_2O_3} \ll K_S$ (because of irreversible removal of $S_2O_3^{2-}$ from interphase to bulk aqueous phase after the detachment of $S_2O_3^{2-}$ from the $Q_{HS^-HSO_3^-}$), Equation 5.23 becomes,

$$[Q^+.HS^-] = [Q]_{tot}\ \frac{K_S\ [S^{2-}]_{aq}^2}{(1 + K_S\ [S^{2-}]_{aq}^2)}$$

Where $[Q]_{tot}$ and $[Q^+.HS^-]$ are the total concentration catalyst and active sites respectively.

According to the overall reaction (Equation 5.1) the conversion can be calculated as

$$\text{Conversion (X)} = 1 - \frac{[ArNO_2]_O}{[ArNO_2]_i} \tag{5.24}$$

Where $[ArNO_2]_i$ and $[ArNO_2]_O$ are the total initial concentration of m-CNB and concentration at any time of m-CNB in the organic phase.

So, $[ArNO_2]_O = (1 - X)\ [ArNO_2]_i$

As it is mentioned before, the reaction (Equation 5.11) presented in Scheme 5.1 is rate limiting step at the interphase, the rate $(-r_A)$ of the reaction can be written as,

$$-r_A = k_O\ [ArNO_2]_O\ .\ [Q^+.HS^-]_S \tag{5.25}$$

$$= \frac{d[ArNO_2]_O}{dt} = k_o\,[Q]_{tot}\,\frac{K_S\,[S^{2-}]^2_{aq}}{(1+K_S\,[S^{2-}]^2_{aq})}\,(1-X)\,[ArNO_2]_i \quad (5.26)$$

$$= -\frac{dX}{dt} = k_o\,[Q]_{tot}\,\frac{K_S\,[S^{2-}]^2_{aq}}{(1+K_S\,[S^{2-}]^2_{aq})}\,(1-X), \quad (5.27)$$

$$= -\frac{dX}{(1-X)} = k_{app}\,dt, \quad (5.28)$$

Where $k_{app} = k_o\,[Q]_{tot}\,\frac{K_S\,[S^{2-}]^2_{aq}}{(1+K_S\,[S^{2-}]^2_{aq})}$

k_{app} can be assumed to be constant for a fixed catalyst loading, a fixed initial sulphide concentration and a fixed temperature. So,

$$-r_A = -\ln(1-X) = k_{app}.t \quad (5.29)$$

From the Equation 5.29 it is clear that the reaction follows the pseudo-first order.

5.2.3. Parametric studies

5.2.3.1. Effect of stirring speed

For carrying out a kinetic study, mass transfer resistance should be minimised during the course of the reaction. So, for determining the influence of external mass transfer on the rate of reaction of m-CNB, reactions in the presence of PTC (Amberlite IR 400 (Cl^- form)) were performed in the range of 800 - 2500 rpm as shown in Figure 5. 2. However other experimental conditions were kept identical. The stirring speed was found to have very little effect on the reaction rate. So the reaction can be assumed to have no mass transfer resistance when it is operated at 1000 rpm. All the experiments were carried out at 1500 rpm to ensure that the reaction is only kinetically controlled one.

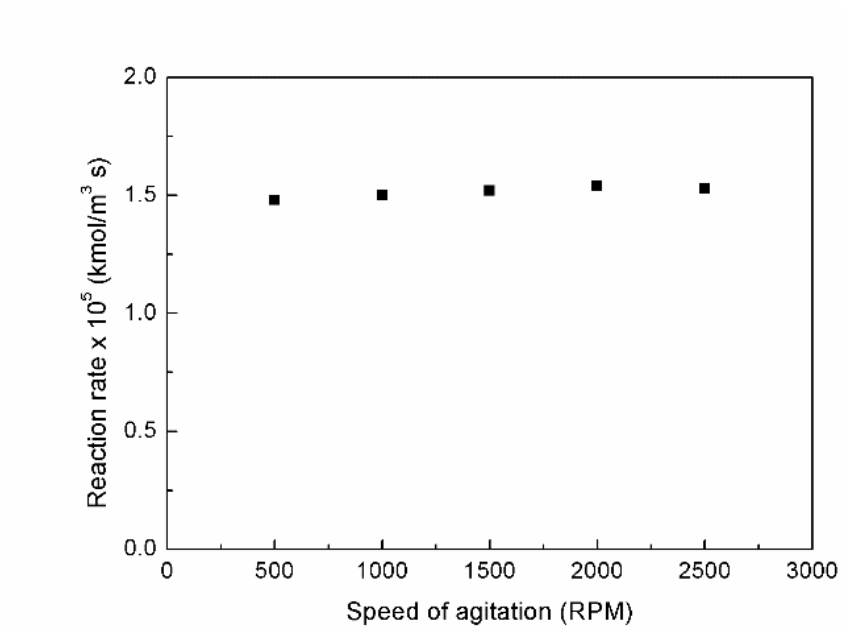

Figure 5.2: Effect of stirring speed on the conversion of m-CNB. Operating conditions: Volume of organic phase =5 x 10^{-3} m^3; concentration of m-CNB = 1.27 kmol/m^3 in org. phase; concentration of toluene = 8.17 kmol/m^3 in org. phase; volume of aqueous phase = 50 ml, concentration of catalyst = 0.58 kmol/m^3 in org. phase; concentration of sulphide = 2.53 kmol/m^3, concentration of MEA = 5.787 kmol/m^3; temperature = 333 K.

5.2.3.2. Effect of temperature

The influence of temperature on the conversion of m-CNB catalysed by Amberlite IR-400 (Cl^- form) was studied under various reaction temperatures in the range of 30–60^oC under otherwise similar reaction conditions as shown in Figure 5.3. As per the transition state theory the rates of most organic reactions increase with the increase in temperature and increasing temperature is likely to enhance the rate of slow organic phase reactions in PTC system. From the figure it is clear that the reactivity (conversion) of m-CNB increases with an increase in the temperature, the activation energy of molecules is overcome and more molecules react to form product. On the other hand, collision among reactant molecules at higher temperature has also resulted in an increase of the reaction rate with increasing temperature.

Arrhenius plot of ln (initial rate) vs. *1/T* was made for m-CNB (Figure 5.4). The apparent activation energy for the kinetically controlled reaction was calculated from the slope of the best fitted straight line as 56.16 kJ/mol. The high values of apparent activation energies again confirm that the reaction is kinetically controlled. Reduction of p-nitrotoluene by aqueous ammonium sulphide catalysed by Anion Exchange Resin

(Serelite SRA-400 in Chloride form) also requires high activation energy of 49.8 kJ/mole.
17

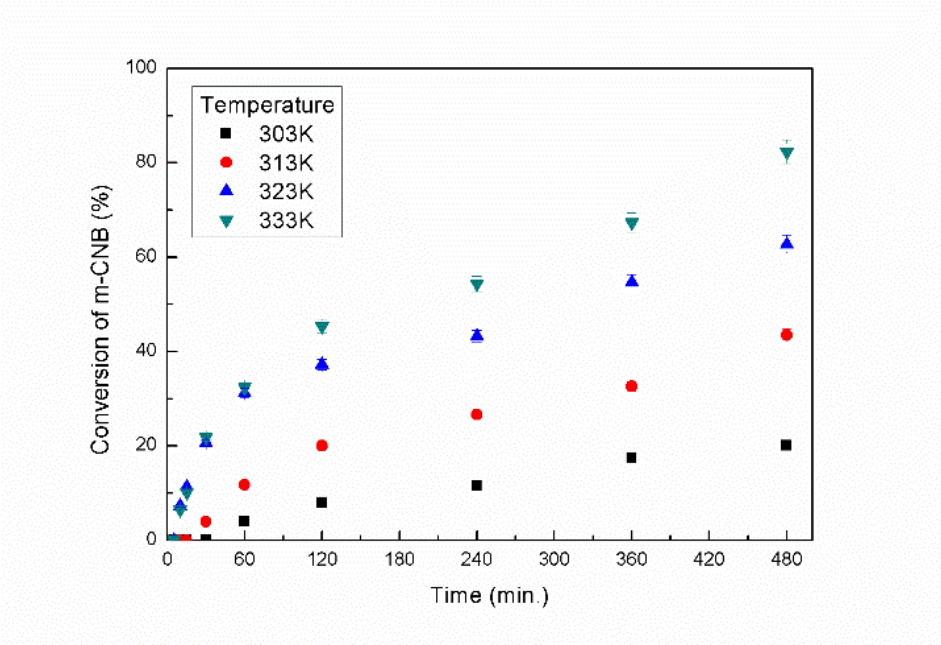

Figure 5.3: Effect of temperature on the conversion of m-CNB. Operating Conditions: Volume of organic phase = 5 x 10^{-3} m^3, Volume of Aqueous Phase = 5 x 10^{-3} m^3, Concentration of m-CNB =1.27 kmol/lit org. phase, concentration of toluene 8.17 kmol/lit in org. phase, concentration of catalyst = 0.58 kmol/lit in org. phase, Sulphide concentration = 2.53 kmol/lit, concentration of MEA = 5.787, Stirring speed = 1500 rpm.

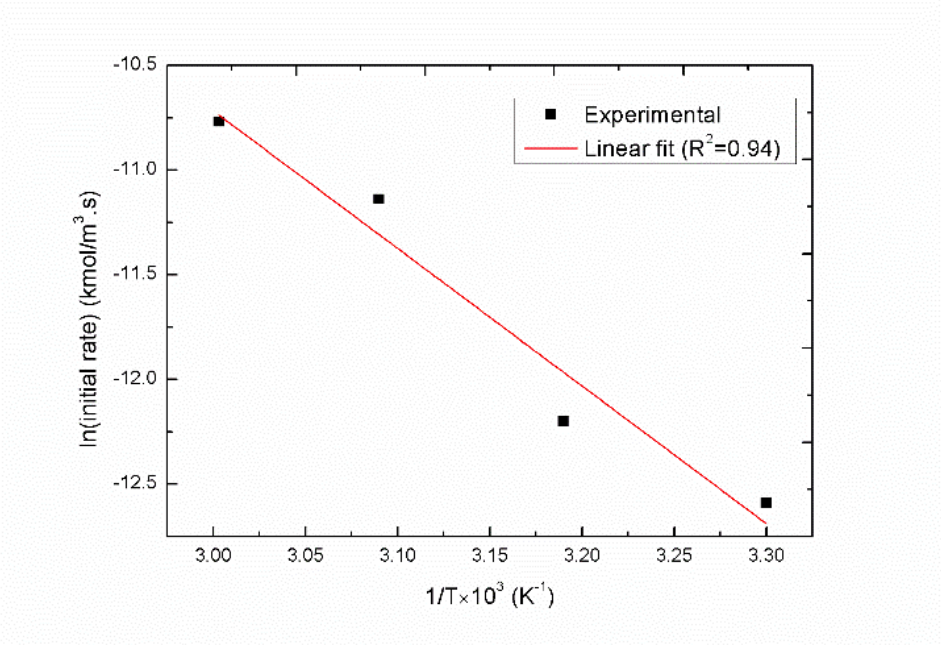

Figure 5.4: Arrhenius Plot of *ln (initial rate)* vs. *1/T*. All other conditions are same as Figure 5.3.

5.2.3.3. Effect of Catalyst loading

For kinetically controlled reduction of m-CNB by H_2S-laden aqueous MEA, the effect of catalyst (Amberlite IR-400) loading on the conversion of m-CNB was studied in the range of 0 – 10% (w/v) under otherwise identical experimental condition as shown in Figure 5.5. With increase in catalyst loading, the conversion of m-CNB as well as the reaction rate increase. Only by increasing the catalyst concentration, reactant conversion of more than 62% was achieved with 10% (w/v) catalyst loading whereas it was about 36% without catalyst even after 8 hours of reaction under otherwise identical conditions. Enhancement factors, which is ratio of rate of reaction in the presence of catalyst to the rate of reaction in the absence of catalyst, were calculated at different catalyst loadings as shown in Table 5.1. Highest enhancement factor of 86 can be seen with 10% (w/v) catalyst loading.

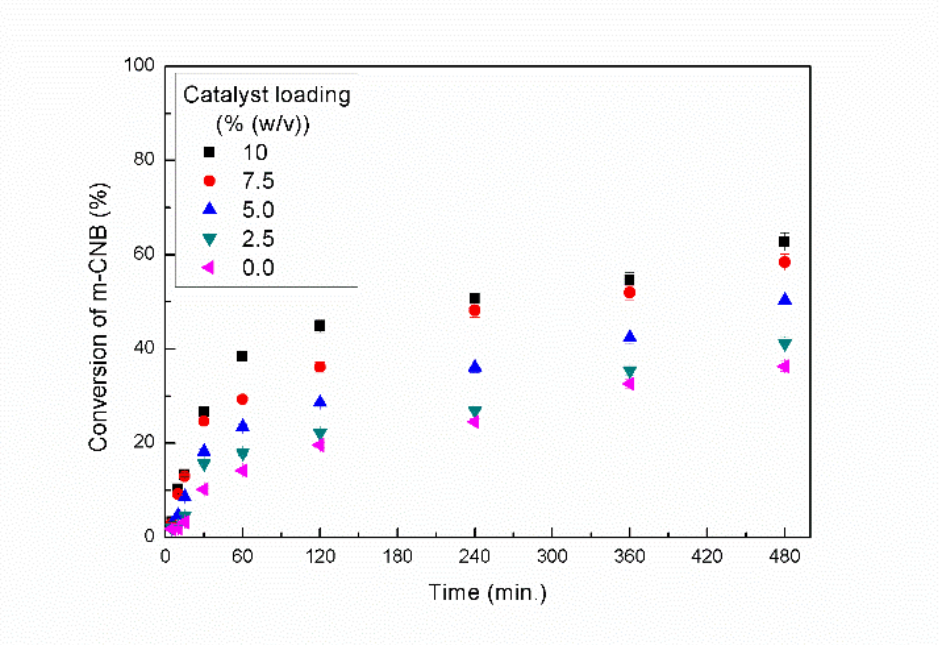

Figure 5.5: Effect of Catalyst (Amberlite IR-400) loading on the conversion of m-CNB. Operating Conditions: Volume of organic phase = 5 x 10^{-3} m^3, Volume of Aqueous Phase = 5 x 10^{-3} m^3, Concentration of m-CNB = 1.27 kmol/m^3 org. phase, concentration of toluene = 8.17 kmol/m^3 in org. phase, concentration of catalyst = 0-0.58 kmol/m^3 in org. phase, Sulphide concentration = 2.53 kmol/m^3, concentration of MEA = 5.787 kmol/m^3, Stirring speed = 1500 rpm, Temperature 323K.

To determine the order of reaction with respect to catalyst concentration, the initial reaction rate was calculated at different catalyst concentrations. A plot of ln (initial rate) against ln (catalyst concentration) was made and shown in Figure 5.6. From the slope of

the linear fit line, the order of reaction was determined. The slope of the line is found out to be 0.88 which is close to unity.

Table 5.1 Effect of catalyst loading on Initial reaction rate[a]

Concentration of Amberlite IR-400 (kmol/m^3 org phase)	**Initial reaction rate × 10^5 (kmol/m^{3}s) at 5% Conversion**	**Enhancement factor**
0	0.29	0
0.146	0.68	2.6
0.290	10.54	36.2
0.438	15.10	51.9
0.580	24.91	85.6

[a]All other conditions are same as that mentioned under **Figure 5.5.**

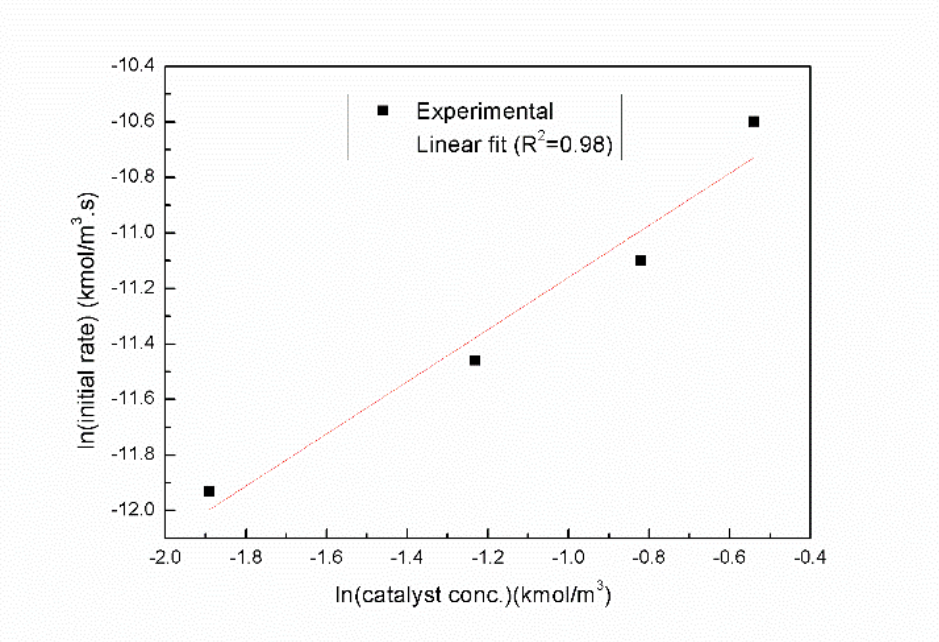

Figure 5.6: Plot of *ln (initial rate)* vs *ln (catalyst concentration)*. All other conditions are same as that mentioned under **Figure 5.5**.

5.2.3.4. Effect of m-chloronitrobenzene concentration

The effect of concentration of m-CNB on its conversion was studied at four different concentrations in the range of 0.371-1.27 kmol/m^3 in the presence of Amberlite IR-400 under otherwise identical experimental conditions, as shown in Figure 5.7. It is clear from the figure that with the increase of the concentration of m-CNB, the conversion of m-

CNB decreases. This is due to the availability of the limited quantity of sulphide in the aqueous phase.

As expected, the increase in the reaction rate during the initial stage of the reaction was due to the increase in the concentration of m-CNB. Since the amount of sulphide in the aqueous phase remained the same for all the experimental runs, the conversion of m-CNB dropped beyond a certain concentration as shown in Figure 5.7. The similar observation was found for o-nitroanisole with H_2S-laden Diethanolamine. [18] After 1 hr of run the rate of reaction along with conversion dropped down due to the availability of fewer amounts of reactants.

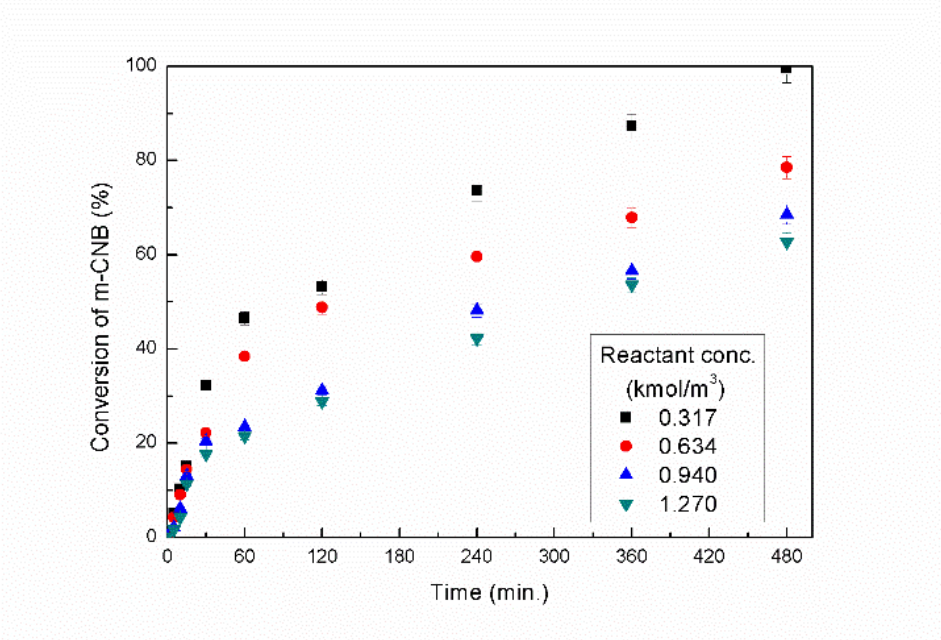

Figure 5.7: Effect of Reactant concentration on % conversion of m-CNB. Operating Conditions: Volume of organic phase = 5 x 10^{-3} m^3, Volume of Aqueous Phase = 5 x 10^{-3} m^3, concentration of toluene = 8.17 kmol/m^3 in org. phase, concentration of catalyst = 0.58 kmol/m^3 in org. phase, Sulphide concentration = 2.53 kmol/m^3, concentration of MEA = 5.787 kmol/m^3, Stirring speed = 1500 rpm, Temperature = 333K.

From the plot of ln (initial rate) vs. ln (m-CNB concentration), (Figure 5.8) the order of reaction with respect to m-CNB concentration was obtained as 0.95, which is close to unity. Hence the reaction is first order with respect to the concentration of reactant. In literature, order for reduction of nitroarenes by aqueous sodium sulphide was also reported as unity with respect to the concentration of p-nitroanisole. [5]

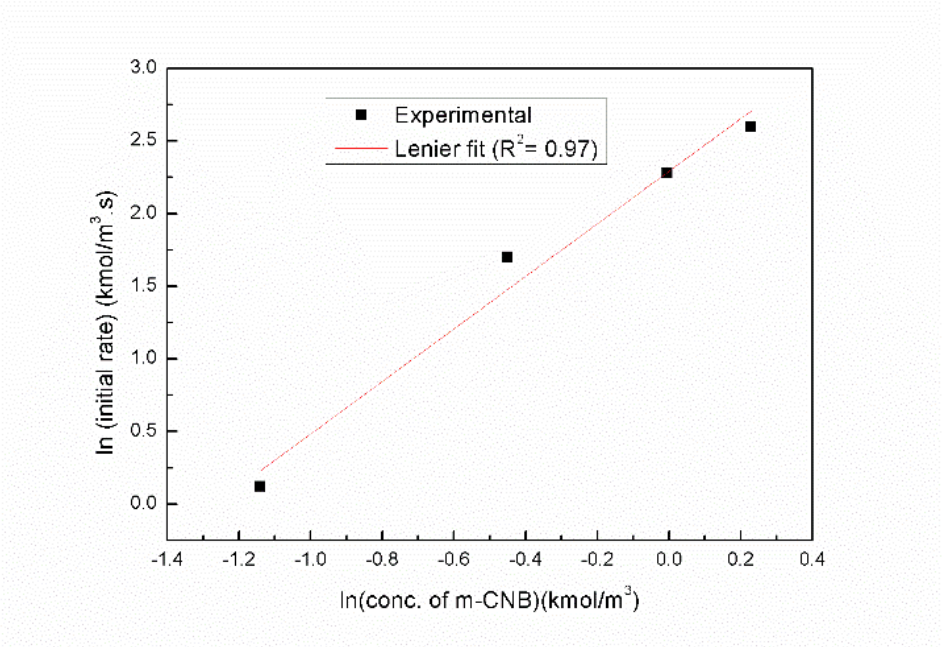

Figure 5.8: Plot of ln (initial rate) vs. ln (reactant concentration). All other conditions are as same that given under **Figure 5.7**.

5.2.3.5. Effect of initial sulphide concentration

Figure 5.9 shows the effect of initial sulphide concentration in the aqueous phase on the conversion of m-CNB. With an increase in the initial sulphide concentration, the conversion of m-CNB increases as expected. Sulphide concentration was varied in the range of 1.5 - 2.53 kmol/m^3 in otherwise identical experimental condition in the presence of catalyst Amberlite IR-400 (Cl^- form).

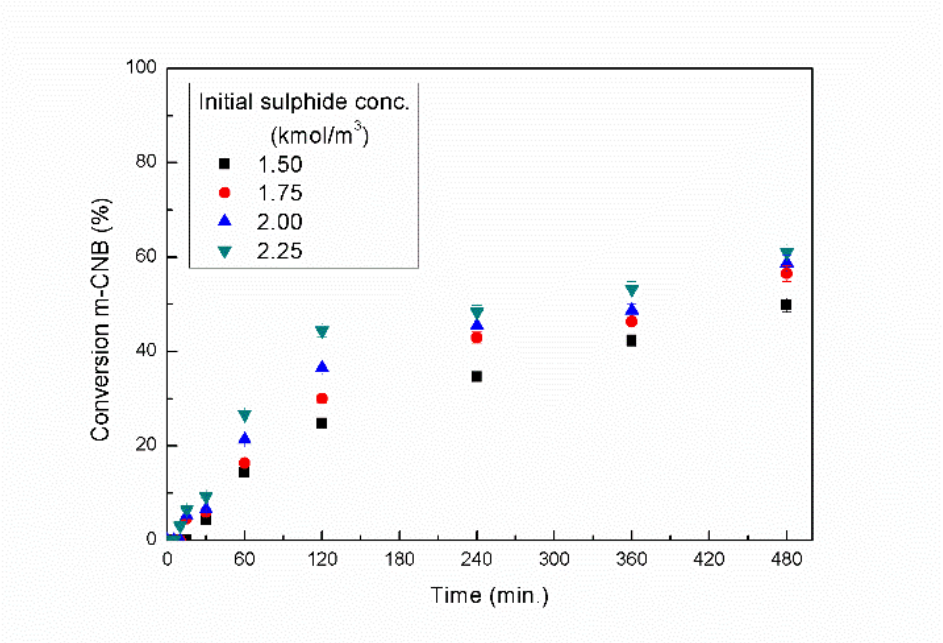

Figure 5.9: Effect of Sulphide Concentration on % conversion of m-CNB. Operating Conditions: Volume of organic phase = 5 x 10^{-3} m^3, Volume of Aqueous Phase = 5 x 10^{-3} m^3, Concentration of m-CNB = 1.27 kmol/m^3 in org. phase, concentration of toluene = 8.17 kmol/m^3 in org. phase, concentration of catalyst = 0.58 kmol/m^3 in org. phase, concentration of MEA = 5.787 kmol/m^3, Stirring speed = 1500 rpm, Temperature = 323K.

From the plot of ln (initial rate) against ln (initial sulphide concentration) (Figure 5.10), the slope of the linear fit line was found out to be to be 1.75. Since this value is closer to 2, the reaction was considered to be second order with respect to the sulphide concentration. Studies on reduction of m-CNB with aqueous ammonium sulphide were also reported to be second order with respect to sulphide concentration. [19]

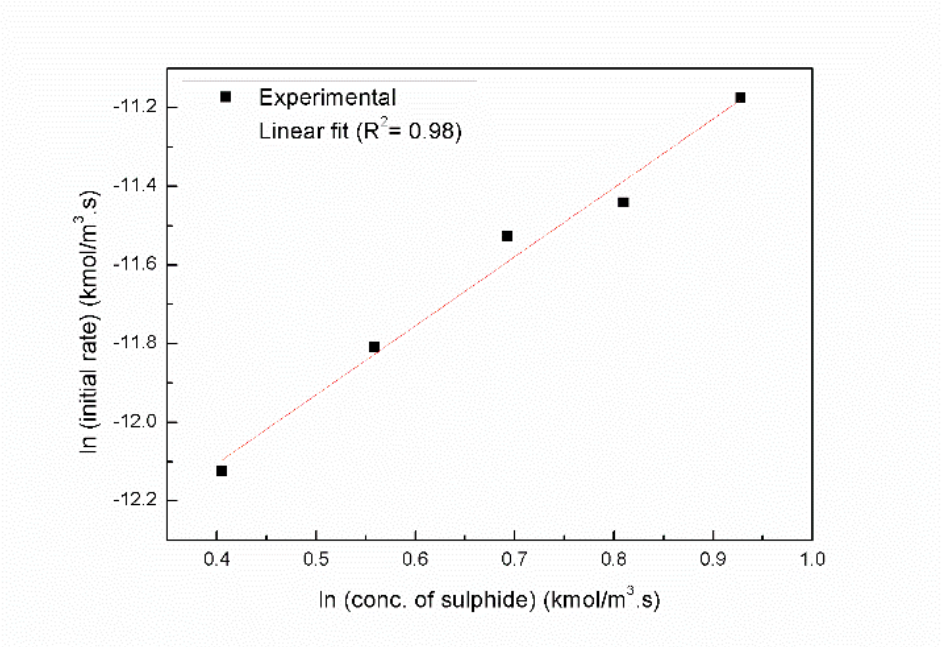

Figure 5.10: Plot of ln (conc. of sulphide) vs. ln (initial rate). All other conditions are same as that reported in **Figure 5.9**.

5.3.6. Effect of MEA concentration

Reactions were carried out at different MEA concentration but at same sulphide concentration, other factors were kept constant. The observations were shown in Figure 5.11. MEA as such does not take part in the reaction, but change of its concentration does affect the equilibrium among MEA, H_2S and water. [10] As mentioned in Scheme 1, in the aqueous phase sulphide (S^{2-}) and hydrosulphide (HS^-) active anions were formed and theses two active anions were responsible for two different reactions (Equation 5.1 & 5.2). Presence of MEA base favours more ionisation and sulphide ions (S^{2-}) dominates over hydrosulphide ions (HS^-) in the aqueous phase. So, the existence of two reactions can be proved only by variation of concentration of MEA in the aqueous phase with a fixed sulphide concentration.

Various MEA concentrations (keeping constant sulphide concentration) were prepared by taking 27 ml of H_2S-laden aqueous MEA (with known sulphide and MEA concentrations) and adding various proportions of pure MEA and distilled water to it to make the total volume to 50 cm^3.

If reduction of m-CNB would follow Equation 5.6 solely and sulphide in aqueous phase got consumed during reaction, then the conversion of m-CNB would have been calculated as 55% from the material balance. Complete conversion of m-CNB can be achieved if

sulphide concentration is provided sufficiently high and reaction follows stoichiometry of Equation 5.5. In this study after 8 hrs of long run 80% conversion of m-CNB was achieved with maximum MEA concentration of 10 kmol/m^3, as shown in the Figure 5.11. This result suggested that the Equation 5.5 was predominant in reduction m-CNB and it is complete disagreement with some researchers worked with ammonium sulphide and suggested that Equation 5.6 is only operative one [7,20,21]. In the literature, the formation of elemental sulphur was not reported for the reduction of nitroarenes with sodium sulphide and it can be assumed that this reaction follows the stoichiometry of Equation 5.5 via transfer of sulphide ions [3,5]. For a fixed sulphide concentration in the aqueous phase, the increase in MEA concentration resulted in higher sulphide ions that pushed the conversion of m-CNB up.

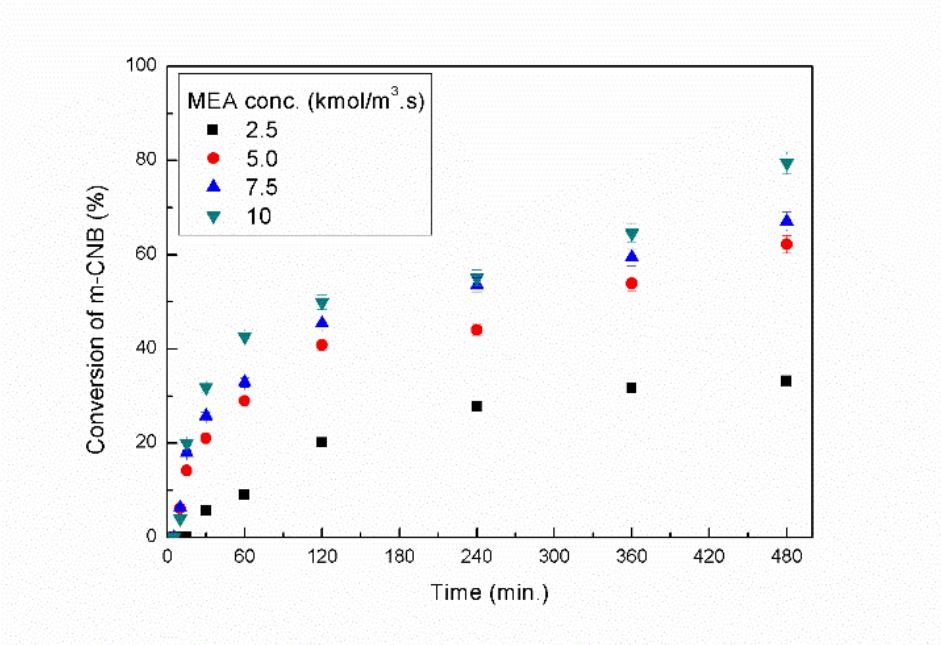

Figure 5.11: Effect of MEA Concentration Operating Conditions: Volume of organic phase = 5 x 10^{-3} m^3, Volume of Aqueous Phase = 5 x 10^{-3} m^3l, Concentration of m-CNB =1.27 kmol/m^3 in org. phase, concentration of toluene = 8.17 kmol/m^3 in org. phase, concentration of catalyst = 0.58 kmol/m^3 in org. phase, Sulphide concentration = 1.39 kmol/m^3, Stirring speed = 1500 rpm, Temperature= 323K.

5.2.3.7. Reusability of the catalyst

After the completion of the kinetic run, the agitation was stopped and the phases were allowed to separate in a separating funnel into three layers (L-L-S). When the phases were clearly separated, then the aqueous phase along with organic phase containing the product was removed and the solid catalyst was filtered and then washed several times with

distilled water. The recovered catalysts are rinsed with NaCl solution and then dried at 50^{o}C to remove any absorbed species. The catalyst obtained was reused and the data obtained was plotted for three reuse as shown in Figure 5.12. It can be seen that up to the three cycles, the catalyst can be used without a significant decrease in conversion, indicating that the catalyst has got excellent reusable and recyclable property and high stability.

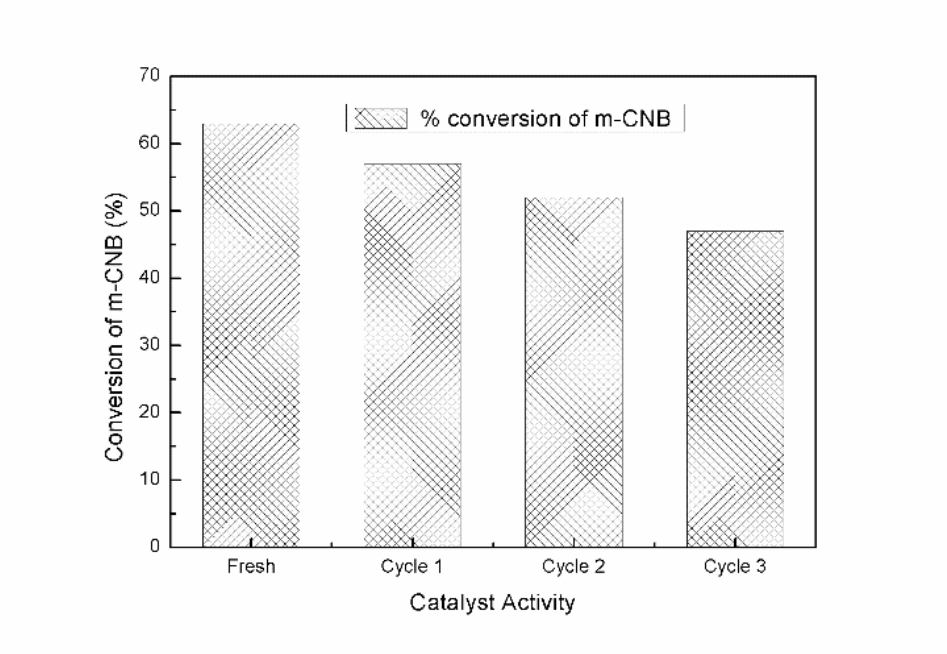

Figure 5.12: Conversion of m-CNB with the cycle number.

5.2.3.8. Validation of kinetic model

The kinetic model was validated by considering Equation 5.29 was valid at different temperatures by plotting of $-ln\ (1- X_A)$ against time (Figure 5.13). The slope of each line gives apparent rate constant k_{app} at different temperatures as shown in Table 5.2. Figure 5.14 represents a comparison of calculated conversions of m-CNB based on these rate constants and experimentally obtained conversions of m-CNB. Good agreement has been observed between calculated and experimental conversions.

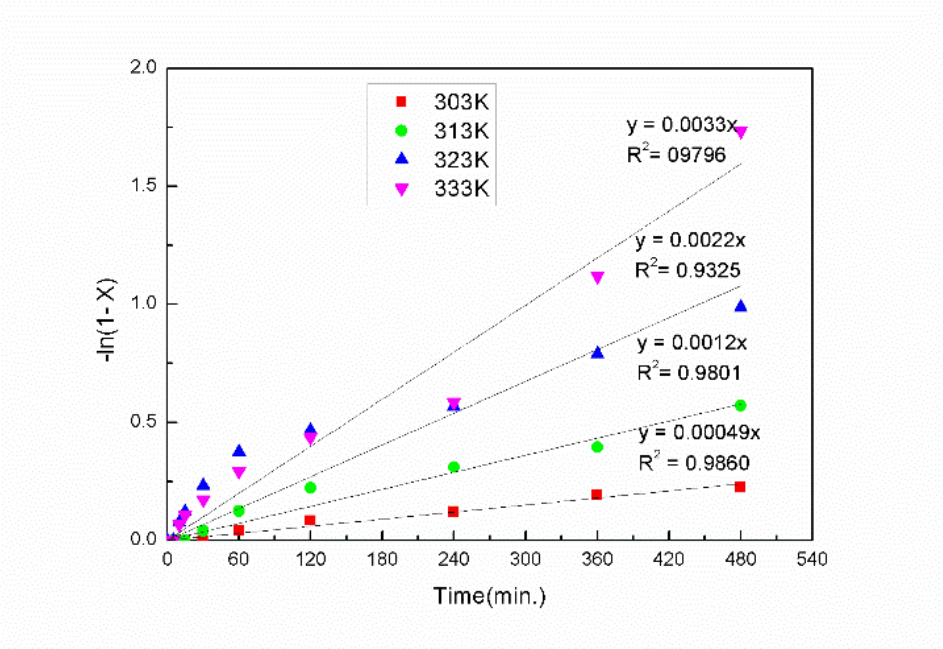

Figure 5.13: Validation of the kinetic model with experimental data at different temperature. Operating Conditions: Volume of organic phase = 5 x 10^{-3} m^3, Volume of Aqueous Phase = 5 x 10^{-3} m^3, concentration of toluene= 8.17 kmol/m^3 in org. phase, concentration of m-CNB = 1.27 kmol/m^3 in org. phase, concentration of catalyst = 0.58 kmol/m^3 in org. phase, Sulphide concentration – 2.53 kmol/m^3, concentration of MEA = 5.787 kmol/m^3, Stirring speed = 1500 rpm.

Table 5.2 Apparent rate (k_{app}) constants at different temperatures[b]

Temperature (^oC)	30	40	50	60
$k_{app} \times 10^3$ (min^{-1})	0.49	1.20	2.25	3.33

[b]All considerations are the same as mentioned in **Figure 5.13**.

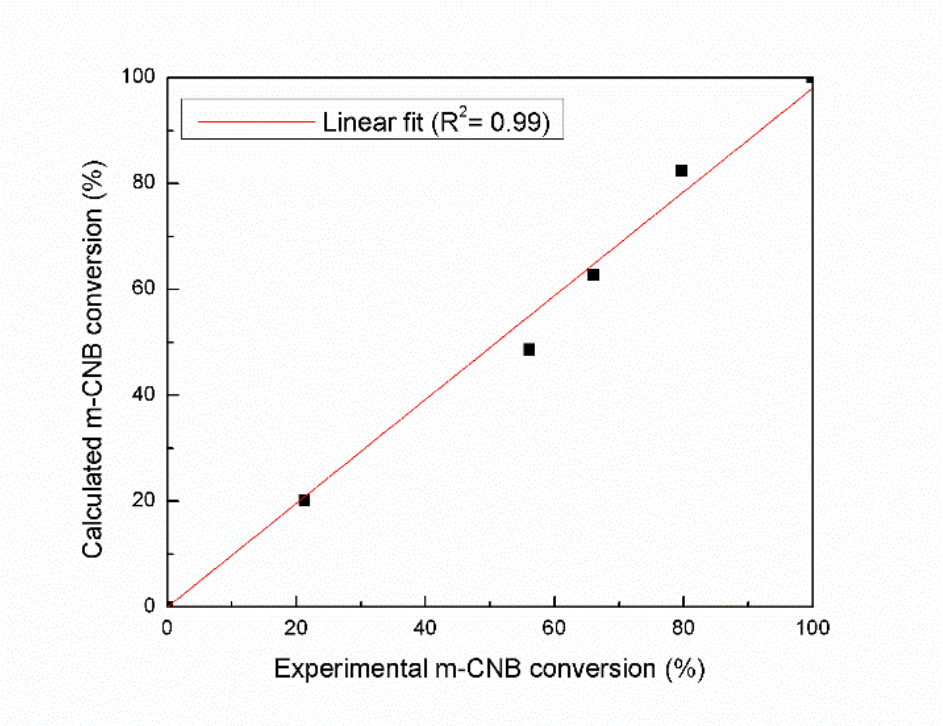

Figure 5.14: Comparison of calculated and experimental m-CNB conversions at 480 min different temperatures. All conditions are as same as **Figure 5.13**.

5.4. Conclusions.

The Zinin reduction of m-CNB by H_2S-laden MEA was studies under L-L-S mode in presence of solid reusable PTC, Amberlite IR-400 to yield m-CA as the sole product. The reaction was found to be kinetically controlled with an apparent activation energy of 56.16 kJ/mol. The rate of reduction was found to be first order with respect to the concentration of catalyst and reactant and second order with respect to the concentration of sulphide. The process was found to follow a complex mechanism involving different ions and molecules. Based on detailed kinetic studies and proposed mechanism, a kinetic model was developed considering aqueous phase equilibria of H_2S-MEA-H_20 system and interfacial mechanism for insoluble PTC. The developed model predicts conversion of m-CNB reasonable well at all temperatures.

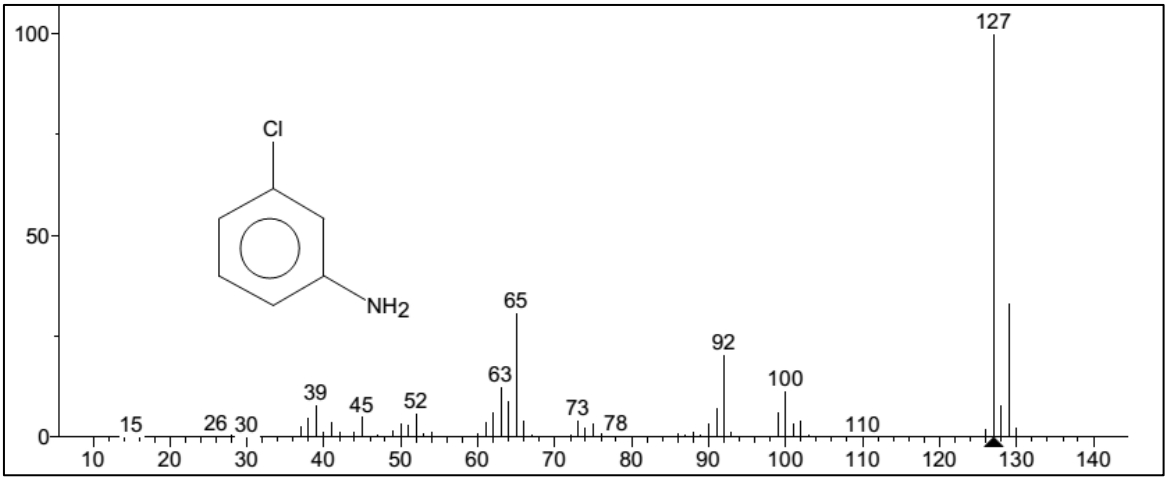

Figure 5.15: MS spectra of m-chloroaniline.

References

1 W. G. Dauben, *Organic reactions*, John Wiley & Sons, Inc., New York, 1973.

2 R. R. Bhave and M. M. Sharma, *J. Chem. Technol. Biotechnol.*, 1981, **31**, 93–102.

3 N. C. Pradhan and M. M. Sharma, *Ind. Eng. Chem. Res.*, 1992, **31**, 1606–1609.

4 N. C. Pradhan, *Indian J. Chem. Technol.*, 2000, **7**, 276–279.

5 G. D. Yadav, Y. B. Jadhav and S. Sengupta, *Chem. Eng. Sci.*, 2003, **58**, 2681–2689.

6 G. D. Yadav, Y. B. Jadhav and S. Sengupta, *J. Mol. Catal. A Chem.*, 2003, **200**, 117–129.

7 H. Gilman, Wiley, New York, 1941, p. 52.

8 H. Beutier, D; Renon, *Ind. Eng. Chem. Process. Des. Dev*, 1978, **17**, 220–230.

9 S. K. Maity, N. C. Pradhan and A. V. Patwardhan, *Appl. Catal. A Gen.*, 2006, 301, 251–258.

10 S. K. Maity, N. C. Pradhan and A. V Patwardhan, *Ind. Eng. Chem. Res.*, 2006, **46**, 7767–7774.

11 S. Desikan and L. K. Doraiswamy, *Ind. Eng. Chem. Res.*, 1999, **38**, 2634–2640.

12 G. D. Yadav and S. V. Lande, *Ind. Eng. Chem. Res.*, 2007, **46**, 2951–2961.

13 M. Wang, H. Yang and T. K. Model, *Ind. Eng. Chem. Res.*, 1991, **30**, 2384–2390.

14 M. Wang and H. Yang, *Ind. Eng. Chem. Res.*, 1992, **31**, 1868–1875.

15 S. Desikan and L. K. Doraiswamy, *Ind. Eng. Chem. Res.*, 1995, **34**, 3524–3537.

16 J. A. B. Satrio, H. J. Glatzer and L. K. Doraiswamy, *Chem. Eng. Sci.*, 2000, **55**, 5013–5033.

17 S. K. Maity, N. C. Pradhan and A. V. Patwardhan, *Chem. Eng. J.*, 2008, **141**, 187–193.

18 S. K. Maity, N. C. Pradhan and A. V. Patwardhan, *Chem. Eng. Sci.*, 2007, **62**, 805–813.

19 S. K. Maity, N. C. Pradhan and A. V. Patwardhan, *Appl. Catal. B Environ.*, 2008, **77**, 418–426.

20 G. R. W. R. Meindl, E. V. Angerer, H. Schonenberger, *J. Med. Chem.*, **27**, 1111–1118.

21 N. F. Lucas, H J, Scudder, *J. Am. Chem. Soc.*, 1928, **50**, 244–249.

Abstract

In this chapter a new and unique method for utilizing H_2S-rich MDEA (which could be obtained from amine treating unit (ATU) of petroleum refinery) for reduction of m-chloronitrobenzene (m-CNB) in the presence of tetra-n-butylphosphoniumbromide (TBPB) as phase transfer catalyst under liquid-liquid mode (LLPTC) has been demonstrated. The kinetic model of LLPTC process has been developed and then validated against experimental data. A suitable mechanism was proposed to explain the complex reaction steps.

6.1 Introduction

In a new and efficient method to capture and utilize hydrogen sulfide (H_2S), commercially important methyldiethanolamine (MDEA) has been utilized to capture H_2S and chloronitrobenzenes (CNBs) have been selectively reduced by this H_2S-rich MDEA. The reduction reaction of CNBs was carried out under liquid-liquid mode mode of reaction in the presence of tetra-n-butylphosphonium bromide (TBPB) as phase transfer catalyst (PTC). The reaction was found to be kinetically controlled and the apparent activation energy was estimated as 33.34 kJ/mol for reduction of m-chloronitrobenzene. Yield and selectivity of the product amine were found to be 100%. Parametric studies were performed to determine the kinetics of the modified Zinin reduction and to optimize the process parameters like stirring speed, reaction temperature, the concentration of catalyst, reactant concentration, concentration of aqueous sulphide, concentration of MDEA, elemental sulfur loading for process intensification and maximizing the yield and selectivity of the product amine. Effect of various phase transfer catalysis such as Tetrabutylammonium bromide (TBAB), Tetrabutylammonium chloride (TBAC), Tetrabutylphosphonium bromide (TBPB), Tetramethylammonium bromide (TMAB), Cetyltrimethylammonium bromide (CTMAB) and Ethyltriphenylphosphonium bromide (ETPPB) was evaluated under otherwise similar experimental conditions. A suitable mechanism was proposed to explain the complex reaction steps. A kinetic model of LLPTC process has been developed based on proposed mechanism and then successfully validated against experimental data. The current approach of utilizing H_2S for the production of valuable chemicals like amines is very much promising and can be utilized to replace energy-expensive Claus process.

6.2 RESULTS AND DISCUSSION

6.2.1 The proposed mechanism of L-L PTC

Zinin in 1842 proposed the overall stoichiometry for the reduction of nitrobenzene by aqueous ammonium sulphide , is shown in Equation (6.1).[1] According to the literature reduction reaction of nitroaromatic compounds by sodium sulphide also follows similar stoichiometry [41, 45, 63–65].

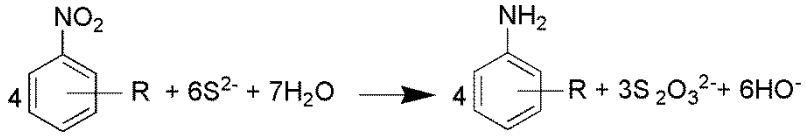

(6.1)

The production of elemental sulphur as a byproduct during reduction of nitroarenes by aqueous ammonium sulphide other than thiosulphate also documented in the literature, when nitroarenes were reduced. Elemental sulphur was produced during the reduction reaction of the p-nitrophenylacetic acid with aqueous ammonium sulphide to prepare p-aminophenylacetic acid and the stoichiometry is shown in Equation (6.2) [7].

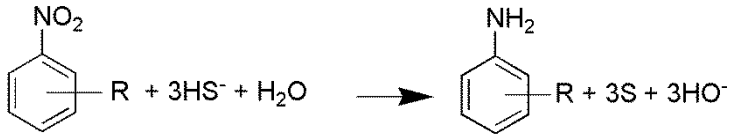

(6.2)

Reactions shown in (Equation (6.1) and (6.2)) suggests that both the anions (S^{2-}& HS^{-}) are participating in the reduction reactions and thiosulphate or elemental sulphur is produced as a byproduct respectively. The presence of a base (ammonia)favours more ionisation in the aqueous phase [8] and with the increase of ammonia concentration in the aqueous phase the concentration of sulphide ions (S^{2-}) in comparison of hydrosulphide (HS^{-}) ions increases.

The reactions shown above suggests that reduction of CNB can lead to the formation of either thiosulphate or elemental sulphur. Therefore a detailed study of the current reaction taken is of great significance for both commercially and academically.

A general reaction mechanism of current reduction reaction has been prepared based on the current investigation and some previous studies on reduction reaction of nitroaromatic compounds by sodium sulphide (Scheme 1) [2,6,9,10]. Sulphur is a multivalency element (-2 to +6) and therefore can in different anionic form ($HS^{-}, HSO^{-}, HSO_2^{-}, HSO_3^{-}$) which can rapidly pair with quaternary cations in comparison with other anions that require more than one quaternary cations ($Q_n^{+}X^{-}$) [6].The nitro group attached to the benzene ring is reduced by the transfer of electrons from the sulphide ions present in the aqueous sulphide solution.

Current liquid-liquid PTC system consists of an organic phase (organic reactant dissolved in organic solvent), an aqueous phase (H_2S absorbed in the aqueous MDEA solution) and quaternary phosphonium salt as a phase transfer catalyst, soluable in both the phases.
PTC mechanism has been expained by two approaches 1. extraction mechanism by Stark's [11] 2. Interfecial mechanism by Makosza's [12]. When increase of reaction rate is proportionately related with higher organophilicity or in terms of longer quaternary ions and catalyst concentration but it is not related with stirring speed i.e. reaction rate remains constant even at higher stirring speed, then the reaction is following extraction mechanism [13,14]. Macosza's interfacial mechanism is highly dependent on stirring speed. From the experimental results it is very clear that reaction rate is independent on stirring speed, but highly dependent on catalyst concentration, sulphide concentration and temperature, which made creent reaction following Stark's extraction mechanism. Reduction reaction of CNB can be explained by Starks extraction mechanism, according to the mechanism the catalyst is partitioned into the both phases, then anions (nucleophiles) present in the aqueous phase is get transferred to the organic phase by attaching with catalyst cations and react with the organic substrate in the organic phase.

H_2S reacts with MDEA in the aqueous phase to form sulphide (S^{2-}) and hydrosulphide ions (HS^-) anions (Scheme 1). Sulphide (S^{2-}) and hydrosulphide (HS^-) ions form an ionic equilibrium in the H_2S-laden aqueous alkanolamine (MDEA) solution as shown in Equation (6.4) to Equation (6.7) (Scheme 1). As stated earlier, because of the presence of the two anions, thiosulphate or elemental sulphur produced as a byproduct in the aqueous phase. But both ions are unavailable in aqueous sodium sulphide solution which makes aqueous ammonium sulphide and H_2S-laden aqueous alkanolamine solutions different.

Quaternary cations (Q^+) readily pairs with hydrosulphide (HS^-) ions at the interphase to form Q^+HS^- ion pair and transfer to the organic phase. Then, active ion pair Q^+HS^- go through a series of reactions in the organic phase, is shown in Scheme 1 (Equation 6.13 to 6.18). Reactions occur in the vicinity of the interphase, as anions (S^{2-} and HS^-) present in the aqueous phase reacts with the organic substrate present in the organic phase, which it is very little soluable in the aqueous phase. Product formation in the absence of catalyst poves this phenomenon.

The following mechnism elaborates the contribution of several elementory reactions in the organic phase to the over all rate of the reaction. After a series of elementary reactions, m-CNB is reduced to form chloroaniline (m-CA). Some intermediates (m-chlorophenylhydroxyl-amine and m-chloronitrosobenzene) have formed during the

cource of reaction, none of them have not been detected in GC-MS analysis. The formation of these two intermediate products during Zinin reduction is confirmed by other scientist [6,15]. As the formation and depletion of those intermediates is very fast, so they remain undetected. Some water molecules also transferred to the organis phase along with the catalyst cation anion pair and took part in the reaction in the organic phase (Equation (6.16) to (6.17)). At the end of the series of elementary reactions, the inactive ion pair $Q^+HSO_3^-$ formed in the organic phase and then returns to the aqueous phase and gets regenarated (Q^+HS^-) after reacting with S^{2-} ions (15). Then the regenerated quaternary cations anion pair is again transferred to the organic phase and take part in the reaction.

According to this proposed mechanism the catalyst cations are pairing with some anions in the organic phase during the reactions, though the most of the catalyst cations remain in Q^+HS^- form and the whole catalysis cycle goes on. In the aqueous phase nine reactions (Equation (6.3) to (6.11)) took place and remaining reactions (Equation (6.12) – Equation (6.17)) occurred in the organic phase. 100% selectivity of the product (m-CA) was achieved at the end of the reaction.

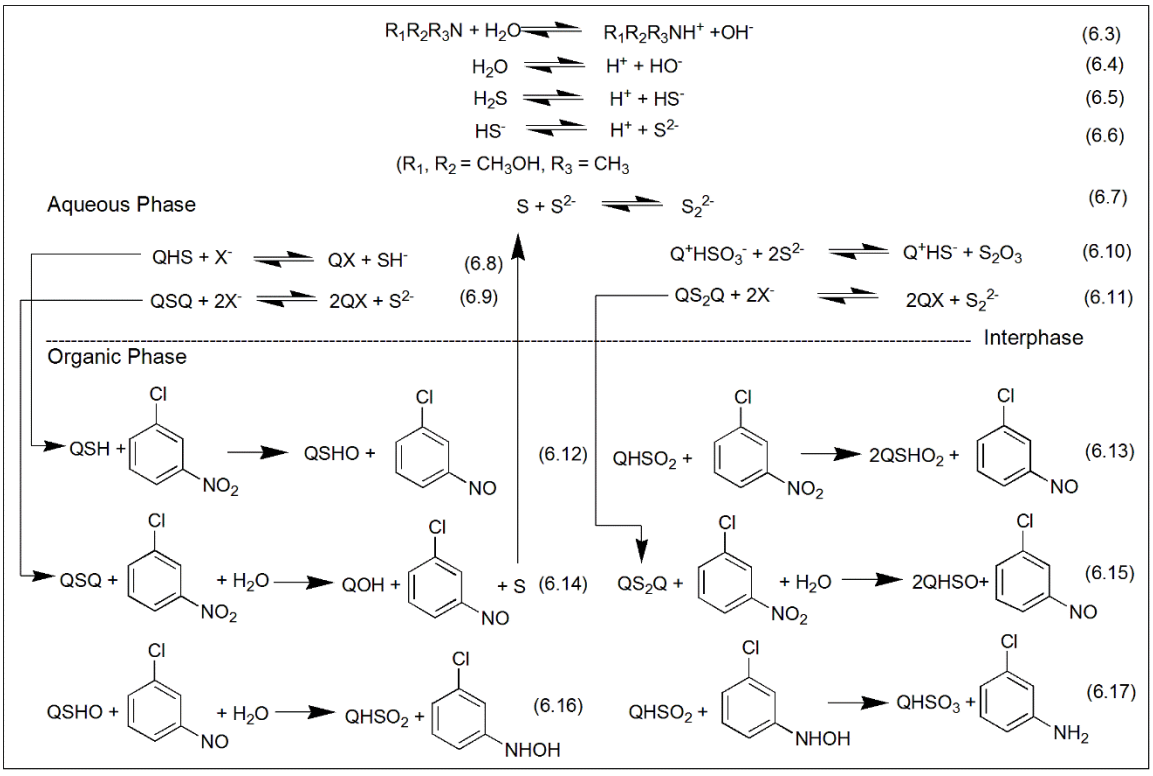

Scheme 6.1. The proposed mechanism of reduction of m-CNB by H_2S-laden MDEA under L-L PTC.

6.2.2 Kinetic modelling

According to the proposed mechanism Scheme 1, the population of Q^+HS^- active ion pair is higher in comparison with other anions. A kinetic model has been prepared based on the following assumptions, (1) aqueous phase reactions reach equilibrium almost instantaneously, (2) the model of the whole PTC reaction is developed accordingly to the proposed mechanism and (3) the interphasic reactions are very slow and not included in modeling as the aqueous phase and organic phase reactions are more significant.

The current study of reduction of m-CNB by H_2S-laden MDEA solution is a liquid-liquid PTC system, where toluene was used as an organic solvent and m-CA was the main product in the organic phase along with $S_2O_3^-$ as a by-product in the aqueous phase. The overall reaction is as shown in the Equation (6.1).

Current L-L PTC system is provided with mechanical stirring at 1500 rpm for eliminating mass transfer effect. In the aqueous phase, reaction between Q^+X^- ($X^- = Cl^-$) and HS^- was the first ion exchange reaction and forms an active ion pair (Q^+HS^-). A number of transition anions were produced during the reduction reaction and finally an inactive ion pair $Q^+ HSO_3^-$ formed in the organic phase. Then the inactive ion pair was transferred to the aqueous phase and got regenerated (Q^+HS^-) after reacting with S^{2-} ions via redox reaction.

Reaction steps involved according to Scheme 1 are:

1. In-active ion pair, being lipophobic in nature, got transferred to the aqueous phase from the organic phase. For the step of reaction equilibrium constant, say K_1, is given by

$$K_1 = \frac{C_{QSHO_3}^{aq}}{C_{QSHO_3}^{org}} \tag{6.18}$$

2. Reaction (11) is the catalyst regeneration step of the reaction mechanism, which can be written as the following equation (6.20),

$$K_2 = \frac{k_1}{k_1'} = \frac{C_{QHSO_3}^{aq} C_{S_2O_3}^{aq}}{C_{QHSO_3}^{aq} C_{S^2}^{aq}} \tag{6.19}$$

3. Initially added catalyst QX migrated from organic phase to aqueous phase. Other active catalysts QSH, QSQ and QS_2Q , which are formed in the aqueous, diffused to organic phase and equilibrium constants for each diffusion step are K_3, K_4, K_5, K_6,

$$K_3 = \frac{C_{QX}^{aq}}{C_{QX}^{org}} \tag{6.20}$$

$$K_4 = \frac{C_{QHS}^{org}}{C_{HS}^{aq}} \tag{6.21}$$

$$K_5 = \frac{C_{QSQ}^{org}}{C_{QSQ}^{oq}} \quad (6.22)$$

$$K_6 = \frac{C_{QS_2Q}^{org}}{C_{QS_2Q}^{aq}} \quad (6.23)$$

4. The rate of the reaction is determined by the reactions occurred in organic phase. Among all the organic phase reactions (Equation (6.12) to Equation (6.17)), The slowest reaction is Equation (6.12) and hence it determines the overall rate, in which ArNO is formed [6]. Elemental sulphur production in the system as a by-product has made the Equation (6.14) as a contributor to the overall rate of the reduction reaction. Some water molecules also get transferred to the oragnic phase along with other ion pairs.

$ArNO_2$is the limiting reactant and thus it is taken as the basis of the reaction. So the rate of reaction of $ArNO_2$ can be expressed by following Equation (6.24), where k_2-k_4 are the reaction rate constants for the reactions of Equation 6.12, 6.14, and 6.15 shown in Scheme 6.1.

$$-\frac{dC_{\mathrm{ArNO_2}}^{org}}{dt} = k_2 C_{\mathrm{ArNO_2}}^{org} C_{QSH}^{org} + k_3 C_{o\,\mathrm{ArNO_2}}^{org} C_{QSQ}^{org} C_{H_2O}^{org} + k_4 C_{\mathrm{ArNO_2}}^{org} C_{QS_2Q}^{org} C_{H_2O}^{org} \quad (6.24)$$

The total number of $[H_2O]$ molecules along with other anions transferred to the organic phase is very little in contrast to that of active ion pairs (Q^+HS^-), so it can be ignored from Equation (6.24) and the reaction in Equation (6.12) is assumed to be the main rate determining step. The reactions shown in Equation (6.14) and Equation (6.15) can be ignored and the Equation (6.24) can be rewritten as

$$-\frac{dC_{\mathrm{ArNO_2}}^{org}}{dt} = k_2 C_{\mathrm{ArNO_2}}^{org} C_{QSH}^{org} \quad (6.25)$$

The mole balance of catalyst cations is given by,

$$V^o C_{QX}^* = V^{aq}\left\{C_{QX}^{aq} + C_{QSH}^{aq} + C_{QSQ}^{aq} + C_{QS_2Q}^{aq} + C_{QHSO_3}^{aq}\right\}_{aq} + V^{org}\left\{C_{QX}^{org} + C_{QSH}^{org} + C_{QSQ}^{org} + C_{QS_2Q}^{org} + C_{QHSO_3}^{org}\right\}_{org} \quad (6.26)$$

The initial concentration of catalyst is denoted by $[QX]^*$, the volume of aqueous phase and organic phase is denoted by V^a and V^o respectively. Therefore,

$$C_{QX}^* = \frac{V^{aq}}{V^{org}}\left\{C_{QX}^{aq} + C_{QSH}^{aq} + C_{QSQ}^{aq} + C_{QS_2Q}^{aq} + C_{QHSO_3}^{aq}\right\}_{aq} + \left\{C_{QX}^{org} + C_{QSH}^{org} + C_{QSQ}^{org} + C_{QS_2Q}^{org} + C_{QHSO_3}^{org}\right\}_{org} \quad (6.27)$$

Substituting Equation (6.18), (6.20), (6.21), (6.22) and (6.23) in the equation (6.27), we get

$$C^*_{QX} = \frac{V^{aq}}{V^{org}}\left\{K_3\, C^{org}_{QX} + \frac{C^{org}_{QSH}}{K_4} + \frac{C^{org}_{QSQ}}{K_5} + \frac{C^{org}_{QS_2Q}}{K_6} + K_1 C^{org}_{QHSO_3}\right\}_{aq} + \left\{ C^{org}_{QX} + C^{org}_{QSH} + C^{org}_{QSQ} + C^{org}_{QS_2Q} + C^{org}_{QHSO_3}\right\}_{org} \quad (6.28)$$

The total concentration of catalyst cations present in the organic phase is given by,

$$C^T_Q = C^{org}_{QX} + C^{org}_{QSH} + C^{org}_{QSQ} + C^{org}_{QS_2Q} + C^{org}_{QHSO_3} \quad (6.29)$$

$$1 = \frac{C^{org}_{QX}}{C^T_Q} + \frac{C^{org}_{QSH}}{C^T_Q} + \frac{C^{org}_{QSQ}}{C^T_Q} + \frac{C^{org}_{QS_2Q}}{C^T_Q} + \frac{C^{org}_{QHSO_3}}{C^T_Q} \quad (6.30)$$

If we consider,

$$\frac{C^{org}_{QSH}}{C^T_Q} = \eta_1;\ \frac{C^{org}_{QSQ}}{C^T_Q} = \eta_2;\ \frac{C^{org}_{QS_2Q}}{C^T_Q} = \eta_3;\ \frac{C^{org}_{QHSO_3}}{C^T_Q} = \eta_4;$$

After substituting $\eta_1, \eta_2, \eta_3, \eta_4$ in the Equation (6.31) we get,

$$C^{org}_{QX} = (1 - \eta_1 - \eta_2 - \eta_3 - \eta_4)\, C^T_Q \quad (6.31)$$

The following expressionof total added catalyst concentration can be obtained from Equation (6.28) and Equation (6.29) as

$$C^*_{QX} = \frac{V^{aq}}{V^{org}}\left\{K_3\, \frac{C^{org}_{QX}\, C^T_Q}{C^T_Q} + \frac{C^{org}_{QSH}}{C^T_Q}\frac{C^T_Q}{K_4} + \frac{C^{org}_{QSQ}}{C^T_Q}\,\frac{C^T_Q}{K_5} + \frac{C^{org}_{QS_2Q}}{C^T_Q}\,\frac{C^T_Q}{K_6} + K_1 \frac{C^{org}_{QHSO_3}}{C^T_Q}\, C^T_Q\right\}_a + C^T_Q \quad (6.32)$$

Combining Equation (6.31) and Equation (6.32) yields,

$$C^*_{QX} = \frac{V^{aq}}{V^{org}}\left\{\mathrm{K}_3\, C^T_Q\, (1 - \eta_1 - \eta_2 - \eta_3 - \eta_4) + \eta_1 \frac{C^T_Q}{\mathrm{K}_4} + \eta_2\, \frac{C^T_Q}{\mathrm{K}_5} + \eta_3\, \frac{C^T_Q}{\mathrm{K}_6} + \eta_4\, K_1 C^T_Q\right\}_{\mathrm{a}} + C^T_Q \quad (6.33)$$

Simplifying we get,

$$C^T_Q = \frac{C^{org}_{QX}}{\frac{V^{aq}}{V^{org}}\left\{K_3(1-\eta_1-\eta_2-\eta_3-\eta_4) + \frac{\eta_1}{K_4} + \frac{\eta_2}{K_5} + \frac{\eta_3}{K_6} + \eta_4 K_1\right\}_a + 1} \quad (6.34)$$

According to the Equation (6.1) which represents the conversion can be written as,

$$\text{Conversion(X)} = 1 - \frac{C^{org}_{\mathrm{ArNO_2}}}{C^*_{\mathrm{ArNO_2}}} \quad (6.35)$$

[Where $ArNO^*_2$ is the total amount of added reagent in organic phase]

$$\text{So, } C^{org}_{\mathrm{ArNO_2}} = (1 - X)\, C^*_{\mathrm{ArNO_2}} \quad (6.36)$$

As it is mentioned previously that the elementary reaction (Equation (6.12)) shown in Scheme 1 is the rate-limiting step and if we combine Equation 6.25 and 6.36 together, we get,

$$C^*_{\mathrm{ArNO_2}} \frac{dX}{dt} = k_2\, (1 - X)\, C^*_{\mathrm{ArNO_2}} C^{org}_{QSH} \quad (6.37)$$

Now putting $\eta_1 C_Q^T$ in the place of C_{QSH}^{org} in the Equation (6.37), we get

$$C_{\mathrm{ArNO_2}}^{*} \frac{dX}{dt} = k_2 \ (1 - X) \ C_{\mathrm{ArNO_2}}^{*} \eta_1 C_Q^T \quad (6.38)$$

$$C_{\mathrm{ArNO_2}}^{*} \frac{dX}{dt} = k_2 \ \eta_1 (1 - X) \ C_{\mathrm{ArNO_2}}^{*} \ C_Q^T \quad (6.39)$$

Substituting Equation (6.34) in the Equation (6.39), the following equation is obtained.

$$\frac{dX}{dt} = \frac{k_2 \ \eta_1 \ (1-X) \ C_{QX}^{*}}{\frac{V^{aq}}{V^{org}} \left\{ K_3 (1-\eta_1 - \ \eta_2 - \eta_3 - \eta_4) + \frac{\eta_1}{K_4} + \frac{\eta_2}{K_5} + \frac{\eta_3}{K_6} + \eta_4 \ K_1 \right\}_a + 1} \quad (6.40)$$

$$\frac{dX}{(1-X)} = k_{app} \ dt, \quad (6.41)$$

Where $k_{app} = \frac{k_2 \ \eta_1 \ C_{QX}^{*}}{\frac{V^{aq}}{V^{org}} \left\{ K_3 \ (1-\eta_1 - \ \eta_2 - \eta_3 - \eta_4) + \frac{\eta_1}{K_4} + \frac{\eta_2}{K_5} + \frac{\eta_3}{K_6} + \eta_4 \ K_1 \right\}_a + 1}$, since all the terms of k_{app} are constants and their values can be calculated obtained experimentally.

$$-\ln(1 - X) = k_{app}.t, \quad (6.42)$$

So, it can be concluded from the final expression (Equation (6.42)) that the order of the current reaction is pseudo first order.

6.2.3 Sensitivity analysis

6.2.3.1. Effect of agitation intensity

The stirring speed was varied in the range of 500-2500 rev/min to study the influence of mass transfer resistance on the reaction kinetics and TBPB was used as phase transfer catalyst is shown in Figure 6.1. It is very clear from the figure that, there is no considerable increase in the reaction rate and conversion while the stirring speed increased more than of 500 rev/min. So the stirring speed was maintained at 1500 rev/min during further studies to eliminate mass transfer resistance.

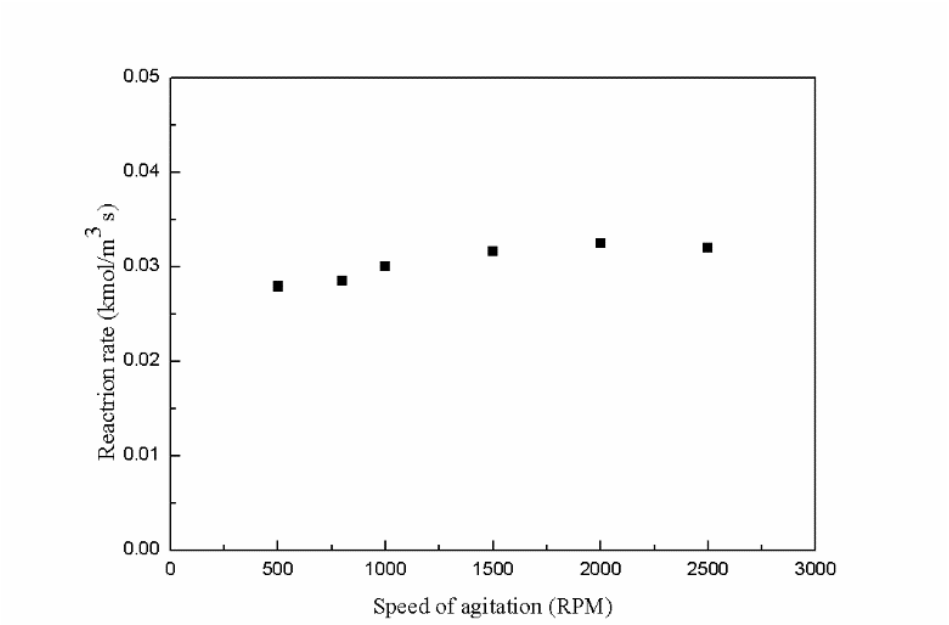

Figure 6.1: Effect of agitation intencity on the reaction rate of m-CNB. Volume of organic phase = 5 x 10^{-5} m^3, m-CNB concentration = 0.63 kmol/m^3 of org. phase, TBPB concentration = 0.044 kmol/m^3 of org. phase, Volume of Aqueous Phase = 5 x 10^{-5} m^3, Sulfide concentration = 2.5 kmol/m^3, MDEA concentration = 3.04 kmol/m^3, temperature = 333 K.

6.2.3.2 Comparison of reactivities of different isomers of CNBs

The conversion of different isomers of CNBs by H_2S-laden aqueous MDEA solution in the L-L PTC mode of reaction has been studied under otherwise identical experimental conditions. The order of the conversion of different isomers of CNBs is MCNB> PCNB> OCNB, as shown in Figure 6.2. The presence of electron donating group in the aromatic ring enhances conversion (or reaction rate) of the reduction reaction and electron withdrawing group play the opposite role. The chloride (Cl^-) group attached to the aromatic ring in the *para* or *ortho* position, is sharing lone pair electrons with the aromatic ring and thus, acts as electron donating group. In this system the nitro group in CNBs is deactivated by external electrophiles (sulphide ions). On the other hand the presence of chloride group in the *meta* position, makes it as an electron withdrawing group and as a result the nitro group become more electron deficient and very prone to attack by sulphide ions. In our results also *meta* isomer has shown more reactivity than other two isomers. The chloride (Cl^-) group present in the *ortho* position felt more

electron withdrawing effect than when it is present in *para* position and therefore the rate of reduction is higher for *ortho* isomer than *para* isomers of CNBs [16].

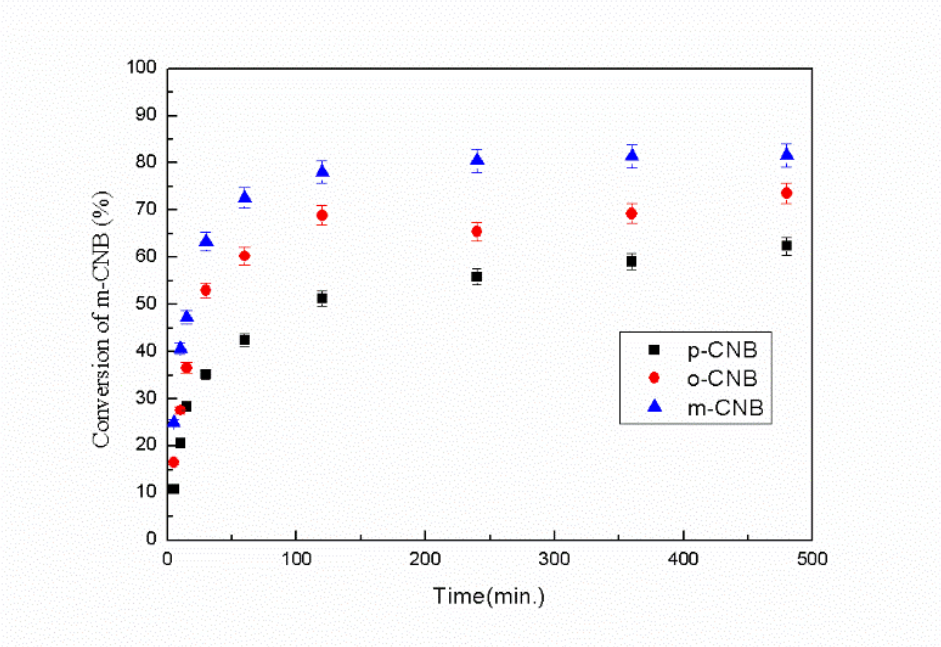

Figure 6.2: Reactivity of different CNBs. Stirring speed = 1500 rpm, Volume of organic phase = 5 x 10^{-5} m^3, CNB concentration = 0.63 kmol/m^3 of org. phase, TBPB concentration = 0.044 kmol/m^3 in org. phase, Volume of Aqueous Phase = 5 x 10^{-5} m^3, Sulfide concentration = 2.5 kmol/m^3, MDEA concentration = 3.04 kmol/m^3, temperature = 333 K.

6.2.3.3 Effect of different phase transfer catalyst. Current reduction process of m-CNB was examined with different phase transfer catalysts. Catalysts were taken for the comparison analysis are Tetrabutylammonium bromide (TBAB), Tetrabutylammonium chloride (TBAC), Tetrabutylphosphonium bromide (TBPB), Tetramethylammonium bromide (TMAB), Cetyltrimethylammonium bromide (CTMAB) and Ethyltriphenylphosphonium bromide (ETPPB). The order of the reactivity of these catalysts is TBPB> TBAB> TBAC> CTMAB> ETPPB> TMAB. A Higher number of carbon atom in the alkyl group of PTC increases lipophilicity and extraction rate, which in turns gives higher productivity. ETPPB which is having higher carbon number although it is showing lower reactivity than other ammonium and phosphonium salts (TBPB, TBAB, and TBAC). As the only single methyl group and three bulky benzyl group attached with quaternary cation in ETPPB, the quaternary cation is not easily accessible for anions and reaction gets slower. The phosphonium salt (TBPB) has shown better reactivity than ammonium salts (TBAB, TBAC). The apparent rate constant are shown in the Table 1 for the six PTC used in the comparison study and TBPB exhibit highest reactivity.

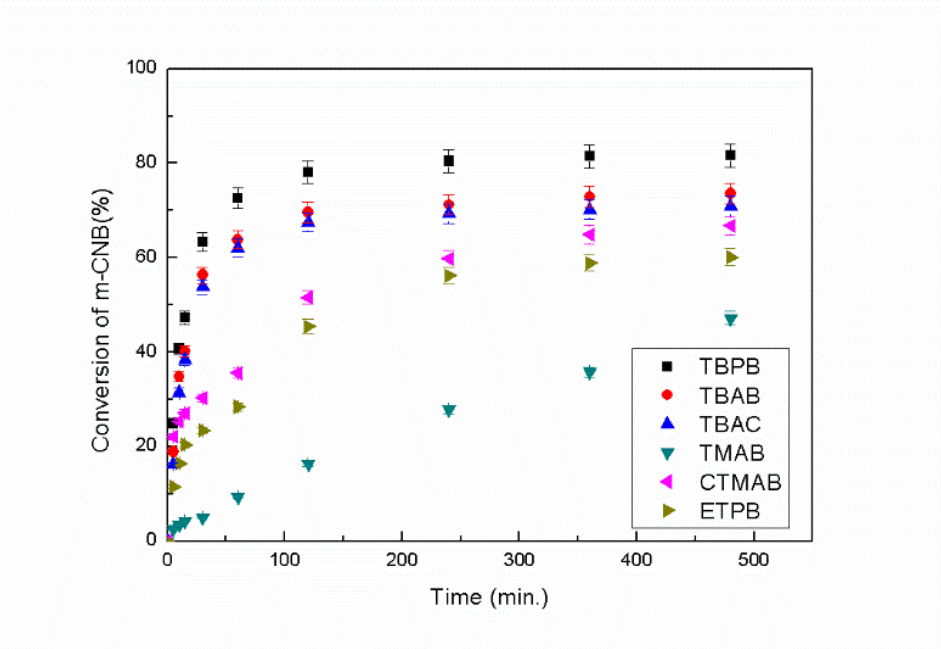

Figure 6.3: Effect of different catalyst on the conversion of m-CNB. Stirring speed = 1500 rpm, Volume of organic phase = 5 x 10^{-5} m^3, m-CNB concentration = 0.63 kmol/m^3 of org. phase, Volume of Aqueous Phase = 5 x 10^{-5} m^3, Sulfide concentration = 2.5 kmol/m^3, MDEA concentration = 3.04 kmol/m^3, temperature = 333 K.

Table 6.1 Effect of the PTC on the apparent rate constants[a]

Catalyst	**k_{app} ($\times 10^2$ min^{-1})**
TBPB	3.61
TBAB	3.03
TBAC	2.80
CTMAB	1.58
ETPPB	1.11
TMAB	0.21

[a]All other conditions are same as Figure 6.3.

6.2.3.4 Effect of temperature

The effect of temperature was investigated under four different reaction temperatures in the range of 313–343K as shown in Figure 6.4. According to the transition state theory, the reaction rate of most organic reactions increases when the reaction temperature is increased and the same phenomenon is also observed for PTC systems. From the Figure 6.4, it is evident that with the rise of reaction temperature the reactivity (conversion) of m-CNB also increases because the activation energy of molecules required is easily achieved and more molecules react to form the product. Collision theory suggests that at higher temperature the number of effective collision between molecules increases and hence the rate of reaction also increases.

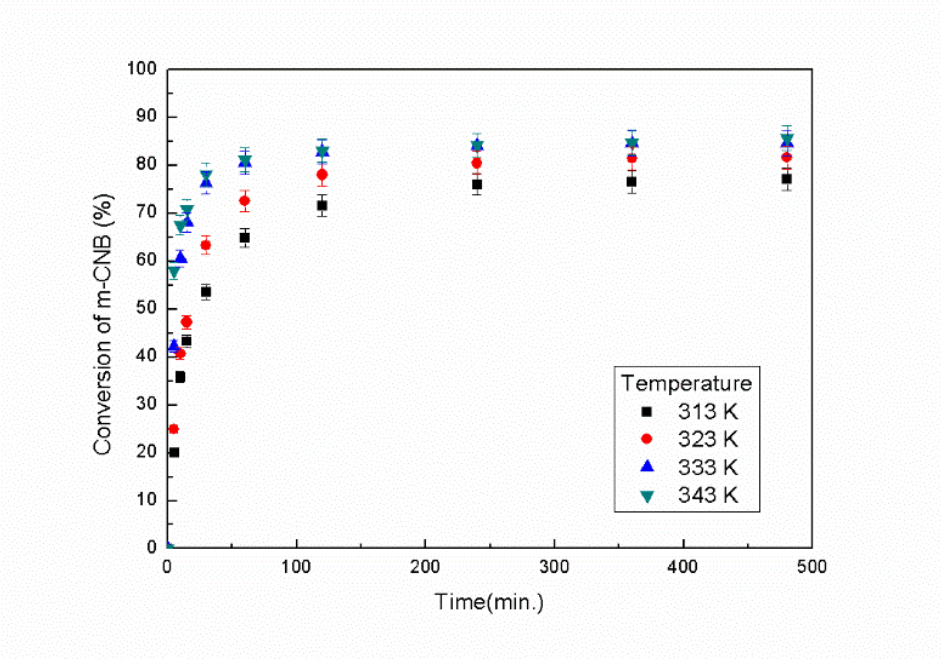

Figure 6.4. Effect of Temperature on the conversion of m-CNB. Stirring speed = 1500 rpm, Volume of organic phase = 5 x 10^{-5} m^3, m-CNB concentration = 0.63 kmol/m^3 of org. phase, TBPB concentration = 0.044 kmol/m^3 in org. phase, Volume of Aqueous Phase = 5 x 10^{-5} m^3, Sulfide concentration = 2.5 kmol/m^3, MDEA concentration = 3.04 kmol/m^3.

Initial rates of reaction at different temperatures were calculated and an Arrhenius plots of *ln* (initial rate) vs. 1/T was plotted (Figure 6.5). The apparent activation energy of current reaction was obtaines as 20.24 kJ/mol. Thus, the current reduction reaction can be considered as a kinetically controlled reaction as the activation energy is high. Reduction reaction of nitrotoluene by ammonium sulphide in L-L PTC system also higher activation energy.

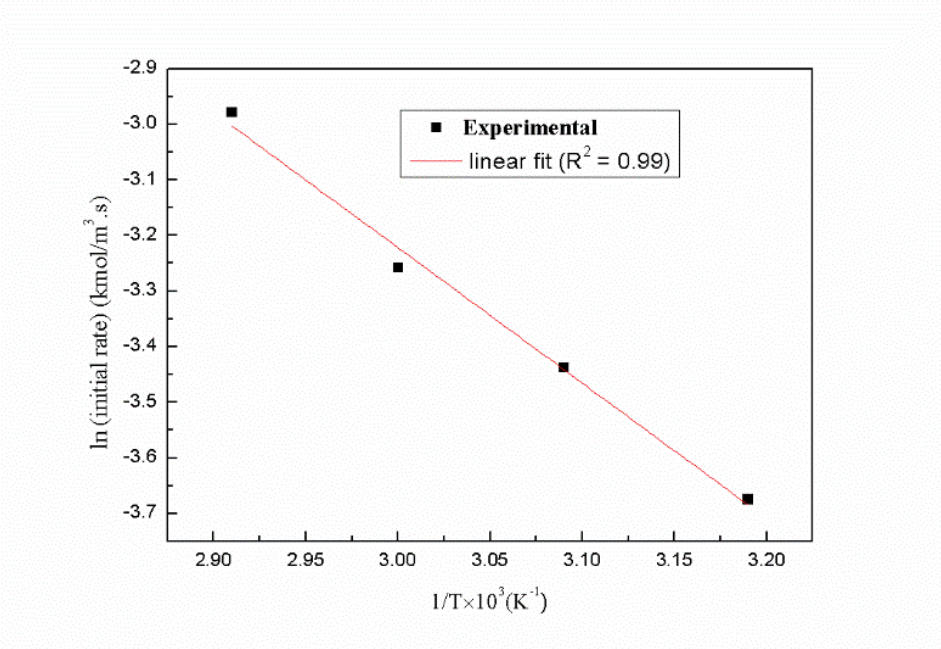

Figure 6.5. Plot of ln (initial rate) vs. vs. 1/T. All other conditions are same as Fig.6. 4.

6.2.3.5. Effect of Catalyst loading. Catalyst loading is a very important parameter for L-L PTC system. In this study catalyst loading is varied in the range of 0 – 0.074 kmol/m^3, as shown in Figure 6.5. The conversion of m-CNB is increased with the increase in catalyst concentration in the L-L PTC system. When the catalyst concentration was increased from zero to 0.074 kmol/m^3, CNB conversion also increased to 83% from 23% after 8 hours of reaction. Table 6.2 shows the enhancement factors, that is a ratio between the rates of reaction at different catalyst loading to that without any catalyst loadings. Table 1 shows the enhancement factors, that is a ratio between the rates of reaction at different catalyst loading to that without any catalyst loadings. The highest enhancement factor obtained was 99 with 0.074 kmol/m^3 of catalyst loading. Similar results also obtained while using TBAB as a phase transfer catalyst and sodium sulphide as reducing agent used for the reduction of p-nitroanisle [6].

Table 6.2. Effect of catalyst loading on Initial reaction rate[a]

Concentration of TBPB (kmol/m^3 org phase)	Initial reaction rate (kmol/m^{3}s)	Enhancement factor
0	0.0005	1
0.0310	0.0273	51
0.0465	0.0346	65
0.0620	0.0412	77
0.0775	0.0527	99

[a]All other conditions are same as Figure 6.4.

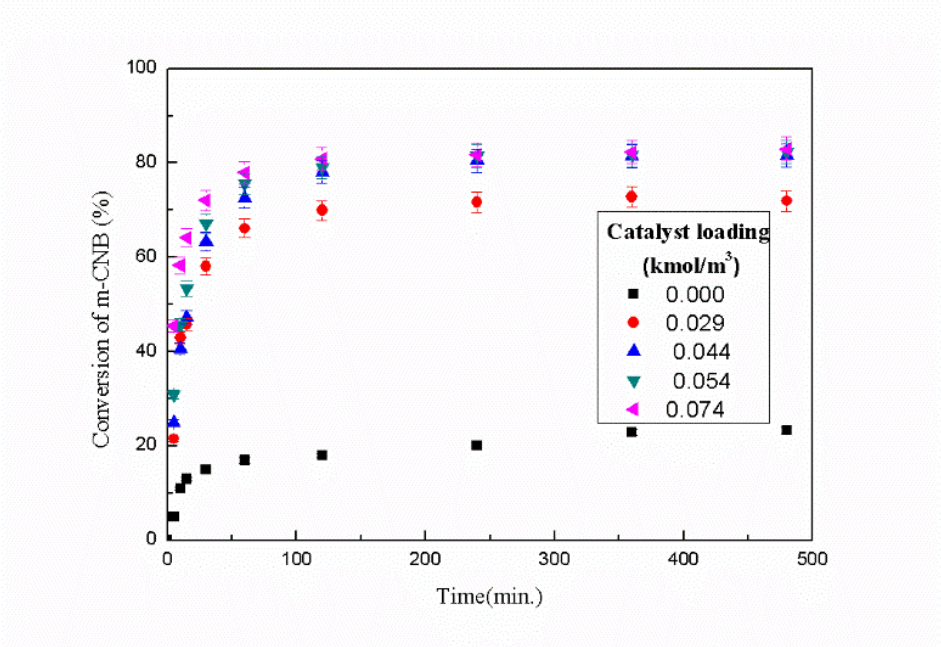

Figure 6.6. Effect of Catalyst loading (TBPB) on the conversion of m-CNB. Stirring speed = 1500 rpm, Volume of organic phase = 5 x 10^{-5} m^3, m-CNB concentration = 0.63 kmol/m^3 of org. phase, Volume of Aqueous Phase = 5 x 10^{-5} m^3, Sulfide concentration = 2.5 kmol/m^3, MDEA concentration = 3.04 kmol/m^3, temperature = 333 K.

6.2.3.6. Effect of concentration of m-CNB

The influence of m-CNB concentration on the conversion was studied in the range of 0.126 -0.952 kmol/m^3 in the L-L PTC system, as shown in Fig.6.7. It is clear from the figure that with the conversion CNB is decreased with a higher concentration of m-CNB. At the beginning the reaction rate increases with higher CNB concentration but it eventually decreases after some time as the total available sulphide concentration is fixed

in the system. A similar phenomenon was observed in the reduction reaction of nitroarenes by aqueous sodium sulphide [6].

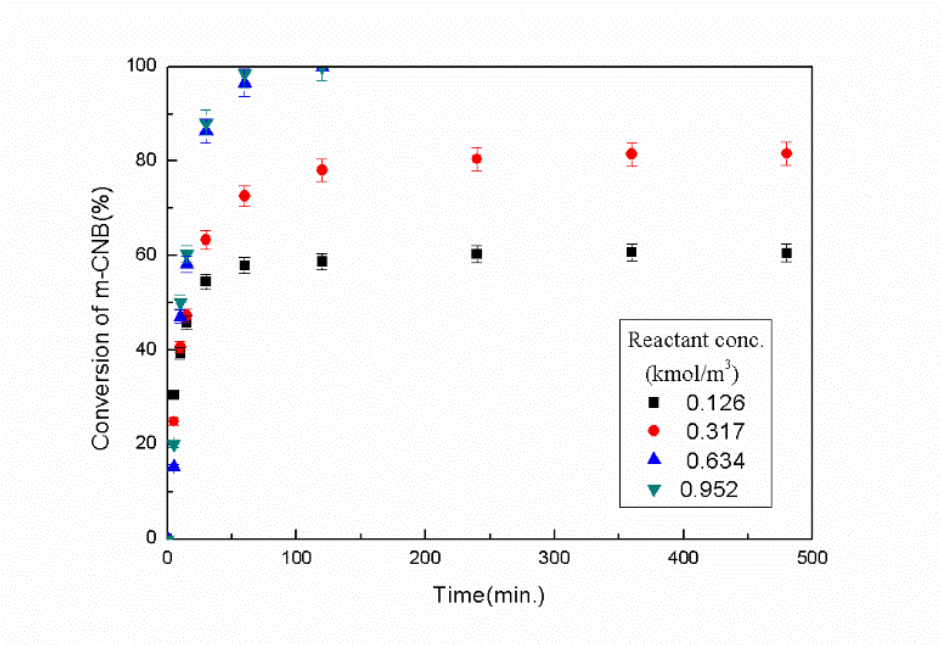

Figure 6.7. Effect of Reactant concentration on the conversion of m-CNB. Stirring speed = 1500 rpm, Volume of organic phase = 5 x 10^{-5} m^3, TBPB concentration = 0.044 kmol/m^3 in org. phase, Volume of Aqueous Phase = 5 x 10^{-5} m^3, Sulfide concentration = 2.5 kmol/m^3, MDEA concentration = 3.04 kmol/m^3, temperature = 333 K.

6.2.3.7. Effect of sulphide concentration

Figure 6.8 shows the effect of aqueous phase sulphide concentration on the conversion of m-CNB at four sulphide concentration in the range of 1 to 2.5 kmol/m^3, keeping other parameters values unchanged, as shown in Figure 6.8. The conversion of m-CNB and the reaction rate enhances with the increase in aqueous phase sulphide concentration.

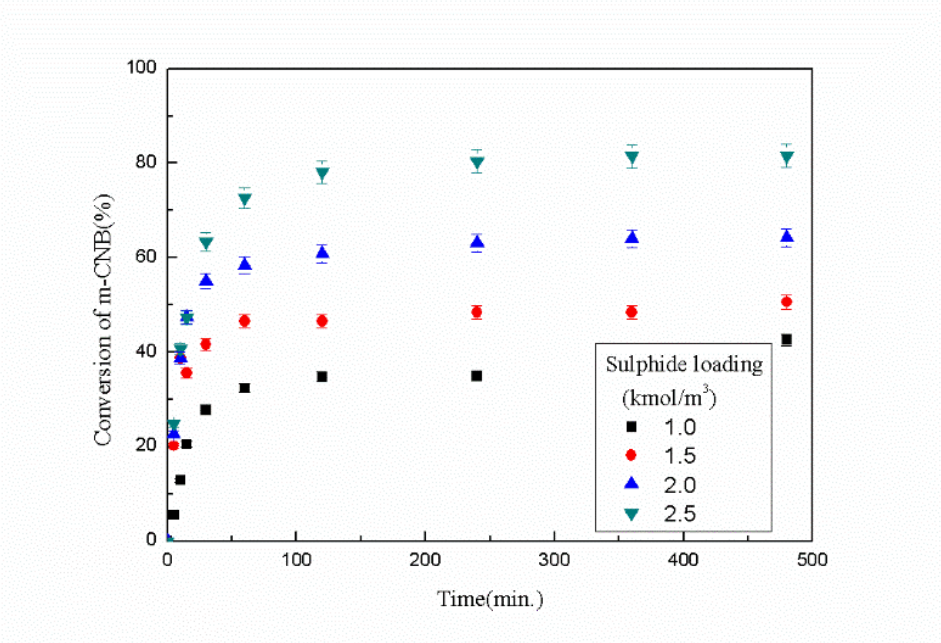

Figure 6.8. Effect of Sulphide Concentration on the conversion of m- CNB. Temperature = 333 K, stirring speed = 1500 rpm, Volume of organic phase = 5 x 10^{-5} m^3, m-CNB concentration = 0.63 kmol/m^3 of org. phase, TBPB concentration = 0.044 kmol/m^3 of org. phase, Volume of Aqueous Phase = 5 x 10^{-5} m^3, MDEA concentration = 3.04 kmol/m^3, temperature = 333 K.

6.2.3.8. Effect of the concentration of MDEA

The reaction rate does not directly influenced by MDEA concentration, but MDEA concentration does influence the equilibrium among MDEA, water and H_2S. As mentioned earlier in the mechanism, hydrosulphide (HS^-) and sulphide (S^{2-}) anions are formed in the aqueous phase and both the active anions are taking part in two different reactions (Equation (6.1) & Equation (6.2)). Basic nature of alkanolamines like MDEA pushes for more ionization of H_2S and the aqueous phase is dominated by sulphide ions (S^{2-}) over hydrosulphide ions (HS^-). So the occurrence of the two reactions in L-L PTC system can be established only by the MDEA variation in the aqueous phase at a fixed sulphide concentration.

Various concentration of aqueous MDEA solution (with constant sulphide concentration) were produced by taking 25 cm^3 of H_2S-laden MDEA solution from stock (sulphide and MDEA concentration was evaluated experimentally) and followed by addition of various amounts of raw MDEA and distilled water in such a manner that the total volume finally become to 50 cm^3.

As the reaction progresses the colour of the reaction mixture changed to orange from greenish yellow and finally at the end tuned into a reddish brown. In can be concluded that polysulphide, which is reddish brown in colour has formed at the end and similar change in colour also observed Lucas and Scudder [17].

The highest conversion achieved after 8 hrs of long run was 73% with utmost MDEA concentration of 6.02 kmol/m^3 and the aqueous phase sulphide concentration was 1.37 kmol/m^3, as shown in Figure 6.9. Experimental results suggest that the operative reaction was Equation (6.1). Other reduction studies with aqueous ammonium sulphide showed similar observations [3,6]. m-CNB conversion achieved was 73%, which is much more than what can be obtained from Equation (6.1) (approx. 60%) or Equation (6.2) (approx. 30%). As the reaction progresses and polysulphide (produced when elemental sulphur produced in Equation (6.2) reacted with sulphide ions present in the aqueous phase) formed during the course of reaction.

Elemental sulphur as a by-product was not reported when aqueous sodium sulphide was used for the reduction of nitroarenes [3,6] and it can be concluded that the current reduction reaction carried out via transfer of sulphide ions by quaternary cations to the organic phase and follows the Equation (6.1) stoichiometry. Initially with higher MDEA concentration low conversion of m-CNB was noticed at the beginning, but after a certain time the reaction rate got enhanced and higher conversion of m-CNB achieved finally. At higher MDEA concertation the number of sulphide ions got increased in the aqueous phase and higher m-CNB conversion achieved

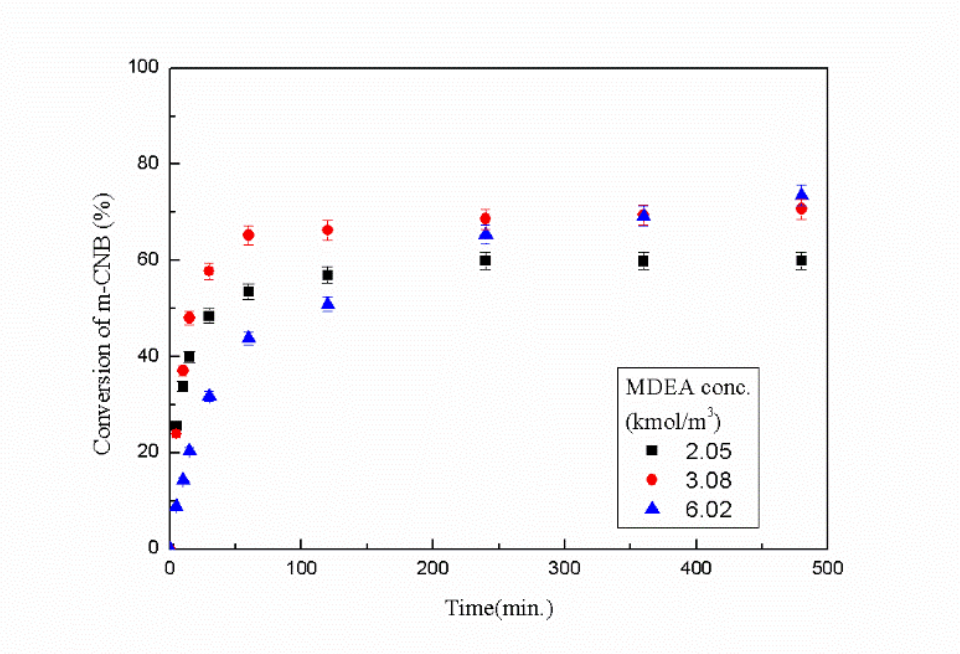

Figure 6.9. Effect of MDEA Concentration on the conversion of m-CNB. Temperature = 333 K, stirring speed = 1500 rpm, Volume of organic phase = 5 x 10^{-5} m^3, m-CNB concentration = 0.63 kmol/m^3 of org. phase, TBPB concentration = 0.044 kmol/m^3 of org. phase, Volume of Aqueous Phase = 5 x 10^{-5} m^3, Sulfide concentration = 2.5 kmol/m^3.

6.2.3.9. Effect of elemental sulphur loading

After addition of elemental sulphur into the aqueous phase, the colour of the H_2S-laden aqueous MDEA solution turns to orange from dark green. Figure 6.10 shows the effect of elemental sulphur loading on the conversion of m-CNB. From the experimental results it is clear that at the beginning of the reaction, the reaction rate was high when elemental sulphur added externally but it slows down as the reaction progress further. During reduction reaction different anions formed other than sulphide (S^{2-}) and hydrosulphide (HS^{-}) ions like, polysulphide (S_n^{2-}, where $2 \leq n \leq 6$), disulphide that are easier to transfer from the aqueous phase to the organic phase and then reacts with CNBs [18]. Lucas and Scudder (1928) [17] also got similar observations.

From the Figure 6.10 it is clear that after 120 min. of reaction the conversion of m-CNB was highest in without elemental sulphur addition study. Based on the previous discussion it can be conclude that the reason for the crossover was the build-up of elemental sulphur in the system and thus reaction rate became higher (Equation (6.2)).

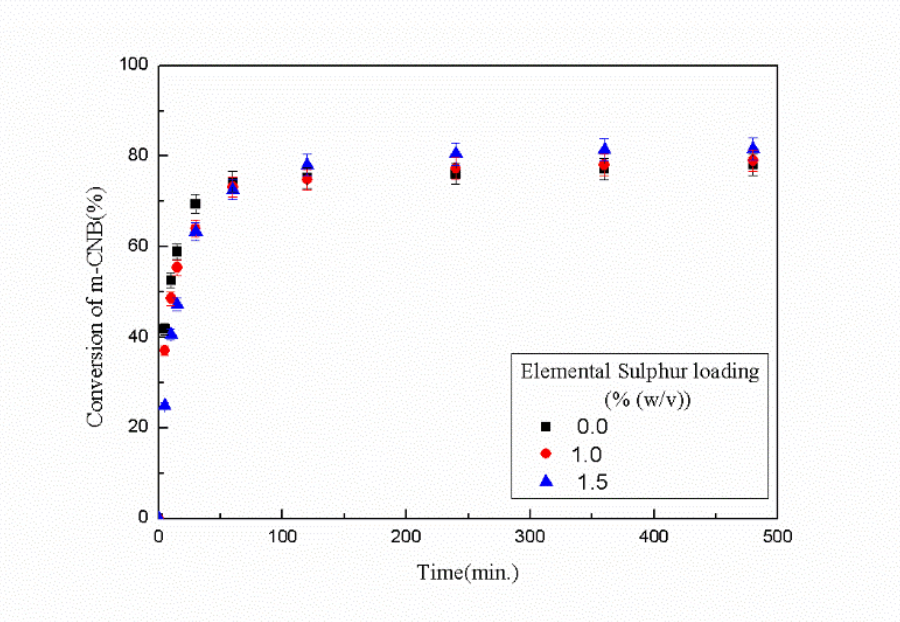

Figure 6.10. Effect of elemental Sulphur loading on the conversion of m-CNB. Stirring speed = 1500 rpm, Volume of organic phase = 5 x 10^{-5} m^3, m-CNB concentration = 0.63 kmol/m^3 of org. phase, TBPB concentration = 0.044 kmol/m^3 in org. phase, Volume of Aqueous Phase = 5 x 10^{-5} m^3, Sulfide concentration = 2.5 kmol/m^3, MDEA concentration = 3.04 kmol/m^3, temperature = 333 K.

6.2.3.10 Validation of the kinetic model. A plot of *–ln (1- X)* against time (Figure 6.11) is shown to validate the kinetic model at different temperatures. Table 2 shows the

apparent rate constant k_{app} was calculated from the slope of each line at different temperatures. (Figure 6.12) shows a comparison study between the conversions of m-CNB at different temperatures, which are calculated accordingly these apparent rate constants and conversions obtained experimentally. A fine match can be observed between experimental and calculated conversions.

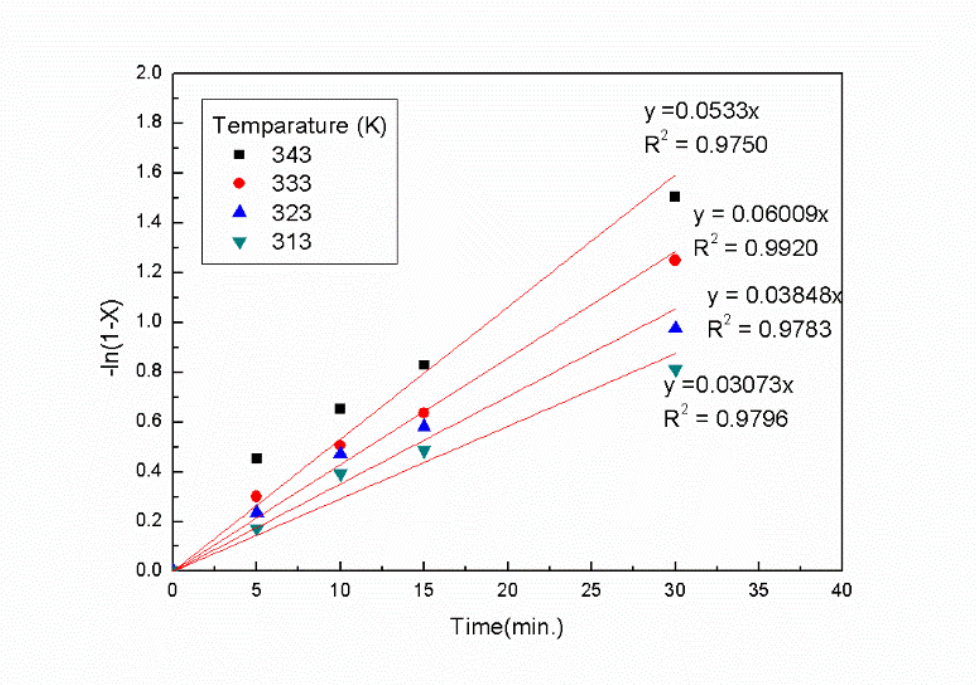

Figure 6.11. Validation of the kinetic model with experimental data at different temperatures. Stirring speed = 1500 rpm, Volume of organic phase = 5 x 10^{-5} m^3, m-CNB concentration = 0.63 kmol/m^3 of org. phase, TBPB concentration = 0.044 kmol/m^3 in org. phase, Volume of Aqueous Phase = 5 x 10^{-5} m^3, Sulfide concentration = 2.5 kmol/m^3, MDEA concentration = 3.04 kmol/m^3, temperature = 333 K.

Table 6.2 Apparent rate (k_{app}) constants at different temperatures[b]

Temperature (K)	313	323	333	343
k_{app} (min^{-1})	0.0291	0.0351	0.0430	0.0531

[b] All considerations are the same as mentioned in Figure 6.11.

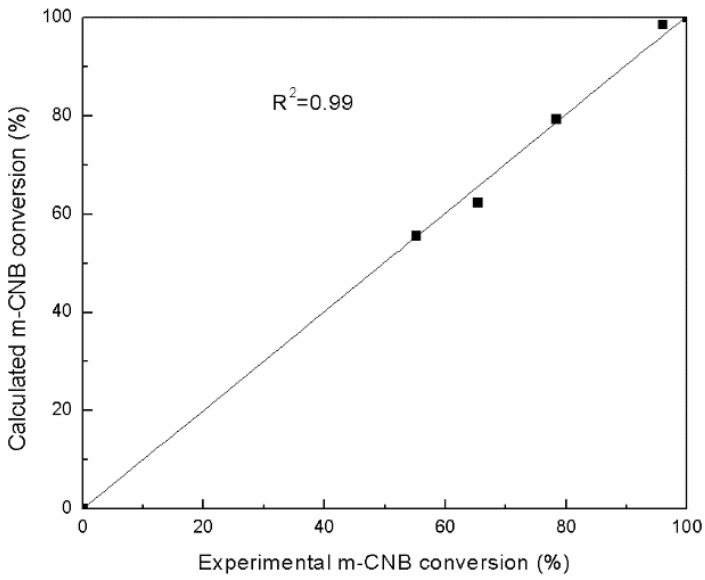

Figure 6.12. Comparison between calculated and experimental m-CNB conversions at 480min at different temperatures. All other parameters are the same as Figure 6.11.

6.3. Conclusion.

The following conclusion can be drawn from the results obtained by experiments

1. H_2S absorbed in industrially important aqueous MDEA has been successfully employed as refined Zinin reagent to reduce CNBs selectively to their respective amines in L-L PTC mode under mild reaction condition.
2. Process intensification was observed with efficient TBPB catalyst and TBPB came out as a best catalyst for our system, when a comparative study was done with different catalyst (TBAB, TBAC, CTMAB, ETPPB and TMAB).
3. Current reduction reaction carried out in a non-polar solvent, which can be used to dissolve a number of nitroaromatic compounds. Separation of product from the reaction mixture is very easy.
4. Parametric studies were performed to optimize the process parameters to get maximum yield and selectivity of the product amine. It leads to 100% yield and selectivity of m-Chlroaniline. So this Zinin reduction of CNB by toxic H_2S gas can be regarded as one of the most economically viable and environment friendly approach till now.
5. The current reduction process is following a complex mechanism which involving different ions and molecules. A kinetic model was developed considering Stark's extraction mechanism for L-L PTC, based on detailed kinetic

studies and proposed mechanism. The current model very accurately predicts the conversion of m-CNB. This versatile reaction can therefore be carried out in the laboratory and for the plant-scale manufacture of aromatic amines when other reduction media are destructive to sensitive nitro compounds and result in undesired side reactions.

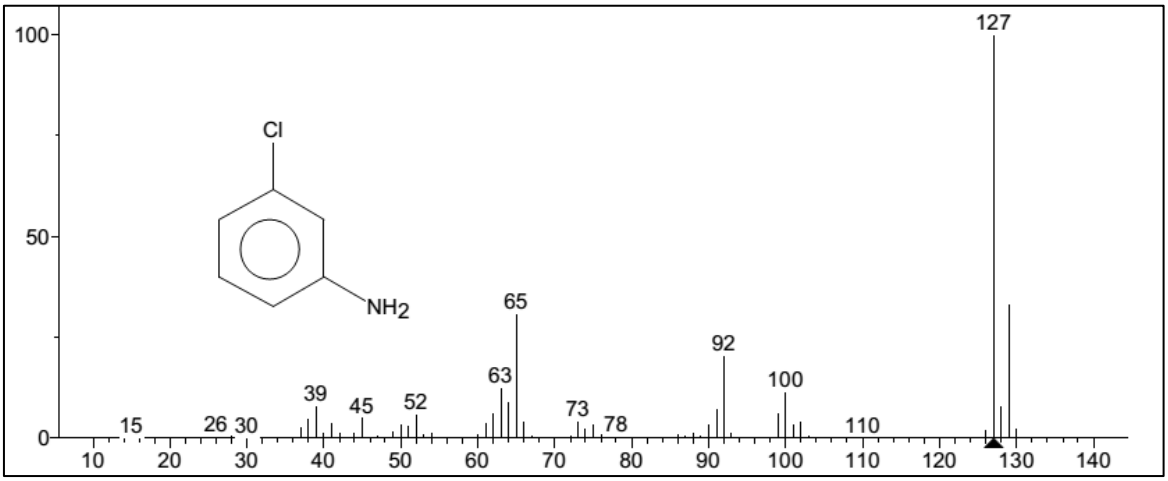

Figure 6.13: MS spectra of m-chloroaniline.

References

1 W. G. Dauben, *Organic reactions*, John Wiley & Sons, Inc., New York, 1973.

2 G. D. Yadav, Y. B. Jadhav and S. Sengupta, *J. Mol. Catal. A Chem.*, 2003, **200**, 117–129.

3 N. C. Pradhan and M. M. Sharma, *Ind. Eng. Chem. Res.*, 1992, **31**, 1606–1609.

4 R. R. Bhave and M. M. Sharma, *J. Chem. Technol. Biotechnol.*, 1981, **31**, 93–102.

5 N. C. Pradhan, *Indian J. Chem. Technol.*, 2000, **7**, 276–279.

6 G. D. Yadav, Y. B. Jadhav and S. Sengupta, *Chem. Eng. Sci.*, 2003, **58**, 2681–2689.

7 H. Gilman, Wiley, New York, 1941, p. 52.

8 H. Beutier, D; Renon, *Ind. Eng. Chem. Process. Des. Dev*, 1978, **17**, 220–230.

9 G. D. Yadav and S. V. Lande, *Adv. Synth. Catal.*, 2005, **347**, 1235–1241.

10 G. D. Yadav and S. V. Lande, *Appl. Catal. A Gen.*, 2005, **287**, 267–275.

11 C. M. Starks, *J. Am. Chem. Soc.*, 1971, **93**, 195.

12 A. Makosza, M ; Jonczyk, *Org. Synth.*, 1976, **55**, 91.

13 P. A. Vivekanand and T. Balakrishnan, *Catal. Commun.*, 2009, **10**, 1962–1966.

14 E. Murugan and A. Siva, *J. Mol. Catal. A Chem.*, 2005, **235**, 220–229.

15 G. D. Yadav and S. V. Lande, *Ind. Eng. Chem. Res.*, 2007, **46**, 2951–2961.

16 J. P. Ldoux and Wendell Plain, *J. Chem. Educ.*, 1972, **49**, 133.

17 N. F. Lucas, H J, Scudder, *J. Am. Chem. Soc.*, 1928, **50**, 244–249.

18 Y. O. M. Hojo, Y. Takagi, *J. Am. Chem. Soc.*, 1960, **82**, 2459–2462.

Abstract

The current study demonstrated the selective reduction of 1-Nitronapthalene (1-NN) by Hydrogen Sulphide (H_2S) absorbed in aqueous N-Methyldiethanolamine (MDEA), which is a commonly encountered process in Amine treating unit (ATU) of petroleum refinery. The modified Zinin reduction has been carried out using Tetra-n-butylphosphonium Bromide (TBPB) as Phase Transfer Catalyst under Liquid-Liquid (L-L) biphasic mode. The kinetic model and mechanism of complex L-L phase transfer catalytic process have been developed and then the same has been validated against the experimental data.

7.1 INTRODUCTION

The current study demonstrated the selective reduction of 1-Nitronapthalene (1-NN) by Hydrogen Sulphide (H_2S) absorbed in aqueous N-Methyldiethanolamine (MDEA), which is a commonly encountered process in Amine treating unit (ATU) of petroleum refinery. The modified Zinin reduction has been carried out using Tetra-n-butylphosphonium Bromide (TBPB) as Phase Transfer Catalyst under Liquid-Liquid (L-L) biphasic mode. The selectivity of product 1-aminonapthalene was found to be 100% and the reaction was kinetically controlled with the activation energy of 20.77 kJ/mol. The influence of the process parameters like stirring speed, concentration of 1-NN, concentration of aqueous sulphide, concentration of catalyst, MDEA concentration, elemental sulphur loading at different reaction time on the reactant conversion and the reaction rate of 1-NN were studied for establishment of the reaction mechanism. The kinetic model and mechanism of complex L-L phase transfer catalytic process has been developed and then the same has been validated against the experimental data. This approach of reducing 1-NN by H_2S – rich MDEA can substitute the energy-expensive Claus process, which gives no other product than sulphur.

7.2 RESULTS AND DISCUSSION

7.2.1 Proposed mechanism of reduction of aromatic nitro compounds under L-L PTC.

The overall stoichiometry of the Zinin's original reduction of nitrobenzene by aqueous ammonium sulphide, as proposed by Zinin in 1842, is given by Equation (7.1).[1] Reduction of nitroarenes by sodium sulphide follows same stoichiometry.[22,23,34,39–8]

$$4ArNO_2 + 6S^{2-} + 7H_2O \rightarrow 4ArNH_2 + 3S_2O_3^{2-} + 6HO^- \quad (7.1)$$

Some other reports show that elemental sulphur can be produced as a by-product instead of thiosulphate when aqueous ammonium sulphide used as a reducing agent in the reaction. P-Aminophenylacetic acid is prepared from p-nitrophenylacetic acid using aqueous ammonium sulphide and it is reported that the sulphide ions are oxidised to elemental sulphur instead of thiosulphate following stoichiometry of Equation (7.2).[9]

$$ArNO_2 + 3HS^- + H_2O \rightarrow ArNH_2 + 3S + 3HO^- \quad (7.2)$$

Above reactions (Equation (7.1) and (7.2)) show that two different anions (S^{2-}& HS^-) have participated in those reduction reactions and elemental sulphur or thiosulphate is produced as a by-product respectively. In the presence of a base, ammonia, the dissociation equilibrium favours toward more ionization and the concentration of sulphide ions (S^{2-}) relative to hydrosulphide (HS^-) ions increases in the aqueous phase with the rise in the ammonia concentration.[10]

The overall stoichiometry of the reduction reaction using sodium disulphide as the reducing agent follows stoichiometry of Equation (7.3).[11]

$$ArNO_2 + S_2^{2-} + H_2O \rightarrow ArNH_2 + S_2O_3^{2-} \quad (7.3)$$

Ionic equilibrium of sulphide ions (S^{2-}) and hydrosulphide ions (HS^-) in H_2S-laden aqueous alkanolamine (MDEA for example) solution should follow the same trend as H_2S-laden aqueous ammonium sulphide solution [12], as represented by Equation (7.4) to Equation (7.7) in the Scheme 7.1. These two ions are responsible for the formation of elemental sulphur or thiosulphate in the process of reduction of nitroarenes by H_2S-laden aqueous MDEA solution. The presence of both ions (sulphide, hydrosulphide) makes H_2S-laden aqueous alkanolamine and aqueous ammonium sulphide solutions different from other reducing agent like sodium sulphide, sodium disulphide.[13].

Based on the current study and some earlier studies on reactions of reduction of nitroaromatic compounds by sodium sulphide [5,6,14,15], a general reaction mechanism has been proposed (Scheme 7.1). Sulphur can exist in multiple valence states ranging from (-2) to (+6) and, therefore, can form different anions ($HS^-, HSO^-, HSO_2^-, HSO_3^-$) which are capable of pairing with quaternary cations in a rapid manner than other anions that require multiple quaternary cations ($Q_n^+X^-$).[5] The nitro group present in the aromatic nitro compounds is reduced by the transfer

of an electron from sulphide ions during reduction of nitro-aromatic compounds by aqueous sulphide solution.

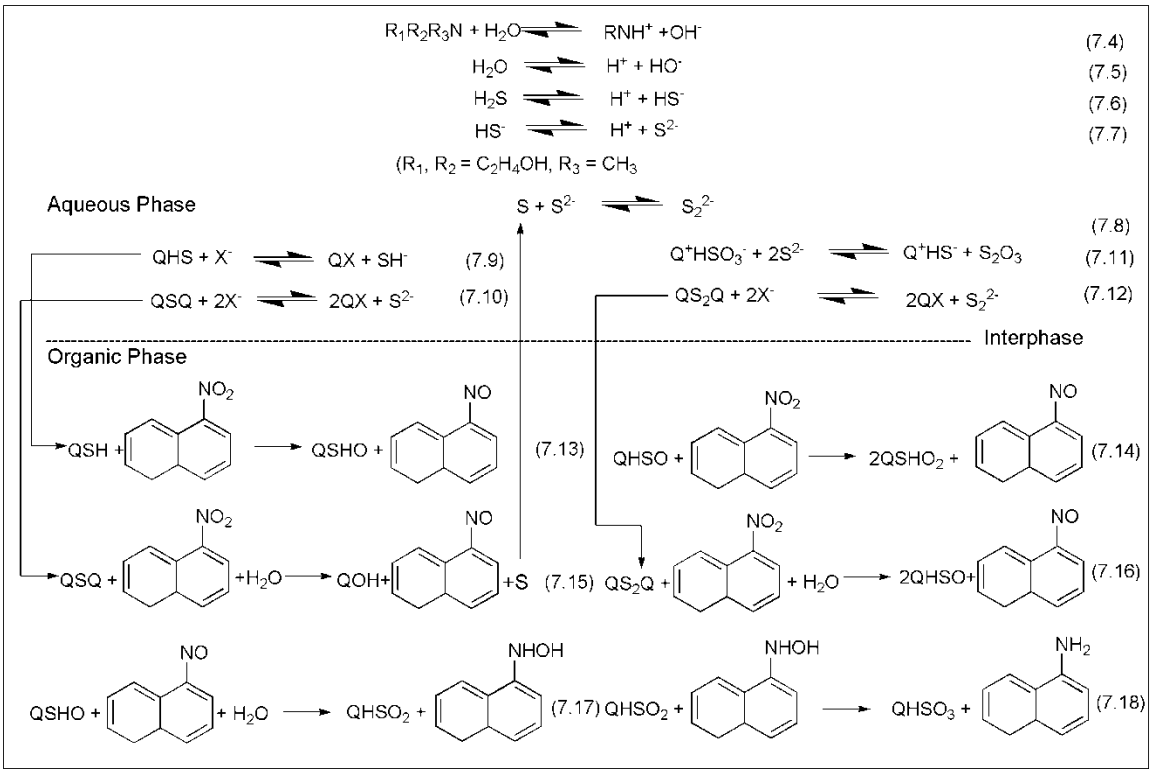

Scheme 7.1. Proposed mechanism of reduction of 1-NN by H_2S-laden MDEA under L-L PTC.

Current reaction system is a liquid-liquid PTC system, which consists of an organic phase (organic substrate dissolved in solvent), an aqueous phase (H_2S absorbed in an aqueous solution of MDEA) and quaternary phosphonium salt, partitioned into both the phases. The organic reactant (1-NN) and product (1-NA) are organophilic in nature.[16] According to Starks extraction mechanism, after the distribution of catalyst in both the phases, nucleophiles (anions) present in the aqueous phase get attached to catalyst cations and then move to the organic phase for taking part in the reaction with organic substrates.

The aqueous phase reaction of H_2S and MDEA is a reversible reaction and instantaneous in nature with respect to the mass transfer. H_2S-MDEA equilibrium exists in the aqueous phase as well in the interfacial liquid film and five ion species are formed $(HS^-, S^{2-}, OH^-, H^+, R_1R_2R_3NH^+)$ in the aqueous phase (Scheme

7.1)[17–21]. Quaternary cations (Q^+) present at the interphase readily form Q^+HS^- ion pair as soon as it comes into contact with the aqueous phase. Then, a series of reactions take place in the organic phase as shown in Scheme 7.1. Reactions also occur near the interphase between anions present in the aqueous phase and organic substrate on the organic phase side as the substrate has limited solubility in the aqueous phase. It is confirmed by the fact that products form even in the absence of the catalyst.

The contribution of several elementary reactions in the organic phase to the overall rate of the reaction is elaborated by the following mechanism. In a series of complex elementary reactions, 1-NN is converted to 1-napthylamine (1-NA) through the formation of intermediates (1-nitrosonapthalene and 1-hydroxyaminonaphthalene), both of which have not been detected by GC-MS analysis. The existence of these two intermediates during Zinin reduction has long been established.[5,15] Those intermediates remain undetected which may be due to the faster disappearance of the intermediates in the organic phase. While the catalyst cations are pairing with the HS^- anions, some water molecules transfer to the interphase and taking part in the reaction (Equation (7.16) to Equation (7.17)). After a series of elementary reaction the ion pair $Q^+HSO_3^-$ formed in the organic phase transfers to the aqueous phase and reacts with S^{2-} to regenerate Q^+HS^- Equation (7.8). The regenerated quaternary cations transferred to the organic phase again for the reduction reaction and that completes a typical catalytic cycle.

According to this mechanism, the quaternary cations are pairing with different anions during the reactions but the majority of the catalyst cations remains in Q^+HS^- form and the catalysis cycle goes on. Nine reactions (Equation (7.4) – Equation (7.12)) took place in the aqueous phase and rest of the reactions (Equation (7.13)–Equation (7.18)) occurred consecutively in the organic phase. During the reaction, 100% selectivity of 1-NA was obtained at the end of the reaction.

7.2.2 Kinetic modelling

From the mechanism shown in Scheme 7.1, it can be said that Q^+HS^- active ion pair forms in large excess although other anions are also present. A few assumptions are made as follows- (7.1) all the aqueous phase reactions have reached equilibrium fast, (7.2) modelling of the whole PTC reaction have done, is based on the mechanism proposed above and (7.3) the reactions occur in the

interphase region are negligible in comparison to aqueous phase and organic phase reactions.

It was assumed to be an L-L PT catalytic reaction where 1-NN dissolved in toluene is reduced by H_2S-laden aqueous MDEA solution to yield 1-NA and $S_2O_3^-$ as a by-product in their respective phases as shown in above Scheme 7.1. The overall reaction can be expressed in a single reaction shown in Equation (7.1).

The reaction medium was agitated with a stirrer at 1500 rpm to make the reaction as kinetically controlled and mass transfer effects can be ignored. With the progress of the reaction, the first ion exchange reaction took place between HS^- and Q^+X^- ($X^- = Cl^-$ for 1st ion exchange reaction) to form an active ion pair (Q^+HS^-). During reduction reaction, different transition anions were brought into existence in the organic phase and finally those ions become the inactive ion-pairs when HSO_3^- ions get attached to quaternary cations. The inactive sites underwent a redox reaction with S^{2-} ions and active sites Q^+HS^- were regenerated.

Steps as indicated in the mechanism in Scheme 7.1 are:

1. Transfer of inactive PT catalyst from organic phase to aqueous phase with equilibrium constant K_1,

$$K_1 = \frac{[\,QSHO_3]_a}{[\,QSHO_3]_o} \tag{7.19}$$

2. Ion exchange reactions are shown in Scheme 7.1 (Equation (7.9) -Equation (7.12)). Reaction (7.11) is the catalyst regeneration reaction, from which we can write,

$$K_2 = \frac{k_1}{k_1'} = \frac{[Q^+HS^-]_a[S_2O_3^{2-}]_a}{[Q^+HSO_3^-]_a[S^{2-}]_a^2} \tag{7.20}$$

3. Transfer of initially added catalyst QX from organic phase to aqueous phase and the active catalysts Q^+HS^-, QSQ and QS_2Q from aqueous phase to organic phase with equilibrium constant K_3, K_4, K_5, K_6,

$$K_3 = \frac{[QX]_a}{[QX]_o} \tag{7.21}$$

$$K_4 = \frac{[QHS]_o}{[QHS]_a} \tag{7.22}$$

$$K_5 = \frac{[QSQ]_o}{[QSQ]_a} \tag{7.23}$$

$$K_6 = \frac{[QS_2Q]_o}{[QS_2Q]_a} \tag{7.24}$$

4. The overall rate is controlled by organic phase reactions. Among all elementary reactions (Equation (7.13) to Equation (7.18)), reaction shown in the Equation (7.13) is the slowest and rate determining step, where the first intermediate product ArNO is produced.[5] The presence of elemental sulphur as one of the byproduct has made reactions shown in Equation (7.15) and Equation (7.16) as a contributor also to overall reaction. During the transfer of ion pairs from the aqueous phase to the organic phase, some water molecules also got transferred.

As $ArNO_2$ is the limiting reactant, it can be taken as a basis of reaction. Rate of disappearance of $ArNO_2$ can, therefore, be expressed as,

$$-\frac{d[ArNO_2]}{dt} = k_2[\mathrm{ArNO_2}]_o[QHS]_O + k_3[\mathrm{ArNO_2}]_o[QSQ]_O[H_2O]_O + k_4[\mathrm{ArNO_2}]_o[QS_2Q]_O[H_2O]_O \tag{7.25}$$

As the number of water molecules transferred to the organic phase are very less in comparison to that of Q^+HS^- ion pairs, it can be assumed that the reaction in Equation (7.13) is the main rate determining step. Reactions shown in Equation (7.15) and Equation (7.16) can, therefore, be ignored.

Therefore, Equation (25) can be rewritten as

$$-\frac{d[ArNO_2]}{dt} = k_2[\mathrm{ArNO_2}]_o\,[QHS]_O \tag{7.26}$$

The mole balance for the catalyst is given by,

$$V^o\,[QX]^* = V^a\,\{[QX] + [QHS] + [QSQ] + [QS_2Q] + [QHSO_3]\}_a + V^o\,\{[QX] + [QHS] + [QSQ] + [QS_2Q] + [QHSO_3]\}_o$$

(7.27)

$[QX]^*$ is the concentration of catalyst initially fed to the organic phase, V^a and V^o are the volume of aqueous the phase and organic phase. Therefore,

$$[QX]^* = \frac{V^a}{V^o}\{[QX] + [QHS] + [QSQ] + [QS_2Q] + [QHSO_3]\}_a + \{[QX] + [QHS] + [QS_2Q] + [QHSO_3]\}_o$$

(7.28)

Substituting Equation (7.19), (7.21), (7.22), (7.23) and (7.24) in the above reaction, we get

$$[QX]^* = \frac{V^a}{V^o}\left\{K_3[QX]_o + \frac{[QHS]_o}{K_4} + \frac{[QSQ]_o}{K_5} + \frac{[QS_2Q]_o}{K_6} + [QHSO_3]_o\right\}_a + \{[QX] + [QHS] + [QSQ] + [QS_2Q] + [QHSO_3]\}_o \quad (7.29)$$

The total catalyst concentration in the organic phase is given by,

$$[Q^T] = [QX]_o + [QHS]_o + [QSQ]_o + [QS_2Q]_o + [QHSO_3]_o \quad (7.30)$$

$$1 = \frac{[QX]_o}{[Q^T]} + \frac{[QHS]_o}{[Q^T]} + \frac{[QSQ]_o}{[Q^T]} + \frac{[QS_2Q]_o}{[Q^T]} + \frac{[QHSO_3]_o}{[Q^T]} \quad (7.31)$$

Let us consider,

$$\frac{[QHS]_o}{[Q^T]} = \eta_1;\ \frac{[QSQ]_o}{[Q^T]} = \eta_2;\ \frac{[QS_2Q]_o}{[Q^T]} = \eta_3;\ \frac{[QHSO_3]_o}{[Q^T]} = \eta_4;$$

After substituting $\eta_1, \eta_2, \eta_3, \eta_4$ in the Equation (7.31) we get,

$$[QX]_o = (1 - \eta_1 - \eta_2 - \eta_3 - \eta_4)[Q^T] \quad (7.32)$$

The following equation can be obtained from Equation (7.29) and Equation (7.30) as

$$[QX]^* = \frac{V^a}{V^o}\left\{K_3\frac{[QX]_o[Q^T]}{[Q^T]} + \frac{[QHS]_o}{[Q^T]}\frac{[Q^T]}{K_4} + \frac{[QSQ]_o}{[Q^T]}\frac{[Q^T]}{K_5} + \frac{[QS_2Q]_o}{[Q^T]}\frac{[Q^T]}{K_6} + K_1\frac{[QHSO_3]_o}{[Q^T]}[Q^T]\right\}_a + [Q^T] \quad (7.33)$$

Combining Equation (7.32) and Equation (7.33) yields,

$$[\mathrm{QX}]^{*} = \frac{V^{a}}{V^{o}}\left\{\mathrm{K}_3\,[\mathrm{Q^T}]\,(1-\eta_1-\ \eta_2-\ \eta_3-\ \eta_4)+\eta_1\frac{[\mathrm{Q^T}]}{\mathrm{K}_4}+\ \ \eta_2\ \frac{[\mathrm{Q^T}]}{\mathrm{K}_5}+\eta_3\ \frac{[\mathrm{Q^T}]}{\mathrm{K}_6}+\right.$$
$$\left.\eta_4\,K_1[Q^T]\right\}_{\mathrm{a}}+[\mathrm{Q^T}] \qquad (7.34)$$

Rearranging we get,

$$[Q^T] = \frac{[QX]^{*}}{\frac{V^{a}}{V^{o}}\left\{K_3(1-\eta_1-\ \eta_2-\eta_3-\eta_4)+\frac{\eta_1}{K_4}+\frac{\eta_2}{K_5}+\frac{\eta_3}{K_6}+\eta_4\,K_1\right\}_{a}+1} \qquad (7.35)$$

According to the overall reaction (Equation (7.1)), the conversion can be calculated as,

$$\text{Conversion (X)} = 1-\frac{[ArNO_2]_O}{[ArNO_2^{*}]} \qquad (7.36)$$

[Where, $ArNO_2^{*}$ is the total reagent added in the organic phase]

$$\text{So,}\quad [ArNO_2]_o = (1-X)\,[ArNO_2^{*}] \qquad (7.37)$$

As it is mentioned before that the reaction (Equation (7.13)) presented in Scheme 7.1 is rate-limiting step in the organic phase, the rate (r_A) of the reaction can be written as,

$$-\frac{d[ArNO_2]}{dt} = k_2[\mathrm{ArNO_2}]_o\,[QHS]_o \qquad (7.38)$$

Now substituting $\eta_1[Q^T]$ in the place of $[QHS]_o$ and Equation (7.38) in the above equation, we have

$$[ArNO_2^{*}]\frac{dX}{dt} = k_2\ [\mathrm{ArNO_2}]_o\eta_1[Q^T] \qquad (7.39)$$

$$[ArNO_2^{*}]\ \frac{dX}{dt} = k_2\,\eta_1(1-X)\,[ArNO_2^{*}]\,[Q^T] \qquad (7.40)$$

Substituting Equation (7.35) in the above equation, the following is obtained.

$$\frac{dX}{dt} = \frac{k_2\,\eta_1\,(1-X)\,[QX]^{*}}{\frac{V^{a}}{V^{o}}\left\{K_3(1-\eta_1-\ \eta_2-\eta_3-\eta_4)+\frac{\eta_1}{K_4}+\frac{\eta_2}{K_5}+\frac{\eta_3}{K_6}+\eta_4\,K_1\right\}_{a}+1} \qquad (7.41)$$

$$\frac{dX}{(1-X)} = k_{app}\,dt, \qquad (7.42)$$

Where $k_{app} = \frac{k_2\,\eta_1\,[QX]^*}{\frac{V^a}{V^o}\left\{K_3\,(1-\eta_1-\,\eta_2-\eta_3-\eta_4)+\frac{\eta_1}{K_4}+\frac{\eta_2}{K_5}+\frac{\eta_3}{K_6}+\eta_4\,K_1\right\}_a+1}$, since all terms are constant and can be calculated experimentally.

$$-\ln(1-X) = k_{app}.t, \tag{7.43}$$

From the Equation (7.43) it is clear that the reaction follows Pseudo first order.

7.2.3 Parametric studies

7.2.3.1. Effect of stirring speed

The effect of mass transfer resistance on reaction kinetics at different stirring speed have been investigated in the range of 500-2500 rev/min under otherwise identical experimental conditions in the presence of TBPB as phase transfer catalyst. It is ascertained from the Figure 1 that, there is no substantial increase in conversion due to the rise of stirring speed beyond stirring speed of 1000 rev/min. During further studies, the stirring speed has been maintained at 1500 rev/min for the complete elimination of mass transfer resistance.

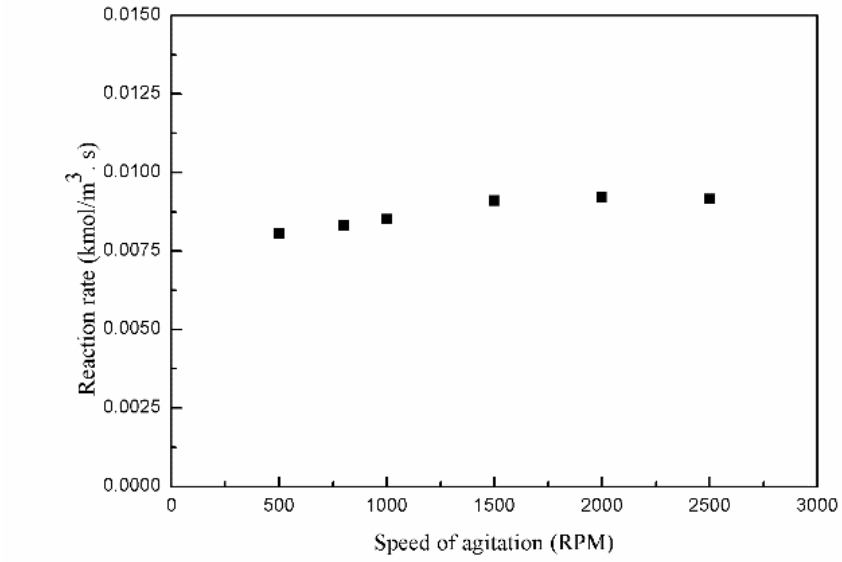

Figure 7.1 Effect of stirring speed on the conversion of 1-NN. Operating conditions: Volume of organic phase = 3 x 10^{-3} m^3, volume of aqueous phase = 3 x 10^{-3} m^3, [1-NN] = 0.577 kmol/m^3 in org. phase, [toluene] = 8.17 kmol/m^3 in org. phase, [catalyst] = 0.046 kmol/m^3 in org. phase, [sulphide] = 2.5 kmol/m^3, [MDEA] = 3.04 kmol/m^3, temperature = 333 K.

7.2.3.2 Effect of temperature

The influence of temperature on the conversion of 1-NN catalysed by TBPB, as phase transfer catalyst was studied under various reaction temperatures in the range of 313–343K under otherwise similar reaction conditions as shown in Figure 7.2. As per the transition state theory, the rates of most organic reactions increase with the rise in temperature. Increasing temperature is likely to enhance the rate of slow organic phase reactions under the PTC system. From the Figure 7.2, it is clear that the reactivity (conversion) of 1-NN augments with an increase in the temperature. The reason is, with the rise in temperature, the activation energy of the molecules is overcome and more molecules can react to form the product. On the other hand, collision among reactant molecules at a higher temperature has also resulted in the increase in reaction rate with increasing temperature.

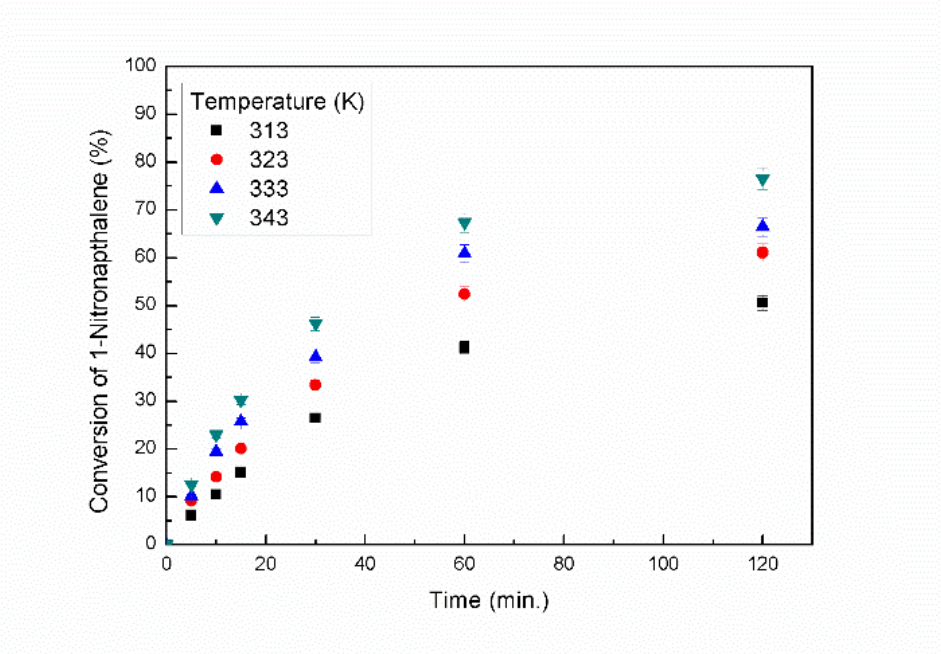

Figure 7.2 Effect of temperature on the conversion of 1-NN. Operating conditions: Volume of organic phase = 3 x 10^{-3} m^3, volume of aqueous phase = 3 x 10^{-3} m^3, [1-NN] = 0.577 kmol/m^3 in org. phase, [toluene] = 8.17 kmol/m^3 in org. phase, [catalyst] = 0.046 kmol/m^3 in org. phase, [sulphide] = 2.5 kmol/m^3, [MDEA] = 3.04 kmol/m^3, temperature = 333 K.

The initial rates were calculated at different temperatures and Arrhenius plots of *ln* (initial rate) vs. 1/T were made (Figure 7.3). The apparent activation energy for the kinetically controlled reaction was calculated from the slope of best fitted the

straight line as 20.77 kJ/mol. The high values of apparent activation energies again confirm the reaction systems to be kinetically controlled. The reduction of 1-NN by aqueous ammonium sulphide catalysed by Tetra-n-butylammonium bromide (TBAB) as phase transfer catalysis have been studied, which requires activation energy of 9.4 kJ/mole.[6]

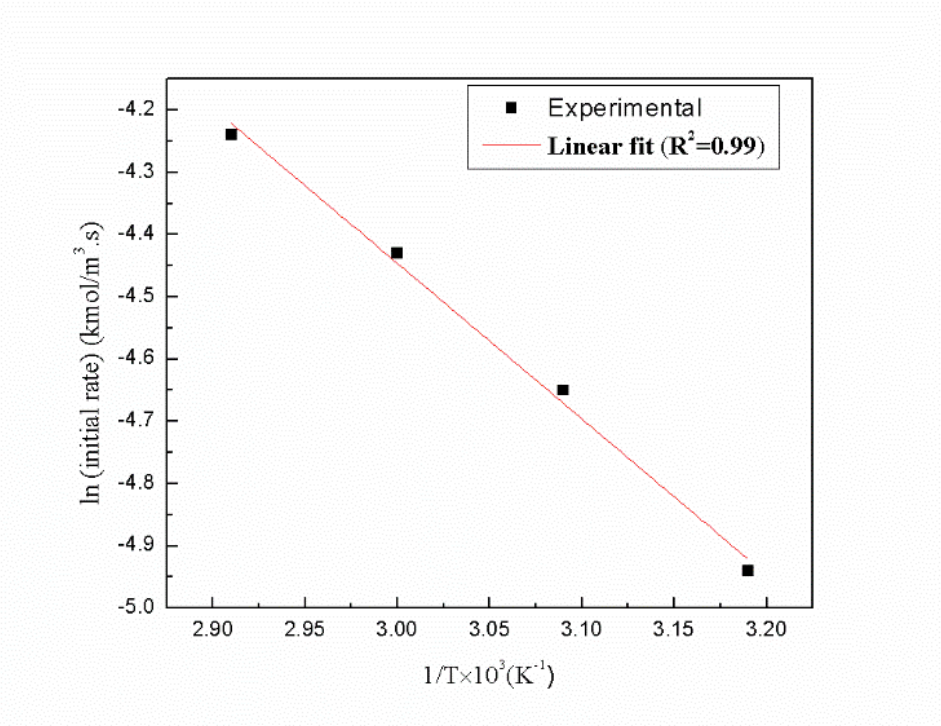

Figure 7.3. Arrhenius Plot (Plot of ln (initial rate) vs. 1/T). All other conditions are same as Figure 7.2.

7.2.3.3. Effect of Catalyst (TBPB) loading.

The effect of catalyst (TBPB) loading on the conversion of 1-NN by H_2S-laden aqueous MDEA was studied in the range of 0.000 – 0.093 kmol/m^3 under otherwise identical experimental conditions, as shown in Figure 7.4. As the catalyst load increases, the conversion of 1-NN as well as the reaction rate increases. Only by increasing the catalyst concentration, reactant conversion of more than 75.4% was achieved with 0.093 kmol/m^3 of catalyst loading whereas it was about 23% without added catalyst even after 2 hours of reaction under otherwise identical conditions. Enhancement factors, which is the ratio of the rate of reaction in the presence of the catalyst to that in the absence of the catalyst, are calculated at different catalyst loadings has shown in Table 7.1. A highest enhancement factor of 75 was observed with 0.093 kmol/m^3 of catalyst loading.

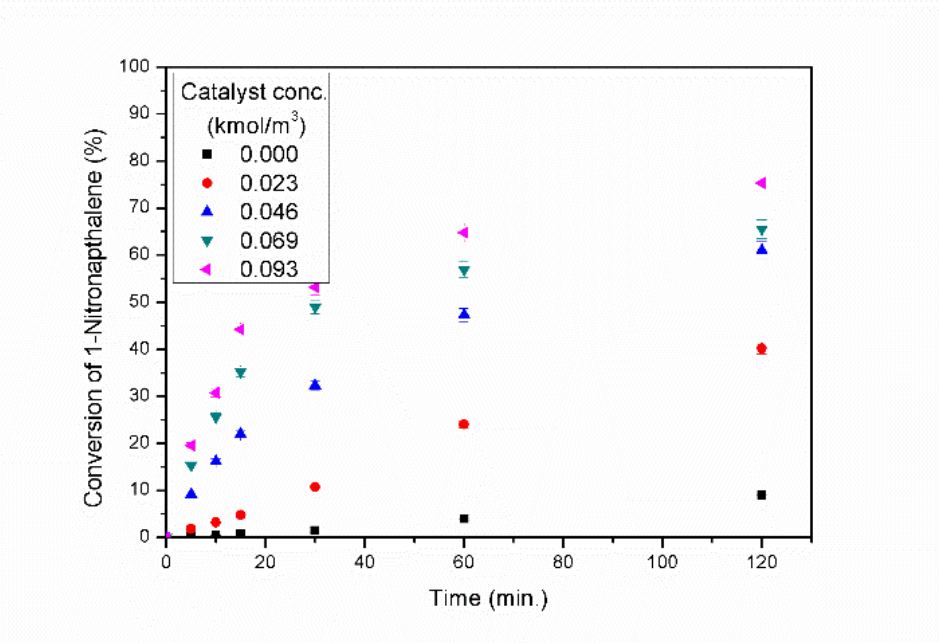

Figure 7.4. Effect of catalyst concentration on the conversion of 1-NN. Operating conditions: Volume of organic phase = 3 x 10^{-3} m^3, volume of aqueous phase = 3 x 10^{-3} m^3, [1-NN] = 0.577 kmol/m^3 in org. phase, [toluene] = 8.17 kmol/m^3 in org. phase, [catalyst] = 0.046 kmol/m^3 in org. phase, [sulphide] = 2.5 kmol/m^3, [MDEA] = 3.04 kmol/m^3, temperature = 333 K

Table 7.1 Effect of catalyst loading on Initial reaction rate[a]

Conc. of TBPB (kmol/m^3 org phase)	**Initial reaction rate (kmol/m^3s)**	**Enhancement factor**
0.000	0.0003	1.0
0.023	0.0022	7.3
0.046	0.0090	30.0
0.069	0.0165	55.0
0.093	0.0225	75.0

[a]All other conditions are same as Figure 7.4.

To determine the order of reaction with respect to the catalyst concentration, the initial reaction rate was calculated at different catalyst concentrations. A plot of *ln*

(initial rate) against *ln* (TBPB concentration) was made and shown in Figure 7.5. From the slope of the linear fit line, the order of reaction was determined. The order of the reaction was found out to be 1.4 with respect to TBPB concentration. Similar observations were made for the reduction of nitrochlorobenzenes by aqueous ammonium sulphide by PTC, TBAB.[22]

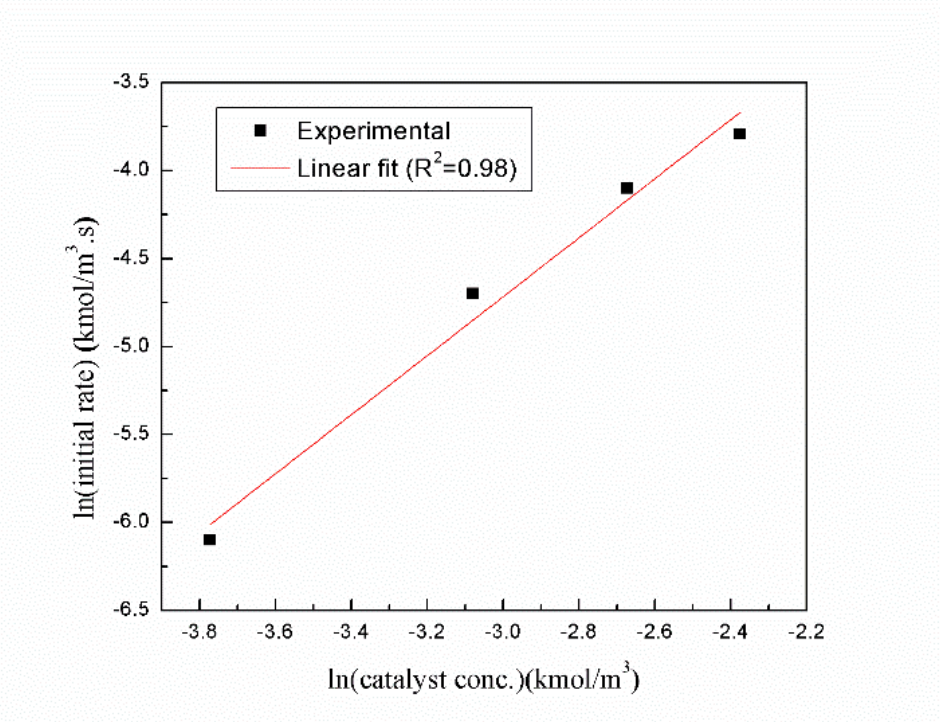

Figure 7.5 Plot of ln (initial rate) vs. ln (catalyst concentration). All other conditions are same as Figure 7.4.

7.3.3.4. Effect of 1-nitronapthalene concentration.

The effect of concentration of 1-NN on its conversion was considered at fourdifferent concentrations in the range of 0.288 to 1.155 kmol/m^3 in the presence TBAB under otherwise identical experimental conditions, as shown in Figure 7.6.

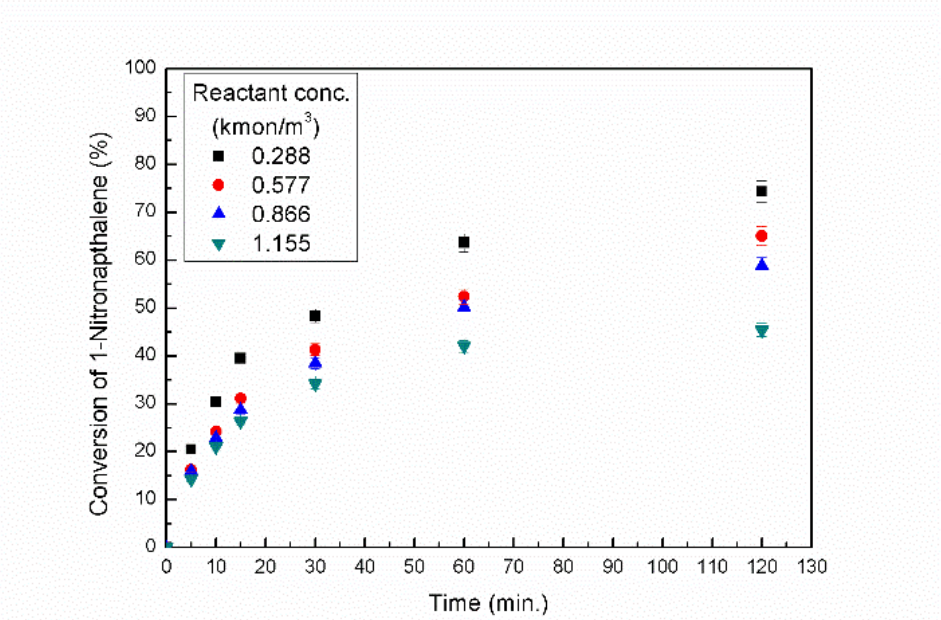

Figure 7.6. Effect of reactant concentration on the conversion of 1-NN. Operating conditions: Volume of organic phase = 3 x 10^{-3} m^3, volume of aqueous phase = 3 x 10^{-3} m^3, [1-NN] = 0.577 kmol/m^3 in org. phase, [toluene] = 8.17 kmol/m^3 in org. phase, [catalyst] = 0.046 kmol/m^3 in org. phase, [sulphide] = 2.5 kmol/m^3, [MDEA] = 3.04 kmol/m^3, temperature = 333 K.

It is evident from the figure that with higher reactant concentration lower conversion of 1-NN was achieved. As expected, the increase in the reaction rate during the initial stage of the reaction is due to the increase in the concentration of 1-NN. Since the amount of sulphide in the aqueous phase has remained the same for all the experimental runs, the conversion of 1-NN dropped beyond a particular concentration as shown in Figure 7.6. For reduction of o-nitroanisole by H_2S rich diethanolamine, a similar observation was found. [12]

Conversion and the reaction rate were found to increase with the decrease in 1-NN concentration at the end of 2 hours of reaction time. From the Figure 7.7, the order of reaction with respect to 1-NN concentration was obtained as 1.13. Hence, the reaction is first order with respect to the concentration of 1-NN. A similar observation was found elsewhere for the reduction of nitroarenes by aqueous sodium sulphide.[5]

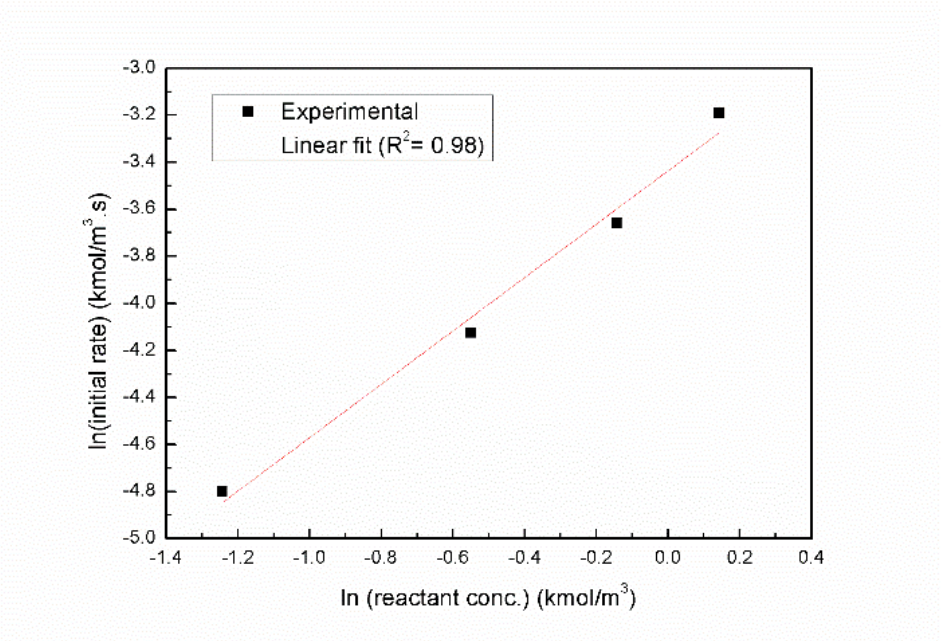

Figure 7.7. Plot of ln (initial rate) vs. ln (reactant concentration). All other conditions are same as Figure 7.6.

7.2.3.5. Effect of sulphide concentration.

Figure 7.8 shows the effect of sulphide concentration in the aqueous phase on the conversion of 1-NN. With an increase in the concentration of sulphide, the conversion of 1-NN and the reaction rate increases which is as expected. Sulphide concentration was varied in the range of 1.0 to 2.5 kmol/m^3 under otherwise identical experimental conditions in the presence of catalyst TBPB. From the plot of *ln* (initial rate) against *ln* (sulphide concentration) (Figure 7.9), the slope of the linear fit line was found out to be to be 1.91. Studies on the reduction of nitrotoluenes with aqueous ammonium sulphide also reported the order of reaction to be 2nd with respect to sulphide concentration.[10]

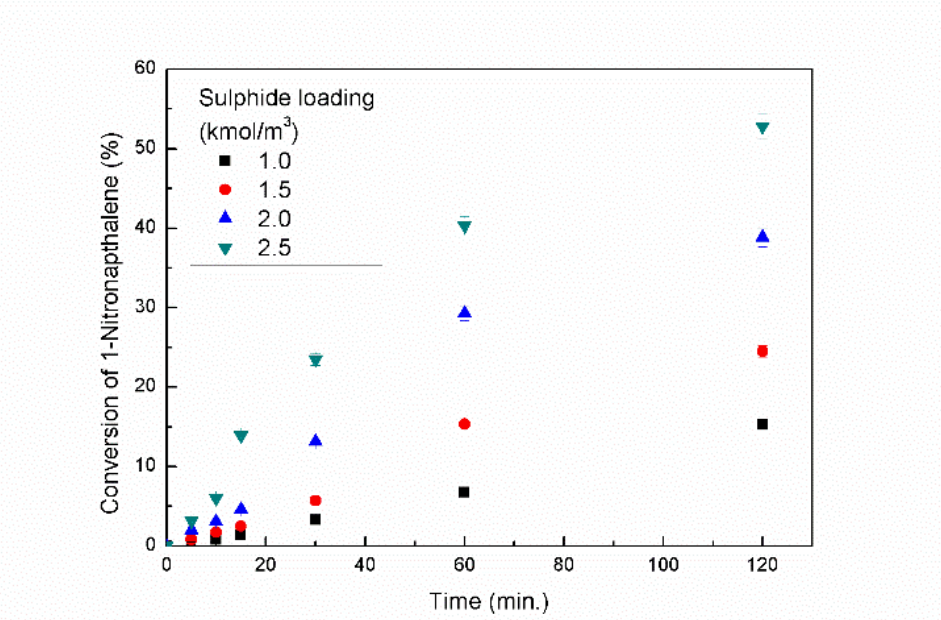

Figure 7.8 Effect of sulphide concentration on the conversion of 1-NN. Operating conditions: Volume of organic phase = 3 x 10^{-3} m^3, volume of aqueous phase = 3 x 10^{-3} m^3, [1-NN] = 0.577 kmol/m^3 in org. phase, [toluene] = 8.17 kmol/m^3 in org. phase, [catalyst] = 0.046 kmol/m^3 in org. phase, [sulphide] = 2.5 kmol/m^3, [MDEA] = 3.04 kmol/m^3, temperature = 333 K.

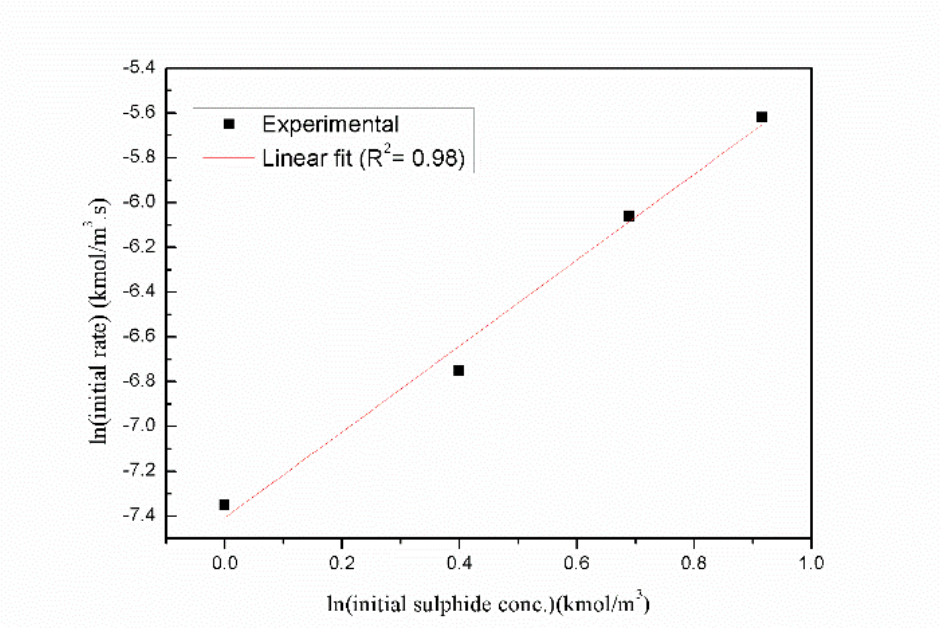

Figure 7.9 Plot of ln (initial rate) vs. ln (sulphide concentration). All other conditions are same as Figure 7.8.

3.2.3.6. Effect of MDEA concentration.

MDEA does not have the direct impact on reaction rate, but it does affect the equilibrium among MDEA, H_2S and water. As mentioned in Scheme 7.1, in aqueous phase, sulphide (S^{2-}) and hydrosulphide (HS^-) active anions are formed and theses two active anions are responsible for two different reactions (Equation (7.1) & Equation (7.2)). Basic nature of MDEA favours more ionisation of H_2S and sulphide ions (S^{2-}) dominates over hydrosulphide ions (HS^-) in the aqueous phase. The existence of two reactions can be proven only by varying MDEA addition in the aqueous phase with a fixed sulphide concentration.

Various MDEA concentrations (sulphide concentration kept constant) were prepared by taking 20 cm^3 of H_2S-laden aqueous MDEA (with known sulphide and MDEA concentrations) solution and adding into its various proportions of pure MDEA and distilled water in such a way that the total volume was made up to 30 cm^3. During the course of the reaction colour of the aqueous solution was changed from greenish yellow to orange and then to reddish brown that is useful in indicating the extent of reaction. With the progress of the reaction, polysulphide that is reddish brown in colour, formed. A similar phenomenon was observed by Lucas and Scudder.[23]

In this study, after 12 hrs of run, 46% conversion of 1-NN was achieved with maximum MDEA concentration of 3.04 $kmol/m^3$ as shown in Figure 7.10. It was observed that increase in MDEA concentration lowers the conversion of 1-NN. The reason is, with increase in MDEA concentration, concentration of HS^- decreases with respect to S^{2-}, and consequently, conversion of 1-NN decreases as concluded from Equation (7.2).

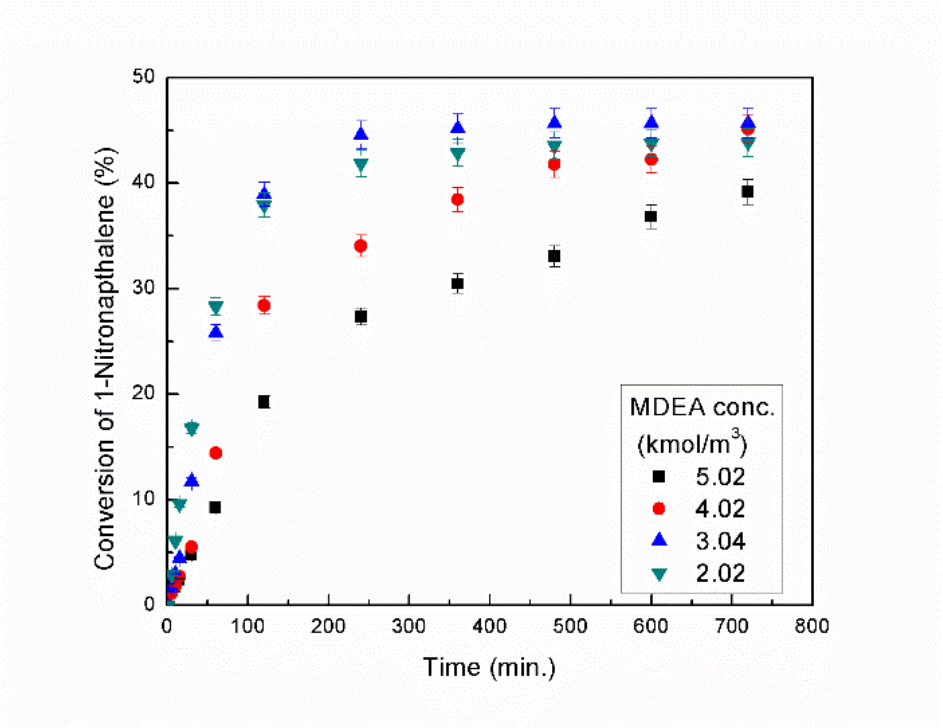

Figure 7.10. Effect of MDEA concentration on the conversion of 1-NN. Operating conditions: Volume of organic phase = 3 x 10^{-3} m^3, volume of aqueous phase = 3 x 10^{-3} m^3, [1-NN] = 0.577 kmol/m^3 in org. phase, [toluene] = 8.17 kmol/m^3 in org. phase, [catalyst] = 0.046 kmol/m^3 in org. phase, [sulphide] = 2.5 kmol/m^3, [MDEA] = 3.04 kmol/m^3, temperature = 333 K.

7.2.3.7. Effect of elemental sulphur loading.

The dark greenish colour of H_2S-laden MDEA solution became orange when elemental sulphur was added to it, the change in colour is attributed to the formation of disulphide. A similar colour change was observed during other parametric studies. The effect of elemental sulphur loading on conversion of 1-NN is shown in Figure 7.11. It is evident from the figure that initially reaction rate has increased with elemental sulphur addition but after certain time reaction rate slowed down.

It was predicted that polysulphide (S_n^{2-}, where $2 \leq n \leq 6$) was produced along with disulphide that can facilely transfer to the organic phase and reacts with aromatic nitro compounds as shown in Equation (7.3). A similar explanation was given by Lucas and Scudder (1928).[23] The transfer of hydrosulphide (HS^-) and sulphide ions (S^{2-}) to the organic phase is slower in comparison to disulphide ions and consequently disulphide ions can reduce nitroaromatic compounds faster.[24] Conversion without elemental sulphur addition was found to be higher after 120 min of reaction. This crossover may be due to the fact that the reaction rate increases as elemental sulphur build up as the reaction proceeds (Equation (7.2)).

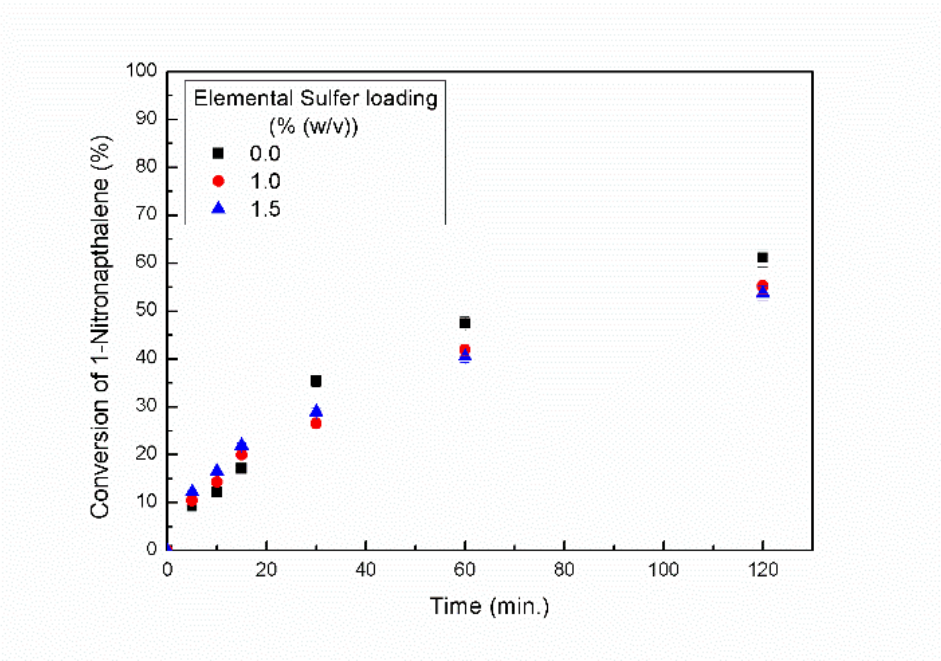

Figure 7.11. Effect of Elemental sulphur on the conversion of 1-NN. Operating conditions: Volume of organic phase = 3 x 10^{-3} m^3, volume of aqueous phase = 3 x 10^{-3} m^3, [1-NN] = 0.577 kmol/m^3 in org. phase, [toluene] = 8.17 kmol/m^3 in org. phase, [catalyst] = 0.046 kmol/m^3 in org. phase, [sulphide] = 2.5 kmol/m^3, [MDEA] = 3.04 kmol/m^3, temperature = 333 K.

7.2.3.8. Validation of the kinetic model.

The kinetic model has been validated by considering Equation (43) to be valid at different catalyst concentrations and plotting of $-ln\ (1-X)$ against time (Figure 7.12). The slope of each line gives apparent rate constant k_{app} at different catalyst concentrations as shown in Table 7.2.

Table 7.2 Apparent rate (k_{app}) constants at different temperatures[b]

Temperature (K)	313	323	333	343
k_{app} (min^{-1})	0.0092	0.0128	0.0161	0.0195

[b] All considerations are the same as mentioned in Figure 7.12.

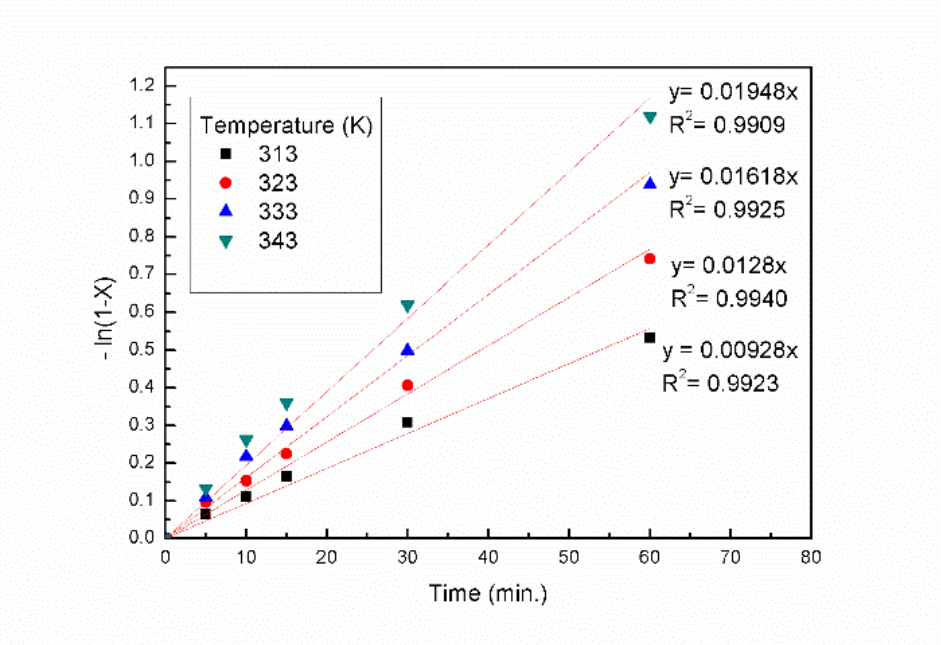

Figure 7.12. Validation of the kinetic model with experimental data at different catalyst concentrations. Operating conditions: Volume of organic phase = 3 x 10^{-3} m^3, volume of aqueous phase = 3 x 10^{-3} m^3, [1-NN] = 0.577 kmol/m^3 in org. phase, [toluene] = 8.17 kmol/m^3 in org. phase, [catalyst] = 0.046 kmol/m^3 in org. phase, [sulphide] = 2.5 kmol/m^3, [MDEA] = 3.04 kmol/m^3, temperature = 333 K.

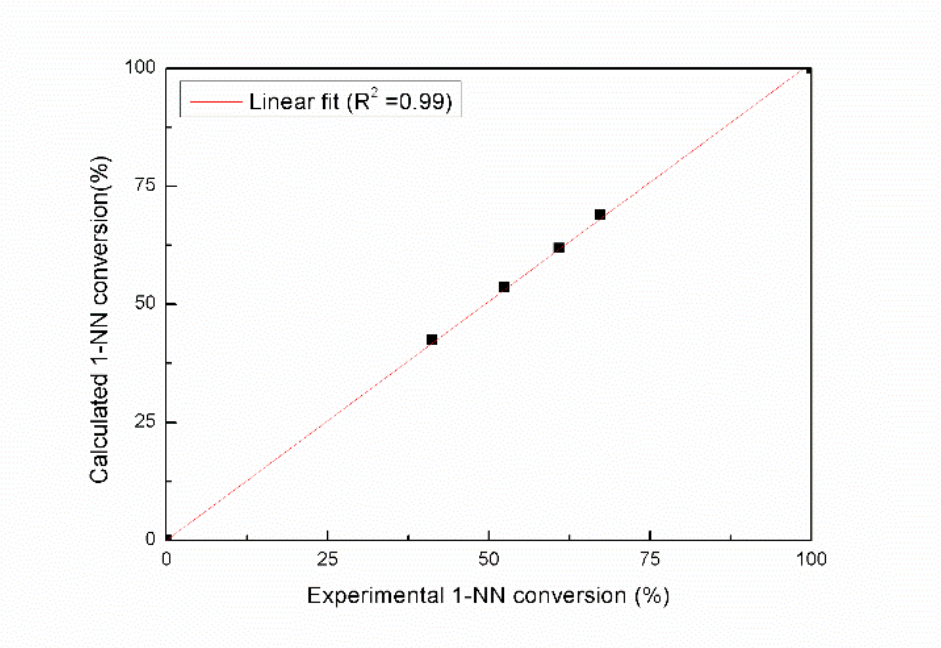

Figure 7.13. Comparison of calculated and experimental 1-NN conversions at 60 min at different temperatures. All considerations are the same as Figure 7.12.

Figure 7.13 represents a comparison of calculated conversions of 1-NN based on these rate constants and experimentally obtained conversions of 1-NN. Good agreement has been observed between calculated and experimental conversions. Mass spectra of 1-napthylamine is shown in Figure 7.14.

7.3. Conclusion.

H_2S-rich MDEA is successfully used as reducing agent for Zinin reduction of 1-NN in this work and 100% selectivity of 1-AN is achieved after the reaction. The reaction is kinetically controlled with an activation energy of 20.77 kJ/mol. This work addresses the novelties of the kinetics and mechanism of the selective reduction of 1-NN to respective amine using hydrogen sulphide absorbed in industrially significant sour gas absorber under L-L PTC. The effects of different parameters such as stirring speed, temperature, MDEA concentration, reactant concentrations (both sulphide and 1-NN), and sulphur loading were studied. The process was found to follow a complex mechanism involving different ions and molecules. Based on detailed kinetic studies and proposed mechanism, a kinetic model was developed considering Stark's extraction mechanism for L-L PTC. The

developed model predicts the conversion of 1-NN reasonable well at all temperatures.

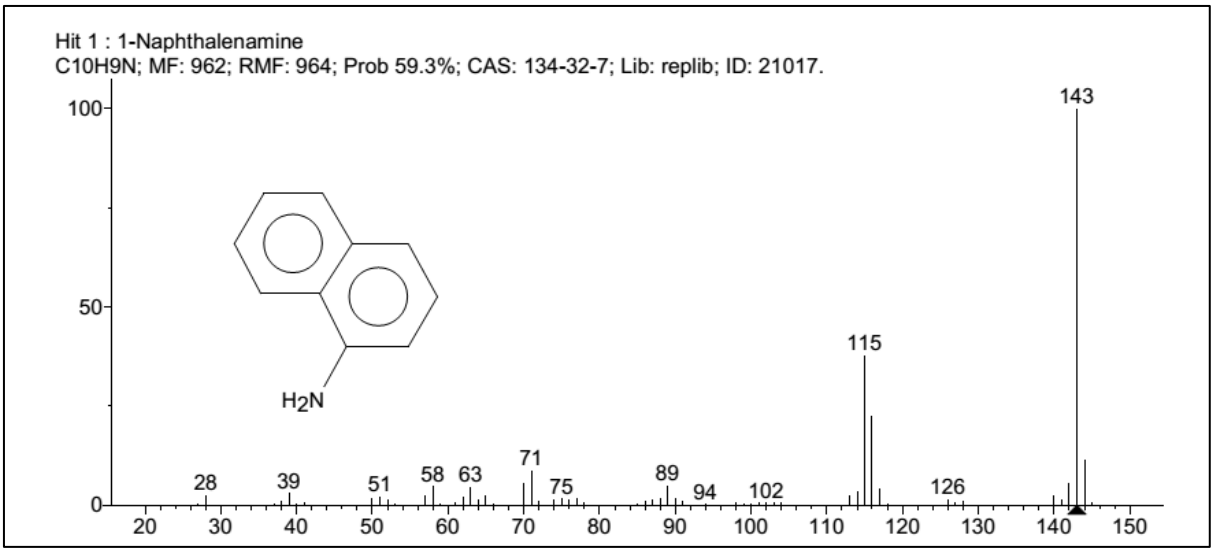

Figure 7.14: Mass spectra of product 1-napthylamine.

References

1 W. G. Dauben, *Organic reactions*, John Wiley & Sons, Inc., New York, 1973.

2 R. R. Bhave and M. M. Sharma, *J. Chem. Technol. Biotechnol.*, 1981, **31**, 93–102.

3 N. C. Pradhan and M. M. Sharma, *Ind. Eng. Chem. Res.*, 1992, **31**, 1606–1609.

4 N. C. Pradhan, *Indian J. Chem. Technol.*, 2000, **7**, 276–279.

5 G. D. Yadav, Y. B. Jadhav and S. Sengupta, *Chem. Eng. Sci.*, 2003, **58**, 2681–2689.

6 G. D. Yadav, Y. B. Jadhav and S. Sengupta, *J. Mol. Catal. A Chem.*, 2003, **200**, 117–129.

7 G. D. Yadav and S. V. Lande, *J. Mol. Catal. A Chem.*, 2006, **247**, 253–259.

8 P. H. Croggins, *Unit Processes in Organic Synthesis*, McCraw-Hill, New York, 5th edn., 1958.

9 H. Gilman, Wiley, New York, 1941, p. 52.

10 S. K. Maity, N. C. Pradhan and A. V. Patwardhan, *Appl. Catal. A Gen.*, 2006, 301, 251–258.

11 L. Kaewsichan, O. Al-Bofersen, V. F. Yesavage and M. S. Selim, *Fluid Phase Equilib.*, 2001, **183**–**184**, 159–171.

12 S. K. Maity, N. C. Pradhan and A. V. Patwardhan, *Chem. Eng. Sci.*, 2007, **62**, 805–813.

13 S. K. Maity, N. C. Pradhan and A. V Patwardhan, *Ind. Eng. Chem. Res.*, 2006, **46**, 7767–7774.

14 G. D. Yadav and S. V. Lande, *Appl. Catal. A Gen.*, 2005, **287**, 267–275.

15 G. D. Yadav and S. V. Lande, *Ind. Eng. Chem. Res.*, 2007, **46**, 2951–2961.

16 K. R. Hoover, W. E. Acree Jr. and M. H. Abraham, *J. Solution Chem.*, 2005, **34**, 1121–1133.

17 F. Jou, A. E. Mather and F. D. Otto, *Ind. Eng. Chem. Process Des. Dev.*, 1982, **21**, 539–544.

18 J. G. Lu, Y. F. Zheng and D. L. He, *Sep. Purif. Technol.*, 2006, **52**, 209–217.

19 Z. Qian, L. Xu, Z. Li, H. Li and K. Guo, *Ind. Eng. Chem. Res.*, 2010, 6196–6203.

20 R. H. Weiland, T. Chakravarty and A. E. Mather, *Ind. Eng. Chem. Res.*, 1993, **32**, 1419–1430.

21 Y. Wang, F. Wang, F. Jin and Z. Jing, *Ind. Eng. Chem. Res.*, 2013, **52**, 5616–5625.

22 S. K. Maity, N. C. Pradhan and A. V. Patwardhan, *Appl. Catal. B Environ.*, 2008, **77**, 418–426.

23 N. F. Lucas, H J, Scudder, *J. Am. Chem. Soc.*, 1928, **50**, 244–249.

24 Y. Hojo, M. Takagi, Y. Ogata, *J. Am. Chem. Soc.*, 1960, **82**, 2459–2462.

Abstract

A novel way of utilizing harmful H_2S gas to produce value-added chemicals has been explored. The improved Zinin reduction of 4-Nitroacetophenone (4-NAP) was studied with refinery generated toxic H_2S dissolved in aqueous N-methyldiethanolamine (MDEA) solution under liquid-liquid phase transfer catalysis. Response Surface Methodology (RSM) was employed to model the system and optimise the controlling parameters for maximum p-NAP conversion.

8.1 Introduction

Response Surface Methodology (RSM) was employed to model and optimize an improved Zinin reduction of a nitroarene, p-Nitroacetophenone (p-NAP), by hydrogen sulphide (H_2S) under bi-liquid phase transfer catalysis. A novel Zinin reagent, H_2S laden aqueous N-methyldiethanolamine (MDEA) solution was prepared and used for this purpose. A quadratic regression model was tested with a multivariate experimental design based on the relationship between p-NAP conversion (Response) and four independent variables - temperature, catalyst concentration, p-NAP: sulfide mole ratio and MDEA concentration. The optimum values of the independent variables were found as: temperature 339.45 K, catalyst concentration of 0.082 kmol/m^3, p-NAP/sulfide mole ratio of 0.452, MDEA concentration of 2.20 kmol/m^3 and maximum p-NAP conversion of 96.31% has been attained. The analysis of variance (ANOVA) has been used to evaluate the goodness of the fit of the model and the desirability function has been used to find the value of the optimized parameters to maximize the p-NAP conversion.

8.2 Result and Discussion

8.2.1 Overall reaction

Reduction of p- Nitroacetophenone (**1**) by H_2S-laden MDEA in the presence of TBPB as phase transfer catalysis to produce p-Aminoacetophenone (**2**) as a sole product with 100% selectivity is following Zinin reduction pathway is shown below.

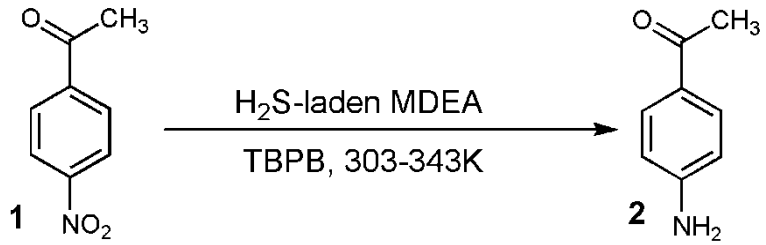

8.2.2. Proposed mechanism of the reaction.

The mechanism of reduction reaction of aromatic nitroaromatic compounds by Zinin reduction under L-L PTC mode of reaction has long been established.[1–3] Current L-L PTC system consists of an aqueous phase (H_2S absorbed in aqueous MDEA solution) and an organic phase (substrate p-NAP dissolved in toluene) and a quaternary phosphonium salt (TBPB). TBPB is a phase transfer catalyst in the reaction, is soluble in both the phases. Thus, the reaction mechanism can be explained by Stark's extraction mechanism. Valency of Sulphur can vary between -2 to +6. Therefore during the course of the reaction sulphur can be in multiple anionic forms (($HS^-, HSO^-, HSO_2^-, HSO_3^-$).

In the aqueous phase H_2S gas reacts with MDEA and forms two anions (Sulphide (S^{2-}) and hydrosulphide (HS^-) ions).[4–6] These two anions form an ionic equilibrium in the aqueous phase, which is same as observed in aqueous ammonium sulphide solution,[7] as shown in Scheme 8.1. Quaternary cations (Q^+) present in the aqueous phase readily binds with hydrosulphide anions (HS^-) and transfer to the organic phase. Then Q^+HS^- ion pair reacts with p-NAP to form p-AAP through the formation of multiple intermediates. The reduction reaction of the aromatic nitro compound to aromatic amines is an electron transfer reaction which requires 6 electron transfer through the formation of intermediates 2 and 3 (nitroso benzene and hydroxyamines).[8,9] The existence of these intermediates was undetected during GC-MS analysis because the formation and disappearance of these molecules are very fast. In the Scheme 8.1 at the end of the organic phase reaction Equation (8.7), the quaternary cation became inactive $Q^+HSO_3^-$. Then it transfers to aqueous phase and reacts with sulphide (S^{2-}) to regenerate again (Q^+HS^-) as shown in Equation (8.6). Like this, the cyclic process is going on. Selectivity of the p-AAP is 100% achieved in the current process of reduction.

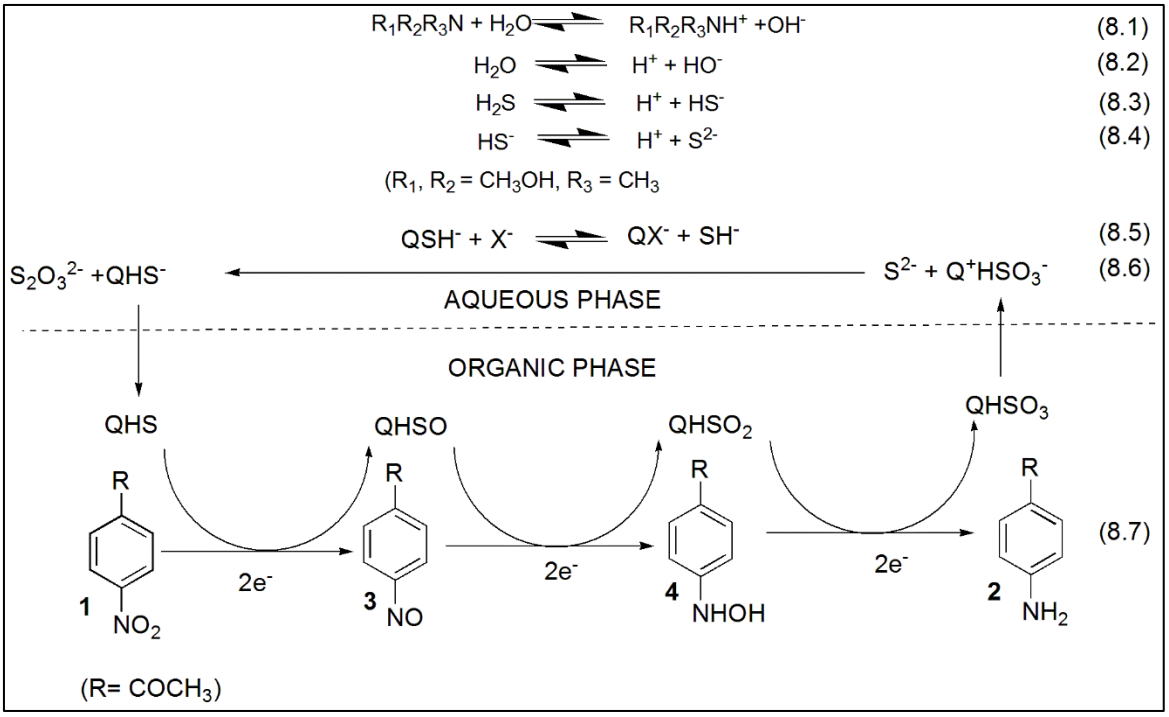

Scheme 8.1. Proposed mechanism for selective reduction of p-NAP by H_2S-laden MDEA solution in Zinin reduction.

8.2.3 Screening of parameters.

The main effect plot is shown in Figure 8.1. The effect of stirring speed and reaction time on p-NAP conversion is insignificant as shown in the figure. Based on the preliminary studies, it can be concluded that increasing stirring speed more than 1000 rev/min does not help to enhance total conversion of substrate.[10] In order to eliminate mass transfer effect entirely the stirring speed was maintained at 1500 rev/min. Reaction rate becomes slower after high initial conversion and to achieve maximum conversion all experiments are carried out for the duration of 8 hours. Catalyst concentration and MDEA concentration is having a strong effect on p-NAP conversion, and the temperature is having a weak effect on the conversion of p-NAP. p-NAP/ sulfide concentration ratio has a negative impact on conversion. As p-Aminoacetophenone (p-AAP) is the only product identified by GC-MS, p-NAP conversion is the only response chosen for our design as 100% selective product was obtained.

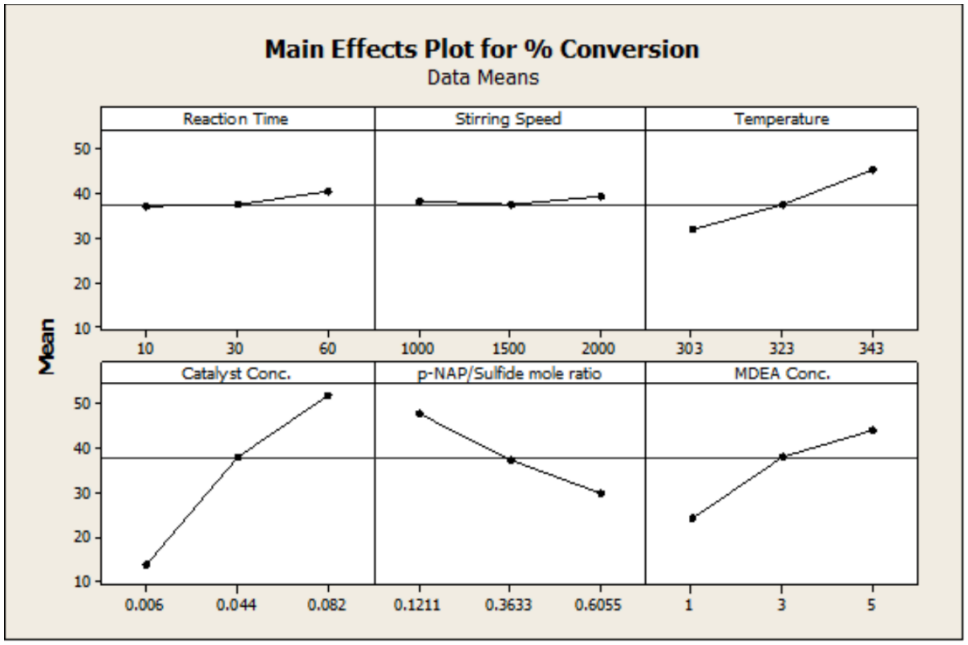

Figure 8.1. The main effect plot of control factors.

The levels and range of all the independent variables taken are listed in Table 8.1. The levels of each independent variable are set accordingly the knowledge gained from preliminary studies to achieve desired results.

Table 8.1 Coded levels and range of independent variables for experimental design.

Level	Coded level X_I	Uncoded level			
		A: Temperature (K)	B: Catalyst Conc. (kmol/m^3)	C: p-NAP/ Sulfide mole ratio	D:MDEA Conc. (kmol/m^3)
lowest	-2	303	0.006	0.1211	1.00
low	-1	313	0.025	0.2422	2.00
mid	0	323	0.044	0.3633	3.00
high	1	333	0.063	0.4844	4.00
highest	2	343	0.082	0.6055	5.00

8.2.4. Development of Regression Model Equation. Table 8.2 is the design matrix generated based on the range and levels of Table 8.1. The total number of experimental runs conducted were 30 as proposed by the central composite design and response (p-NAP conversion) was calculated to fit in a second order polynomial model. The centre points of the design are comprised of the variables at the zero level. To terminate the effects of the uncontrolled factors, a random experimental sequence is adopted. Runs 2,

13, 19, 23, 25 and 30 at the centre point of the design were utilised for the determination of the experimental error. Actual levels of independent variables, temperature (A), Catalyst concentration (B), p-NAP: sulfide mole ratio (C) and MDEA concentration (D) with ranges are shown in Table 8.2.

8.2.5 Model Selection and Fitting

The model is selected on the basis of different statistical parameters which were accurately analyzed by DOE. Fitting and significance of developed model can be understood by "p-value" and "F-value" of ANOVA analysis. Further refinement of the model can be done based on the results obtained by ANOVA analysis.

The software suggested that the quadratic model is the most suitable for the provided data based on the best lack of fit test, favorable F value, "prob>F" value, standard deviation, and R^2 value. It is shown in the form of the quadratic polynomial equation:

$$Y = \beta_0 + \sum_{i=1}^{4} \beta_i X_i + \sum_{i=1}^{4} \beta_{ii} X_i^2 + \sum_{i=1}^{4} \sum_{j=i+1}^{4} \beta_{ij} X_i X_j \tag{8.3}$$

Table 8.2. Experimental design matrix and results - A 2^4 full factorial CCD with six replicates of the Centre point.

Run	Actual level of variables				Response
	Temperature (K)	Catalyst Conc. (kmol/m^3)	p-NAP/Sulfide mole ratio	MDEA Conc. (kmol/m^3)	p-NAP Conversion (%)
1	323	0.044	0.6055	3.00	44.20
2	323	0.044	0.3633	3.00	47.92
3	313	0.025	0.2422	2.00	50.16
4	333	0.063	0.4844	2.00	61.60
5	313	0.025	0.2422	4.00	66.50
6	323	0.006	0.3633	3.00	44.49
7	313	0.063	0.4844	2.00	46.10
8	333	0.025	0.4844	4.00	49.33
9	333	0.025	0.2422	2.00	60.91
10	333	0.025	0.2422	4.00	72.00
11	313	0.025	0.4844	4.00	45.10
12	323	0.082	0.3633	3.00	82.40
13	323	0.044	0.3633	3.00	47.00

14	333	0.063	0.4844	4.00	73.11
15	323	0.044	0.3633	1.00	43.63
16	313	0.063	0.4844	4.00	58.46
17	323	0.044	0.1211	3.00	88.50
18	343	0.044	0.3633	3.00	70.00
19	323	0.044	0.3633	3.00	48.00
20	313	0.063	0.2422	2.00	66.73
21	333	0.063	0.2422	2.00	82.00
22	333	0.063	0.2422	4.00	95.21
23	323	0.044	0.3633	3.00	47.50
24	323	0.044	0.3633	5.00	69.00
25	323	0.044	0.3633	3.00	47.40
26	313	0.025	0.4844	2.00	32.83
27	303	0.044	0.3633	3.00	45.69
28	313	0.063	0.2422	4.00	81.22
29	333	0.025	0.4844	2.00	41.87
30	323	0.044	0.3633	3.00	46.40

Where Y is (the response of dependent variable) the conversion of p-NAP conversion (%) and β_is are the model coefficients calculated from experimental data.

Table 8.3 is showing the ANOVA result summary of the quadratic response surface model fitting. With 0.0001 probability and F-value of the model of 602.37 at the 0.01% level suggests a high degree of precision of the model. The "Lack of Fit F-value" is low as 3.28 signifies that there is a 10.12% chance of occurring of the large "Lack of Fit F-value" due to noise. The coefficient of determination (R^2) of 99.82% implies that the model fitting was accurate (Table 8.3) and only 0.18% of the total variability was unable to explain by the model. The "Pred R-Squared" value of 0.9908 in comparison with the "Adj R-Squared" of 0.9966; which signifies that the model prepared can give a very well estimation of the response of the system. The low value of the coefficient of variation (CV = 1.62%) of the model also suggests a high accuracy and better reliability of the experimental data. Adequate precision was also found to be more than 4. Figure 8.3 shows the comparison between predicted values and actual values for p-NAP conversion. From Figure 8.3, it is clear that the experimental values obtained are close to the predicted ones. Thus, we may imply that the developed model can successfully predict the conversion of p-NAP. The normal plot of residues for p-NAP (Figure 8.4) was found significant as didn't show any deviation of the variance.

All the linear, quadratic and interaction model terms are found to be significant as P-value for all terms are below 0.01. AC, BD are the interaction parameter that is having P-value

more than 0.15 and considered as insignificant. From the coded values of the main effect, quadratic and interaction parameters, it could be seen that A, B, C, D, AB, AD, BC, CD, A^2, B^2, C^2 and D^2 are major influencing parameters. AC and BD are the insignificant terms and are not necessary for explaining the conversion of p-NAP. Therefore, the insignificant terms are ignored for better fitting of the model. The significance of these quadratic and interaction effects between the variables had indeed been lost in earlier studies[11] where experiments were carried out following OVAT approach.

Final model equation for p-NAP conversion in terms of actual factors (subjected to range shown in Table 8.1) has been obtained as follows:

$$\% \text{ NAP Conversion} = 2798.27028 - 17.00191 \times A - 3678.47998 \times B - 267.31403 \times C + 18.49510 \times D\ 9.83453 \times AB - 0.10802 \times AC - 0.07620 \times AD - 148.06706 \times B + 14.43749 \times BD - 5.95633 \times CD + 0.02695 \times A^2 + 11343.68074 \times B^2\ 328.75893 \times C^2 + 2.31256 \times D^2 \quad (8.4)$$

Table 8.3 ANOVA for response surface quadratic model for p-NAP conversion[a]

Source	Sum of Squares	Degree of Freedom	Mean Square	F-Value	p-value Prob > F
Model	7612.22	14	543.73	602.37	< 0.0001
Residual	13.54	15	0.90		
Lack of Fit	11.75	10	1.17	3.28	0.1012
Pure Error	1.79	5	0.36		
Cor Total	7625.76	29			

[a]Coefficient of determination (R^2) =0.9982; Adj. R^2 =0.9966; Pred. R^2 =0.9908; C.V. % = 1.62; Adeq. Precision = 94.703; Std. Dev.= 0.95.

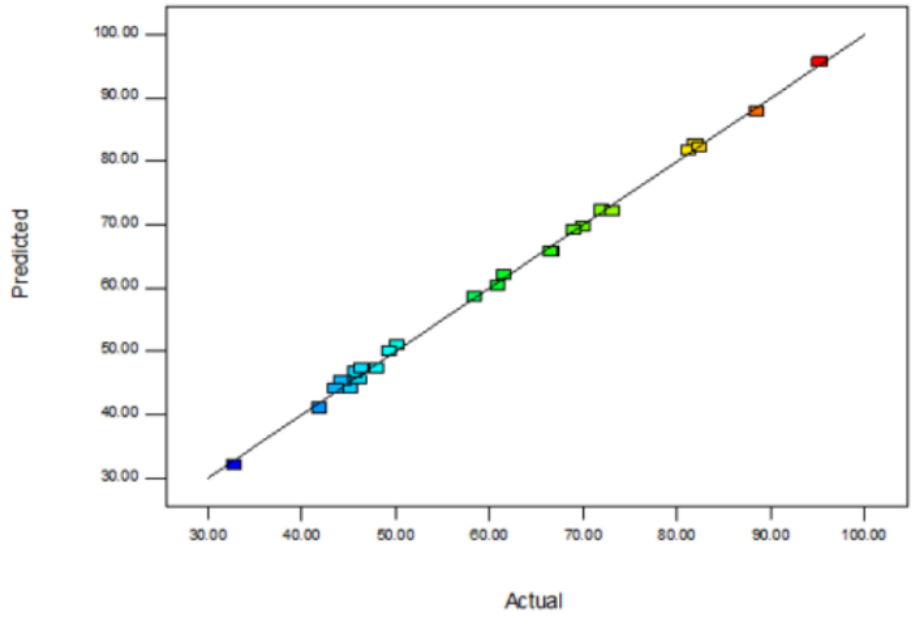

Figure 8.2 Plot of predicted values versus actual values for p-NAP conversion.

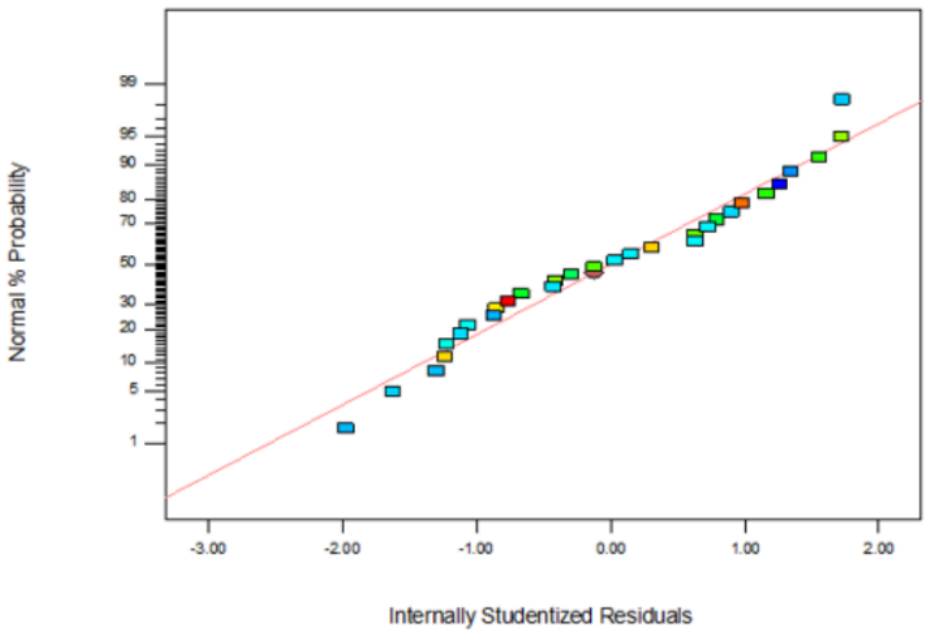

Figure 8.3 Normal plot of residuals for p-NAP conversion.

8.2.6. Model Analysis.

The regression analysis suggests that the p-NAP conversion was affected by Temperature (A), Catalyst conc. (B), p-NAP: Sulfide mole ratio (C), MDEA Conc. (D) and their respective higher order terms (A^2, B^2, C^2, D^2). The interaction between Temperatures – catalyst conc. (AB) is most significant. Moderate significant terms are temperature – MDEA conc. (AD), p-NAP: sulfide mole ratio – MDEA conc. (CD) and least significant interaction term is catalyst – p-NAP: sulfide mole ratio (BC). So, the value of each coefficient in the equation (8.4) symbolizes the extent of the influence made by the specific variable and sign signifies whether the effect is positive or negative. Earlier studies on a similar type of system[3] showed only the variation of responses with each parameter without giving any clue to the comparative influence of each main effect on each response.

8.2.7. Response surface analysis.

3D surface and contour plots are the graphical representation of the regression equations implemented to achieve or predict the optimum influence of variables and to gain a better understanding of combined interaction variables the range provided.[12,13] 3D surface plots show not only the combined but also the sole impact of the variables on the response. While the circular or elliptical nature of the contour (2D) helps to identify the major interactions between the process variables.

Figure 8.4A & 8.4B shows the interaction effect of catalyst concentration and temperature on the conversion of p-NAP. Conversion increased with the increase of catalyst concentration and temperature, either individually or combined. The catalyst concentration is having pronounced effect on conversion. Highest conversion of 71% achieved with 0.063 kmol/m^3 catalyst concentration and at 333K temperature. As the catalyst loading increased the number of active catalyst increase in the reaction mixture and so the conversion. The transition state theory explains that the rates of most organic reactions can be enhanced by the increase of reaction temperature, and the collision theory suggests that at higher temperature the number of effective collision between molecules increases and hence the rate of reaction also increases. Reaction under PTC mode also shows similar observations. It is evident from the Figure (8.4A & 8.4B) that the conversion of p-NAP amplifies with an increase in the temperature.

The Figure 8.4C & 8.4D shows the interaction between MDEA concentration ratio and temperature on p-NAP conversion. The effect of MDEA concentration has a positive influence on p-NAP conversion and the effect of temperature if very feeble. MDEA does not react with p-NAP but it is affecting equilibrium among MDEA-H_2S-water and which is dominated by sulfide and hydrosulfide anions. With more MDEA concentration the equilibrium between active anions shift towards more concentration of sulfide anions and

the conversion p-NAP is enhanced (Equation 8.1). Highest conversion of 63.5% achieved with MDEA concentration of 4 and at 333K.

Figure 8.5A & 8.5B is showing the interactive effect of p-NAP: sulfide concentration ratio and MDEA concentration on the conversion of p-NAP. According to the figure, the conversion of p-NAP is decreased with the increased ratio of p-NAP/sulfide concentration ratio. MDEA concentration is the feeble effect on p-NAP in comparison to p-NAP/sulfide concentration ratio. Reducing the p-NAP/sulfide concentration ratio from 0.48 to 0.24, have increased the conversion 49% to 72%. As the ratio of p-NAP/sulfide concentration decreases the number of moles of sulfide molecules par moles of p-NAP increases as the conversion is also enhanced.

Figure 8.5C & 8.5D is showing the combined effect of p-NAP/sulfide concentration ratio and catalyst concentration on the p- NAP conversion. With the highest catalyst concentration of 0.063 and lowest p-NAP/sulfide concentration ratio 76% conversion achieved.

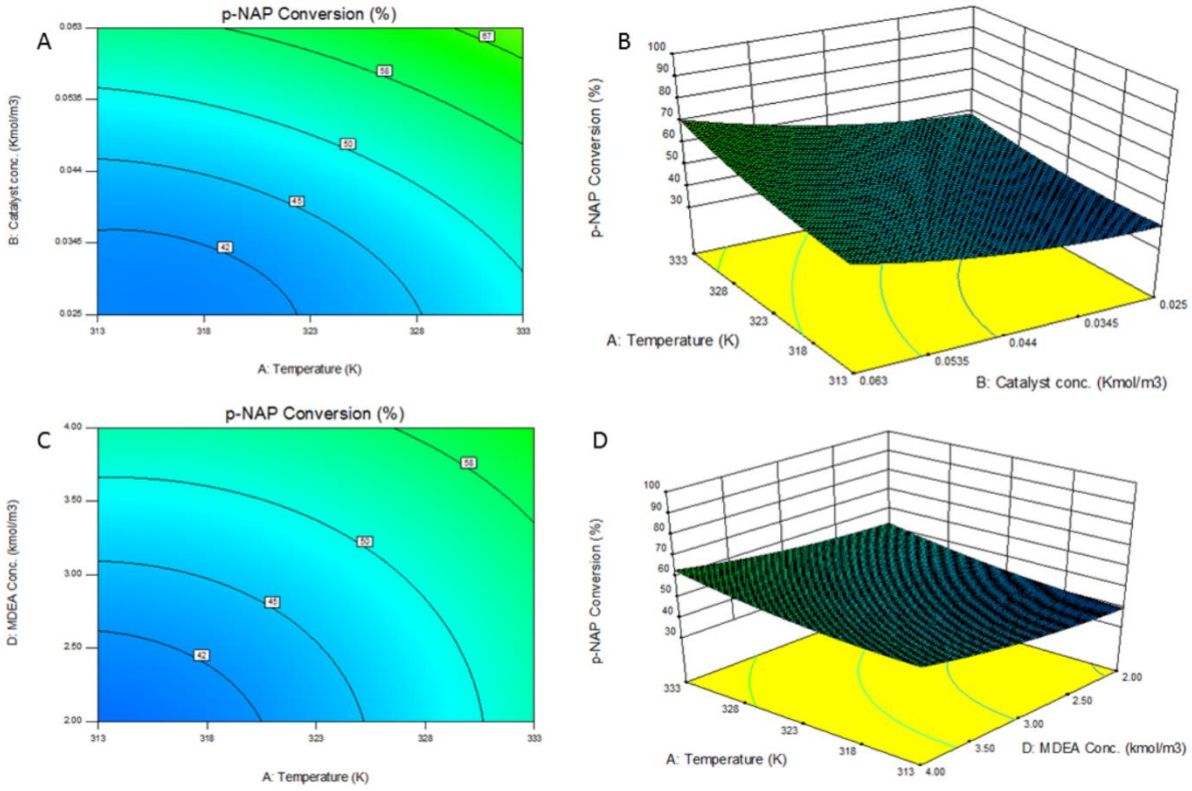

Figure 8.4 Contour and 3D surface plot of the effect of different parameters on the conversion of p-NAP (A) contour plot of the interaction of Temperature and Catalyst concentration. (B) 3D surface plot of the interaction of Temperature and Catalyst concentration. (C) Contour plot of the interaction of Temperature and MDEA concentration. (D) 3D surface plot of the interaction of Temperature and MDEA concentration.

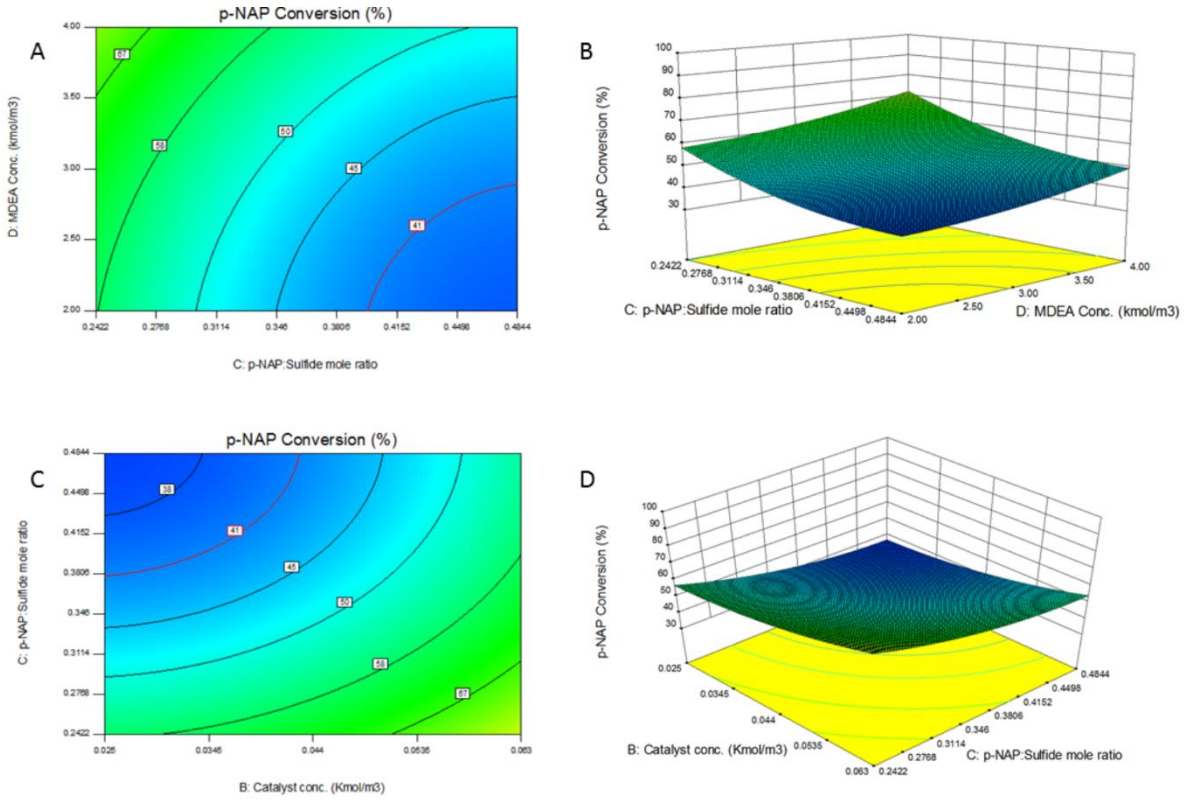

Figure 8.5 Contour and 3D surface plot of the effect of different parameters on the conversion of p-NAP (A) Contour plot of the interaction of Catalyst concentration and MDEA concentration. (B) 3D surface plot of the interaction of Catalyst concentration and MDEA concentration. (C) Contour plot of the interaction of Catalyst concentration and p-NAP: sulfide concentration ration. (D) 3D surface plot of the interaction of Catalyst concentration and p-NAP: sulfide concentration ration.

8.2.8 Optimization of influencing factors.

The numerical optimization function of the software has been utilized in search of the specific points where desirability reaches the maximum. The weight or importance of the goal is set accordingly to achieve the desired goal. Optimum conditions for conversion of p-NAP is obtained with the response surface methodology on the basis of the desirability function. The goal set for each constraint is in range among four other possibilities (none, minimum, maximum, and target). The criterion for all parameters that are adopted to

achieve maximum p-NAP conversion are shown in Table 8.4. Based on the range of the parameters provided, the optimum criteria for p-NAP conversion (96.31%) were found to be temperature fixed at 339.45 K, with a catalyst concentration of 0.082 kmol/m^3, p-NAP/sulfide concentration ratio of 0.452 and MDEA concentration of 2.20 (Figure 8.6).

Table 8.4 Optimization of the individual Responses (d_i) to find the Overall Desirability Response (D).

Name	Goal	Lower Limit	Upper Limit	Lower Weight	Upper Weight	Importance
Temperature	is in range	303	343	1	1	3
Catalyst conc.	is in range	0.006	0.082	1	1	3
p-NAP:Sulfide mole ratio	is in range	0.1211	0.6055	1	1	3
MDEA Conc.	is in range	1	5	1	1	3
Conversion	maximize	32.83	95.21	1	1	5

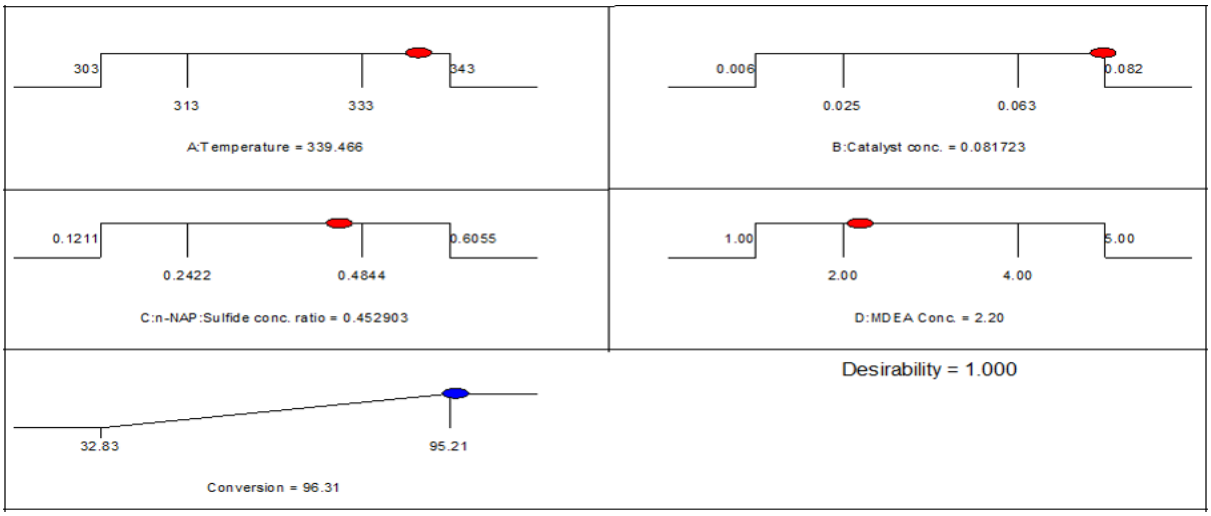

Figure 8.6 Desirability ramp for numerical optimization.

8.3 Model verification and confirmation

In order to confirm the established model, a number of verification experiments were carried out based on the optimum conditions for achieving maximum p-NAP conversion. After three replicate experiments, an average of 96.07% conversion achieved, as shown in Table 8.5. So it can be concluded that there is a good agreement between the models

predicted value and experimental value and thus the validity of the model simulated for p-NAP is confirm.

Table 8.5. Results of validation experiments[a].

Run No.	Conversion%	Selectivity%
1	96.0	100.0
2	96.12	100.0
3	96.09	100.0
Average	96.07	100.0
Predicted by Eq. (5)	96.07	-

[a] Experiments conducted at conditions: Temperature = 339.5K; Catalyst conc. =0.082 kmol/m^3; p-NAP: Sulfide mole ratio=0.452; MDEA Conc. = 2.20 kmol/m^3.

8.4 Conclusion

Based on experimental design methodology a statistical model of single response surface optimization was carried out on the liquid-liquid phase transfer catalyzed the reaction of p-NAP with H_2S-ladden MDEA. A quadratic model developed based on the relationship between p-NAP conversion and four independent variables (temperature, catalyst conc., p-NAP/sulfide mole ratio and MDEA conc.). The contour plots, 3D surface plots and the value of different regression coefficients have clearly explained the single parameter effect and interaction effects of dual parameters on the p-NAP conversion. The model fits well and is verified with optimum conditions for highest p-NAP conversion. R^2 value of the regression analysis confirms a good agreement between the experimental data and predicted response. From the response surface analysis it is very clear that temperature and catalyst loading in the reaction system amplifies the reaction rate and product yield. The concentration of MDEA and concentration sulphide ions increase in the reaction system enhances the reaction rate and reactant conversion also. Figure 8.7 shows the MS Spectra of the product 3-aminoacetophenone.

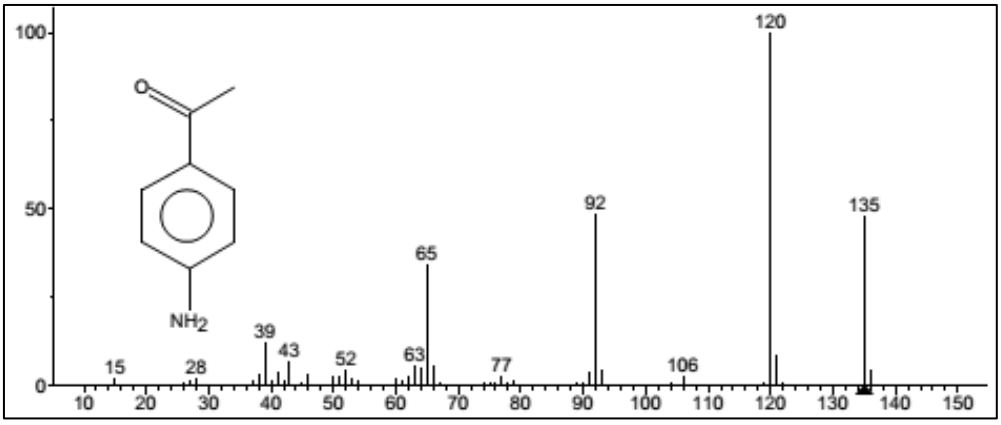

Figure 8.7: MS Spectra of the product 3-aminoacetophenone.

References

1 G. D. Yadav and S. V. Lande, *Adv. Synth. Catal.*, 2005, **347**, 1235–1241.

2 G. D. Yadav and S. V. Lande, *Ind. Eng. Chem. Res.*, 2007, **46**, 2951–2961.

3 G. D. Yadav, Y. B. Jadhav and S. Sengupta, *Chem. Eng. Sci.*, 2003, **58**, 2681–2689.

4 H. Xu, C. Zhang and Z. Zheng, *Society*, 2002, 6175–6180.

5 H. Xu, C. Zhang and Z. Zheng, *Simulation*, 2002, 2953–2956.

6 S. K. Maity, N. C. Pradhan and A. V Patwardhan, *Ind. Eng. Chem. Res.*, 2006, **46**, 7767–7774.

7 S. K. Maity, N. C. Pradhan and A. V. Patwardhan, *Appl. Catal. A Gen.*, 2006, 301, 251–258.

8 J. Klausen, J. Ranke and R. P. Schwarzenbach, *Chemosphere*, 2001, **44**, 511–517.

9 B. Zhou, J. Song, H. Zhou, T. Wu and B. Han, *Chem. Sci.*, 2016, **7**, 463–468.

10 G. Singh, P. G. Nakade, P. Mishra, P. Jha, S. Sen and U. Mondal, *J. Mol. Catal. A Chem.*, 2016, **411**, 78–86.

11 S. K. Maity, N. C. Pradhan and A. V. Patwardhan, *Appl. Catal. A Gen.*, 2006, **301**, 251–258.

12 H. L. Liu and Y. R. Chiou, *Chem. Eng. J.*, 2005, **112**, 173–179.

13 D. Vildozo, C. Ferronato, M. Sleiman and J.-M. Chovelon, *Appl. Catal. B Environ.*, 2010, **94**, 303–310.

Abstract

Selective reduction of one of the nitro group present in dinitro aromatic compounds by a novel Zinin reagent, H_2S-laden N-methyldiethanolamine (MDEA) solution, has been explored in the presence of Tetra-n-butyl phosphonium bromide (TBPB) as phase transfer catalyst (PTC) under the liquid-liquid (L-L) mode of reaction. Under the present condition, reduction 2,4-dinitrotoluene (2,4-DNT) with H_2S-laden MDEA leads to the selective reduction of one nitro group present either at the fourth position to obtain 4-amino-2-nitrotoluene (4A2NT) or at the second position to get 2-amino-4-nitrotoluene (2A4NT).

9.1 Introduction

Selective reduction of one of the nitro group present in dinitro aromatic compounds by a novel Zinin reagent, H_2S-laden N-methyldiethanolamine (MDEA) solution, has been explored in the presence of Tetra-n-butyl phosphonium bromide (TBPB) as phase transfer catalyst (PTC) under the liquid-liquid (L-L) mode of reaction. Under the present condition, reduction 2,4-dinitrotoluene (2,4-DNT) with H_2S-laden MDEA leads to the selective reduction of one nitro group present either at the fourth position to obtain 4-amino-2-nitrotoluene (4A2NT) or at the second position to get 2-amino-4-nitrotoluene (2A4NT). The reaction was very fast to achieve 100% conversion, and the selectivity of 4A2NT is much higher than the 2A4NT. A detailed parametric study was performed to analyse the effect of parameters on 2,4-DNT conversion and selectivity of both the isomers. The apparent activation energy was found to be as high as 46.25 kJ/mol, which indicates that the reaction was kinetically controlled. A mathematical model has been developed for the complex system, and it was validated against the experimental data. The present system dealt with an industrial problem in dealing with H_2S, present in by-product gaseous streams of many petroleum and natural gas industries. Novelties in the selective mono-reduction lie in that fact that the reaction was done at room temperature (303 K), with a novel reagent, H_2S-laden MDEA solution. Therefore waste-minimization was effected to yield a value-added fine chemicals, i.e., amines.

9.2 Results and Discussion

Two products namely 4-amino-2-nitrotoluene (4A2NT) and 2-amino-4-nitrotoluene (2A4NT) were identified by GC-MS (Agilent 5977A model). No diamines or other products like nitroso or hydroxylamine were found out. So, the overall reaction can be written as follows:

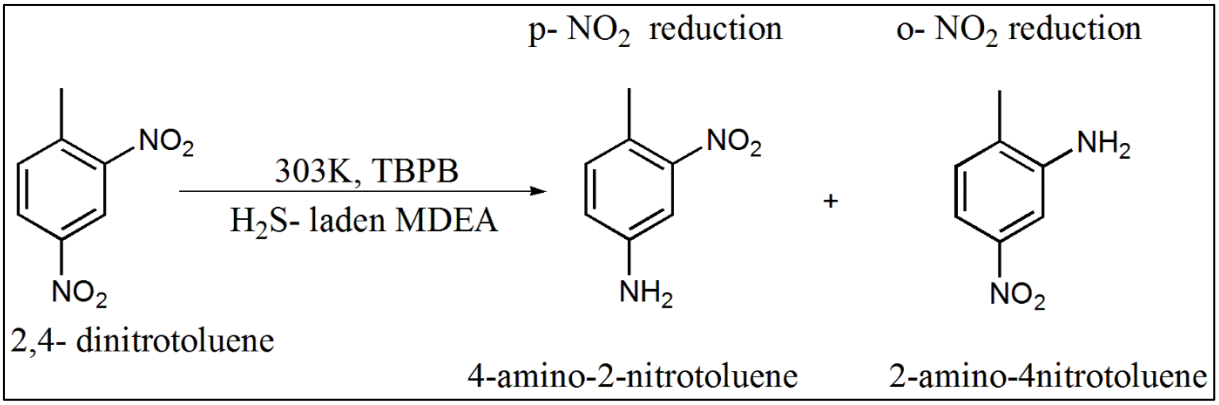

9.2.1. Proposed mechanism of reduction of 2,4-DNT under L-L PTC

As proposed by Zinin in 1842, the overall stoichiometry of the reduction reaction of nitroarenes by aqueous ammonium sulphide is given by Equation (9.1) [1]. Sodium sulphide as a reducing agent for the reduction of aromatic nitro compounds also follows same stoichiometry [2–6].

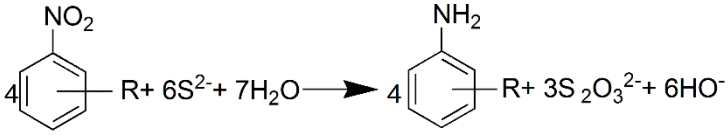

(9.1)

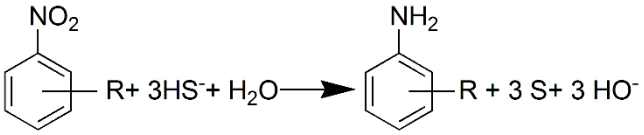

(9.2)

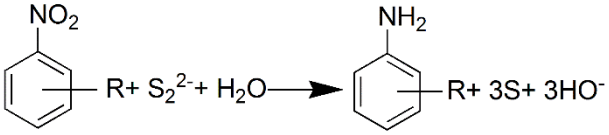

(9.3)

Elemental sulphur was found as a by-product of the reduction reaction of *p*-nitrophenylacetic acid with aqueous ammonium sulphide as shown in the Equation (9.2) [7]. Thiosulphate or elemental sulphur is generated as a by-product in two different reactions as shown in Equation (9.1) and (9.2). In the presence of a base, ammonia, the dissociation equilibrium favours toward more ionisation [8] and as the concentration of ammonia increases, the concentration of sulphide ions (S^{2-}) become more than hydrosulphide (HS^{-}) ions. Sodium disulphide was also used as the reducing agent, and the overall

stoichiometry is shown in Equation (9.3) [7]. Zinin reduction of 2,4-DNT with H_2S-laden MDEA is assumed to follow Equation (9.1) or (9.2).

9.2.1.1. Aqueous Phase Equilibrium

In the aqueous MDEA phase, sulphide (S^{2-}) and hydrosulphide (HS^-) ions exist in an ionic equilibrium which is affected by the concentration of the MDEA [9]. Formation of both the anions is shown in the Scheme 9.1 from Equation (9.4) to Equation (9.6). Similar results were shown by ammonium sulphide solution [10].

9.2.1.2. Phase Transfer Catalysis in biphasic liquid-liquid system

A general reaction mechanism of current reduction reaction has been proposed based on the current work and some previously published work (Scheme 9.1) [2,6,11,12]. Valency of sulphur can vary in a wide range (-2 to +6) and thus the presence of sulphur in different anionic forms ($HS^-, HSO^-, HSO_2^-, HSO_3^-$) in the reaction media is very much possible and an established fact, and those anions can bind to single quaternary cations very easily [6].

The catalyst used for our study was TBPB, which is soluble in both the phases. The LLPTC reaction pathway can be easily explained by Stark's extraction mechanism, as according to the mechanism the phase transfer catalyst partitioned into both phases. The catalyst captions present in the aqueous phase transfers the inorganic anions to the organic phase where it took part in the reaction with the organic substrate.

L-L PTC system is cyclic process; it starts at the aqueous phase where quaternary cations (Q^+) rapidly pair with hydrosulphide ions (HS^-) to form Q^+HS^- ion pair, and then the ion pair transfer to the organic phase. After that, it took part in some complex elementary reaction as shown in Scheme 9.1(Equation 9.12 to Equation 9.17). Without the presence of phase transfer catalyst, the similar reaction also occurs but it is rather a slow reaction. The end product of the reduction reaction of 2,4-DNT is 4-amino-4-nitrotoluene (4A2NT) and 2-amino-4-nitrotoluene (2A4NT). The reduction reaction of the aromatic nitro compound to aromatic amines is an electron transfer reaction which requires 6 electron transfer through the formation of intermediates- nitrosobenzene and benzene hydroxylamines)[13,14]. GC-MS analysis of the samples was not able to detect those intermediates; this may be due to the fast appearance and disappearance of those intermediates[6,13,15–17]. The selectivity of 2A4NT is less because of the nitro group present at the 2nd position that is sterically hindered by the methyl group present on the aromatic ring. So the reduction of nitro group present at the 4th position is easier than the 2nd position and as a result selectivity of 4A2NT is higher [16]. A few water molecules also

transfer to the organic phase along with the Q^+HS^- ion pair and taking part in the reaction (Equation (9.14) & Equation (9.16)). Quaternary ion pair gets inactivated ($Q^+HSO_3^-$) after the formation of the product (Equation (9.17) and when it transfers back to the aqueous phase it gets regenerated (Q^+HS^-) after reacting with S^{2-} (Equation (9.9)). Then the same catalytic cycle started when reactivated ion pair transfer to the organic phase.

The developed mechanism for the reduction of 2,4-DNT suggests that the Q^+HS^- is the majorly available ion pair among other ions available. In the aqueous phase, nine reactions (Equation (9.4) – Equation (9.11)) took place and remaining reactions (Equation (9.12) – Equation (9.17)) occurred sequentially in the organic phase.

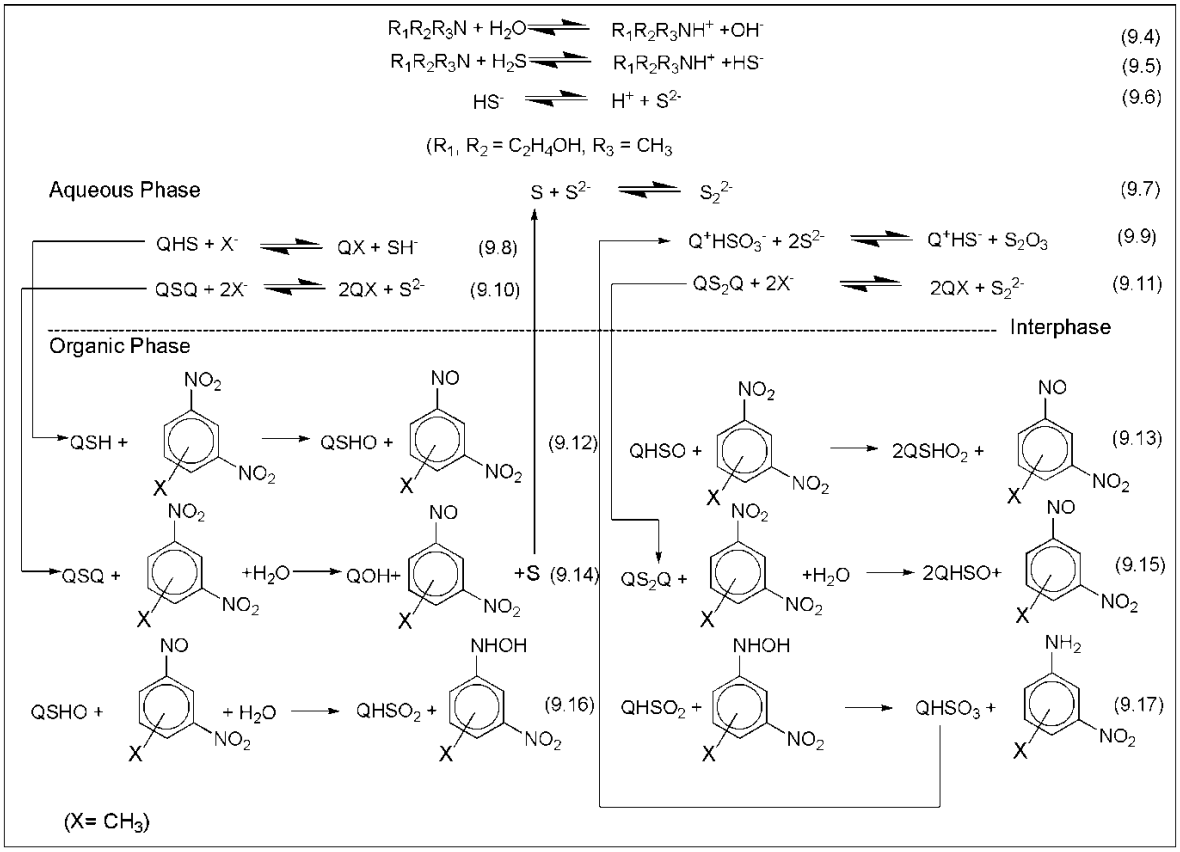

Scheme 9.1 Proposed mechanism of reduction of 2,4-DNT by H_2S-laden MDEA under L-L PTC.

9.2.2 Parametric studies

9.2.2.1. Effect of agitation intensity

The effect of stirring speed on the reaction rate of 2,4-DNT disappearance in L-L PTC system has been explored in the range of 500-2500 rev/min in the presence of PTC. It is very clear from the Figure 9.1 that, the variation of initial reaction rate is very small due to change in stirring speed. So it can be concluded that the reaction is kinetically controlled and free from any mass transfer resistance. For elimination of the mass transfer effect, the stirring speed has been fixed at 1500 rev/min during other parameter variation studies.

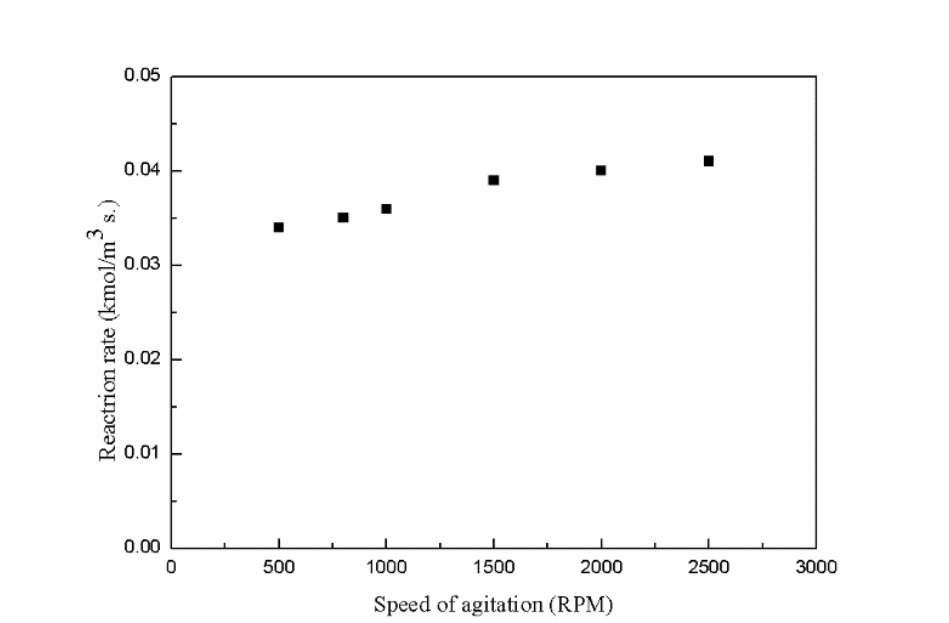

Figure 9.1 Effect of Stirring speed on the reaction rate. Temperature = 303 K, Organic phase volume = 3 x 10^{-5} m^3, Concentration of 2,4-DNT in organic phase = 0.549 kmol/m^3, Concentration of TBPB = 0.0232 kmol/m^3, Aqueous phase volume = 3 x 10^{-5} m^3, Concentration of MDEA in aqueous phase = 3.04 kmol/m^3, Concentration of sulphide in aqueous phase = 2.5 kmol/m^3.

9.2.2.2. Comparison of conversion between different dinitrotoluenes

In this study, the effectiveness of the developed reduction process by using H_2S-laden MDEA has been analysed on different isomers of dinitrotoluenes, as shown in Figure 9.2. For the current study, 2,4 dinitrotoluene (2,4-DNT) and 2,6 dinitrotoluene (2,6-DNT) have been used as a study material. From the Figure 9.2a, it is very clear that reactivity of 2,4-DNT is higher and selectively reduced to 4A2NT (79.6%) and 2A4NT (20.4%). Reduction of 2,6 DNT results only 2-amino-6-nitrotoluene (2A6NT) and conversion achieved was 76.23% after 120 min of reaction. The nitro group present at the 2^{nd} and 6^{th} position that are sterically hindered by the methyl group attached to the aromatic ring. So

the reduction of nitro group present at the 4th position is easier compared to 2nd and 6th position. As a result reactivity of 2,4 DNT was found of being higher than 2,6 DNT.

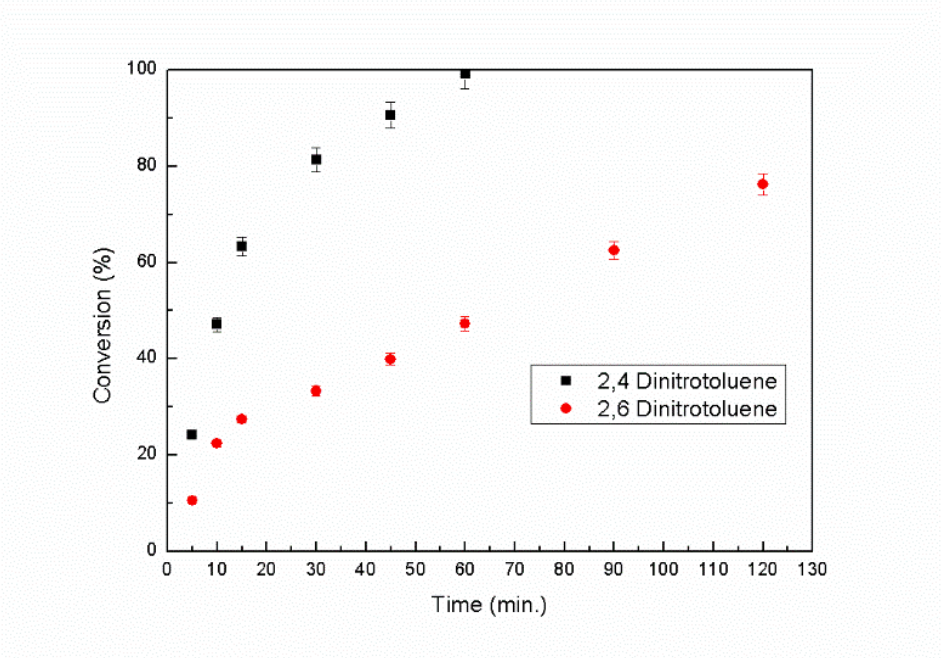

Figure 9.2 Conversion-time plot obtained experimentally of two isomers of dinitrotoluenes. Stirring speed = 1500 rpm, Temperature = 303 K, Organic phase volume = 3 x 10^{-5} m^3, Concentration of reactant in organic phase = 0.549 kmol/m^3, Concentration of TBPB = 0.0232 kmol/m^3, Aqueous phase volume = 3 x 10^{-5} m^3, Concentration of MDEA in aqueous phase = 3.04 kmol/m^3, Concentration of sulphide in aqueous phase = 2.5 kmol/m^3.

9.2.2.3 Effect of different phase transfers catalyst

The selective reduction of 2,4-DNT was studied with different phase transfer catalysts as shown in Figure 9.3. Catalysts taken for the comparison studies are Tetrabutylammonium bromide (TBAB), Tetrabutylphosphonium bromide (TBPB), Tetramethylammonium bromide (TMAB), Tetrabutylammonium iodide (TBAI) and Ethyltriphenylphosphonium bromide (ETPPB), Tetrapropylammonium bromide (TPAB). The order of the reactivity of these catalysts is TBPB> TBAB> TPAB> ETPB> TBAI> TMAB. With a higher number of carbon atom in the alkyl group of PTC, the lipophilicity and extraction rate of PTC enhances, which in turns generates higher productivity. ETPPB is having higher carbon number although it is showing less reactivity than other ammonium and phosphonium salts (TBPB, TBAB, and TPAB). As the only single methyl group and three big benzyl group attached with the quaternary cation in ETPPB, the quaternary cation is not easily accessible for anions, and reaction rate gets slower. The phosphonium salt (TBPB) has shown better reactivity than ammonium salts (TBAB, TBAI). The apparent rate constant

is shown in Table 9.2 for the six PTC used in the comparison study and TBPB exhibit the highest reactivity.

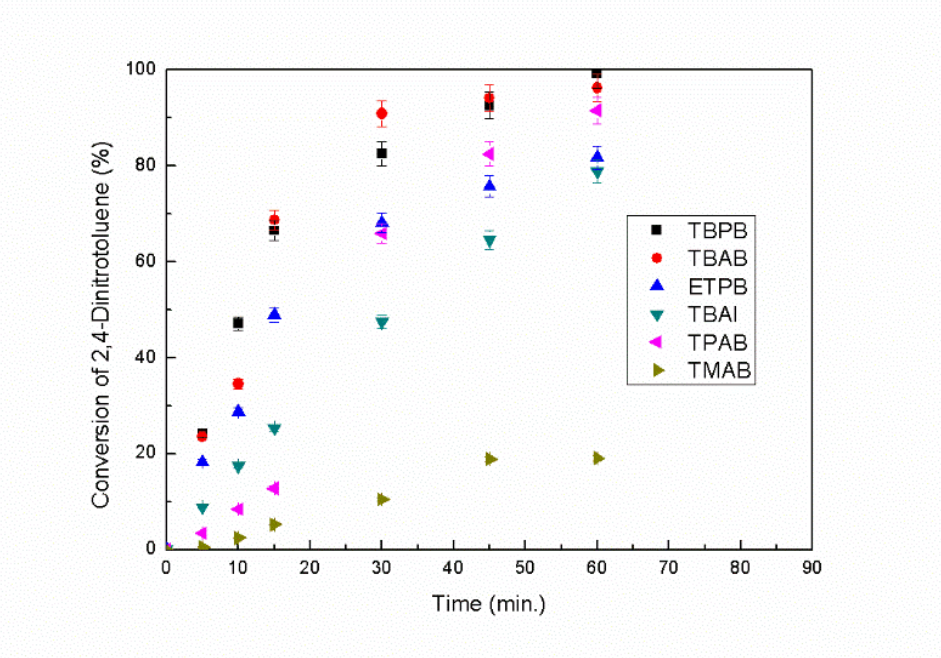

Figure 9.3 Effect of different catalysts on the conversion of 2,4-DNT. Stirring speed = 1500 rpm, Temperature = 303 K, Organic phase volume = 3 x 10^{-5} m^3, Concentration of 2,4-DNT in organic phase = 0.549 kmol/m^3, Concentration of TBPB = 0.0232 kmol/m^3, Aqueous phase volume = 3 x 10^{-5} m^3, Concentration of MDEA in aqueous phase = 3.04 kmol/m^3, Concentration of sulphide in aqueous phase = 2.5 kmol/m^3.

9.2.2.4. Effect of other organic solvents

In this study, organic solvents such as Chloroform, Benzene, and Toluene were employed to analyse the effect of their polarities (dielectric constant) on the reactivity of the reduction reaction as shown in Figure 9.4. According to the stark's mechanism phase transfer catalyst must transfer the reactive anions into the organic phase to react with the organic substrate. If the reactive anions are firmly held by a cation, then reaction rate will be hindered. Strong solvation (including hydration) of the anions in the solvent also affects the reactivity. Non–polar solvents promote higher reactivity by reducing the extent of solvation of anions and by increasing the concentration of phase transfer catalyst in the organic phase. But if the polarity of the solvent is low then the catalyst is unable to ionise, and hence, reactivity will be very low and the distribution of the catalyst in both the phases is also affected by the solvent. The maximum deviation in conversion of 2,4-DNT was found to be 7% because of the change of a solvent. So, the effect of solvent is not significant, and therefore solvent effect can be ignored. Therefore, in kinetic modeling we

didn't consider the solvent effect.The dielectric constant of the solvents used is in order of Chloroform> Benzene> Toluene. And the conversion (and reactivity) of 2,4-DNT in the solvents follows in the order Benzene> Toluene> Chloroform. Thus, in the current reaction system, toluene has been used as an effective solvent. . Like in our present case, toluene was found to be a better solvent in other biphasic phase transfer catalytic reaction systems [19]

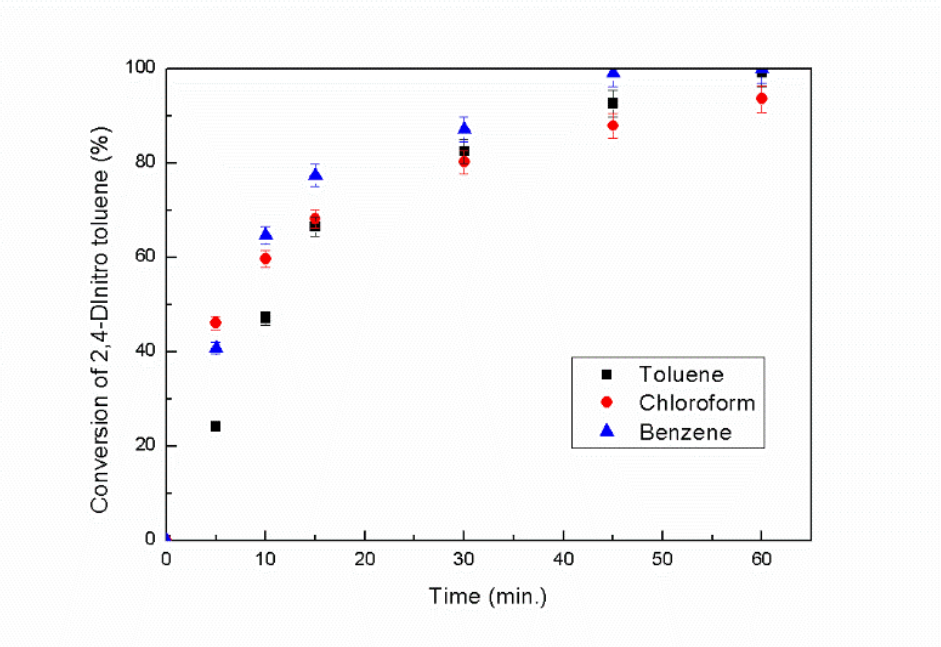

Figure 9.4. Effect of different solvents on the conversion of 2,4-DNT. Stirring speed = 1500 rpm, Temperature = 303 K, Organic phase volume = 3 x 10^{-5} m^3, Concentration of 2,4-DNT in organic phase = 0.549 kmol/m^3, Concentration of TBPB = 0.0232 kmol/m^3, Aqueous phase volume = 3 x 10^{-5} m^3, Concentration of MDEA in aqueous phase = 3.04 kmol/m^3, Concentration of sulphide in aqueous phase = 2.5 kmol/m^3.

9.2.3.5. Effect of temperature of the reaction

To study the effect of temperature on the conversion of 2,4-DNT in L-L PTC system the temperature of the reaction is varied in the range of 313–343K and rest of all reaction conditions were kept same (Figure 9.5a). From the theory of transition state, the rate of a reaction increases with the rise in temperature because increasing temperature provides the energy required to overcome the reaction barrier. It is evident from the figure that the temperature variation has a great impact on reactivity (conversion) of 2,4-DNT. With increasing temperature, the collision between reactant molecules are becoming more frequent, and thus reaction rate gets enhanced.

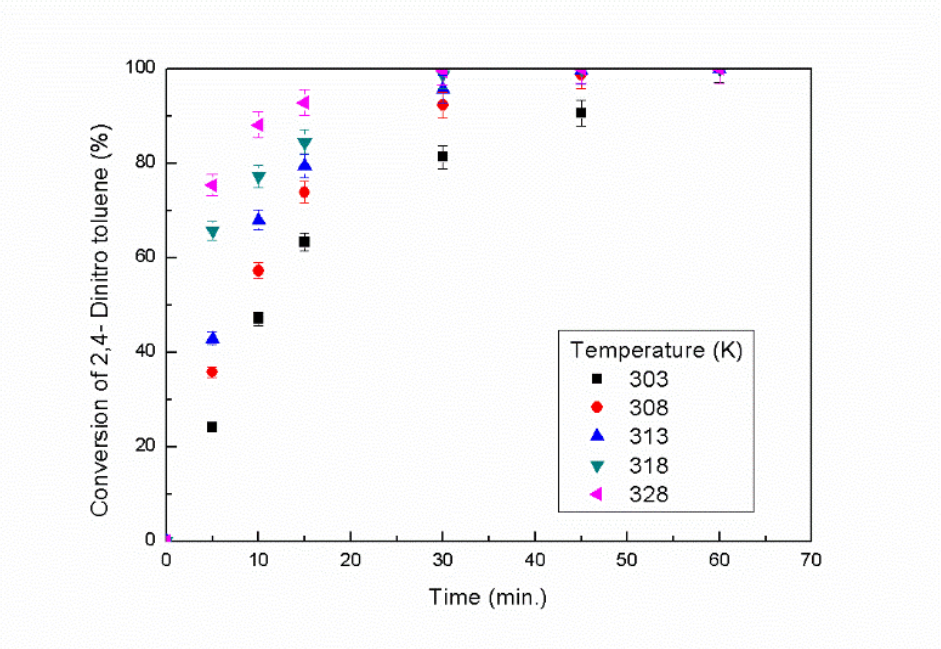
Conversion of 2,4- Dinitro toluene (%)
Time (min.)
Temperature (K)
303
308
313
318
328

(a)

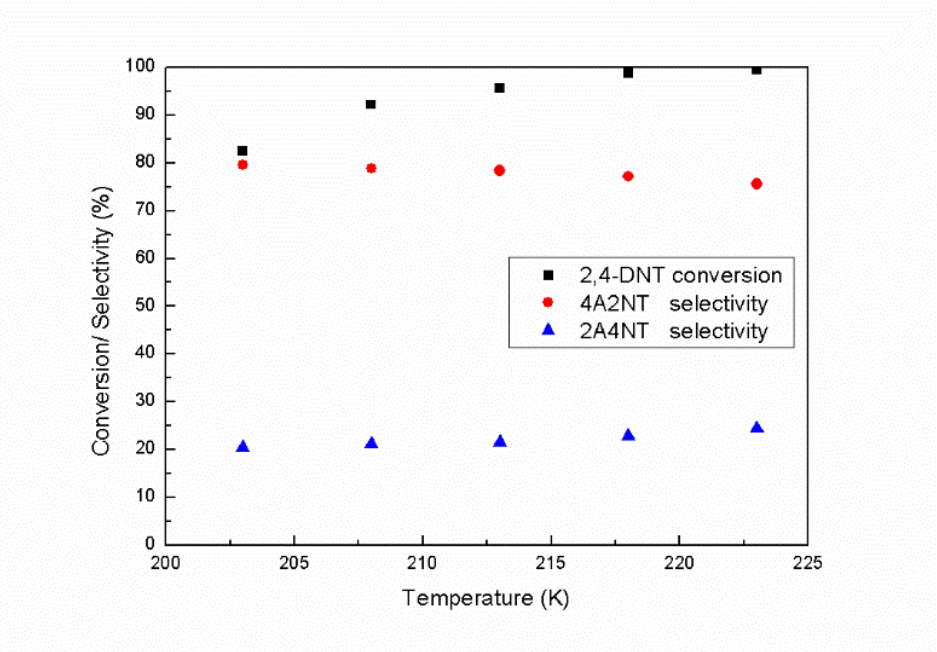
Conversion/ Selectivity (%)
Temperature (K)
2,4-DNT conversion
4A2NT selectivity
2A4NT selectivity

(b)

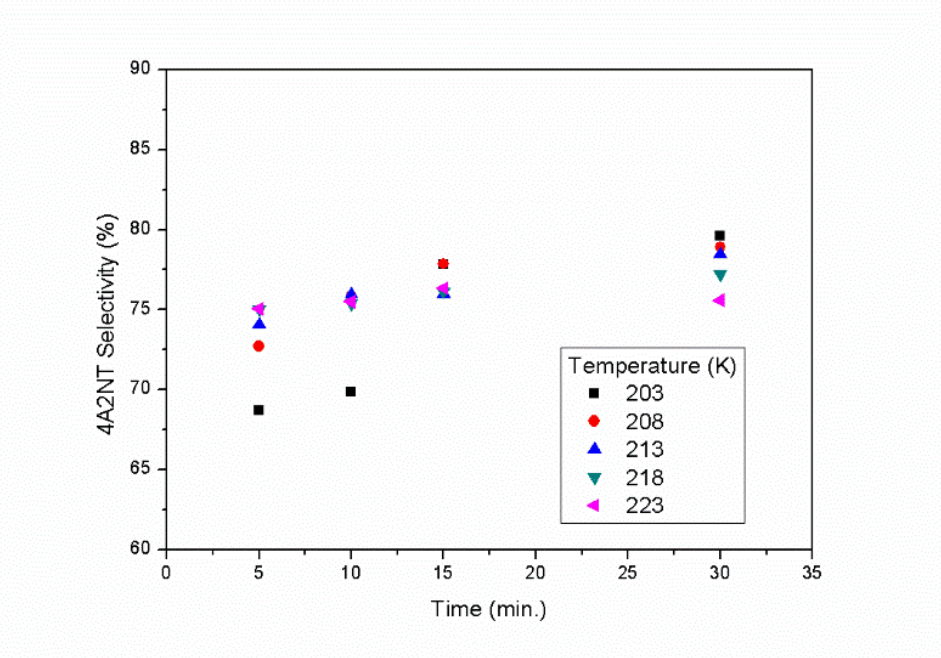

(c)

Figure 9.5. Effect of temperature on (a) the conversion of 2,4-DNT and (b) selectivity of 4A2NT & 2A4NT with respect to temperature and (c) selectivity of 4A2NT with respect to reaction time. Stirring speed = 1500 rpm, Organic phase volume = 3 x 10^{-5} m^3, Concentration of 2,4-DNT in organic phase = 0.549 kmol/m^3, Concentration of TBPB = 0.0232 kmol/m^3, Aqueous phase volume = 3 x 10^{-5} m^3, Concentration of MDEA in aqueous phase = 3.04 kmol/m^3, Concentration of sulphide in aqueous phase = 2.5 kmol/m^3.

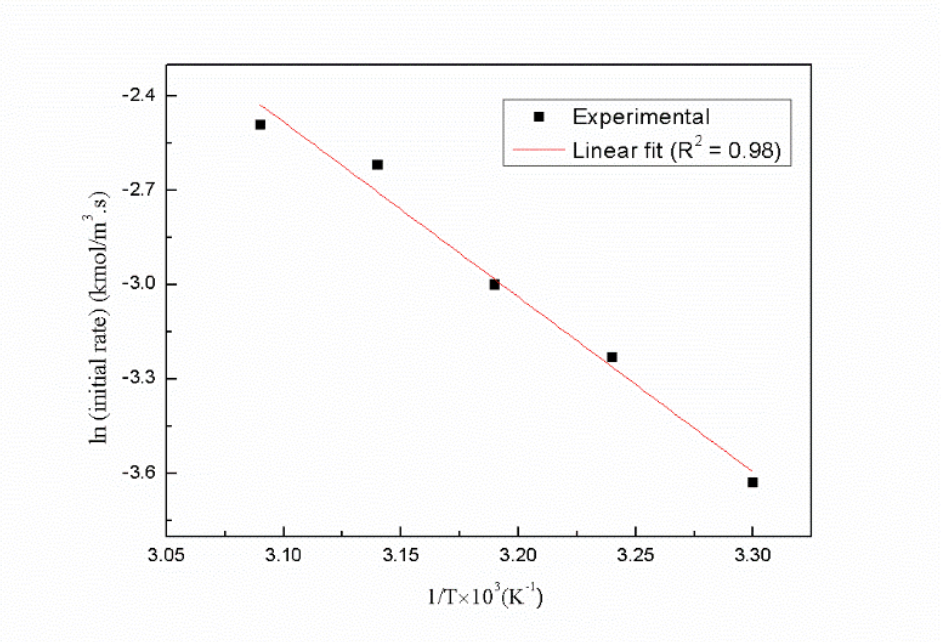

Figure 9.6. Arrhenius plot of ln (Initial Reaction Rate) vs. 1/T. All other conditions are same as Figure 9.5.

The initial rates at different temperatures were determined, and Arrhenius plot of *ln* (initial rate) vs. 1/T was made (Figure 9.6). The slope of the best fitted straight line gives us apparent activation energy as 46.25 kJ/mol. As the value of the apparent activation energy is high, the reaction is kinetically controlled. The activation energy of the same order of magnitude has been obtained in selective reduction of other nitro-compounds and there also, it was proposed to be kinetically controlled one [6,10]. As the conversion reached 100% after 60 min. of reaction for each temperature study, selectivity plot (Figure 9.5b) is drawn based on the data of 30 min. of reaction. The selectivity of the two isomers of aminonitrotoluene follows different trends with increasing temperature although there was an enhancement of the overall conversion of 2,4-DNT. From the plot Figure 9.5c it is clear that with increasing temperature, selectivity of 4A2NT has decreased.

9.2.2.6. Effect of Catalyst Concentration

To study the effect of catalyst concentration, at five different catalyst concentrations (0 – 0.093 kmol/m^3), the conversion of 2,4-DNT was determined and is shown in Figure 9.7a, keeping all the other reaction conditions same as shown in Figure 9.5. The conversion of 2,4-DNT, as well as the reaction rate, enhances when catalyst concentration increases. Reactant conversion was found to be 100% with 0.0232 kmol/m^3 of catalyst loading whereas it was about 70% without catalyst after 60 minutes of reaction. The highest enhancement factor of 5.2 was achieved with the catalyst concentration of 0.093 Kmol/m^3, as shown in Table 9.1. The influence of catalyst loading on the selectivity of 4A2NT and 2A4NT is shown in Figure 9.7b after 30 min. of reaction. From the Figure 9.7c, it is evident that with the catalyst concentration of 0.0465 Kmol/m^3 highest selectivity of 4A2NT was achieved and with further catalyst loading the selectivity of 4A2NT has been decreasing gradually.

To determine the order of reaction with respect to the catalyst concentration, the initial reaction rate was calculated at different catalyst concentrations. A plot of *ln* (initial rate) against *ln* (Catalyst concentration) was made and shown in Figure 9.8. From the slope of the linear fit line, the order of reaction was determined. The order of the reaction was found out to be 0.64 with respect to TBPB concentration.

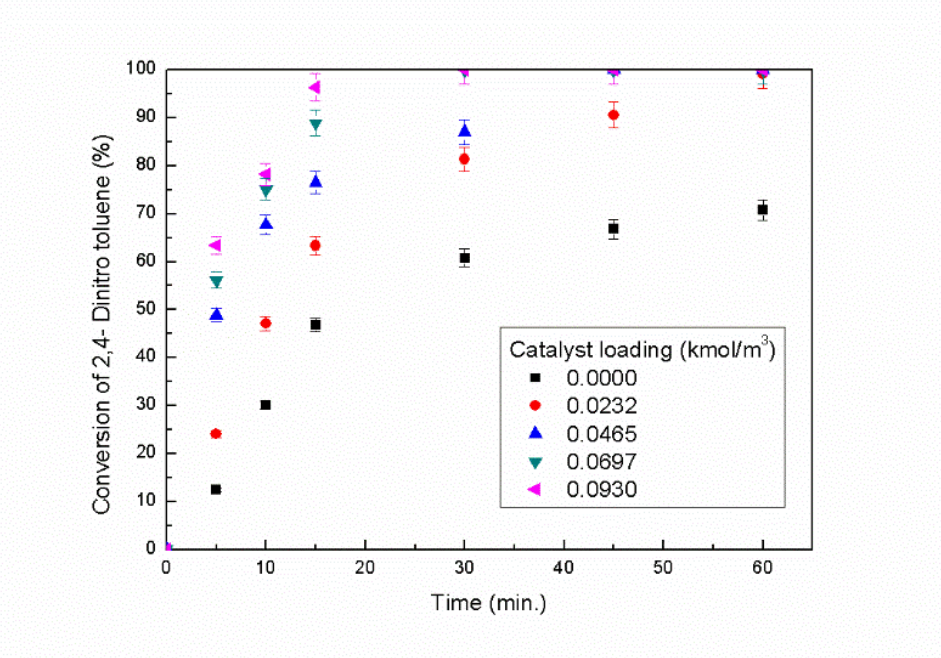
Conversion of 2,4- Dinitro toluene (%)
Time (min.)
Catalyst loading (kmol/m3)
0.0000
0.0232
0.0465
0.0697
0.0930

(a)

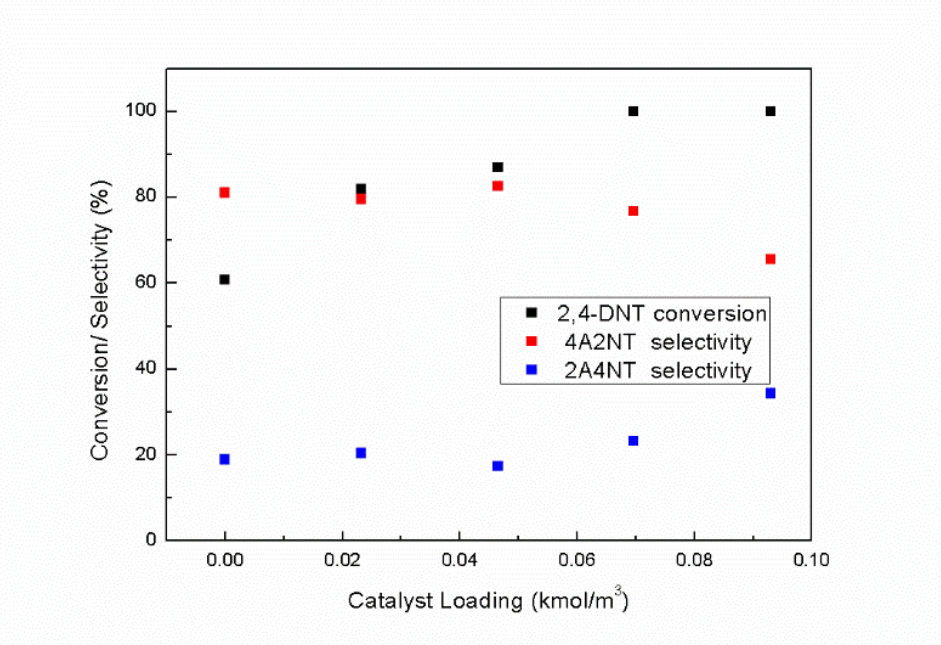
Conversion/ Selectivity (%)
Catalyst Loading (kmol/m3)
2,4-DNT conversion
4A2NT selectivity
2A4NT selectivity

(b)

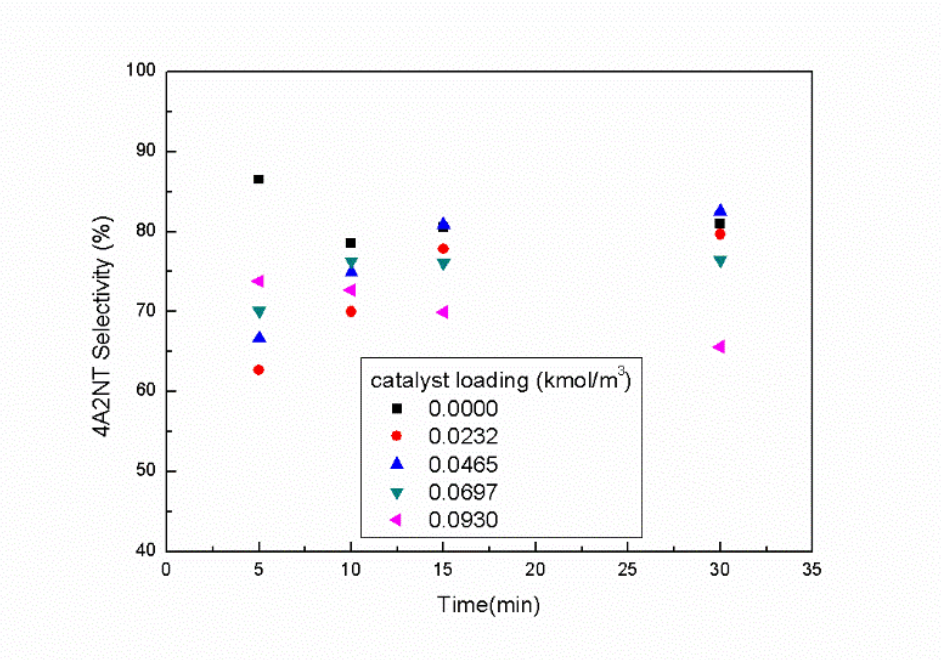

(c)

Figure 9.7 Effect of TBPB concentration on (a) the conversion of 2,4-DNT and (b) selectivity of 4A2NT & 2A4NT with respect to catalyst loading and (c) selectivity of 4A2NT with respect to reaction time. Stirring speed = 1500 rpm, Temperature = 303 K, Organic phase volume = 3 x 10^{-5} m^3, Concentration of 2,4-DNT in organic phase = 0.549 kmol/m^3, Concentration of TBPB = 0.0232 kmol/m^3, Aqueous phase volume = 3 x 10^{-5} m^3, Concentration of MDEA in aqueous phase = 3.04 kmol/m^3, Concentration of sulphide in aqueous phase = 2.5 kmol/m^3.

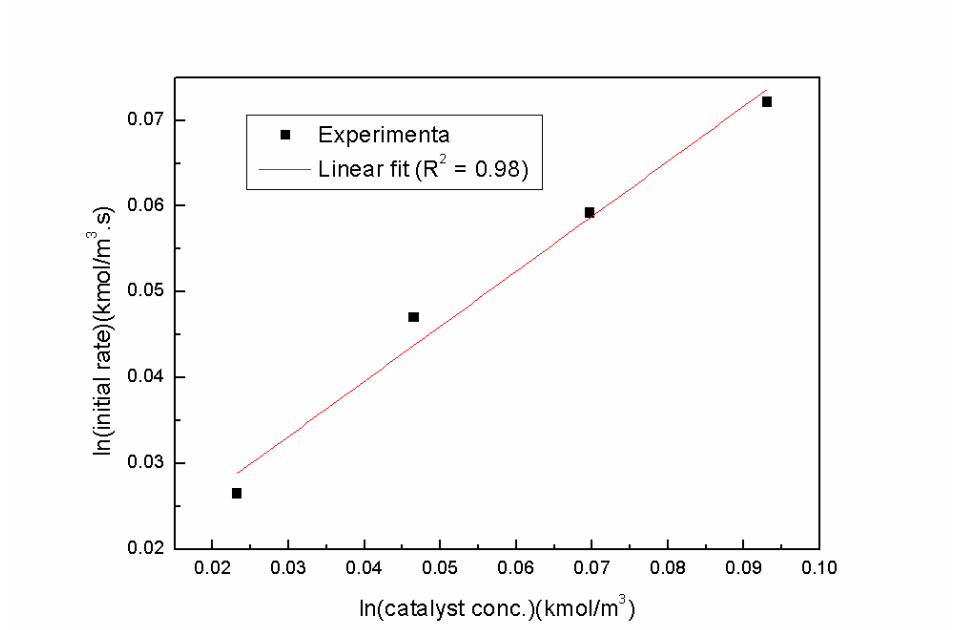

Figure.9.8.ln (Initial Reaction Rate) vs. ln (Catalyst concentration). All other conditions are same as Figure 9.7.

Table 9.1 Effect of catalyst concentration on Initial reaction rate[a]

TBPB concentration (kmol/m^3 of org phase)	**Initial reaction rate (kmol/m^{3}s)**	**Enhancement factor**
0.0000	0.0136	1.0
0.0232	0.0264	2.0
0.0465	0.0536	3.0
0.0697	0.0613	4.5
0.0930	0.0696	5.2

[a]All other conditions are same as Figure 9.7.

9.2.3.7. Effect of 2,4-Dinitrotoluene concentration

The influence of the concentration of 2,4-DNT, on the kinetics of the reaction, was studied in the concentration range of 0.2745 -1.0981 kmol/m^3 and presented in Figure 9.9a. It can be understood from the figure that with the increase of the concentration of 2,4-DNT, the conversion of 2,4-DNT has reduced. The selectivity of 4A2NT and 2N4AT was studied at different concentrations of 2,4-DNT, is shown in the Figure 9.9b. According to the Figure 9.9c the selectivity of 4A2NT is increased gradually as the concentration of 2,4-DNT is increased. At the highest concentration of 1.0981 kmol/m^3 of reactant, the selectivity of 4A2NT was 82.26%. From the Figure 9.10, the order of reaction with respect to 2,4-DNT concentration was obtained as 0.47.

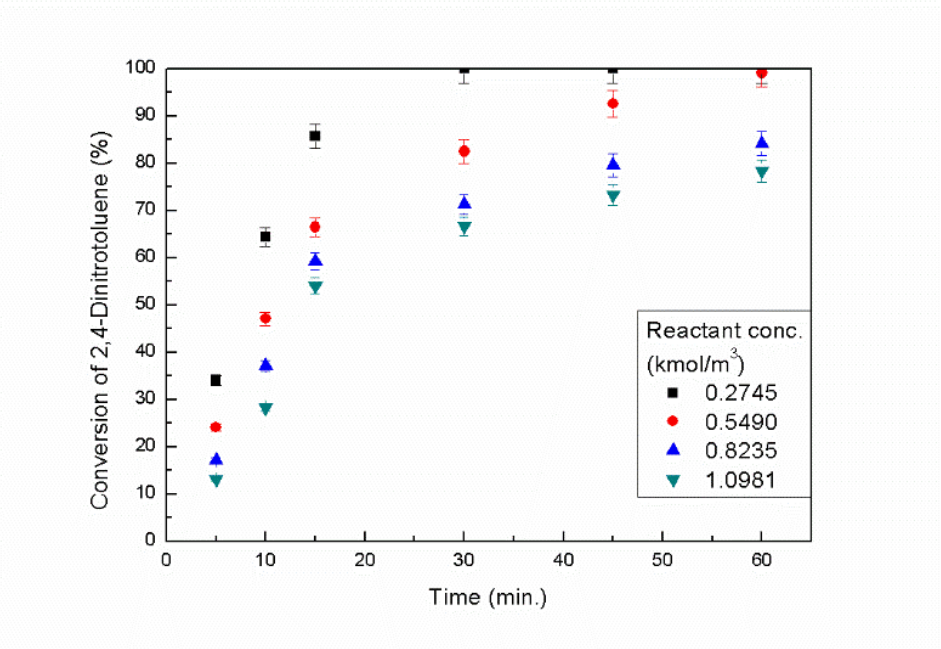
Conversion of 2,4-Dinitrotoluene (%)
Time (min.)
Reactant conc. (kmol/m3)
0.2745
0.5490
0.8235
1.0981

(a)

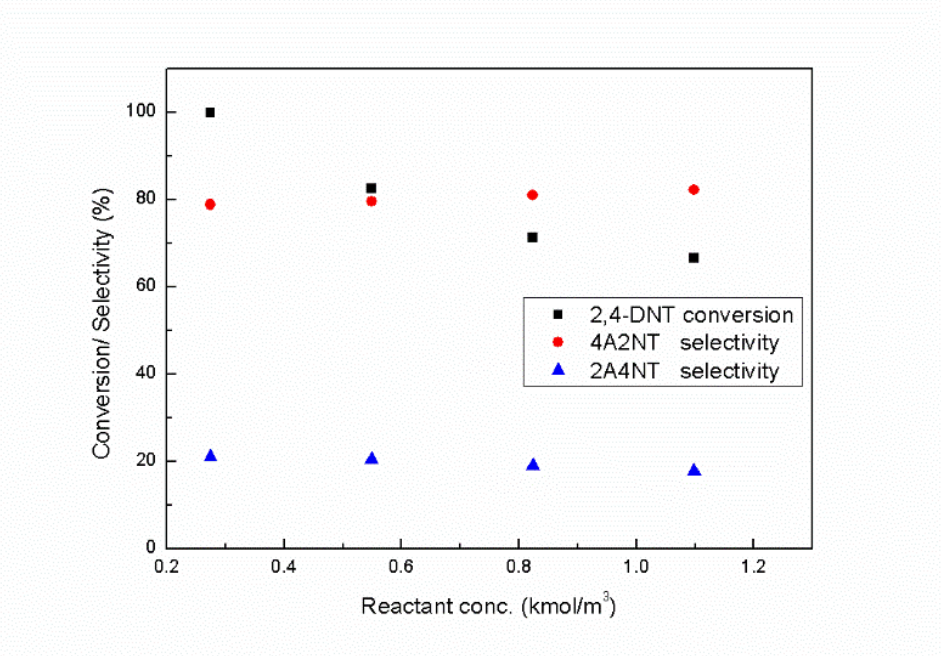
Conversion/ Selectivity (%)
Reactant conc. (kmol/m3)
2,4-DNT conversion
4A2NT selectivity
2A4NT selectivity

(b)

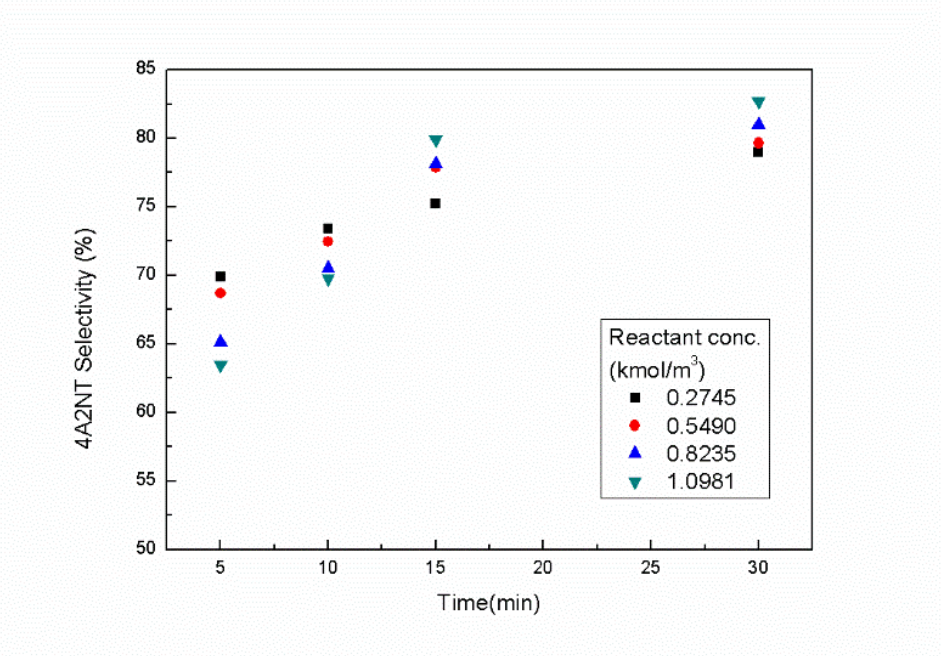

(c)

Figure 9.9 Effect of 2,4-DNT concentration on (a) the conversion of 2,4-DNT and (b) selectivity of 4A2NT & 2A4NT with respect to reactant concentration and (c) selectivity of 4A2NT with respect to reaction time. Stirring speed = 1500 rpm, Temperature = 303 K, Organic phase volume = 3 x 10^{-5} m^3, Concentration of TBPB = 0.0232 kmol/m^3, Aqueous phase volume = 3 x 10^{-5} m^3, Concentration of MDEA in aqueous phase = 3.04 kmol/m^3, Concentration of sulphide in aqueous phase = 2.5 kmol/m^3.

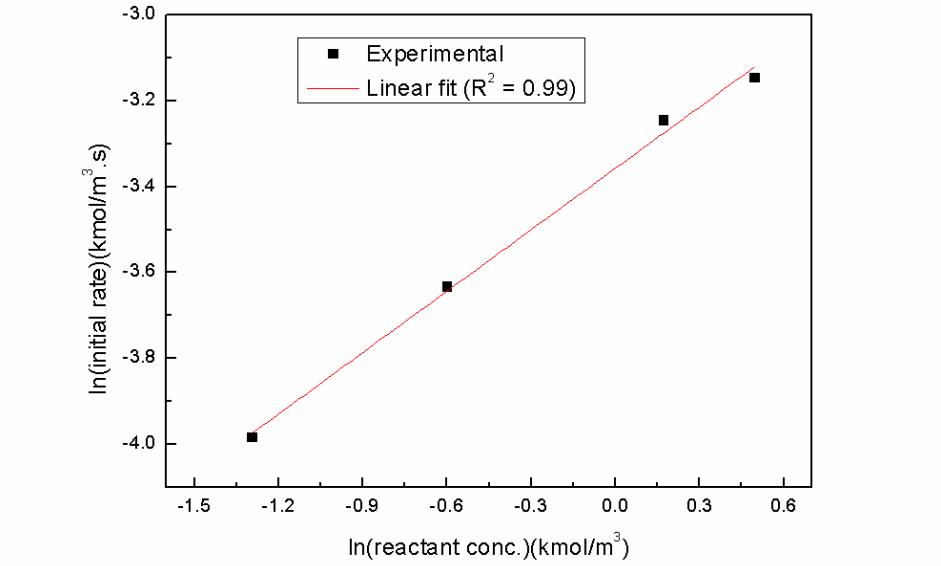

Figure 9.10. Plot of ln (initial rate) vs. ln (reactant concentration). All other conditions are same as Figure 9.8.

9.2.3.8. Effect of concentration of sulphide ion in the aqueous phase

The conversion of 2,4-DNT is greatly influenced by sulphide ions concentration in the aqueous phase as shown in the Figure 9.11a. For this study, the sulphide concentration in the aqueous phase was varied in the range of 1.0 to 2.5 kmol/m^3. As the concentration of sulphide increases, the conversion of 2,4-DNT also gets enhanced. Figure 9.11b shows how the selectivity of 4A2NT is affected by the change of sulphide concentration, and it is found from the Figure 9.11c that with a higher concentration of sulphide, selectivity of 4A2NT is gradually decreased. From the plot of *ln* (initial rate) against *ln* (sulphide concentration) (Figure 9.12), the slope of the linear fit line was found out to be to be 1.93.

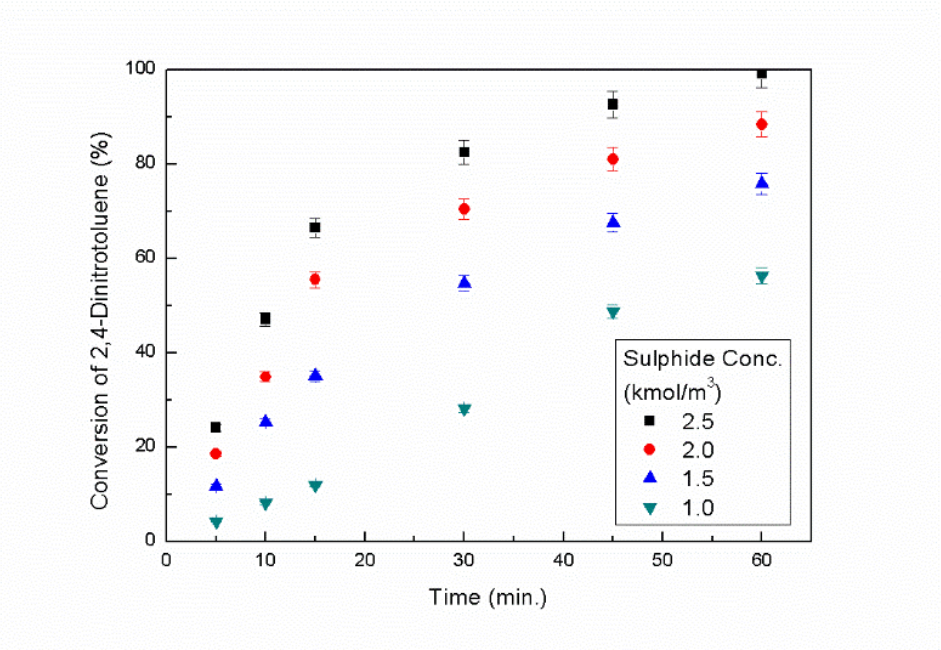

(a)

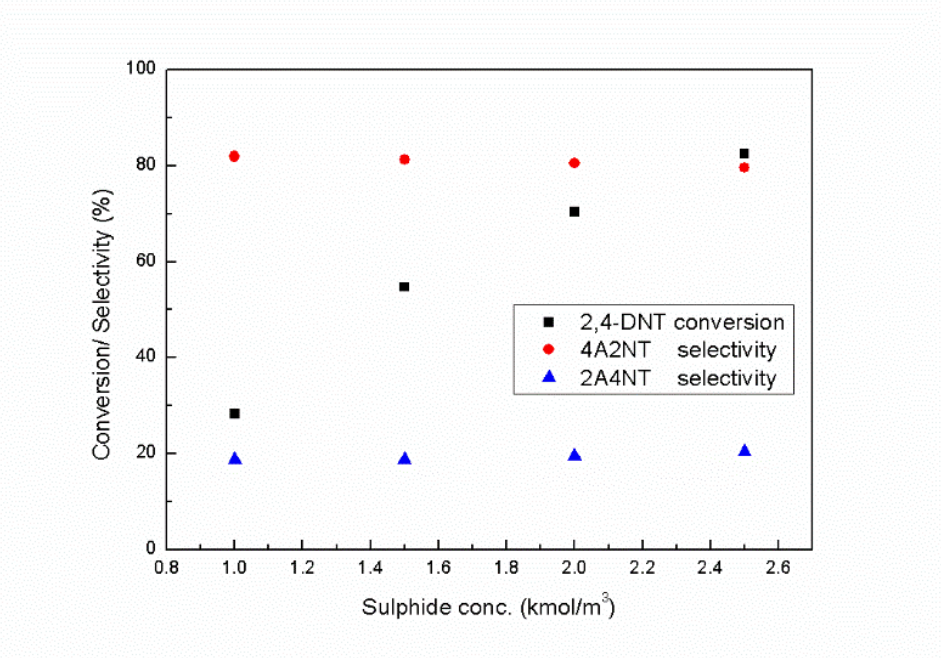

(b)

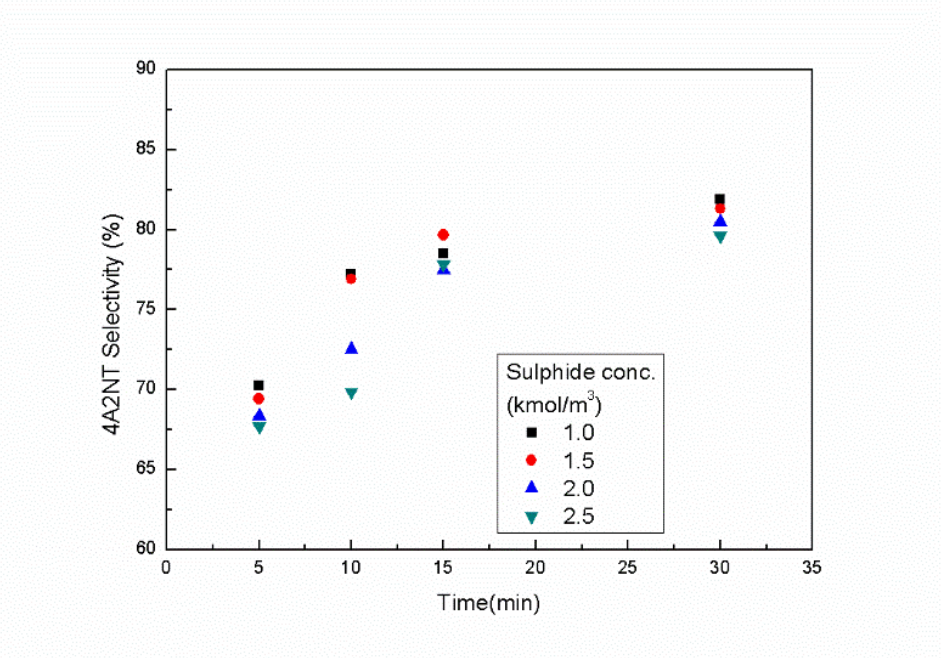

(c)

Figure 9.11 Effect of Sulphide concentration on (a) the conversion of 2,4-DNT and (b) selectivity of 4A2NT & 2A4NT with respect to sulphide concentration and (c) selectivity of 4A2NT with respect to reaction time. Stirring speed = 1500 rpm, Temperature = 303 K, Organic phase volume = 3 x 10^{-5} m^3, Concentration of 2,4-DNT in organic phase = 0.549 kmol/m^3, Concentration of TBPB = 0.0232 kmol/m^3, Aqueous phase volume = 3 x 10^{-5} m^3, Concentration of MDEA in aqueous phase = 3.04 kmol/m^3, Concentration of sulphide in aqueous phase = 2.5 kmol/m^3.

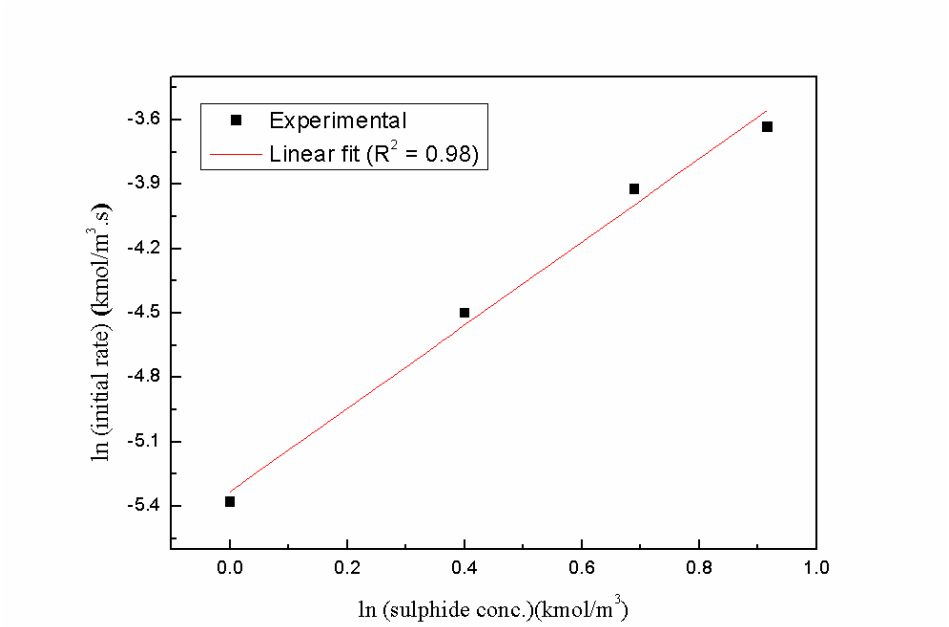

Figure 9.12. Plot of ln (initial rate) vs. ln (sulphide concentration). All other conditions are same as Figure 9.11.

9.2.2.9. Effect of MDEA concentration

There is no direct influence of MDEA in the reaction kinetics but, it still affects the chemical equilibria of MDEA-H_2O-H_2S system. As shown in Scheme 9.1, active anions like sulphide (S^{2-}) and hydrosulphide (HS^-) are formed in the aqueous phase and both the active anions take part in the reactions as shown in Equation (9.1) & Equation (9.2). Due to the basic nature of MDEA, ionisation of H_2S in aqueous phase is easier, and availability of sulphide ions (S^{2-}) is more than hydrosulphide ions (HS^-). MDEA variation with a fixed sulphide concentration can give some idea about the existence of both the reactions.

The colour of the aqueous solution changes from greenish yellow to orange and then finally to reddish brown during the whole process of the reaction, this phenomenon helpfully indicates the progress of the reaction. The reddish brown colour is due to polysulphide ions formed which formed as the reaction proceeds further. Similar kind of observations was witnessed by Lucas and Scudder [20].

In the present study, after 60min of run time, 87.34% conversion of 2,4-DNT was achieved with highest MDEA concentration of 5.02 kmol/m^3 with a sulphide concentration 1.37kmol/m^3 in the aqueous phase, as shown in the Figure 9.13a. These results support that the reaction follows Equation (9.1). Similar observations were found

when scientist used aqueous ammonium sulphide solution for nitroaromatic compound reduction reaction [3,6]. Highest conversion achieved during MDEA variation was 87.34%, and the current result is much higher than the conversion obtained according to Equation (9.1) (approx. 60%) or Equation (9.2) (approx. 30%). It can be explained by assuming that the reaction either follows both equation (9.1) and (9.2) or it follows Equation (9.3). As reaction proceeds, polysulphide ions formed (as colour intensifies to red), when sulphide ions react with elemental sulphur (produced in Equation (9.2)), and higher conversion can be achieved.

So it can be concluded that the increase in MDEA concentration with fixed sulphide concentration enhances the number of sulphide ions, and that boost the conversion of 2,4-DNT. Figure 9.13b and Figure 9.13c shows effect MDEA concentration on the selectivity of 4A2NT. From the figure, it is clear that there is a slight influence of MDEA on the selectivity between 4A2NT and 2A4NT. With increasing MDEA 2.02 to 5.02 kmol/m^3 concentration, the conversion of 2,4-DNT increases but the selectivity of 4A2NT decreases from 82.5% to 80.2%.

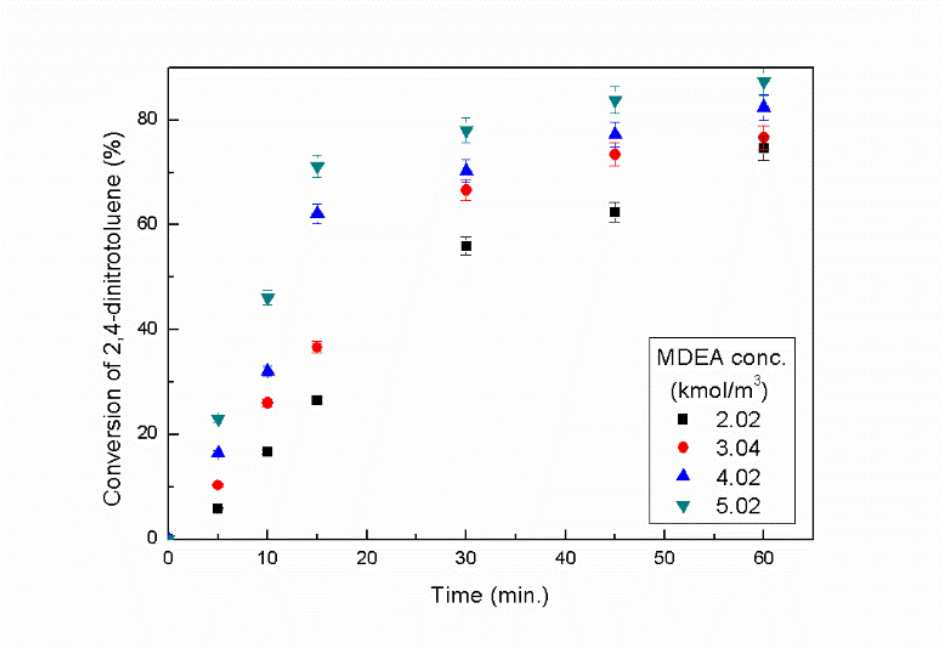

(a)

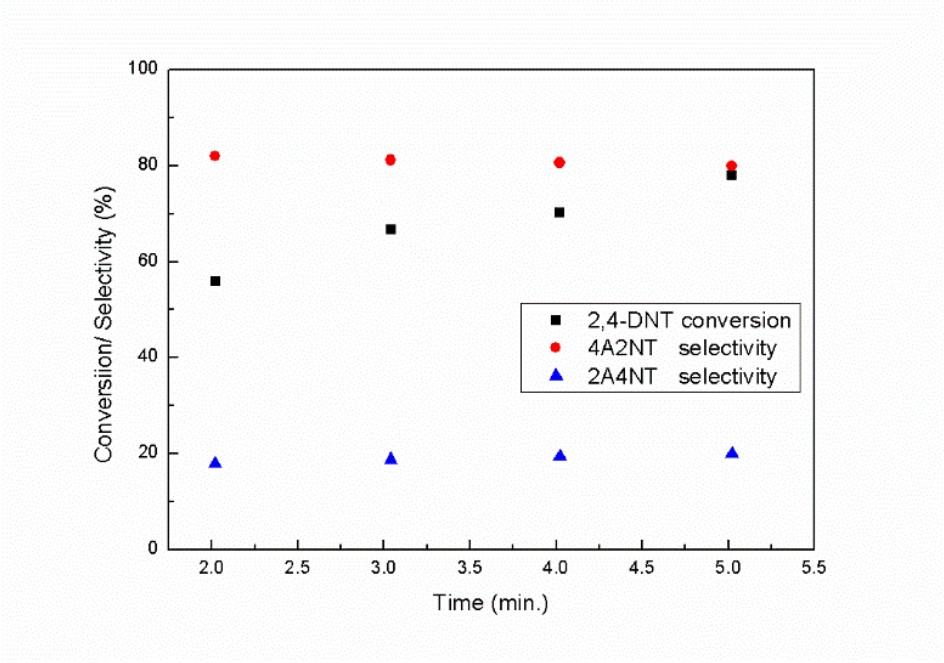

(b)

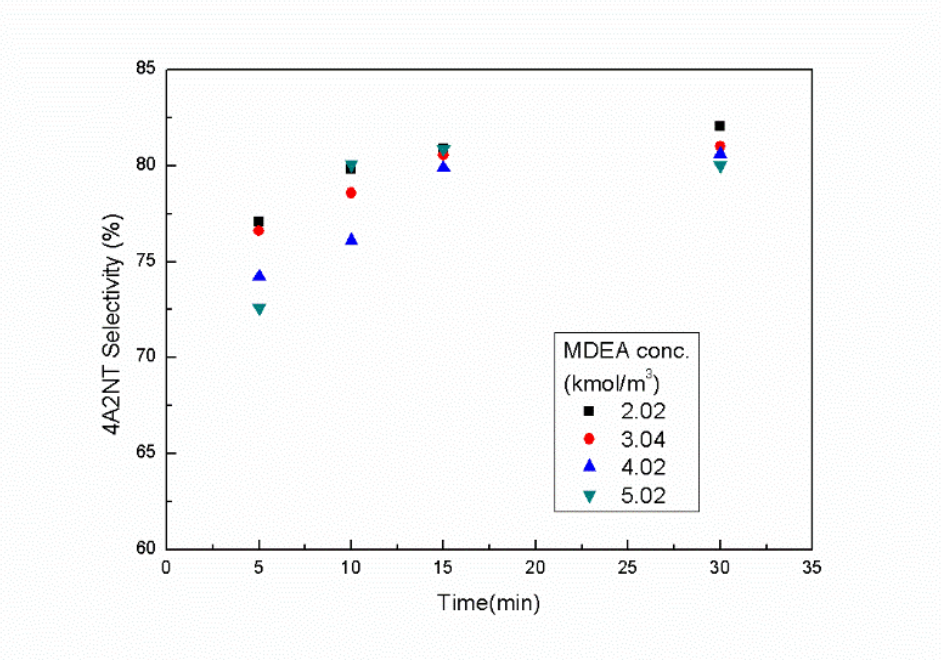

(c)

Figure 9.13 Effect of MDEA concentration on (a) the conversion of 2,4-DNT (b) selectivity of 4A2NT & 2A4NT with respect to MDEA concentration and (c) selectivity of 4A2NT with respect to reaction time. Stirring speed = 1500 rpm, temperature = 303 K, Organic phase volume = 3 x 10^{-5} m^3, Concentration of 2,4-DNT in organic phase = 0.549 kmol/m^3, Concentration of TBPB = 0.0232 kmol/m^3, Aqueous phase volume = 3 x 10^{-5} m^3, Concentration of sulphide in aqueous phase = 2.5 kmol/m^3.

9.2.2.10. Effect of elemental sulphur loading

Due to addition of sulphur powder, a change in the colour of H_2S-laden MDEA solution i.e. from dark green to orange. A similar phenomenon of colour change was noticed during MDEA variation. The effect of sulphur powder loading on the reactivity of 2,4-DNT is shown in Figure 9.14 and the "S" nature of the curve is unclear. Initial hike in reaction rate is observed in the figure because of the addition of elemental sulphur but as the reaction proceeds reaction rate became slower. It can be assumed that polysulphide ions (S_n^{2-}, where $2 \leq n \leq 6$) were formed among which disulphide ions were in majority (Equation (9.7)), these ions can easily transfer to the organic phase in comparison with sulphide (S^{2-}), hydrosulphide (HS^-) and other polysulphide ions (S_n^{2-}, where $3 \leq n \leq 6$). The reduction rate of 2,4-DNT with disulphide ions is faster. It is an established fact that polysulfide is a selective reducing agent for nitro reduction. Conversion of 2,4-DNT in the run without elemental sulphur addition became higher after 15 min of reaction. The sole reason for this crossover may be the formation of elemental sulphur as reaction proceeds (Equation (9.2)). The sharp rise in conversion of reactant for no-sulphur addition case is due to in-situ production of elemental sulphur and consequent production of disulphide and other polysulfides that enhance the reduction process.

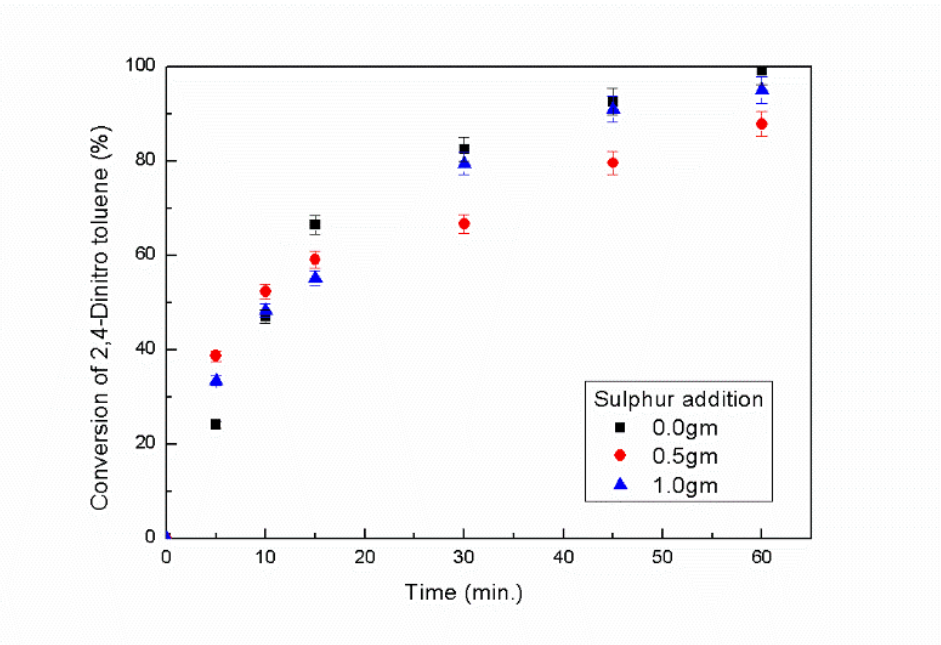

Figure 9.14 Effect of elemental Sulphur addition on the conversion of 2,4-DNT. Stirring speed = 1500 rpm, Temperature = 303 K, Organic phase volume = 3 x 10^{-5} m^3, Concentration of 2,4-DNT in organic phase = 0.549 kmol/m^3, Concentration of TBPB = 0.0232 kmol/m^3, Aqueous phase volume = 3 x 10^{-5} m^3, Concentration of sulphide in aqueous phase = 2.5 kmol/m^3, Concentration of MDEA in aqueous phase = 3.04 kmol/m^3.

9.2.3. Kinetic modeling of L-L PTC

A kinetic model has been developed based on the proposed mechanism shown in Scheme 9.1. The reaction occuring at interphase between the aqueous and organic phases is also contributing significantly to the overall reaction. From the Figure (9.7.a) the without catalyst run shows 70% conversion.

It is further assumed that the overall L-L PTC reaction follows both Equation (9.1) and (9.2) where 2,4-DNT present in the organic phase is selectively reduced by sulphide and hydrosulphide anions present in the aqueous phase to yield 4A2NT and 2A4NT as the main products.

To eliminate the mass transfer effect, the reaction mixture was agitated with at an optimum stirring speed of 1500 rpm. As the reaction commences, the PTC catalyst ion-pair Q^+X^- ($X^- = Cl^-$) exchanges its anions with HS^- ions very rapidly in the aqueous phase to transform into active catalyst ion-pair (Q^+HS^-). The active catalyst ion-pair is then transferred to the organic phase crossing the interface. After that the reaction proceeds in the organic phase, and different transition anions are formed. Finally, the active catalyst became inactive as the HSO_3^- ion gets attached to quaternary cations Q^+. $Q^+HSO_3^-$ ions transfer to the aqueous phase and reacts with S^{2-} to get reactivated as Q^+HS^- again.

The elemental sulphur produced in the rection is enhancing the reaction rate initially and it is the reason behind the 'S' nature of the conversion versus time curve (Figure 9.12). The formation polysulphide occurs when elemental sulphur reacts with H_2S-laden MDEA solution. Previously it was discussed that the overall conversion is decreased with the addition of elemental sulphur due to the formation of polysulphide in large number in comparison with disulphide ions, which the catalyst cation can not tranfer easily to the organic phase. According to the Equation (3), the disulphide (S^{2-}) ions are forming ion pair with two catalyst cations ($Q^+ S^{2-}Q^+$) in the aqueous phase and tranfer to the organic phase.

Development of a mathemetical model based on the mechnism proposed is quite diffficult job because of the complexities involved in the current reaction as the selective reaction of dinitro compound gives us two products i.e. 4A2NT and 2A4NT. So in our current study, an empirical kinetic model has been developed to correlate with the conversion version time data obtained experimentaly. In our current study the reaction order respect to catlyst, reactant and sulphide concentration term has been evaluated and based on

those, the rate of the reduction reaction of 2,4-DNT ($-r_R$) is expressed by the Equation (9.18)

$$-r_R = k_1 C_R^{0.47} C_S^{1.93} C_C^{0.64} + k_2 C_R^{0.47} C_S^{1.93} C_C^{0.64} C_E \quad (9.18)$$

Where C_R and C_c are the concentration of 2,4-DNT and catalyst (TBPB) in the aqueous phase. Due to the formation of elemental sulpur in reaction medium, the curve is of 'S' natue and it is defined by the second term of the reaction rate (Equation 9.18). The concentration of sulphide (C_S) and elemental sulphur (C_E) in the aqueous phase is derived from the over all mass balance based on the stoichiometry of the Equation (9.2) and those are shown in following expressions:

$$C_S = C_{SO} - 3f(C_{RO} - C_R) \quad (9.19)$$

$$C_E = f(C_{RO} - C_R) \quad (9.20)$$

Where C_{SO} and C_{RO} are the concentration of the initial sulphide concentration in the aqueous phase and 2,4-DNT concentration added in the organic phase. f is the volume ratio between the organic and aqueous phase and parameter estimation is done by a non-linear regression algorithm. The optimum values of the rate constants k_1 and k_2 were calculated at different temperatures by minimizing the objective function (E) as given by the following equation:

$$E = \sum_{i=1}^{n} [\{(-r)_{pred}\}_i - \{(-r)_{expt}\}_i]^2 \quad (9.21)$$

In the Table () the calculated values of k_1 and k_2 are listed. From the slope of the Arrhenious plots shown in Figure (9.15a) and (9.15b), the activation energies are calculated for both rate constants (k_1 and k_2)and it is 75.65 and 48.72 respectively.

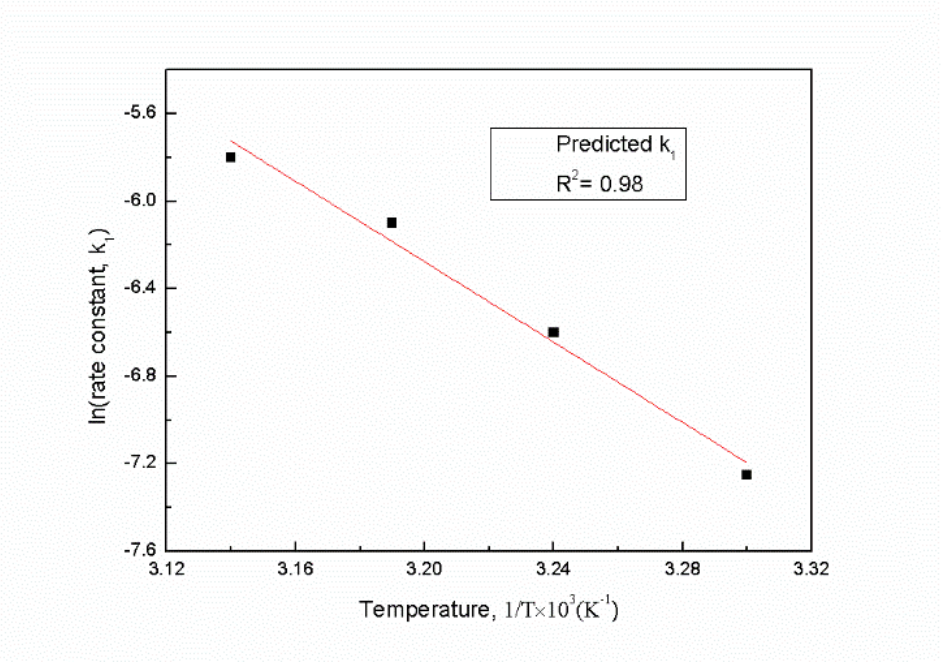

(a)

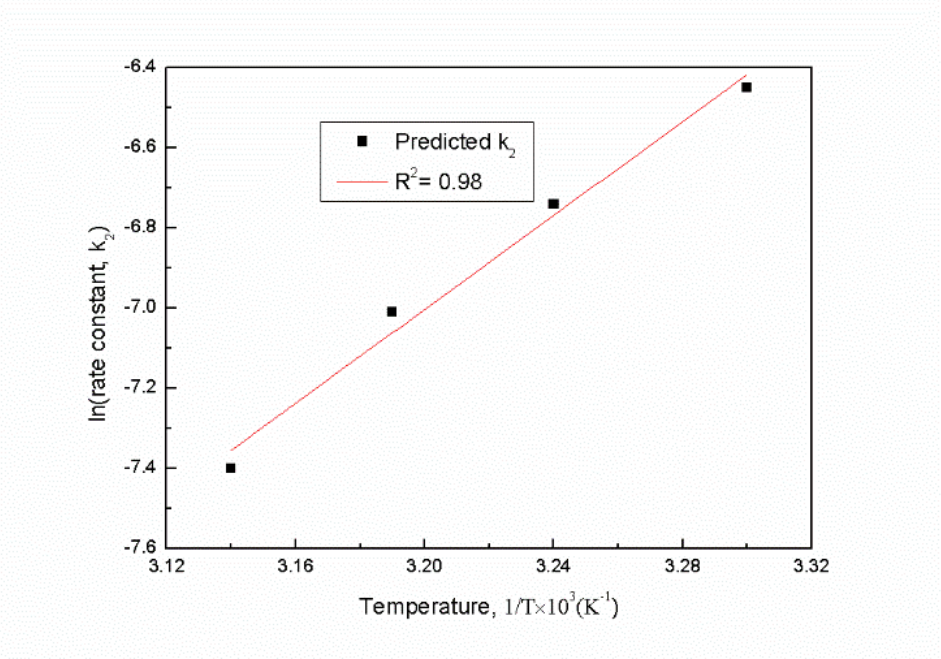

(b)

Figure. 9.15.. Arrhenius plot of (a) ln (rate constant, k_1) vs. 1/T and (b) ln (rate constant, k_2) vs. 1/T.

Table 9.2 Rate constants of the model different temperatures[b]

Temperature (K)	$k_1 \times 10^{-4}$ ((kmol/m^3) $^{-3.04}$ s^{-1})	$k_1 \times 10^{-4}$ ((kmol/m^3) $^{-4.04}$ s^{-1})
303	7.10	15.80
308	13.60	11.82
313	22.42	9.02
318	30.27	6.11

[b] All considerations are the same as mentioned in Figure 9.15.

9.2.4. Kinetic model validation

From the regression model the predicted reaction rate is evaluated and based on the predicted rates a comparison study between the predicted conversion versus experimental conversion is ploted in Figure 9.16. Excellent agreement was obsered between the predicted and experimental conversion.

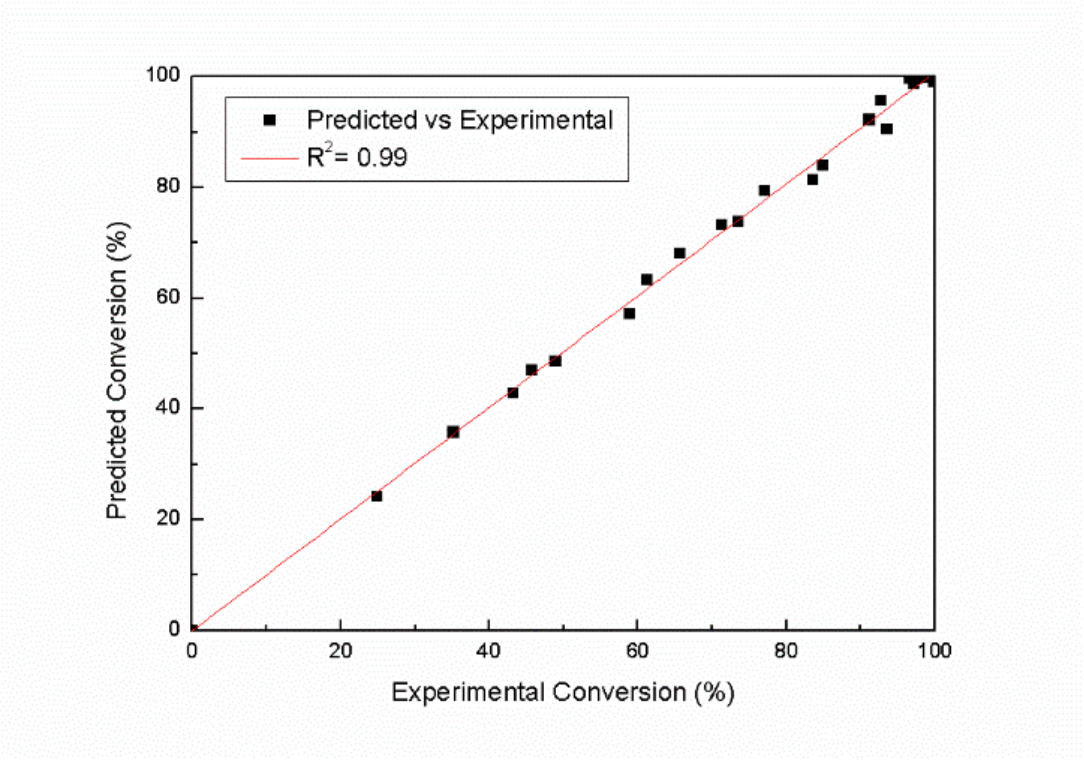

Figure 9.16. Comparison between calculated conversion and experimental conversion of 2,4-DNT at different temperatures after 60 min of reaction.

9.3 Conclusion

The current study shows the novelties of L-L PTC in the selective reduction of 2,4-DNT to the corresponding amino compound by novel Zinin reagent, H_2S-laden MDEA under milder reaction conditions, thereby eliminating the use of a costly metallic catalyst, high-temperature, and high-pressure reaction. As the reaction was very fast, 100% conversion was achieved in a very short time room temperature (303K). Selective reduction leads to the formation of two isomers- 2A4NT and 4A2NT, among them 4A2NT was much more abundant than 2A4NT. The detailed parametric study suggested that with the increase of temperature, catalyst concentration, sulphide ion concentration, MDEA concentration, the selectivity of 4A2NT decreases and that of 2A4NT increases. Highest selectivity of 4A2NT was observed as 82.26% when reactant concentration in the reactor was 1.0981 kmol/m^3. Reaction kinetics has been evaluated after details parametric studies and a mechanistic model also been proposed, which was further confirmed by experimental data. The activation energy of 46.25 kJ/mol makes current reaction a kinetically controlled one. Figure 9.17-9.19 are the mass spectra of 2,4DNT, 4A2NT and 2A4NT respectively.

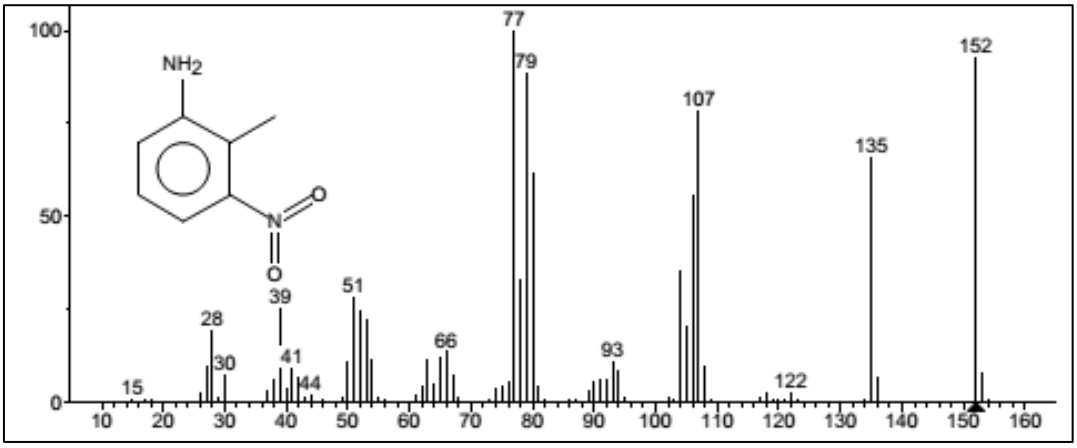

Figure 9.17: MS spectra of 2-amino-6-nitrotoluene (2A6NT).

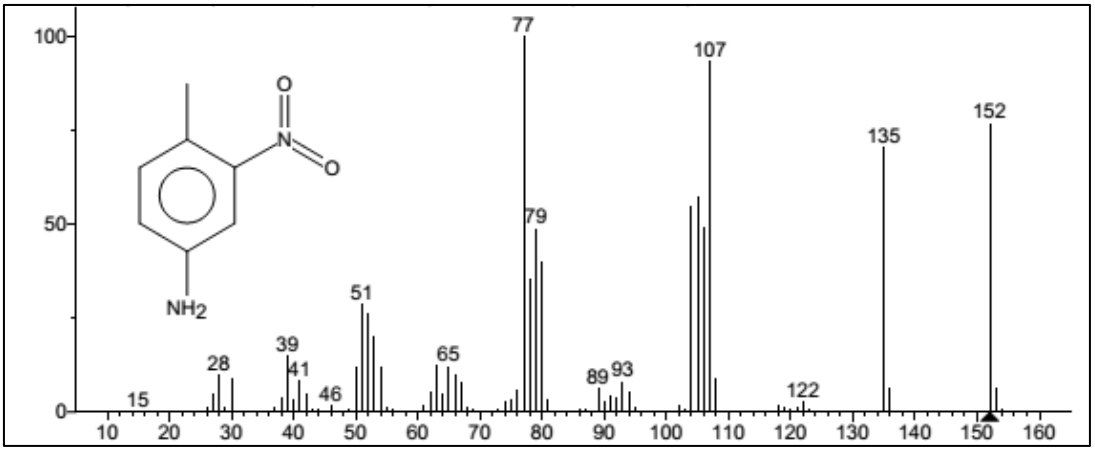

Figure 9.18: MS spectra of 4-amino-2-nitrotoluene (4A2NT).

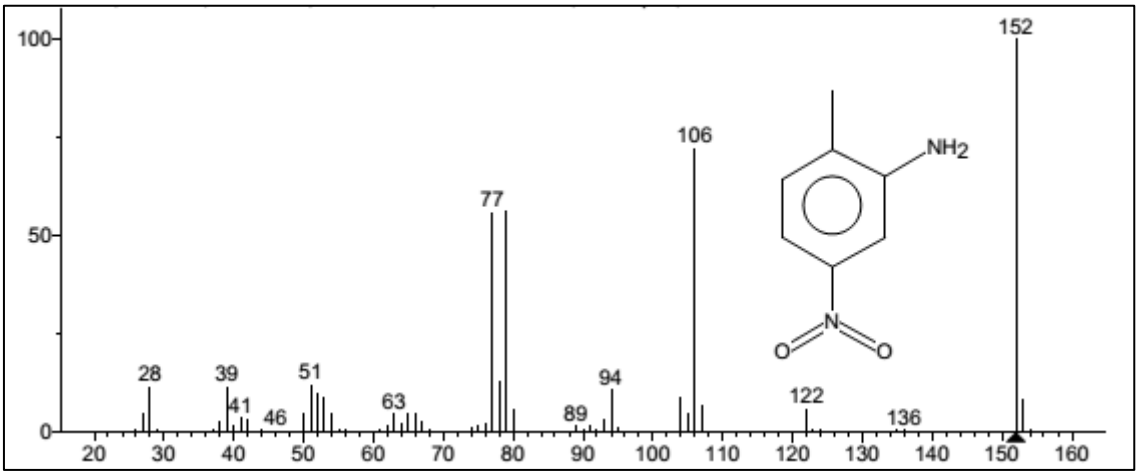

Figure 9.19: MS spectra of 2-amino-4-nitrotoluene (2A4NT).

References

1 W. G. Dauben, *Organic reactions*, John Wiley & Sons, Inc., New York, 1973.

2 G. D. Yadav, Y. B. Jadhav and S. Sengupta, *J. Mol. Catal. A Chem.*, 2003, **200**, 117–129.

3 N. C. Pradhan and M. M. Sharma, *Ind. Eng. Chem. Res.*, 1992, **31**, 1606–1609.

4 R. R. Bhave and M. M. Sharma, *J. Chem. Technol. Biotechnol.*, 1981, **31**, 93–102.

5 N. C. Pradhan, *Indian J. Chem. Technol.*, 2000, **7**, 276–279.

6 G. D. Yadav, Y. B. Jadhav and S. Sengupta, *Chem. Eng. Sci.*, 2003, **58**, 2681–

2689.

7 H. Gilman, Wiley, New York, 1941, p. 52.

8 H. Beutier, D; Renon, *Ind. Eng. Chem. Process. Des. Dev*, 1978, **17**, 220–230.

9 N. Sadegh, E. H. Stenby and K. Thomsen, *Fluid Phase Equilib.*, 2015, **392**, 24–32.

10 S. K. Maity, N. C. Pradhan and A. V. Patwardhan, *Chem. Eng. J.*, 2008, **141**, 187–193.

11 G. D. Yadav and S. V. Lande, *Adv. Synth. Catal.*, 2005, **347**, 1235–1241.

12 G. D. Yadav and S. V. Lande, *Appl. Catal. A Gen.*, 2005, **287**, 267–275.

13 J. Klausen, J. Ranke and R. P. Schwarzenbach, *Chemosphere*, 2001, **44**, 511–517.

14 B. Zhou, J. Song, H. Zhou, T. Wu and B. Han, *Chem. Sci.*, 2016, **7**, 463–468.

15 G. D. Yadav and S. V. Lande, *Ind. Eng. Chem. Res.*, 2007, **46**, 2951–2961.

16 R. V. M. and R. V. Chaudhari, *Ind. Eng. Chem. Res.*, 1999, **38**, 906–915.

17 E. C. Division, *Appl. Environ. Microbiol.*, 1984, **47**, 1295–1298.

18 M. L. Wang and Z. F. Lee, *Ind. Eng. Chem. Res.*, 2006, **45**, 4918–4926.

19 M. L. Wang and Y. H. Tseng, *J. Mol. Catal. A Chem.*, 2003, **203**, 79–93.

20 N. F. Lucas, H J, Scudder, *J. Am. Chem. Soc.*, 1928, **50**, 244–249.

21 Y. Hojo, M. Takagi, Y. Ogata, *J. Am. Chem. Soc.*, 1960, **82**, 2459–2462.

Abstract

This study revolves around finding an alternative usage of a toxic and hazardous waste i.e. Hydrogen sulphide other than industrially popular Claus process. In our current approach we used H_2S-laden Methyldiethanol amine as a reducing agent for the selective reduction of mono/di-nitro arenes under the Liquid-Liquid mode of reaction with utilizing n-tetrabutylphosphonium bromide (TBPB) as a phase transfer catalyst.

10.1 Introduction

Selective reduction of nitro aromatic compounds is an industrially important reaction as the amino group can be further derivetize to give commercially important products[1]. The production of Aniline and its derivative is a cornerstone of modern chemical industry. In 2013 value of global aniline market was £6.25 billion and expected to reach £ 10.17 billion by 2020[2]. Aniline its derivatives are found to be very useful in plenty industries such as pharmaceutical, polymer and materials (e. g. rubber, polyurethane), herbicides, pesticide, bulk chemicals, photographic chemicals, and sometimes as an inhibitor of the polymerization reaction and as stabilizing agent for many chemicals [3–7]. Azo and azoxy compounds are prepared thorough oxidation of aromatic amines which is having ubiquitous usage in dye industry as a raw material for the production of dyes and pigments (e.g. indigo) [4,8,9].

A plethora methods are available for the reduction of nitro compounds including Bechamp reduction [10], catalytic hydrogenation[11], metal catalysed reduction but reducing agent other than molecular hydrogen, stoichiometric reducing agent. Bechamp reduction process involved stoichiometric amount metal catalyst (Fe, Zn, Al and Sn) or a metal sulphide (Na_2S) in the presence of acid. However selective reduction of a single nitro group in the presence of carbonyl group in very difficult. On the other hand catalytic hydrogenation reaction requires high reaction temperature and pressure for enhancing reactivity because of lower intensive reactivity of the catalyst. So this makes whole process energy expensive and difficult to operate as hydrogen handling is difficulty process [3,12–18]. Use of potentially explosive hydrogen source in catalytic hydrogenation is very risky job[19]. Chemoselective hydrogenation also utilises stoichiometric reducing agents such as sodium hydrosulphide [20], hydrazine hydrate [1], silanes [21], decaborane [22] and formats [23] as a hydrogen source.

All the existing catalysis methods are failing to meet the confluence of reactivity and selectivity. Reaction involves highly active catalyst lacks selective reduction which leads to production undesired side product which makes the purification process difficult.

Another drawback of the process mentioned above includes the reagents utilised are expensive and moisture sensitive, extreme process handling conditions and high number of safety concerns. Selective reduction of nitroaromatic compounds can be achieved by Zinin reduction [1]. The reduction reaction of nitroaromatic compounds by negative divalent sulphur in the form of sulphide, hydrosulphide and polysulphide is called Zinin reduction [24]. Ammonium sulphide, sodium sulphide have been used a reducing agent in Zinin reduction for the reduction of several nitroaromatic compounds [25–30].

Hydrogen sulphide (H_2S) gas is normally a toxic and hazardous gas, but it can be used as a reducing agent in Zinin reduction as H_2S absorbed in amine or alkanolamine solution also producing sulphide and hydrosulphide ions. H_2S is produced as a gaseous by-product in several industries like petroleum, natural gas processing industries, coal, kraft pulping [31,32]. Currently available crude petroleum is enriched with sulphur and nitrogen and refineries are forces process this heavy crude. As a result after hydrotreating and hydrodesulfurization, tons of H_2S gas is generated as a gaseous by-product. Amine treating unit (ATU) is a place where H_2S gas is absorbed in amine or alkanolamine solution to separate it from the gasious stream. Then H_2S gas is regenerated from the amine or alkanolamine solution ATU regenarator is treated by Claus process, which is a high-temperature oxidation process and the end product is elemental sulphur [33].

As the environmental emission rule become stricter and huge amount of elemental sulphur produced in Claus process does not find any other use other than possessing hazardous effect, other approaches of H_2S utilization have to be taken. Ample approaches have been taken such as thermal [34], photochemical [35], electrochemical [36–38], thermochemical processes [39] to convert H_2S into some useful product like hydrogen(H_2) and sulphur (S_2). Syngas (H_2, CO) have been produced from acid gas (H_2S, CO_2) and can be used as fuel for gas engines [40]. All the above approaches are costly to operate, laborious and not enviro-friendly, so these setbacks are forcing to think for an innovative and better utilization of H_2S.

Removal of H_2S gas from gas stream s difficult job and Alkanolamines are mostly used for removal Acid gases (H_2S, CO_2) from the natural gas and synthetic ammonia gas industry and petrochemical plants around the globe[41]. Industrially important alkanolamines are monoethanolamine (MEA), diethnolamine (DEA), N-methyldiethanolamine (MDEA) and di-2-propanolamine (DIPA). Primary amine (MEA) and secondary amine (DEA) react with CO_2 and forms stable carbamates but tertiary amine (MDEA) can selectively remove H_2S gas from a gas stream which contains CO_2 and H_2S. Other advantages of MDEA includes high loading capacity and low heat of

reaction which make regeneration process an economical and energy efficient process[41–44].

Our proposed reaction is biphasic reaction system where aqueous phase is H_2S laden aqueous MDEA solution which constitutes reducing ions and organic phase contains soluble PTC along with nitro compound dissolved in organic solvent. The main role of PTC is to accelerate reaction rate by transferring aqueous phase inorganic anions to the organic phase through the interphase. Two types of biphasic reaction are available in literature involving soluble PTC catalyst are Liquid-Solid (L-S) and Liquid-Liquid (L-L) systems and one multiphasic reaction system available which is Liquid-Liquid-Liquid (L-L-L) system. L-L PTC system is the most simple and widely accepted system, because of its simpleness, little requirement for solvent and raw materials, feasible operating conditions, high selectivity and enhanced reaction rate.

PTC of different types have been utilised in multiphase reactions and PTCs can be categorised into quaternary ammonium and phosphonium salts, Cryptands, Crown ethers, Polyethylene glycols (PEG) [45]. Ammonium and phosphonium salts are most popular because of their high reactivity, operational at higher temperature and cheaper. Ethyltriphenylphosphonium bromide (ETPPB) have been used in Zinin reduction and the quaternary phosphonium salt has shown good results in comparison with ammonium salts [25]. Tetra-n-butylphosphonium bromide (TBPB) is a type of quaternary phosphonium salt, is used as PTC in several reactions which include synthesis of alkyl, aryl thioglycoside and thiodisaccharide utilizing the thioiminium salt, synthesizing o-nitrophenyl octyl ether, one-pot synthesis of pyrano- and furanoquinolines are available in several kinds of literature [46–48]. Use of TBPB for selective reduction of di-nitro aromatic compounds by H_2S- laden MDEA as reducing agent at room temperature is a unique approach and taken into consideration for the current study.

10.2 Experimental setup and procedure:

H_2S gas was bubbled through the chilled aqueous MDEA solution to prepare aqueous phase and this process was carried out till desired sulphide concentration attained in the aqueous phase, which was measured by iodometric titration method [49]. The proposed reactions were done in a 150ml capacity isothermal baffled stirred tank reactor. The isothermal bath temperature was regulated with a PID controller (±1°C) and it was provided with a digital regulation system. Our reaction system was composed with of two equal volume phases, the aqueous phase was H_2S-laden aqueous MDEA solution and the other phase was organic phase which was a mixture of reactant (nitroaromatic

compound), PT catalyst (quaternary phosphonium salt) and organic solvent (toluene). At the beginning of the process 30ml of aqueous phase was poured into reactor and it was stirred until it reaches desired temperature. Then stirring was paused and the organic phase was introduced into the reactor. The reaction commenced as soon as the stirrer was switched on. For kinetic analysis organic phase samples were withdrawn at a particular time interval from the organic phase. In order to take sample the stirrer was switched off and when the phases got separated, 0.1ml of organic phase sample was collected by pipette.

10.3 Result and discussion:

In 1844 Zinin proposed overall stoichiometric equation of the reduction reaction of nitroaromatic compounds by ammonium sulphide [24]. Sodium sulphide is also following similar stoichiometry when it is used as a reducing agent [25,50–52,28]. During reaction another by-product is formed such as thiosulphate or elemental sulphur by two different reaction Equation (10.1) [24] and Equation (10.2) [53]. For our current research H_2S-laden MDEA solution is taken as reducing agent.

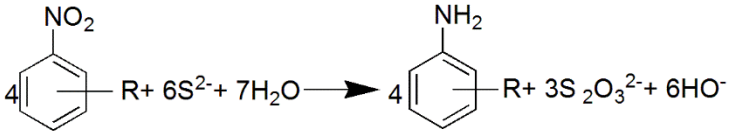

(10.1)

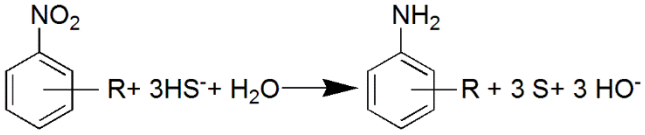

(10.2)

The selective reduction reaction rate depends on the speed of agitation due to the mass transfer effect possess by the inorganic anion while transferring from the aqueous phase to organic phase. Thus stirring speed effect was studied in the range of 500-2500 RPM. It was discovered that there is no significant increase in reaction rate as we increase the stirring speed beyond 1500 RPM. Thus the agitation speed was fixed at 1500 rpm for further reaction.

We have chosen a number of quaternary cations as phase transfer catalyst for the initial investigation of reduction reaction Table 10.1. To our delight the reaction between 4C3NT and H_2S-laden MDEA in the presence of An as PTC proceeded smoothly to produce desired product () in 96% yield and 100% selectivity after 90 minutes of reaction. After getting this excellent preliminary results we started to compare it with other PT catalysts shown in Table 10.1. The order of reactivity of these PT catalysts is

A>C>B>D>E>F. Catalyst with higher carbon number in the alkyl group is more lipophilic and thus it can be easily extracted to organic phase, which is responsible for higher activity of this catalyst. Although D is having higher carbon number in its alkyl group, it is showing lower activity than the rest of the phosphonium and ammonium salts (A, B and C). In its structure D is having a single methyl group and three big benzyl group attached with the quaternary cation, so the quaternary cation core is inaccessible for other anions which are needed to get transferred to another phase, thus reaction rate slows down. Catalyst A is a phosphonium salt, it is showing highest activity among all the catalyst we have used. The quaternary phosphonium cation is more advantageous for the role of transferring hydrosulphide ions (HS^-) from aqueous phase to organic phase, as phosphonium cation is soft base and HS^- ion is soft acid and according to the Pearson's HSAB theory soft bases prefers to bind soft acid. The reaction yield with different PT catalyst is shown in Table 10.1.

Table 10.1 Screening of different catalyst and yield achieved.

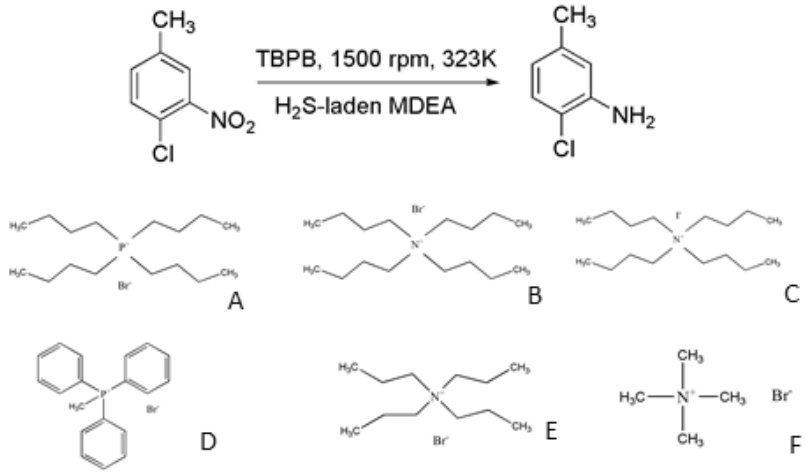

Entry	Catalyst	Yeild (%)
1	N/A	5
2	A	96
3	B	37
4	C	55
5	D	15
6	E	12
7	F	10

10.4 Mechanism of L-L PTC:

Current reduction reaction follows a complex mechanism and the number of elementary reaction steps involved is envisaged. In the aqueous phase an ionic equilibrium exists between sulphide (S^{2-}) and hydrosulphide (HS^-) ions. This ionic equilibrum is affected by the concentration of basic MDEA. Formation of the (S^{2-}) and (HS^-) ion is shown in the Scheme 10.1 from Equation (10.4) to Equation (10.6). Similar ionic equilibrium is also reported in aqueous ammonium sulphide solution [54].

Reaction mechanism of current reaction is proposed based on some previously published work (Scheme 10.1) [25,28,55,56]. Sulphur can remain in multiple valence states (-2 to +6) and in the aqueous phase sulphur exist in multiple anionic forms ($HS^-, HSO^-, HSO_2^-, HSO_3^-$). These anion can easily bind to the quaternary cations and get transfer to the organic phase. On the other hand quaternary cations, Q^+, pairs up with the anions available in aqueous phase for its reaction with organic substrate, but most of the quaternary cations are found in the form of Q^+HS^-in the reaction medium.

Generally PTC mechanism can be expained by two approaches 1. extraction mechanism by Stark's [57] 2. Interfecial mechanism by Makosza's [58]. According to the extraction mechanism when reaction rate increases proportionately with higher organophilicity of quaternary catlyst and catalyst concentration but it is not related with stirring speed i.e. reaction rate remains constant even at higher stirring speed, then the reaction is following extraction mechanism [59,60]. Macosza's interfacial mechanism is highly dependent on stirring speed. As our reaction is mass transfer effect free beyond 1500 rpm and above this the reaction rate does not change, which made creent reaction following Stark's extraction mechanism.

Current L-L PTC system is a cyclic process and it starts with the formation of ion pair between quaternary cations (Q^+) and hydrosulphide ions (HS^-) to form Q^+HS^- ion pair, then in the next step the ion pair transferred to the organic phase to react with the organic substrate. After that a number of elementary reaction took place in the organic phase and which leads to the formation of aromatic amines as shown in Scheme 10.1 (Equation 10.11 to Equation 10.16). In the organic phase a number of intermediates has formed (nitrosobenzene and benzene hydroxylamines) [61,62], but during GC-MS analysis these intermediates have not been detected, which may be due to the fast appearance and disappearance of those intermediates[28,61,30,63,64]. At the last step of PTC cycle the quaternary ion pair gets inactivated ($Q^+HSO_3^-$) (Equation (10.17) and then it returns back to the aqueous phase and reacts with with S^{2-} and got regenerated (Q^+HS^-) (Equation

(10.8)). This cyclic process is carried out till the organic substrate got converted to product.

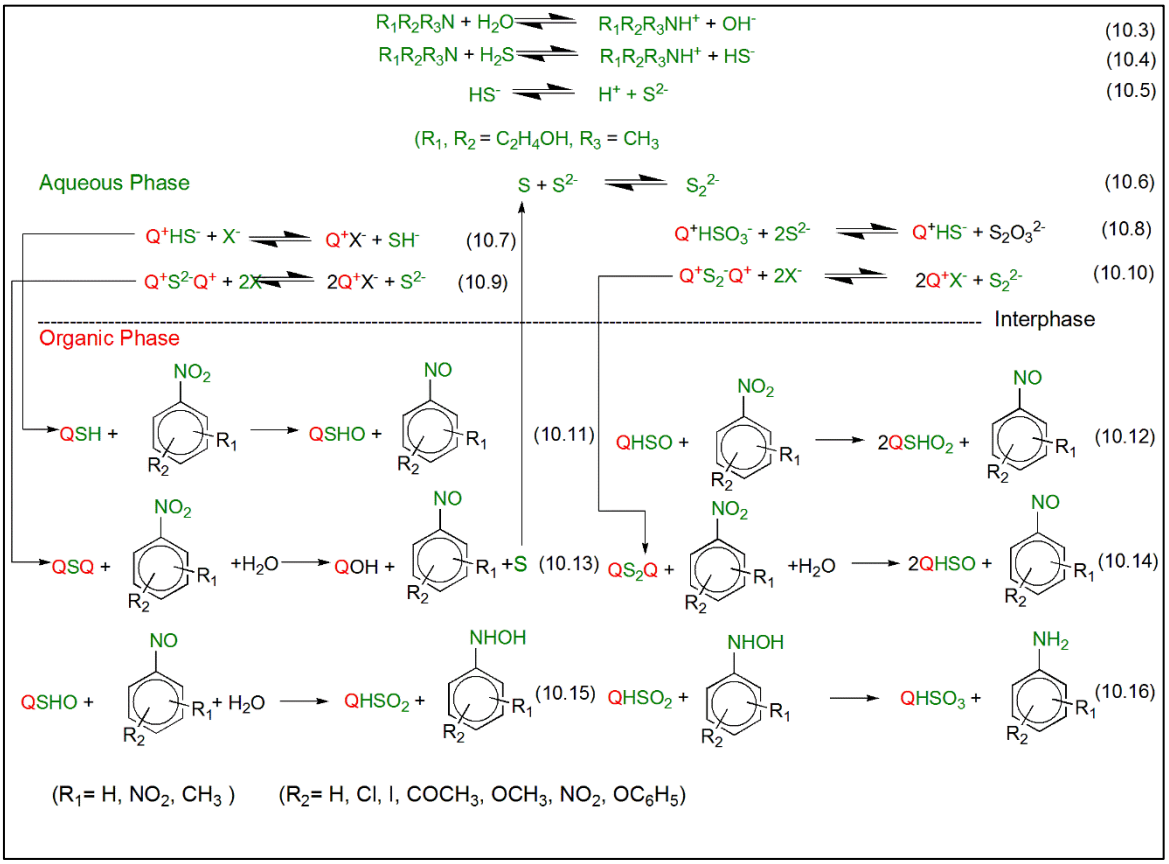

Scheme 10.1 Mechanism of selective reduction substituted nitroaromatic compounds under L-L PTC.

10.5 Reaction scope

After optimizing reaction condition we proceed further to utilise this reaction method to reduce selectively other nitro aromatic compounds (Table 10.2). 4-chloro-3nitrotoluene and 4chloro-2nitro toluene reacted with H_2S-laden MDEA and fully reduced after 90 and 100 minutes of reaction time (Table 10.2, 1a, b). O, m and p isomers of chloronitrbenzene (Table 10.2, 1c-e) have shown excellent conversion with 100% selectivity. Among all isomers *meta* isomer has shown highest reactivity because chloride ion present at the meta position behaves as an electron withdrawing group and as a result the nitro group becomes more electron deficient and very prone to attack by sulphide ions [65]. Very fast reduction of nitro group in iodonitrobenzene (Table 10.2, 1f) is observed with 100% selectivity of corresponding amine. In the same manner 3-nitroacetophenone and 4-

nitroacetophenone (Table 10.2, 1g, h) gone under reduction reaction and completely converted after 45 and 60 minutes of reaction time. While reacting with o,p-nitroanisole (Table 10.2, 1i,j) compounds the *para* isomer (Table 10.2, 1j) have shown higher reactivity and as the nitro group present at *ortho* position (Table 10.2, 1i) is sterically hindered by the methoxy group, it reduced only 20% after 180 min of reaction. The reduction reaction of a polynuclear compound i.e. 1-Nitronaphthalene (Table 10.2, 1k) and a heterocyclic compound i.e. 8-nitroquinolene (Table 10.2, 1l) underwent smoothly. After 120 minutes of reaction 1-naphthyleamine produced with 85% conversion and 8-aminoquinolene (Table 10.2, 2l) produced with 100% conversion after 30 minutes of reaction. Selective reduction of a dinitro compounds also tried out. The synthetically interesting selective reduction of 2,6-dinitrotoluene (Table 10.2, 1m) and 2,4-dinitrotoluene (Table 10.2, 1n) successfully gave mono nitro reduced product. The end product of the reduction reaction of **1n** is 4-amino-4-nitrotoluene (4A2NT) (Scheme 10.2, $2n_1$) and 2-amino-4-nitrotoluene (2A4NT) (Table 10.2, $2n_2$). The selectivity of 2A4NT is less because of the nitro group present at the 2nd position that is sterically hindered by the methyl group present on the aromatic ring. So the reduction of nitro group present at the 4^{th} position is easier than the 2^{nd} position and as a result selectivity of 4A2NT is higher [63]. The substrate scope is further extended to 1-(2-nitrophenoxy) benzene (Table 10.2, 1o) and 1-(4-nitrophenoxy) benzene (Table 10.2, 1p) reduction they converted to their corresponding amines.

Table 10.2 substrate scope of selective reduction of substituted nitroaromatic compounds under L-L PTC.

Reactant	Product	Conversion/selectivity	Time (min.)
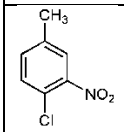 1a	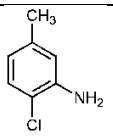 2a	100/100	90
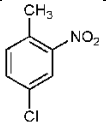 1b	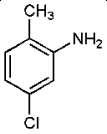 2b	100/100	100
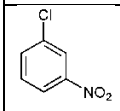 1c	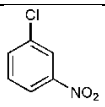 2c	100/100	45

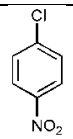 1d	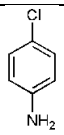 2d	97/100	60
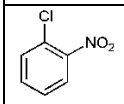 1e	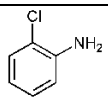 2e	80/100	75
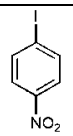 1f	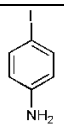 2f	100/100	60
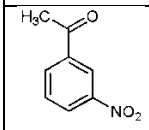 1g	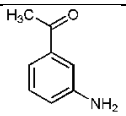 2g	100/100	45
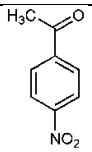 1h	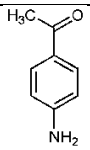 2h	100/100	60
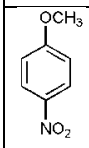 1i	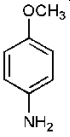 2i	100/100	180
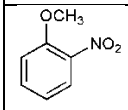 1j	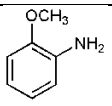 2j	25/100	180
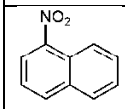 1k	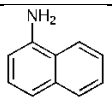 2k	85/100	120
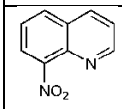 1l	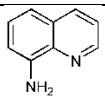 2l	100/100	30
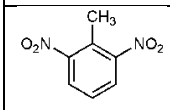 1m	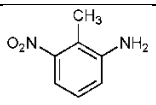 2m	100	60

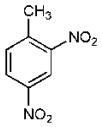 1n	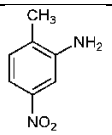 $2n_1$ 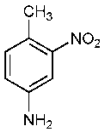 $2n_2$	100/83[a], 17[b]	20
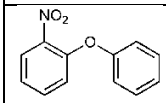 1o	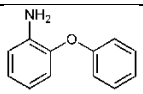 2o	74/100	420
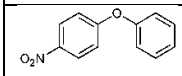 1p	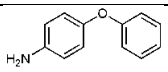 2p	40/100	420

The yield is the amount of product produced in comparison to the amount of substrate added. L-L PTC reaction conditions : TBAB (A) 0.00136 mol, nitroaromatics 0.00409 mol, sulphide conc. 2.50 kmol/m^3, toluene 30 cm^3, aqueous phase 30 cm^3, temperature 323 K, speed of agitation 1500 rpm.

10.6 Conclusion

The novel application of an industrial waste i.e. H_2S as a reducing agent for the selective reduction of mono/di nitroaromatics is successfully developed. For this process a number of phase transfer catalyst have been adopted as it is a biphasic reaction (L-L PTC) and the PT catalyst which is best suited for our current reaction have been identified, that is the TBPB. Our current research opens up the possibility of the alternative usage of H_2S-laden amine solution which can be acquired from amine treating unit (ATU) and the toxic waste can be utilised and removed, which is normally treated by Claus process. Our present approach is to find a total waste free process and current L-L PTC system uses milder reaction condition, inexpensive solvents without compromising the speed of the reaction and improved selectivity has been achieved for desired products. Mass spectra of the products from 2a to 2p is shown in Figure 10.1 to 10.17.

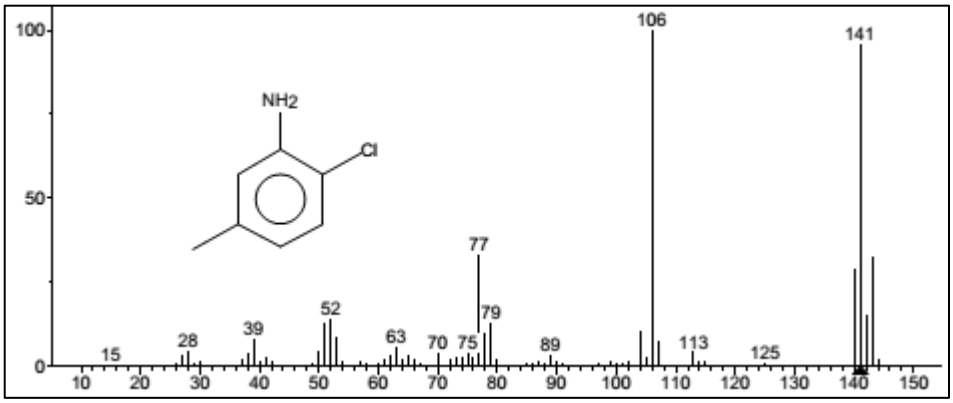

Figure 10.1: Mass spectra of product 4-chloro-3-aminotoluene (**2a**)

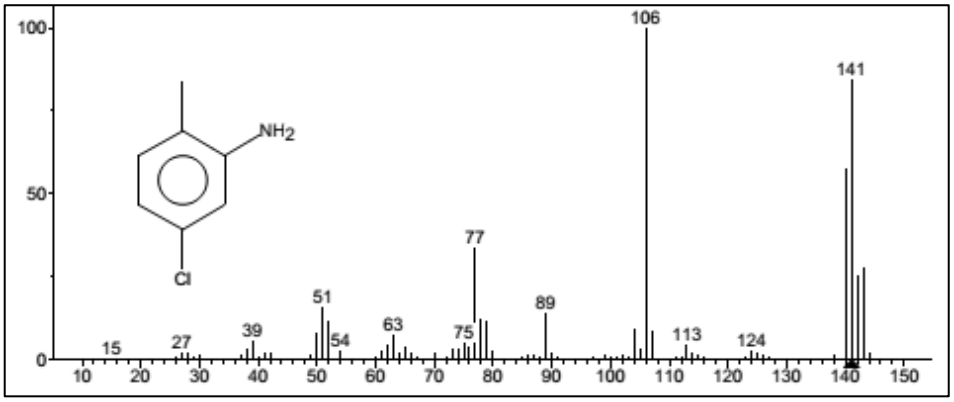

Figure 10.2: Mass spectra of product 4-chloro-2-aminotoluene (**2b**)

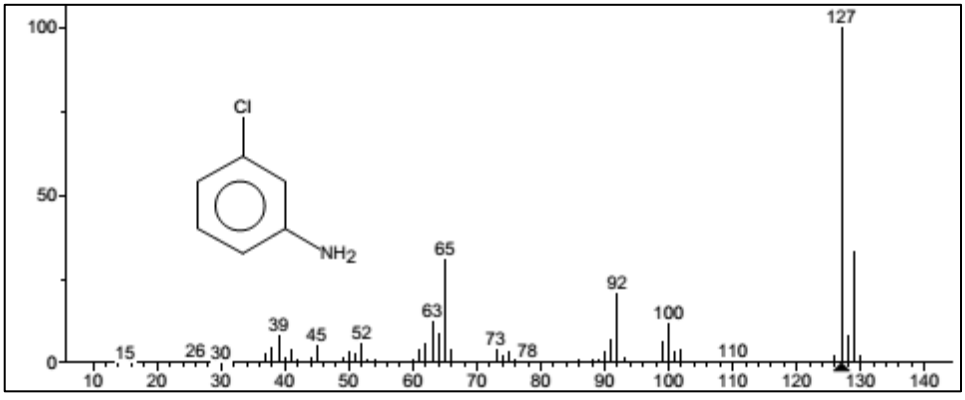

Figure 10.3: Mass spectra of product 3-chloroaniline (**2c**)

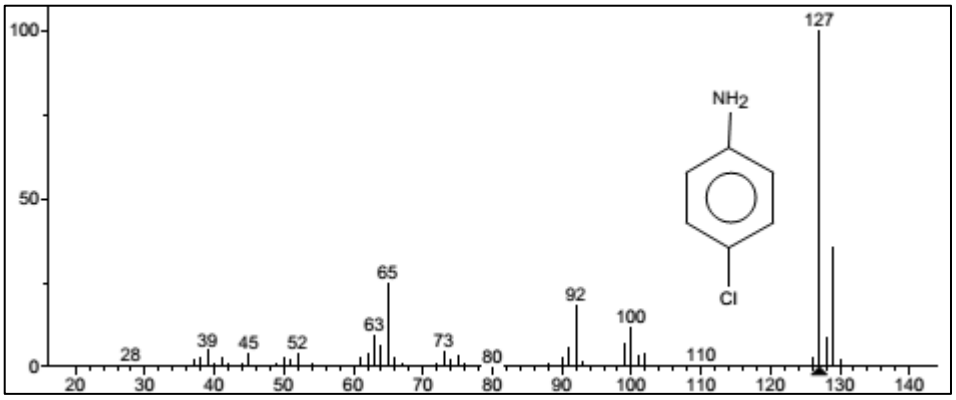

Figure 10.4: Mass spectra of product 4-chloroaniline (**2d**)

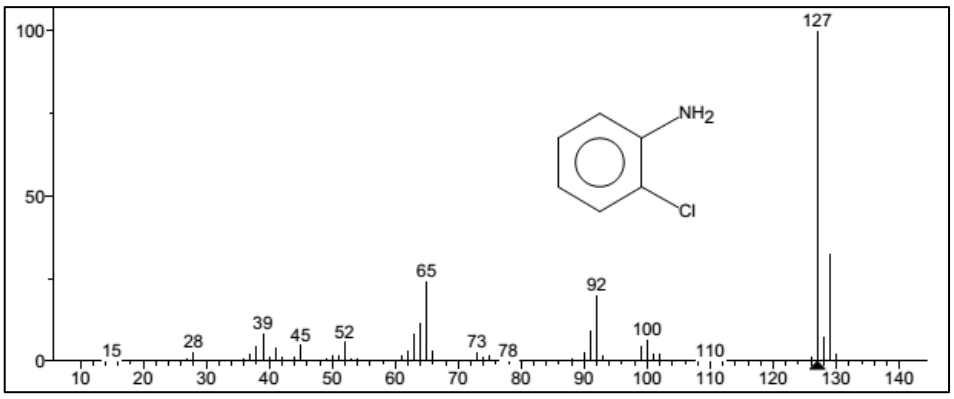

Figure 10.5: Mass spectra of product 2-chloroaniline (**2e**)

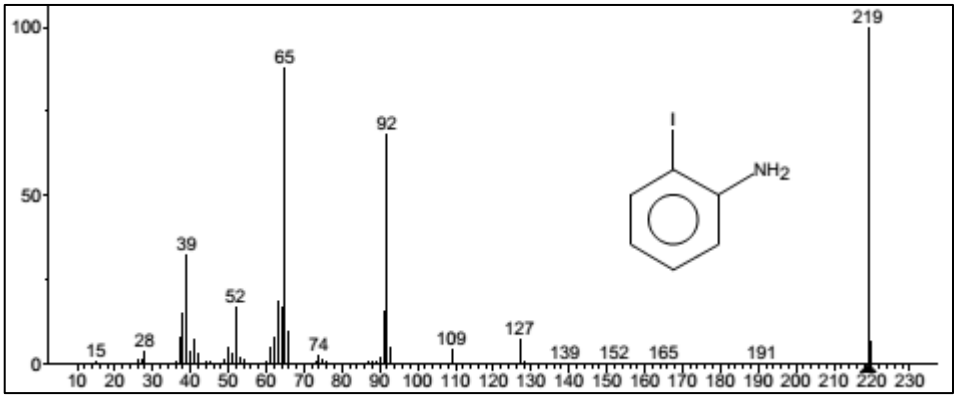

Figure 10.6: Mass spectra of product Iodo-2-aniline (**2f**)

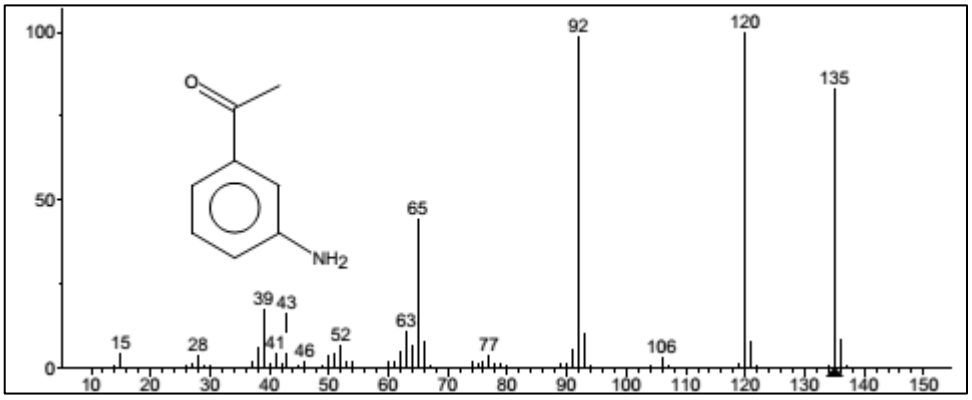

Figure 10.7: Mass spectra of product 3-aminoacetophenone (**2g**)

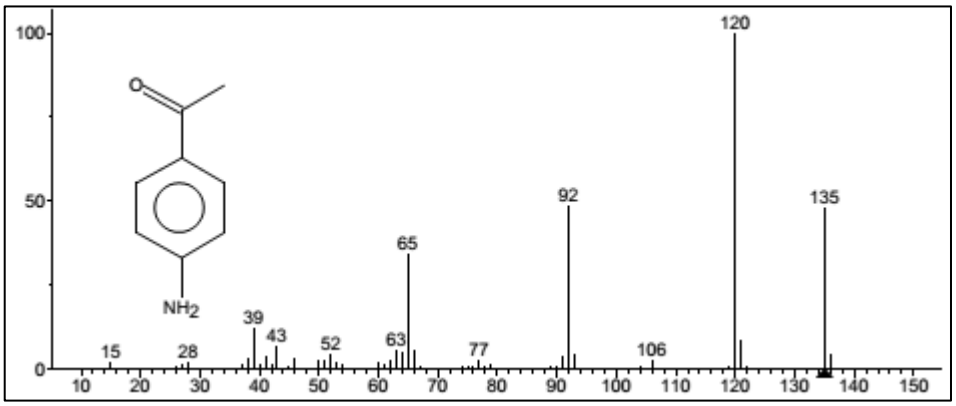

Figure 10.8: Mass spectra of product 4-aminoacetophenone (**2h**)

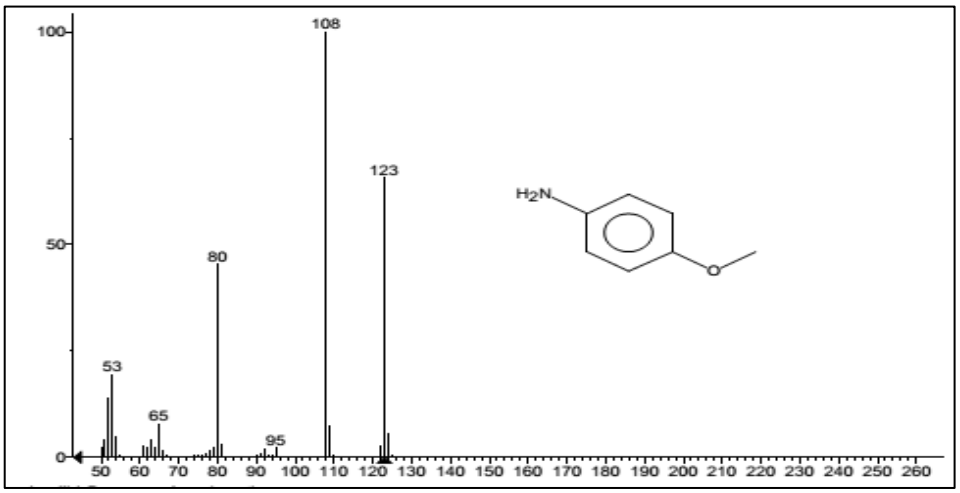

Figure 10.9: Mass spectra of product 4-aminoanisole (**2i**)

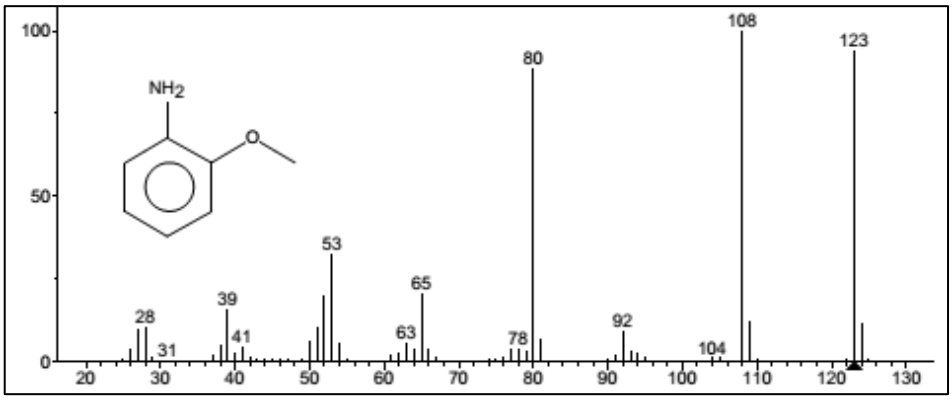

Figure 10.10: Mass spectra of product 2-aminoanisole (**2j**)

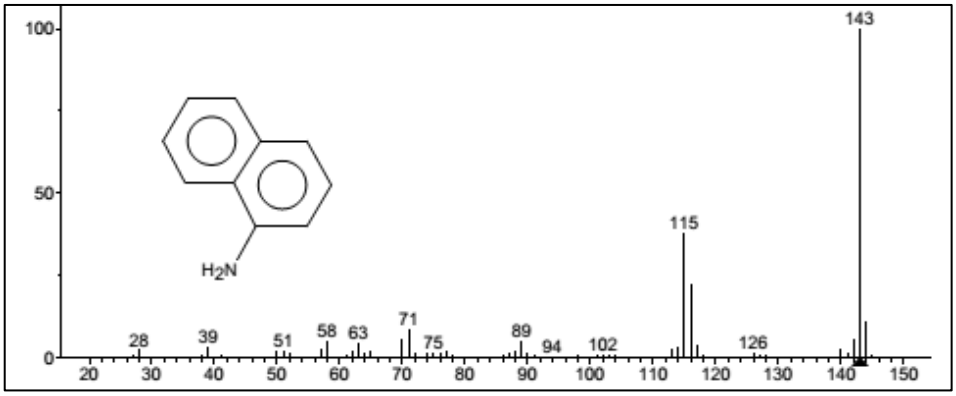

Figure 10.11: Mass spectra of product 1-aminonapthalene (**2k**)

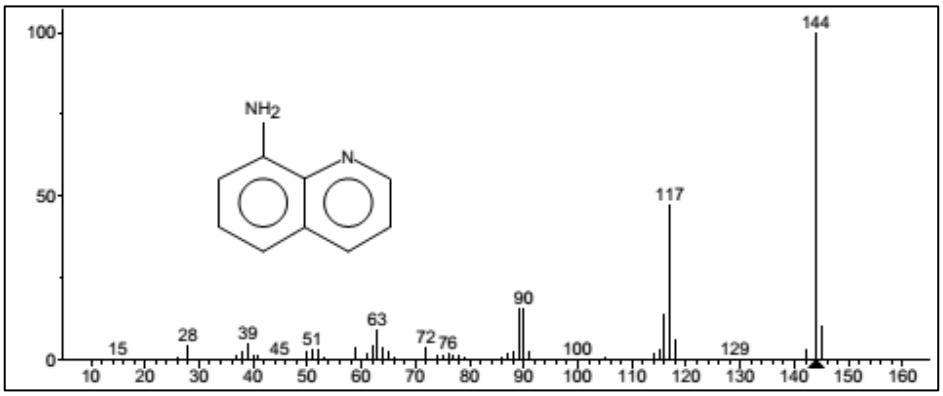

Figure 10.12: Mass spectra of product 8-aminoquinoline (**2l**)

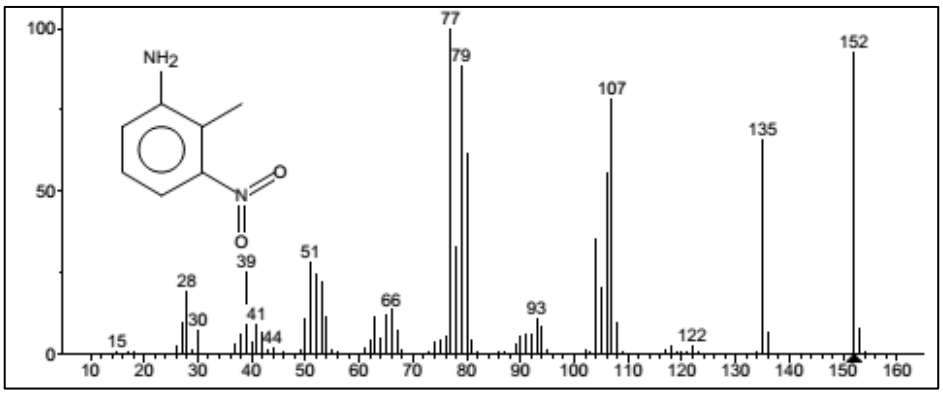

Figure 10.13: Mass spectra of product 2-amino-6-nitrotoluene (**2m**)

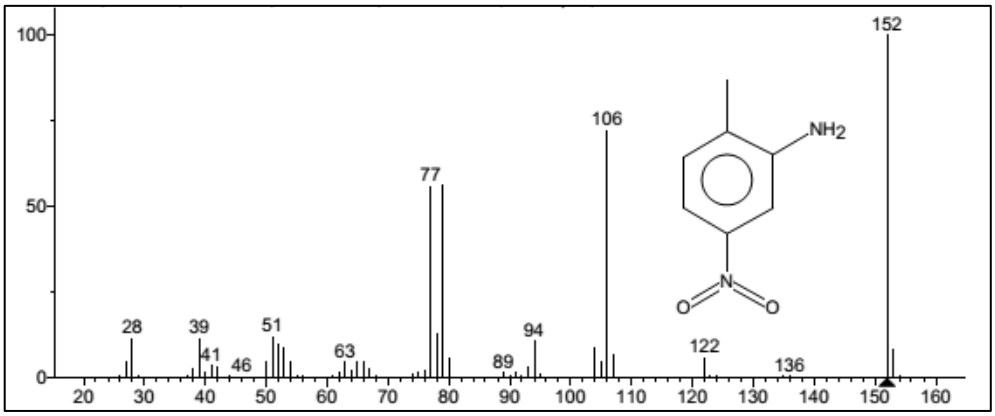

Figure 10.14: Mass spectra of product 2-amino-4-nitrotoluene (**$2n_1$**)

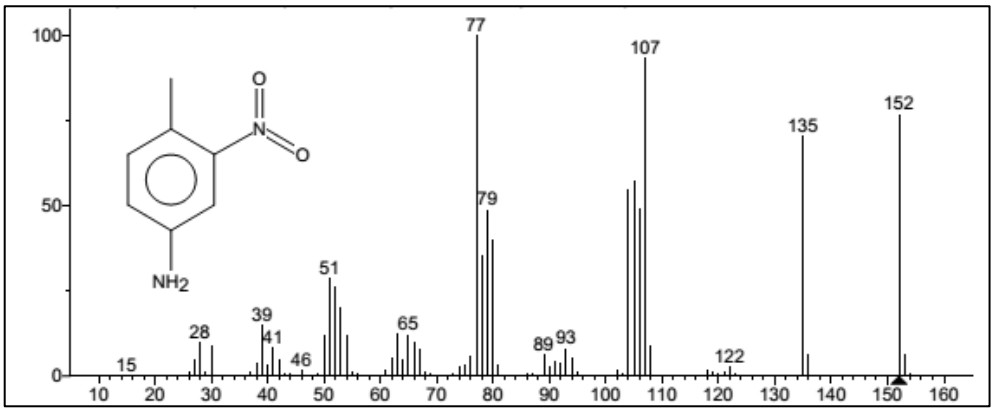

Figure 10.15: Mass spectra of product 4-amino-2-nitrotoluene (**$2n_2$**)

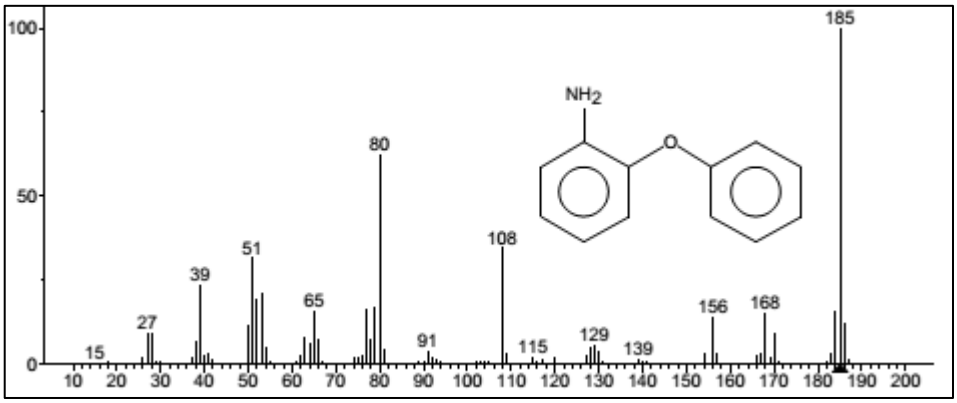

Figure 10.16: Mass spectra of product 1-(2-aminophenoxy) benzene (**2o**)

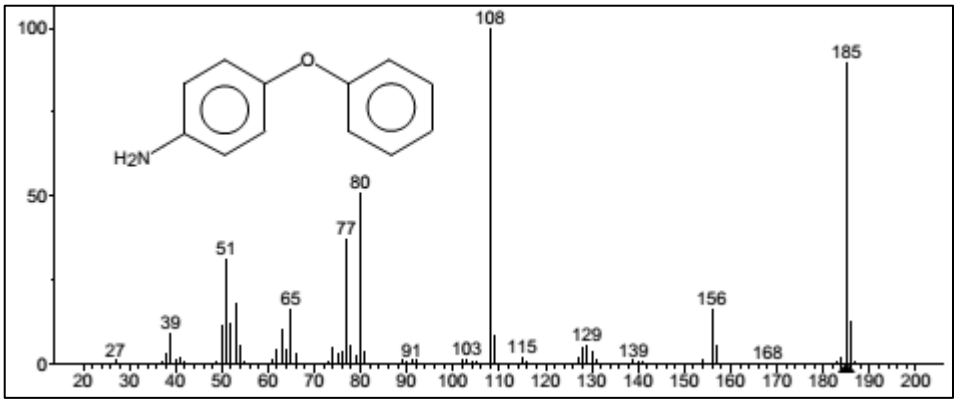

Figure 10.17: Mass spectra of product 1-(4-aminophenoxy) benzene (**2p**)

References

1 M. Kumarraja and K. Pitchumani, *Appl. Catal. A Gen.*, 2004, **265**, 135–139.

2 K. Zhu, M. P. Shaver and S. P. Thomas, *Chem. Sci.*, 2016, **7**, 3031–3035.

3 M. H. Lin, B. Zhao and Y. W. Chen, *Ind. Eng. Chem. Res.*, 2009, **48**, 7037–7043.

4 F. E. Catino SC, *Concise Encyclopaedia of Chemical Technology*, John Wiley & Sons, New York, 1985.

5 S. Sakaue, T. Tsubakino, Y. Nishiyama and Y. Ishii, *J. Org. Chem.*, 1993, **58**, 3633–3638.

6 A. P. A. Shabbir H. Gheewala, *Water Sci. Technol.*, 1997, **36**, 53–63.

7 N. Boon, L. De Gelder, H. Lievens, S. D. Siciliano, E. M. Top and W. Verstraete, *Environ. Sci. Technol.*, 2002, **36**, 4698–4704.

8 R. S. Downing, P. J. Kunkeler and H. vanBekkum, *Catal. Today*, 1997, **37**, 121–136.

9 H. G. Abdessamad Grirrane, Avelino Corma, *Science*, 2008, **322**, 1661–1664.

10 Y. Zheng, K. Ma, H. Wang, X. Sun, J. Jiang, C. Wang, R. Li and J. Ma, *Catal. Letters*, 2008, **124**, 268–276.

11 P. G. Jessop, T. Ikariya and R. Noyori, *Nature*, 1994, **368**, 231–233.

12 M. M. Dell'Anna, V. Gallo, P. Mastrorilli and G. Romanazzi, *Molecules*, 2010, **15**,

3311–3318.

13 M. L. Kantam, R. Chakravarti, U. Pal, B. Sreedhar and S. Bhargava, *Adv. Synth. Catal.*, 2008, **350**, 822–827.

14 A. Corma, P. Serna, P. Concepcin and J. J. Calvino, *J. Am. Chem. Soc.*, 2008, **130**, 8748–8753.

15 M. Boronat, P. Concepción, A. Corma, S. González, F. Illas and P. Serna, *J. Am. Chem. Soc.*, 2007, **129**, 16230–16237.

16 L. F. Chen and Y. W. Chen, *Ind. Eng. Chem. Res.*, 2006, **45**, 8866–8873.

17 P. Corma, A.; Serna, *Science (80-.).*, 2006, 332–334.

18 H. Liu, J. Deng and W. Li, *Catal. Letters*, 2010, **137**, 261–266.

19 M. Kumar, U. Sharma, S. Sharma, V. Kumar, B. Singh and N. Kumar, *RSC Adv.*, 2013, **3**, 4894–4898.

20 C. T. Redemann and C. Ernst Redemann, *Org. Synth.*, 1949, **29**, 8.

21 K. Junge, B. Wendt, N. Shaikh and M. Beller, *Chem. Commun.*, 2010, 1769–1771.

22 J. W. Bae, Y. J. Cho, S. H. Lee, C.-O. M. Yoon and C. M. Yoon, *Chem. Commun.*, 2000, 1857–1858.

23 G. R. Srinivasa, K. Abiraj and D. C. Gowda, *Indian J. Chem. - Sect. B Org. Med. Chem.*, 2004, **43**, 192–195.

24 W. G. Dauben, *Organic reactions*, John Wiley & Sons, Inc., New York, 1973.

25 G. D. Yadav, Y. B. Jadhav and S. Sengupta, *J. Mol. Catal. A Chem.*, 2003, **200**, 117–129.

26 S. K. Maity, N. C. Pradhan and A. V. Patwardhan, *Appl. Catal. B Environ.*, 2008, **77**, 418–426.

27 S. K. Maity, N. C. Pradhan and A. V. Patwardhan, *Appl. Catal. A Gen.*, 2006, 301, 251–258.

28 G. D. Yadav, Y. B. Jadhav and S. Sengupta, *Chem. Eng. Sci.*, 2003, **58**, 2681–2689.

29 C. Wright, *US Pat.*, US 8835677 B2, 2014, 1–8.

30 G. D. Yadav and S. V. Lande, *Ind. Eng. Chem. Res.*, 2007, **46**, 2951–2961.

31 Y. Belmabkhout, G. De Weireld and A. Sayari, *Langmuir*, 2009, **25**, 13275–13278.

32 D. D. E. Koyuncu and S. Yasyerli, *Ind. Eng. Chem. Res.*, 2009, **48**, 5223–5229.

33 M. A. Plummer, *US Pat.*, US5334363 A, 1994.

34 F. Faraji, *Int. J. Hydrogen Energy*, 1998, **23**, 451–456.

35 J. M. A. S. Cervera-March, L. Borrell, J. Giménez, R. Simarro, *Int. J. Hydrogen Energy*, 1992, **17**, 683–688.

36 H. Huang, Y. Yu and K. H. Chung, *Energy & Fuels*, 2009, **23**, 4420–4425.

37 K. Petrov and S. Srinivasan, *Int. J. Hydrogen Energy*, 1996, **21**, 163–169.

38 S. S Srinivasan. and A. J. A. Z. Mao, A. Anani, R. E. White, *J. Electrochem. Soc.*, 1991, **138**, 1299–1303.

39 J. O. N. E. Noringt and E. A. Fletchers, *Energy*, 1982, **7**, 651–666.

40 M. Groisil, S. Ibrahim, A. K. Gupta and A. AlShoaibi, *Energy Procedia*, 2015, **75**, 3066–3070.

41 M.-H and K. Shen, *J. Chem. Eng. Data*, 1993, 105–108.

42 H. Xu, C. Zhang and Z. Zheng, *Society*, 2002, 6175–6180.

43 H. Xu, C. Zhang and Z. Zheng, *Simulation*, 2002, 2953–2956.

44 W. Pohl, J. Menzel, *US Pat.*, US5607594 A, 1997.

45 G. D. Yadav, *Top. Catal.*, 2004, **29**, 145–161.

46 Z. Li, A. Zhu and J. Yang, *J. Heterocycl. Chem.*, 2012, **49**, 1458–1461.

47 P.-J. Lin and H.-M. Yang, *J. Mol. Catal. A Chem.*, 2005, **235**, 293–301.

48 T. T. Fujihira T. and M. S. Seno, *J. Mol. Catal. A Chem.*, 1999, **137**, 65–75.

49 W. W. Scott, *Standard Methods of Chemical Analysis*, Van Nostrand, New York, 6th Editio., 1966.

50 N. C. Pradhan and M. M. Sharma, *Ind. Eng. Chem. Res.*, 1992, **31**, 1606–1609.

51 R. R. Bhave and M. M. Sharma, *J. Chem. Technol. Biotechnol.*, 1981, **31**, 93–102.

52 N. C. Pradhan, *Indian J. Chem. Technol.*, 2000, **7**, 276–279.

53 H. Gilman, Wiley, New York, 1941, p. 52.

54 S. K. Maity, N. C. Pradhan and A. V. Patwardhan, *Chem. Eng. J.*, 2008, **141**, 187–193.

55 G. D. Yadav and S. V. Lande, *Adv. Synth. Catal.*, 2005, **347**, 1235–1241.

56 G. D. Yadav and S. V. Lande, *Appl. Catal. A Gen.*, 2005, **287**, 267–275.

57 C. M. Starks, *J. Am. Chem. Soc.*, 1971, **93**, 195.

58 A. Makosza, M ; Jonczyk, *Org. Synth.*, 1976, **55**, 91.

59 P. A. Vivekanand and T. Balakrishnan, *Catal. Commun.*, 2009, **10**, 1962–1966.

60 E. Murugan and A. Siva, *J. Mol. Catal. A Chem.*, 2005, **235**, 220–229.

61 J. Klausen, J. Ranke and R. P. Schwarzenbach, *Chemosphere*, 2001, **44**, 511–517.

62 B. Zhou, J. Song, H. Zhou, T. Wu and B. Han, *Chem. Sci.*, 2016, **7**, 463–468.

63 R. V. M. and R. V. Chaudhari, *Ind. Eng. Chem. Res.*, 1999, **38**, 906–915.

64 E. C. Division, *Appl. Environ. Microbiol.*, 1984, **47**, 1295–1298.

65 J. P. Ldoux and Wendell Plain, *J. Chem. Educ.*, 1972, **49**, 133.

Abstract

This chapter outlines the conclusions which are gathered from the previous chapters. Few suggestions for the future work have been proposed based on the observations, results and conclusions encapsulated from the present study. How the present study can be utilised to improve the knowledge and utilization of phase transfer catalysis are shown.

11.1 Introduction

Present work carried out in the thesis emphasises a state of the art approach to the utilization of a pollutant and hazardous gas, H_2S, which is one of the most common bi-product of many industries to synthesise value added fine chemicals. Our current approach is a two-step process, first H_2S gas is removed from the gas stream by chemisorption in conventional solvents and second stage is the utilisation of the solution obtained from the first stage to produce fine chemicals. The first stage is an industrially adopted process which utilises alkanolamines as an absorbent and it can be imported from the amine treating unit (ATU). The present work is stressed on the detailed study of the synthesis of the fine chemicals like aromatic amines with utilization of the H_2S-laden aqueous alkanolamies in a batch reactor.

A number of aromatic amines have been successfully produced by Zinin reduction from respective substituted nitro aromatic compounds. The reduction of chloronnitrobenzene (CNB) by H_2S-laden monoethanolamine (MEA) in the presence of Amberlite IR400 (Cl^-) as an insoluble PT catalyst (chapter 5), reduction CNB by H_2S-laden n-methyl diethanol amine (MDEA) in the presence of n-tetra butyl phosphonium bromide (TBPB) as PT catalyst (chapter 6), reduction 1-nitronapthalene (1-NN) by H_2S-(MDEA) in the presence of TBPB as PT catalyst (chapter 7), reduction 3-nitroacetophenone (3-NAP) by H_2S-(MDEA) in the presence of TBPB as PT catalyst (chapter 8), reduction dinitrotoluenes (DNT) by H_2S-(MDEA) in the presence of TBPB as PT catalyst (chapter 9) and finally a number of mono nitro, dinitro, heterocyclic nitro compound has been reduced to identical reaction condition in the presence of TBPB as PT catalyst in bi-phasic reaction has been investigated (chapter 10). During the present studies variety of reaction parameters (i. e. stirring speed, temperature, catalyst loading, reactant loading, suphide concentration, MEA/MDEA concentration and elemental sulphur loading) has been studied and their influence on the conversion, yield and selectivity have been correctly enquired. Reaction mechanism of either liquid-liquid-solid (L-L-S) or liquid-liquid (L-L) phase transfer catalysis has been developed for all the reaction studied. The stirring speed was found to have very little effect on the reaction rate. So the reaction can be assumed to have no mass

transfer resistance when it is operated at 1000 rpm. All the experiments were carried out at 1500 rpm to ensure that the reaction is only kinetically controlled one. Based on the kinetic studies a mathematical model has been developed (Chapter 5, 6, 7, 9) and the model is able to predict the conversion correctly. Statistical method for the designing of experiments has also been adopted in chapter 8 to optimise controlling process parameters in order to enhance the conversion and selectivity of desired product.

11. 2 Conclusions

11.2.1 The salient achievements and major conclusions of chapter 5:

- ✓ The Zinin reduction of m-CNB by H_2S-laden MEA was studying under L-L-S mode in presence of solid reusable PTC, Amberlite IR-400 to yield m-CA as the sole product.
- ✓ The reaction was found to be kinetically controlled with apparent activation energy of 56.16 kJ/mol. The rate of reduction was found to be first order with respect to the concentration of catalyst and reactant and second order with respect to the concentration of sulphide.
- ✓ Only by increasing the catalyst concentration, reactant conversion of more than 62% was achieved with 10 grams (10% w/v) of catalyst loading whereas it was about 36% without catalyst even after 8 hours of reaction under otherwise identical conditions.
- ✓ It can be seen that up to the three cycles, the catalyst can be used without significant decrease in conversion, indicating that the catalyst has got excellent reusable and recyclable property and high stability.
- ✓ The process was found to follow a complex mechanism involving different ions and molecules. Based on detailed kinetic studies and proposed mechanism, a kinetic model was developed considering aqueous phase equilibria of H_2S-MEA-H_20 system and interfacial mechanism for insoluble PTC. The developed model predicts conversion of

11.2.2 The salient achievements and major conclusions of chapter 6:

- ✓ The liquid-liquid (L-L) phase transfer catalysis (PTC) reactions are carried out under milder conditions, using less-expensive solvents at much faster reaction rate and improved selectivity to desired products and, thus by definition, are waste minimization processes.
- ✓ This work addresses the novelties of the kinetics and mechanism of the selective reduction of CNBs to respective amines using hydrogen sulphide absorbed in industrially important sour gas absorber under L-L PTC.

- ✓ The effects of different parameters such as stirring speed, temperature, MDEA concentration, reactant concentrations (both sulphide and CNB), and sulphur loading were studied. It was observed that the reaction rates were intensified under L-L PTC. It leads to 100% selectivity of m-Chlroaniline.
- ✓ The process was found to follow a complex mechanism involving different ions and molecules. Based on detailed kinetic studies and proposed mechanism, a kinetic model was developed considering Stark's extraction mechanism for L-L PTC. The developed model predicts the conversion of m-CNB reasonable well at all temperatures.
- ✓ For this process, a number of phase transfer catalyst have been adopted as it is a biphasic reaction (L-L PTC) and the PTC which is best suited for our current reaction has been identified, that is TBPB.

11.2.3 The salient achievements and major conclusions of chapter 7:

- ✓ H_2S-rich MDEA is successfully used as reducing agent for Zinin reduction of 1-NN in this work and 100% selectivity of 1-AN is achieved after the reaction. The reaction is kinetically controlled with an activation energy of 20.77 kJ/mol.
- ✓ This work addresses the novelties of the kinetics and mechanism of the selective reduction of CNBs to respective amines using hydrogen sulphide absorbed in industrially significant sour gas absorber under L-L PTC. The effects of different parameters such as stirring speed, temperature, MDEA concentration, reactant concentrations (both sulphide and 1-NN), and sulphur loading were studied.
- ✓ The process was found to follow a complex mechanism involving different ions and molecules. Based on detailed kinetic studies and proposed mechanism, a kinetic model was developed considering Stark's extraction mechanism for L-L PTC. The developed model predicts the conversion of 1-NN reasonable well at all temperatures.

11.2.4 The salient achievements and major conclusions of chapter 8:

- ✓ Based on experimental design methodology a statistical model of single response surface optimization was carried out on the liquid-liquid phase transfer catalyzed the reaction of p-NAP with H_2S-ladden MDEA.
- ✓ A quadratic model developed based on the relationship between p-NAP conversion and four independent variables (temperature, catalyst conc., p-NAP/sulfide mole ratio and MDEA conc.).
- ✓ The contour plots, 3D surface plots and the value of different regression coefficients have clearly explained the single parameter effect and interaction effects of dual parameters on the p-NAP conversion.

- ✓ The model fits well and is verified with optimum conditions for highest p-NAP conversion. R^2 value of the regression analysis confirms a good agreement between the experimental data and predicted response.

11.2.5 The salient achievements and major conclusions of chapter 9:

- ✓ The current study shows the novelties of L-L PTC in the selective reduction of 2,4-DNT to the corresponding amino compound by novel Zinin reagent, H_2S-laden MDEA under milder reaction conditions, thereby eliminating the use of a costly metallic catalyst, high-temperature, and high-pressure reaction.
- ✓ As the reaction was very fast, 100% conversion was achieved in a very short time room temperature (303K). Selective reduction leads to the formation of two isomers- 2A4NT and 4A2NT, among them 4A2NT was much more abundant than 2A4NT.
- ✓ The detailed parametric study suggested that with the increase of temperature, catalyst concentration, sulphide ion concentration, MDEA concentration, the selectivity of 4A2NT decreases and that of 2A4NT increases.
- ✓ Highest selectivity of 4A2NT was observed as 82.26% when reactant concentration in the reactor was 1.0981 kmol/m^3. Reaction kinetics has been evaluated after details parametric studies and a mechanistic model also been proposed, which was further confirmed by experimental data.
- ✓ The activation energy of 46.25 kJ/mol makes current reaction a kinetically controlled one.

11.2.6 The salient achievements and major conclusions of chapter 10:

- ✓ In summary, the novel application of an industrial waste i.e. H_2S as a reducing agent for the chemoselective reduction of mono/di-substituted nitroaromatics is successfully developed.
- ✓ For this process, a number of phase transfer catalyst have been adopted as it is a biphasic reaction (L-L PTC) and the PTC which is best suited for our current reaction has been identified, that is TBPB.
- ✓ Our current research opens up the possibility of the alternative usage of H_2S-laden amine solution which can be acquired from amine treating unit (ATU) and is being normally treated by Claus process.
- ✓ Our present approach is to find a total waste free process and current L-L PTC system uses milder reaction condition, inexpensive solvents without compromising the speed of the reaction and improved selectivity has been achieved for desired products.

11. 3 Future recommendations

This present work is based upon the idea of reducing nitroaromatic compounds by H_2S-laden aqueous alkanolamine solution under either L-L PTC or L-L-S PTC reaction condition. Based on the current findings a number of future recommendations can be stated for the improvement of current process and for further reducing the cost and labour of the process.

- Current study is a two pot system which requires multiple subsystems to prepare reducing agent (H_2S-laden alkanolamines) and reducing reaction was performed in a separate batch reactor. The whole system can be transformed into a single pot system where autoclave reactor is the only equipment to be used. H_2S can be directly fed into the autoclave and organic substrate and catalyst mixed with organic solvent will be added separately.
- Solvent free process is unique approach which is more environment friendly and possesses many advantages compared to present approaches such as requirement of small size reactor, cheaper operation and easier handling, easy mode of separation of product.
- The influence of other parameters on the conversion and selectivity can also be enquired. The pH of aqueous phase (H_2S-laden alkanolamines), addition of other anions (example NaCl), addition of co-catalyst etc.

- In our present work for elimination the mass transfer effect we provide stirring effect with a 6 blade stirrer at 1500 rpm which is quite energy intensive process. So this stirring can be replaced with ultrasound sonication which can make this work green technology.
- For the increasing the reaction rate heating effect is provided with water bath in our present work. Instead of using water bath the whole reaction can be operated in microwave reactor which makes this work as a green technology.

- The aqueous phase is an aqueous solution of alkanolamines (MEA/ MDEA) which absorbed with H_2S. There are other industrially used alkanolamines present such as di-2-propanolamine (DIPA), secondary amine diethnolamine (DEA), triethnolamine (TEA) which can be compared with current alkanolamines used.

- This current system is an L-L or L-L-S PTC system which can be converted to liquid-liquid-liquid (L-L-L) PTC system. By doing so product separation problem can be avoided and faster reaction can be achieved.

- Reusable catalyst is more favourable for any catalyst reaction because it not only saves lots of money but it is easy to use also if we can little compromise the reaction rate. Single or multisite solid phase transfer catalyst can be manufactured or procured commercially and utilised in the current systems.

- The aqueous amine solution can be reused for after the completion of the reaction. The used alkanolamine solution can be again bubbled with H_2S gas to get regenerated and used to generate industrially important value added chemicals.

Dissemination

International Journals

1. **Ujjal Mondal**, Sujit Sen and Gaurav Singh,"Advances in hydrogen sulphide utilisation: phase transfer catalysed selective reduction of nitronaphthalene", RSC Advances 2015, 5, 102942–102952

2. **Ujjal Mondal**, Aslam Puthankot, Sujit Sen and Gaurav Singh,"Novelties of triphasic phase transfer catalysed Zinin reduction of nitrochlorobenzene by H_2S-laden monoethanolamine", RSC Advances 2015, 2016, 6, 23666–23676

3. **Ujjal Mondal**, Sujit Sen, "Multivariate analysis in selective nitroacetophenone conversion by toxic hydrogen sulfide under phase transfer catalysis '', Org. Process Res. Dev. Org. Process Res. Dev., 2017, 21 (1), 23–30

4. Preeti Jha, **Ujjal Mondal**, Devipriya Gogoi, Gaurav Singh and Sujit Sen, "Novelties of selective triphasic synthesis of bis-(p-chlorobenzyl) sulfide using hydrogen sulfide and reusable phase transfer catalyst'', J. Mol. Catal. A Chem. 2016. DOI: 10.1016/j.molcata.2016.03.030

5. Sujit Sen, **Ujjal Mondal**, Gaurav Singh, "Dual Optimization in Phase Transfer Catalyzed Synthesis of Dibenzyl Sulfide using Response Surface Methodology (RSM)", *Accepted* in Org. Process Res. Dev. 2016.

6. Gaurav Singh, Priya G. Nakade, Dorothy Chetia, Preeti Jha, **Ujjal Mondal**, Saroj Kumari and Sujit Sen, "Kinetics and mechanism of phase transfer catalyzed synthesis of aromatic thioethers by H_2S-rich methyldiethanolamine'', J. Ind. Eng. Chjem. 2016. DOI: 10.1016/j.jiec.2016.03.022.

7. Gaurav Singh, Priya G. Nakade, Pratik Mishra, Preeti Jha, Sujit Sen, **Ujjal Mondal**,"Kinetic investigation on liquid–liquid–solid phase transfer catalyzed synthesis

of dibenzyl disulfide with H_2S-laden monoethanolamine", J. Mol. Catal. A Chem. 2015, 411, 78–86

8. **Ujjal Mondal**, Sujit Sen "Modified Zinin Reduction of Nitroarenes by H_2S-laden Aqueous Methyldiethanolamine under Liquid-Liquid Phase Transfer Catalytic Condition'', J. Ind. Eng. Chem. (under review).

9. **Ujjal Mondal**, Sujit Sen "Selective Zinin reduction of dinitro arenes at room temperature under Liquid-Liquid phase transfer catalysis'', Appl. Catal., A. (under review).

10. **Ujjal Mondal**, Sujit Sen "Hydrogen sulphide as an efficient reducing agent for selective reduction mono/dinitro arenes under Liquid-Liquid Phase transfer catalysis'', Chem. Comn. (under review)

International Conferences

1. **Ujjal Mondal**, Sujit Sen, Gaurav Sing. "H_2S-rich Alkanolamine: A new reagent for Zinin Reduction", Indian Chemical Engineering Congress (CHEMCON-2013), ICT Mumbai, India, December 27-30, 2013

2. Gaurav Singh, Sujit Sen, **Ujjal Mondal**, Priya G. Nakade. "Synthesis of Symmetrical Thioethers from Hydrogen Sulfide", Indian Chemical Engineering Congress (CHEMCON-2013), ICT Mumbai, India, December 27-30, 2013.

UJJAL MONDAL

Communication

Business Address
Department of Chemical Engineering
National Institute of Technology
Rourkela – 769008, Odisha, India
Email: ujjal.mondal130887@gmail.com
Phone: +91-8902766097 (M)

Home Address
C/O Uttam Kumar Mondal
29, Purbasha, Ichapore
24 pgs (N), West Bengal
Pin code-743144

Education

2012 - Present	**Doctoral Fellow (PhD)** Mentor: **Prof. Sujit Sen** Department of Chemical Engineering **National Institute Of Technology,** Rourkela Title**: "Chemoselective Reduction of Nitroarenes using Hydrogen Sulphide under Phase Transfer Catalysis."**
2010 – 2012	**Master of Technology (M.Tech.) in Chemical Engineering.** Department of Chemical Engineering. **Manipal Institute Of Technology**, Manipal First Class (7.77 CGPA).
2005 – 2009	**Bachelor of Technology (B.Tech.) in Biotechnology.** Department of Biotechnology. **Haldia Institute Of Technology**, Haldia West Bengal University of Technology

First Class (7.25 CGPA).

Personal Dossier

Date of Birth: 13th August 1987
Marital Status: Single
Nationality: Indian